

IntechOpen

# Gasification

*Edited by Valter Silva  
and Celso Eduardo Tuna*





---

# Gasification

*Edited by Valter Silva  
and Celso Eduardo Tuna*

Published in London, United Kingdom

---



## IntechOpen





*Supporting open minds since 2005*



## Gasification

<http://dx.doi.org/10.5772/intechopen.87865>

Edited by Valter Silva and Celso Eduardo Tuna

## Contributors

Viktors Gutakovskis, Vladimirs Gudakovskis, Xianhui Zhao, Kai Li, Meghan Lamm, Serdar Celik, Lin Wei, Soydan Ozcan, Shehzaad Kauchali, Alessia Borgogna, Gaetano Iaquaniello, Annarita Salladini, Emanuela Agostini, Mirko Boccacci, Seyede Masoumeh Safavi, Runar Unnthorsson, Christiaan Richter, Oleg Aleksandrovich Ivanin, Olga Mihailovna Larina, Vladimir Aleksandrovich Lavrenov, Vladimir Aleksandrovich Sinelshchikov, Georgij Aleksandrovich Sytchev, Viktor Mihajlovich Zaichenko, Md Emdadul Hoque, Fazlur Rashid, Jose Antonio Mayoral Chavando, Valter Silva, Luís António Da Cruz Tarelho, João Sousa Cardoso, Daniela Eusébio, Danielle Regina Da Silva

© The Editor(s) and the Author(s) 2021

The rights of the editor(s) and the author(s) have been asserted in accordance with the Copyright, Designs and Patents Act 1988. All rights to the book as a whole are reserved by INTECHOPEN LIMITED. The book as a whole (compilation) cannot be reproduced, distributed or used for commercial or non-commercial purposes without INTECHOPEN LIMITED's written permission. Enquiries concerning the use of the book should be directed to INTECHOPEN LIMITED rights and permissions department ([permissions@intechopen.com](mailto:permissions@intechopen.com)).

Violations are liable to prosecution under the governing Copyright Law.



Individual chapters of this publication are distributed under the terms of the Creative Commons Attribution 3.0 Unported License which permits commercial use, distribution and reproduction of the individual chapters, provided the original author(s) and source publication are appropriately acknowledged. If so indicated, certain images may not be included under the Creative Commons license. In such cases users will need to obtain permission from the license holder to reproduce the material. More details and guidelines concerning content reuse and adaptation can be found at <http://www.intechopen.com/copyright-policy.html>.

## Notice

Statements and opinions expressed in the chapters are these of the individual contributors and not necessarily those of the editors or publisher. No responsibility is accepted for the accuracy of information contained in the published chapters. The publisher assumes no responsibility for any damage or injury to persons or property arising out of the use of any materials, instructions, methods or ideas contained in the book.

First published in London, United Kingdom, 2021 by IntechOpen

IntechOpen is the global imprint of INTECHOPEN LIMITED, registered in England and Wales, registration number: 11086078, 5 Princes Gate Court, London, SW7 2QJ, United Kingdom  
Printed in Croatia

British Library Cataloguing-in-Publication Data

A catalogue record for this book is available from the British Library

Additional hard and PDF copies can be obtained from [orders@intechopen.com](mailto:orders@intechopen.com)

## Gasification

Edited by Valter Silva and Celso Eduardo Tuna

p. cm.

Print ISBN 978-1-83968-795-2

Online ISBN 978-1-83968-796-9

eBook (PDF) ISBN 978-1-83968-797-6

# We are IntechOpen, the world's leading publisher of Open Access books Built by scientists, for scientists

**5,400+**

Open access books available

**134,000+**

International authors and editors

**165M+**

Downloads

**156**

Countries delivered to

Our authors are among the  
**Top 1%**

most cited scientists

**12.2%**

Contributors from top 500 universities



**WEB OF SCIENCE™**

Selection of our books indexed in the Book Citation Index  
in Web of Science™ Core Collection (BKCI)

Interested in publishing with us?  
Contact [book.department@intechopen.com](mailto:book.department@intechopen.com)

Numbers displayed above are based on latest data collected.  
For more information visit [www.intechopen.com](http://www.intechopen.com)







# Meet the editors



Valter Silva is a senior researcher in the area of environment and energy at the Portuguese Collaborative Laboratory for Integrated Forest & Fire Management and Senior Collaborator Researcher at the Polytechnic Institute of Portalegre, Portugal. He graduated in Chemical Engineering from the University of Porto, Portugal, in 2004, obtained his Ph.D. in Chemical and Biological Engineering at the same university in 2009, and his degree as Specialist in Numerical Simulation (combustion and fluid dynamics) at Technical University of Madrid and Ansys, Inc., in 2017. Since 2012, he has led a research team devoted to the application of experimental and numerical solutions on the environment and energy topics (gasification, combustion, fuel cells, techno-economic analysis, LCA, CFD, and optimization). In the last five years, he coordinated national and international projects with leading universities across the world (e.g., MIT and Carnegie Mellon) raising approximately \$2.5 million in funds. He has supervised more than thirty students (postdoc, Ph.D., master, and diploma students). He has participated in more than twenty-five national and international projects in energy and environment and has authored two books, eleven book chapters, and more than sixty papers in international peer-reviewed journals.



Celso Eduardo Tuna is a mechanical engineer who graduated from the São Paulo State University (UNESP), Brazil, in 1989. He obtained a master's degree and Ph.D. in Mechanical Engineering from UNESP, where he is also an associate professor, in 1995 and 1999, respectively. Dr. Tuna is a CNPq research and productivity fellow, professor of the post-graduate course in Mechanical Engineering, and coordinator of the Bioenergy Research Institute laboratory of UNESP in Guaratinguetá. He has published six book chapters and twenty-eight indexed scientific articles. His research interests include bioenergy, hydrogen generation, renewable energy, and cogeneration.



# Contents

<b>Preface</b>	<b>XIII</b>
<b>Section 1</b> Pyrolysis	<b>1</b>
<b>Chapter 1</b> Review Chapter: Waste to Energy through Pyrolysis and Gasification in Brazil and Mexico <i>by José Antonio Mayoral Chavando, Valter Silva, Danielle Regina Da Silva Guerra, Daniela Eusébio, João Sousa Cardoso and Luís A.C. Tarelho</i>	<b>3</b>
<b>Chapter 2</b> Two-Stage Pyrolytic Conversion of Biomass <i>by Oleg Aleksandrovich Ivanin, Viktor Zaichenko Mikhailovich, Georgy Aleksandrovich Sytchev, Vladimir Aleksandrovich Sinelshchikov, Vladimir Aleksandrovich Lavrenov and Olga Mihailovna Larina</i>	<b>43</b>
<b>Chapter 3</b> Co-Pyrolysis of Biomass Solid Waste and Aquatic Plants <i>by Md. Emdadul Hoque and Fazlur Rashid</i>	<b>65</b>
<b>Section 2</b> Gasification	<b>83</b>
<b>Chapter 4</b> Chemical Carbon and Hydrogen Recycle through Waste Gasification: The Methanol Route <i>by Alessia Borgogna, Gaetano Iaquaniello, Annarita Salladini, Emanuela Agostini and Mirko Boccacci</i>	<b>85</b>
<b>Chapter 5</b> Dioxin and Furan Emissions from Gasification <i>by Seyedeh Masoumeh Safavi, Christiaan Richter and Runar Unnthorsson</i>	<b>105</b>
<b>Chapter 6</b> Solid Waste Gasification: Comparison of Single- and Multi-Staged Reactors <i>by Xianhui Zhao, Kai Li, Meghan E. Lamm, Serdar Celik, Lin Wei and Soydan Ozcan</i>	<b>123</b>

<b>Chapter 7</b>	<b>145</b>
Gasification Process Using Downdraft Fixed-Bed Gasifier for Different Feedstock <i>by Md. Emdadul Hoque and Fazlur Rashid</i>	
<b>Chapter 8</b>	<b>167</b>
Performance Assessment of the Thermodynamic Cycle in a Multi-Mode Gas Turbine Engine <i>by Viktors Gutakovskis and Vladimirs Gudakovskis</i>	
<b>Chapter 9</b>	<b>191</b>
Graphical Analysis of Gasification Processes <i>by Shehzaad Kauchali</i>	

# Preface

Gasification is the thermochemical process of converting carbonaceous material in the presence of an oxidant less than stoichiometric to form a gaseous product at a high temperature. This gas is known as synthesis gas or syngas. Depending on quality, the gas produced can have different uses, including driving internal combustion engines and gas turbines, direct burning, and synthesis of chemical components.

Gasification transforms a solid material into a gas that can be used as fuel or raw material (methane, ammonia, methanol, gasoline). Different from pyrolysis, which mainly aims to obtain solids and sometimes to obtain liquids, gasification seeks a high production of gases, fundamentally containing CO (10%–20%), H<sub>2</sub> (4%–17%), CH<sub>4</sub> (2%–5%), and N<sub>2</sub> (40%–60%). This difference in objectives characterizes the operating conditions since gasification operates at temperatures higher than those used in pyrolysis and in the presence of gasifying agents such as water vapor to force the production of H<sub>2</sub> and CO.

The main objective of gasification is the conversion of biomass into fuel gas, through its partial oxidation at elevated temperatures. Syngas is an intermediate energy source and can be used later in another conversion process to generate heat or mechanical or electrical power, adapting to systems in which solid biomass cannot be used. This fuel gas has a relatively low calorific value, around 4 to 6 MJ/Nm<sup>3</sup> (using air as a gasifying agent).

When the biomass enters a gasifier, it first heats up, causing it to dry. Once the temperature is above 400°C, pyrolysis starts, giving rise to a carbon residue (char) formed mainly by carbon and condensable gases (light and heavy hydrocarbons) and non-condensable gases (CH<sub>4</sub>, water vapor, CO, H<sub>2</sub>, CO<sub>2</sub>). When the temperature of the “char” exceeds 700°C, gasification reactions take place, which are divided into heterogeneous (gas-solid) and homogeneous (gas-gas) reactions. This “char” reacts with O<sub>2</sub>, water vapor, CO<sub>2</sub>, and H<sub>2</sub>, and the gases react with each other to produce the final gas mixture.

The result of the process is a gas, whose main constituents are CO, H<sub>2</sub>, N<sub>2</sub>, CO<sub>2</sub>, water vapor, and hydrocarbons or tar (tar). The composition of this gas varies with the characteristics of the biomass, the gasifying agent, and the process conditions. As the C, H, and O reactions for different types of biomass are very similar, the main biomass parameter that influences the gas composition is its moisture content. Thus, with higher moisture content in the biomass, more gasifying agent is needed because the water has to be heated and evaporated. A gas that comes from wet biomass contains relatively large amounts of steam, H<sub>2</sub>, and N<sub>2</sub>, compared to dry biomass. For gasification with air, the mixture obtained is a lean gas or gas with a low calorific value (4000 to 6000 kJ/Nm<sup>3</sup>) since it contains 40% to 60% N<sub>2</sub>. The addition of water in the gasifying agent is necessary when one intends to enrich the gas with H<sub>2</sub>, producing a gaseous mixture of average calorific value.

Overall, thermochemical gasification takes place inside a reactor, which is classified according to the way in which the reactions are carried out: concurrent or

countercurrent fixed bed, bubbling or circulating fluidized bed. They are also classified according to working pressure: atmospheric or pressurized (such as entrained flow gasifiers), and according to the gasifying agent, either air, oxygen, steam, hydrogen, or mixtures of these gases.

This book provides a comprehensive overview of the various gasification techniques and applications developed so far to contribute to a better understanding of this important process of obtaining a renewable fuel, essential for the development of a sustainable economy. It presents a collection of works carried out by several researchers addressing a wide range of gasification features, including operating conditions, gasifying agents, coupling with pyrolysis, syngas generation, geographical involvement in Europe and South America, and many other topics of interest.

The authors would like to thank the Coordination for the Improvement of Higher Education Personnel (CAPES) and the Portuguese Foundation for Science and Technology (FCT) for the funding provided through project number 88881.156267/2017-01 and DMAIC-AGROGAS: 02/SAICT/2018. This book is also a result of the project "Apoio à Contratação de Recursos Humanos Altamente Qualificados" (Norte-06-3559-FSE-000045), supported by Norte Portugal Regional Operational Programme (NORTE 2020), under the PORTUGAL 2020 Partnership Agreement.

**Valter Silva**

Polytechnic Institute of Portalegre,  
Portalegre, Portugal

Forestwise, Portuguese Collaborative Laboratory for Integrated Forest and Fire  
Management,  
Portugal

**Celso Eduardo Tuna**

UNESP-Sao Paulo State University (IPBEN - Bioenergy Research Institute),  
Guaratinguetá, Brazil

---

Section 1

# Pyrolysis

---





# Review Chapter: Waste to Energy through Pyrolysis and Gasification in Brazil and Mexico

*José Antonio Mayoral Chavando, Valter Silva,  
Danielle Regina Da Silva Guerra, Daniela Eusébio,  
João Sousa Cardoso and Luís A.C. Tarelho*

## Abstract

Millions of tons of forest residues, agricultural residues, and municipal solid waste are generated in Latin America (LATAM) each year. Regularly, municipal solid waste is diverted to landfills or dumpsites. Meanwhile, forest and agricultural residues end up decomposing in the open air or burnt, releasing greenhouse gases. Those residues can be transformed into a set of energy vectors and organic/chemical products through thermochemical conversion processes, such as pyrolysis and gasification. This book chapter provides information on current examples of gasification on large scale in the world, which typically operate at 700°C, atmospheric pressure, and in a fluidized bed reactor. The produced gas is used for heat and energy generation. Whereas pyrolysis at a large scale operates around 500°C, atmospheric pressure, and in an inert atmosphere, using a fluidized bed reactor. The produced combustible liquid is used for heat and energy generation. The decision of using any of these technologies will depend on the nature and availability of residues, energy carries, techno-socio-economic aspects, and the local interest. In this regard, the particular situation of Brazil and Mexico is analyzed to implement these technologies. Its implementation could reduce the utilization of fossil fuels, generate extra income for small farmers or regions, and reduce the problem derived from the accumulation of residues. However, it is concluded that it is more convenient to use decentralized gasification and pyrolysis stations than full-scale processes, which could be an intermediate step to a large-scale process. The capabilities of numerical models to describe these processes are also provided to assess the potential composition of a gas produced from some biomass species available in these countries.

**Keywords:** Gasification, Pyrolysis, biomass, MSW, RDF

## 1. Introduction

LATAM has a rising renewable energy market, where more than a quarter of its primary energy is generated from renewable sources, twice the world average [1]. Across the continent, hydropower plays a pivotal role in the energy sector. However, LATAM has also access to biomass resources, which may enable the production of bioenergy, providing the opportunity to exploit a domestic, low carbon, and

Region	Total Renewable energy		Hydropower		Wind Energy		Solar Energy		Geothermal Energy		Bioenergy	
	Cap.(MW) 2019	Prod. (GWh) 2018	Cap.(MW) 2019	Prod. (GWh) 2018	Cap. (MW) 2019	Prod. (GWh) 2018	Cap.(MW) 2019	Prod. (GWh) 2018	Cap.(MW) 2019	Prod. (GWh) 2018	Cap.(MW) 2019	Prod. (GWh) 2018
BR	141,933	495,945	109,092	388,971	15,364	48,489	2485	3987	0	0	14,992	54,498
MX	25,648	54,770	12,671	32,526	6591	12,877	4440	1363	936	5375	1010	2628
VE	16,598	25,278	16,521	25,183	71	88	5	6	0	0	0	0
CO	12,375	58,433	11,927	56,661	18	43	90	14	0	0	340	1715
AR	12,776	42,501	11,314	39,957	1609	1413	441	108	40	214	298	1846
CL	11,488	38,515	6679	23,367	1620	3588	2648	5218	0	0	502	6128
PY	8822	59,912	8810	59,211	0	0	0	0	0	0	22	701
PE	6640	33,483	5715	30,731	372	1502	326	797	0	0	186	452
EC	5279	21,224	5079	20,678	21	80	28	38	0	0	152	428
UY	3772	14,234	1538	6557	1521	4732	258	415	0	0	425	2529
BO	1036	2967	736	2612	27	59	120	127	0	0	154	169
CAM*	15,691	47,658	8147	29,160	1942	5838	2218	2625	722	3969	2663	6066
Lat	262,058	894,920	198,229	715,614	29,156	78,709	13,059	14,698	1698	9558	20,744	77,160
EU	497,267	1,052,187	156,412	379,820	191,277	377,494	132,500	128,358	916	6765	41,179	188,053
W**	2,532,866	6,586,124	1,307,994	4,267,085	622,408	1,262,914	584,842	562,033	13,909	88,408	124,026	522,552

Note: Numbers followed by the letter “o” are figures that have been obtained from official sources such as national statistical offices, government departments, regulators, and power companies. The letter “u” follows figures that have been obtained from unofficial sources, such as industry associations and news articles. The letter “e” follows figures that have been estimated by IRENA from a variety of different data sources. All figures from the IRENA questionnaire are presented without any indicator.

\*In refers to central America and the Caribbean area.

\*\*World.

**Table 1.**  
Renewable Energy in LATAM [2].

sustainable energy source, strengthening the renewable energy sector, and generating profits in rural areas. **Table 1** shows the renewable power capacity, considering the maximum net generating capacity of power plants and other installations that use renewable energy sources to produce electricity in LATAM. This information is also available for the European Union (EU), and the world to highlight where LATAM is in terms of renewable energy. It is interesting to notice Brazil's share of renewable energy production in LATAM is ~55%, from which ~78% comes from hydropower and ~10% from bioenergy. In contrast with the EU, whose hydro-power represents ~36%, and bioenergy ~18%. On the other hand, Mexico's renewable energy in LATAM share is 6%.

Renewable energy production in Brazil accounts for ~82.63% [3]. Brazil relies on hydroelectricity for 65% of its electricity, and it plans to expand the ~6% share for biomass and wind energy [4]. While renewable energy production in Mexico is around 16.92% [3]. Without a doubt, Mexico has lagged in the development of renewable energy, comparing with other LATAM countries.

Although LATAM has been a remarkable positive development in renewable energies, the energy demand is increasing at the time, similarly to the impacts of climate change derived from the overconsumption of fossil fuels. Thus, it makes

Region	Total Solid Biofuels and Renewable Waste		Renewable Municipal Solid Waste		Bagasse		Other Solid Biofuels	
	Cap. (MW) 2019	Prod. (GWh) 2018	Cap. (MW) 2019	Prod. (GWh) 2018	Cap. (MW) 2019	Prod. (GWh) 2018	Cap. (MW) 2019	Prod. (GWh) 2018
BR	14,670	53,364	0	0	11,462 o	35,435 °	3195	17,928
MX	811	2368	0	0	791 e	1770	21	598
VE	0	0	0	0	0	0	0	0
CO	336	1711	0	0	336 e	1711	0	0
AR	254	1701	0	0	56 o	351	198	1350
CL	442	6059	0	0	0	0	442	6059
PY	20	700	0	0	20 e	700	0	0
PE	175	402	0	0	175	402	0	0
EC	144	382	0	0	144 o	382 o	0	0
UY	423	2482	0	0	10 e	18	413	2464
BO	149	168	0	0	149 o	168 o	0	0
CAM*	2620	5937	6	23	2509	5599	10	315
Latam**	20,044	75,274	6	23	15,596	46,536	4279	28,714
EU	26,051	122,078	4664	22,969	155	318	21,228	98,680
W***	101,426	426,830	14,518	62,148	19,070	55,355	67,702	309,214

Note: Numbers followed by the letter "o" are figures that have been obtained from official sources such as national statistical offices, government departments, regulators, and power companies. The letter "u" follows figures that have been obtained from unofficial sources, such as industry associations and news articles. The letter "e" follows figures that have been estimated by IRENA from a variety of different data sources. All figures from the IRENA questionnaire are presented without any indicator.

<sup>o</sup>In refers to central America and the Caribbean area.

\*\*World.

\*\*\*From Martinique.

**Table 2.**  
 Solid Biofuels and Renewable Waste [2].

sense today more than ever to take advantage of LATAM's potential for producing bioenergy. **Table 2** shows the production and capacity of the different solid biofuels and renewable waste to produce bioenergy, where bagasse is the main solid biofuel source to produce bioenergy. Brazil is a key player having a 70% share of the total bioenergy production from solid biofuels and renewable waste, occupying first place in LATAM. Regarding renewable municipal waste as a source to produce bioenergy, Martinique is the only one that utilizes them. This situation can be seen as a wise and potential solution to deal with the problems that municipal solid waste (MSW) in landfills and open dumps areas bring out. Therefore, it could be produced a refuse-derived fuel (RDF) to produce bioenergy through gasification or pyrolysis as some developed countries are already doing it at a large-scale, adding value to a material that has no other valorization option and is disposed of in landfills.

Other materials that need better valorization are the biomass residues from agricultural and forestry activities (agroforestry residues) since they are sometimes burnt in the field, causing a range of health issues and significantly raise pollution levels [5]. Similar to Municipal Solid Waste (MSW), agroforestry residues can turn into alternative products. For example, briquettes and pellets made from those residues can partially replace coal in thermal power plants.

Together, RDF and agroforestry residues can be used to generate a set of energy vectors and organic products in LATAM, implementing pyrolysis and gasification at a large-scale, like some countries in the world are already doing. Those products can be used in distinct applications to partially replace fossil fuels. This strategy can add value to the solid waste management sector and the agriculture sector. In this regard, Section 2 presents how some companies in the world utilize pyrolysis and gasification on a large-scale, and Section 3 shows the feedstock availability in Brazil and Mexico, as well as a brief analysis of the current situation in bioenergy in these countries. Section 4 shows an Experimental and Numerical Analysis of two important biomasses in Brazil and Mexico (Wood and coffee husk). Section 5 analyzes the viability of these technologies in Brazil and Mexico. Finally, the conclusion will present, highlighting the main remarks.

## **2. Large-scale pyrolysis and gasification process**

Pyrolysis and gasification are thermochemical conversion processes like combustion, where biomass is broken down into smaller hydrocarbon chains by applying heat and chemical interactions. Unlike combustion that only produces heat, pyrolysis and gasification produce components that can be turned into higher-value commercial products, for example, transportation fuels, chemicals, and fertilizers [6]. Below is a brief description of each technology.

- **Combustion:** it burns biomass directly with excess oxygen at 800 to 1000°C. It generates heat to be transformed into mechanical power and produce electricity. It is already a well-known commercial technology and broadly accessible at domestic and industrial scales [7].
- **Gasification:** it transforms biomass into a combustible gas mixture throughout partial biomass oxidation. It operates normally at temperatures from 700 to 900°C [7].
- **Pyrolysis:** it is the thermal destruction of biomass in the absence of air/oxygen. Pyrolysis of biomass starts at 350 to 500°C and can go to 700 °C, producing bio-oil, gases, and char [7].

These three technologies have not only different operating conditions but also different products, as is described in **Figure 1**.

The oldest thermochemical conversion process to produce energy is certainly biomass combustion. Besides, it is the most dominant process in the thermochemical conversion field. However, pyrolysis and gasification are two promising technologies since their products can be transformed into multiple energy vectors and some chemicals. In fact, some companies already commercialize these technologies on a large-scale to produce power and heat mainly. The following section presents some of those companies and their general process to transform different kinds of biomass into power and heat.

## 2.1 Large-scale fast pyrolysis

The main objective of fast pyrolysis is to produce bio-oil, which can be utilized as a replacement for fossil fuels in energy production, and transport. Bio-oil is a complex mixture of organic fuels containing some water and a small amount of fine carbon [10]. It aims to mobilize biomass into the energy sectors (heat, power, and transport). It is more manageable to transport and handle, and more cost-effective than solid wood-based fuels or biomass, to be successfully commercialized, its characteristics should follow the ASTM D7544–09 and EN16900/2017 standards. **Table 3** presents the main physical and chemical requirements for bio-oils produced from biomass [12].

Bio-oil production on a large-scale involves multiple processes, working together to set up a functional bio-oil refinery. The heart of bio-oil production is in the fast pyrolysis process, where pre-treated biomass is converted into bio-oil. Pre-treated biomass has basically (1) appropriate particle size (<5 mm) and (2) proper moisture content (<10% w) [13]. Then it is fed into the reactor (approximately 500°C), causing the biomass to become a gas. This process occurs in nearly oxygen-free conditions to prevent combustion. The resulting gas enters a cyclone, where carbon

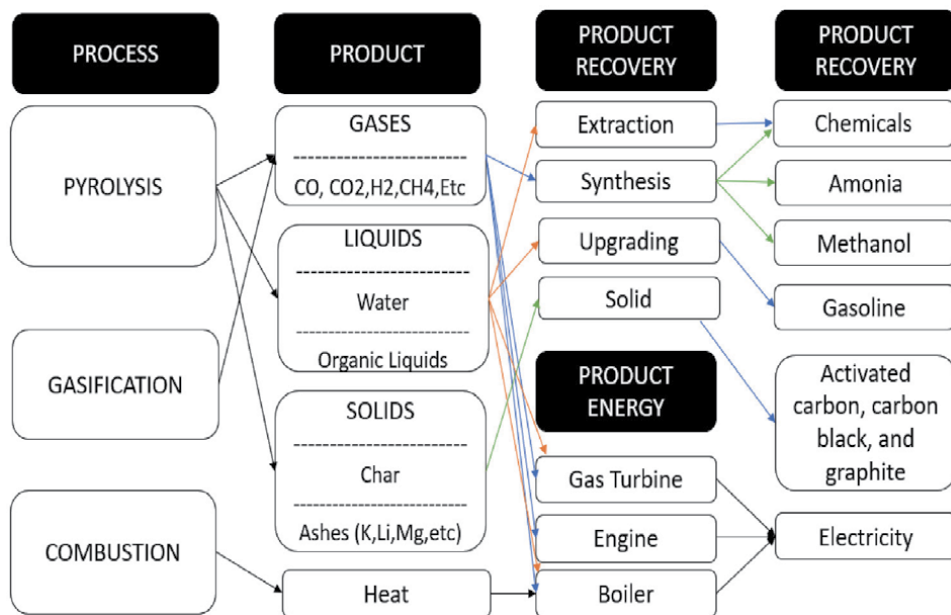


**Figure 1.**  
 Biomass thermal conversion adapted from [8, 9].

Property	Unit	Test Method	Requirement
LHV	MJ/kg	ASTM D240	15 minimums
Solid content	Mass %	ASTM D7544	2.5 maximum
Water content	Mass %	ASTM E202	30 maximums
Acidity	pH	ASTM E70	4.1
Kinematic viscosity	cSt (40 °C)	ASTM D445	125 maximums
Density	kg/dm <sup>3</sup> (20 °C)	ASTM 4052	1.1–1.3
Sulfur	Mass %	ASTM 4294	0.05
Ash content	Mass %	ASTM 482	0.25

**Table 3.**

Main physical and chemical requirements for bio-oils produced from biomass [11].

and other solids are mechanically separated from the gas flow. Then, the gas passes through a condenser system, where it cools down and condenses into bio-oil, then it is filtered. Finally, non-condensable gases are used to produce heat [13].

According to The Green Fuel Nordic company, Bio-oil can be used as a replacement for fossil fuels in the energy production, and transport sector [11]. Furthermore, bio-oil can be transformed into high value-added products like chemical compounds, food ingredients, cosmetics compounds, etc. **Table 4** presents large-scale fast pyrolysis examples in different countries, where the produced bio-oil is used to produce transport fuels, electricity, and heat or to be refined, as appropriate in each case.

A successful example of a bio-oil refinery is Green Fuel Nordic company, whose business model is based on utilizing pyrolysis technology to produce an advanced bio-oil. Then this bio-oil is commercialized and send to its customers like the Savon Voima heating plant to produce heat [16]. Another successful and profitable example is Fortum company, which is a Finnish company that invested €30 million in its bio-oil plant in Joensuu, receiving about €8 million in government investment subsidies for new technology demonstration [13]. This company signed a contract to supply bio-oil produced in Joensuu to Savon Voima, which uses bio-oil to replace the use of heavy and light fuel oil in its district heat production in Iisalmi [13]. In December 2019, Fortum signed an agreement to sell its district heating business in Joensuu Finland to Savon Voima Oyj. The contract concluded in January 2020, registering a tax-exempt capital gain of €430 million in the City Solutions segment's first-quarter 2020 results [28].

The integrated Coal handling plant (CHP) in Joensuu was constructed in 2012 and began full operation in 2015, producing heat, electricity, and 50,000 tons of bio-oil (maximum planned capacity per year). The process consists of a fluidized bed boiler that supplies heat for the pyrolysis reactor and burns the coke, biochar, and non-condensed gases produced during the pyrolysis process to produce electricity and heat (See **Figure 2**). In such a way, high efficiency can be reached for the pyrolyzed fuel production process. Additionally, when a fluidized bed boiler is integrated, pyrolysis is a cost-efficient way of producing bio-oil to replace fossil oils.

It is also interesting to notice that Brazil has already taken a leading role in LATAM with the partnership 50/50 between Ensyn and Suzano to produce 2 million gallons/year of Ensyn biocrude. The project is located at Suzano's pulp facilities at Aracruz city, in the State of Espirito Santo, Brazil. The company derivated from this partnership (NYSE: SUZ) is now the world's largest eucalyptus pulp company in America Latina [25].

Country	REF	Company/entity	Technology/Information	Product	Biomass	For Producing	Feed rate/Production	Status
SE	[14]	Pyrocell-Setra	BTG-BTL Rotating cone	Bio-oil	Sawdust	Transportation fuels	40,000d ton/year of biomass	Construction Start:2021
FI	[15, 16]	Green Fuel Nordic	BTG-BTL Rotating cone	Bio-oil	Wood	Electricity and heat	24,000 ton/y of bio-oil	Operational 2020
CA	[17]	Ensyn	Ensyn Fluid bed/riser	Biocrude	Wood	Heat & refinery	65,000d ton/y of biomass	Operational
NL	[18]	Twence / Twence / EMPYRO	BTG-BTL Rotating cone	Bio-oil	Wood	Electricity 450 GWh	-	Operational
USA	[19]	Ensyn and Renova Capita	circulating fluidized bed reactor	Bio-oil	Wood residues	To refinery	76 ML/y	To Start-up
USA	[20]	Biogas Energy	Ablative reactor	Bio-oil	Wood and agricultural residues	Intermediate fuels	500 kg /h of biomass	Operational
IE	[21]	Kerry Group PLC	RTP (Ensyn)	Biocrude	Wood residues	Food ingredients	30–40 tons/d of biomass	Operational
DE	[22]	KIT	Twin-screw mixing reactor	Biosyncrude	Wheat Straw	Intermediate fuel	500 kg/hr. of biomass	Operational
FI	[23] [24]	Fortum - Valment	Fluid bed (VTT)	Bio-oil	Wood residues	Electricity and heat	50,000 ton/y bio-oil	Operational
BZ	[25]	Ensyn, Suzano S.A	circulating fluidized	Bio-oil	Eucalyptus forest residues	—	83 ML/y	Detailed engineering underway
CH	[26]	Shanxi Yingjiliang Biomass Company	circulating fluidized bed reactor	Bio-oil	Rice Husk	—	2–6 ML	Operational
IN	[27]	MASH Energy	—	Bio-oil	Waste materials	—	—	—

*d. dry.*

**Table 4.**  
 Large-scale Fast Pyrolysis Examples.

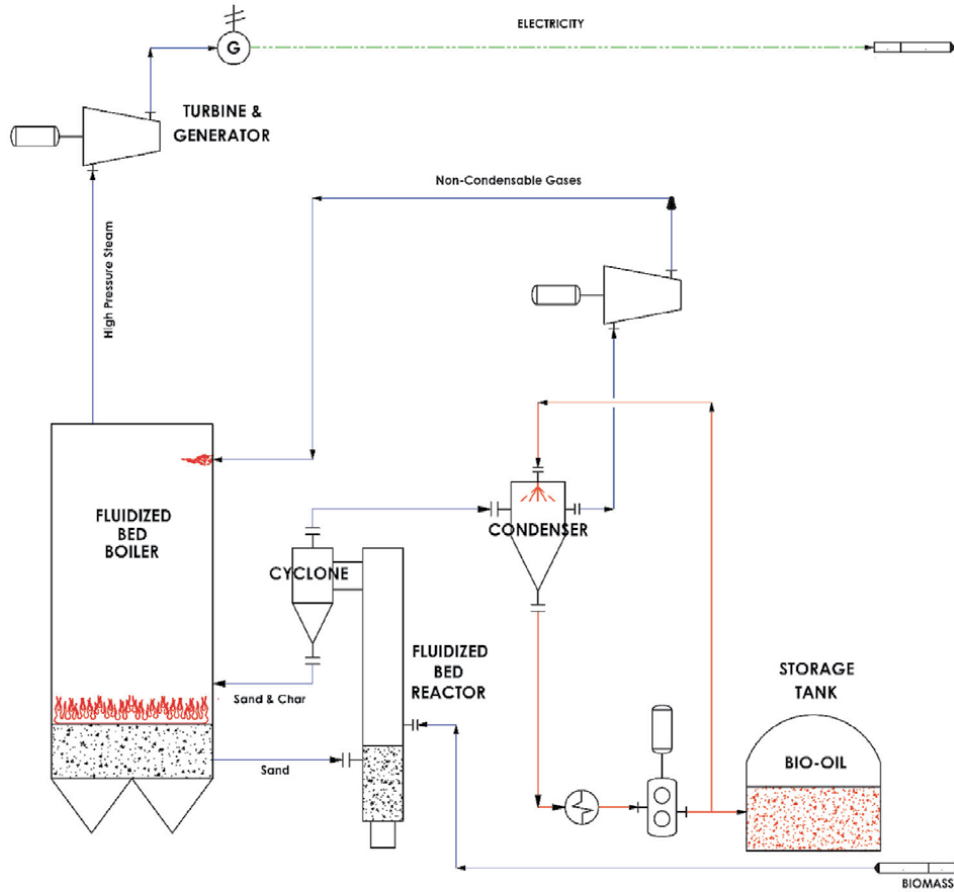
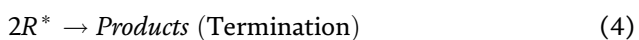
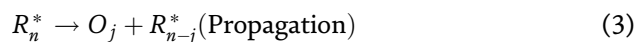
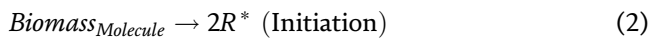
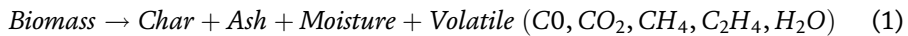


**Figure 2.** Large-Scale Fast Pyrolysis Process (Valmet) adapted from [13].

These success cases seem to support the pyrolysis of biomass as a wise way to reduce the use of fossil fuels, adding value to biomass and contributing to mitigate the impact of greenhouse gases without losing sight of profitability. Applying technologies might make sense to countries with a vast biomass availability. However, as in any process, it is necessary to evaluate the performance of the process to look for continuous improvements. The following section contains some of these performance parameters.

### 2.1.1 Pyrolysis performance

Pyrolysis is a thermochemical cracking process in which organic material is transformed into a carbon-rich solid and volatile matter (gas and liquids) by heating in the absence of oxygen as Eqs. (1)-(4) describe [29].





Eq. (1) is the general pyrolysis reaction. The other reactions represent the thermal cracking process, where  $R_n^*$  is a free radical with a chain length  $n$ .  $O_j$  is an alkene from olefins with a chain length  $j$  [29].

Pyrolysis temperature ranges from 350 to 600°C and it plays a critical role in the cracking process since, at higher temperatures, molecules move violently, which causes the breaking of shorter chains from the main C-C chain. Therefore, shorter hydrocarbon products are favored as in fast pyrolysis or gasification. While biochar is boosted under low temperatures and large residence times as in slow pyrolysis [29].

General measures of performance are often quoted as measures of how effective a given pyrolysis scheme may be. These parameters can be oriented to a mass balance and an energy balance.

### 2.1.1.1 Product yields

Some parameters can affect the product yield of pyrolysis, such as temperature, particle size, heating rate, etc. If the desired product is liquid, then producing more liquids will indicate a more effective process. While, if the desired product is solid, then producing more solids will indicate a more effective process. Eqs. (5)-(8) describe the pyrolysis yield calculations.

$$m_F = m_{solid} + m_{gas} + m_{liquid} \quad (5)$$

$$Y_{solid} = \frac{m_{solid}}{m_F} * 100 \quad (6)$$

$$Y_{gas} = \frac{m_{gas}}{m_F} * 100 \quad (7)$$

$$Y_{liquid} = \frac{m_{liquid}}{m_F} * 100 \quad (8)$$

where  $m_F$  represents the feedstock mass,  $m_{solid}$  is the solid mass,  $m_{gas}$  is the gas mass,  $m_{liquid}$  is the liquid mass,  $m_F$  is the feedstock mass,  $Y_{solid}$  is the solid yield,  $Y_{gas}$  is the gas yield, and  $Y_{liquid}$  is the liquid yield.

### 2.1.1.2 Lower heating value (LHV)

The lower heating value of the products is determined by the contribution of each of the compounds contained in a specific phase. This parameter is important because it indicates the amount of energy contained in the products. The LHV of the gas, liquid, and solid yield is calculated as the following equations describe.

$$LHV_{gas} = \frac{\sum y_{igas} * m_i * LHV_i}{m_{gas}} \quad (9)$$

$$LHV_{liquid} = \frac{\sum y_{iliquid} * m_i * LHV_i}{m_{liquid}} \quad (10)$$

$$LHV_{solid} = \frac{\sum y_{isolid} * m_i * LHV_i}{m_{solid}} \quad (11)$$

where  $y_{igas}$  is the mass fraction of the component “i” in the gas,  $y_{iliquid}$  is the mass fraction of the component “i” in the liquid,  $y_{isolid}$  is the Mass fraction of the component “i” in the solid,  $m_i$  is the mass of the component “i”,  $m_{solid}$  is the solid mass,  $m_{gas}$  is the gas mass,  $m_{liquid}$  is the liquid mass,  $LHV_i$  is the LHV of the component “i”,

$LHV_{gas}$  is the LHV of the gas,  $LHV_{liquid}$  is the LHV of the liquid and  $LHV_{solid}$  is the LHV of the solid.

## 2.2 Large-scale gasification

Similar to pyrolysis on large-scale, gasification on a large-scale involves other processes working together. The main product of gasification is combustible gas. But unlike pyrolysis, the main product is not stored and then transported to be used somewhere else but used in the same facilities where it was produced. Even so, gasification offers great benefits, namely reducing CO<sub>2</sub> emissions for replacing fossil fuels and avoiding their extraction. Another benefit is that gasification can use materials that currently have no other valorization option but to be disposed of in landfills. Waste gasification provides much better electrical efficiency compared with the direct combustion of waste [30].

A perfect successful gasification example is its integration with an existed coal-fired plant in Vaskiluodon Voima Oy, Vaasa, Finland. This integration of gasification into the coal-fired facilities had several advantages, such as the investment cost was kept to about one-third of a similar-sized new biomass plant, it was also kept the full original coal capacity, and the use of coal was cut off by 40% by using local biomasses like wood, peat, and straw [31]. The Plant generates 230 MW electricity and 170 MW district heating.

Another example is ThyssenKrupp, whose main product is syngas, which can be used in multiple processes. While its byproducts are slags, ash, and sulfur components. These byproducts can be employed in road building, cement industry, or recovered [32]. The typical gas composition is CO + H<sub>2</sub> > 85 (vol.%), CO<sub>2</sub> 2–4 (vol.%), and CH<sub>4</sub> 0.1 (vol.%) [32].

More examples of large-scale gasification in the world are provided in **Table 5**, where one can notice several examples are using materials like MSW, plastics, and solid recovered fuels (SRF). The resulting gas is being used to produce heat and electricity.

ThyssenKrupp facilities have a feed dust system, so the biomass must be smaller than 0.1 mm. Then, biomass is gasified using oxygen and steam as gasification agents. The operational temperature is higher than the ash melting temperature to remove ash as slag. While the pressure is around 40 bar. The technology has multiple, horizontally arranged burners to provide heat to the gasifier and produce steam in a drum boiler (see **Figure 3**) [32].

On the other hand, **Figure 4** presents the Valmet equipment that has a screw feeder system, so it allows biomass with higher particle size, it also has a cyclone, which separates solids from the gas. After the cyclone, the gas goes through a gas cleaning system, delivering a clean gas, which enables the production of high pressure and temperature steam for the turbine without risk of boiler corrosion. In Lahti, the electrical efficiency is over 30% (540°C and 120 bar). Furthermore, this plant operates with RDF (250,000 ton/y) and wood, producing 2 x 80 MW hot gas cleaning [50]. VASKILUODON VOIMA OY (formerly Fortum) produces 230 MW electricity and 170 MW district heating, by integrating the gasification capability with the original coal-fired plant. The biomass gasification plant contributes 140 MW and a woodchip dryer. The gas produced in the gasifier and coal enters a circulating fluidized bed boiler, where hot water is transformed into steam, that goes to high-pressure superheaters and then continues to the high-pressure turbine (HPT). From HPT, the steam returns to the boiler's preheaters and ends in the intermediate-pressure turbine (IPT). Here the steam is divided into different streams (1) district heat exchangers, (2) storage water tank to preheat it, and (3)

Country	REF	Company/ entity	Technology/ Information	Biomass	For Producing	Feed rate/ Production (ton/day)	Status
USA	[33]	Energy Products of Idaho <sup>*</sup>	Bubbling bed	—	—	1040	—
DE	[34]	HTW-Plant Berrenrath / Germany	ThyssenKrupp Fluidized-Bed	High-ash coal	methanol	25 ton/h	Shut down 1986– 1997
FI	[35]	Kemira Oy	ThyssenKrupp	Peat	NH <sub>3</sub>	30 ton/h Peat	Shut down 1988– 1991
FI	[36] [37]	NSE Biofuels Oy Ltd.	Sumitomo heavy industries ltd CFB	Wood residues	Heat 12 MWth	—	Start- up 2009
FI	[38]	Corenso United Ltd.	Sumitomo heavy industries ltd	Plastic Waste	50 MWth	—	Start- up 2000
BE	[39]	Electrabe	Sumitomo heavy industries ltd	Wood residues	Heat 50 MWth	—	Start- up 2002
JP	[40]	HTW-Precon	ThyssenKrupp	MSW	—	48 ton/day	Start- up 1999
FI	[41]	Lahti Energia Oy,	Valmet CFB	SRF	160 MW	250,000 ton/y	Start- up 2012
FI	[31]	Vaskiluodon Voima Oy	Valmet CFB	Wood, peat, and straw	230 MW electricity 170 MW heating	—	Start- up 2012
FI	[42]	RENUGAS	ANDRITZ Carbona Bubbling Fluidized Bed (BFB)	Wood pellets, or chip	—	100–150 ton/ day	Start- up 2013
SE	[43]	GoBiGas	Valmet CFB	Wood residues	20 MW	—	Start- up 2013
ID	[44]	OKI Pulp & Paper	Valmet CFB	Bark and wood residues	110 MW X2	—	Start- up 2017
USA	[45] [46]	Taylor Biomass Energy	Dual bed	MSW	—	300–400 ton/ day	2021
UK	[47] [48]	Amec Foster Wheeler	VESTA patented technology	Coal, biomass, waste	—	250,000 Nm <sup>3</sup> /h of Sin gas	—

<sup>\*</sup>It was bought by Outotec.

**Table 5.**  
 Large-Scale Gasification Examples.

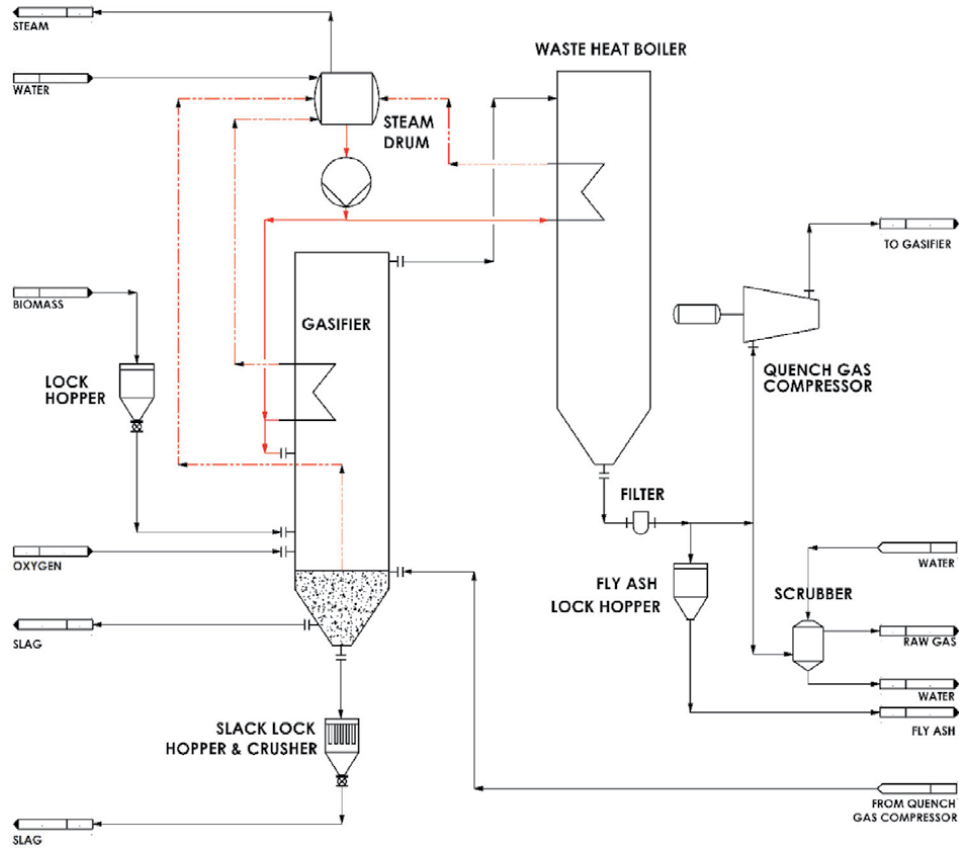


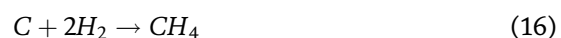
**Figure 3.** Large Scale Gasification Process (Thyssenkrupp PRENFLO), adapted from [32].

the low-pressure turbine (LPT), where steam rotates the turbine’s rotor, and a generator produces electricity for the electrical network. Finally, the gas resulting from the combustion goes to the flue-gas desulphurization, the cleaning process creates gypsum.

The gasification process is a potential solution to deal with problems linked to MSW, plastics, and other residues, producing energy vectors at the same time. This could be a massive opportunity for LATAM countries that are dealing with exorbitant amounts of waste. Similar to pyrolysis, the gasification performance can be evaluated for a continuous improvement process.

### 2.2.1 Gasification performance

Gasification is a partial oxidation process in which organic material is transformed mainly into gases through heterogeneous (Eqs. (12)-(16)) and homogeneous reactions (Eqs. (17)-(21)), as the following reactions describe.



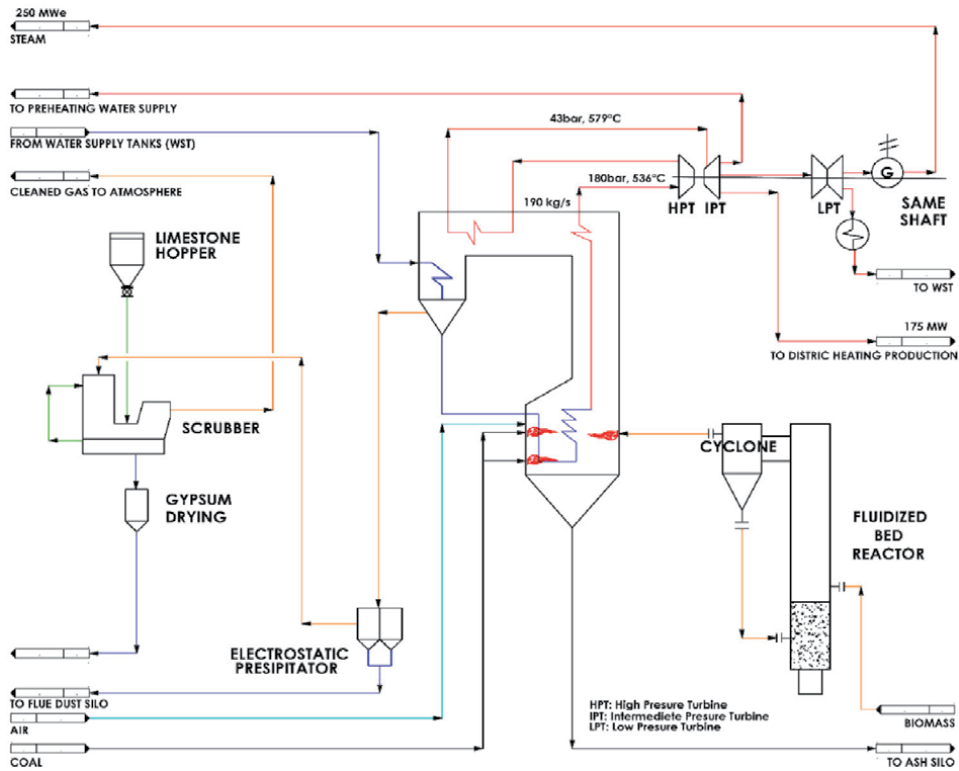
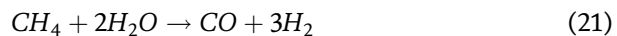
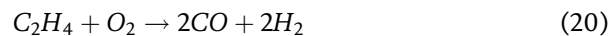
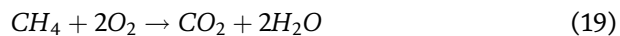


Figure 4. Pioneer of Biofuel Plants, Producer of Combined Heat and Power adapted from [49].



The temperature in the gasification ranges between 600 and 700°C and plays an important role in the product yields and gas composition [51]. Besides, the product yields and LHV of the products exist another parameter to evaluate the performance of the gasification process like Cold Gas Efficiency (CGE) and Gas Efficiency ( $Y_{gas}$ ).

#### 2.2.1.1 Cold gas efficiency (CGE)

Cold gas efficiency is the output energy by input energy [52], and it can be described mathematically with the following equation:

$$CGE = \frac{LHV_{gas} * m_{gas}}{LHV_F * m_F} * 100\% \quad (22)$$

where  $CGE$  is the cold gas efficiency,  $LHV_F$  is the lower heating value of the feed stream,  $LHV_{gas}$  is the lower heating value of the gas mixture,  $m_{gas}$  is the mass of the gas mixture, and  $m_F$  is the mass of the feed stream.

### 2.2.1.2 Gas efficiency ( $y_{gas}$ )

$Y$  gas can be also described as the ratio of the produced gas volume by the feedstock mass as the following equation expresses:

$$y_{gas} = \frac{V_{gas}}{m_F} \quad (23)$$

where  $m_F$  is the mass of the feed stream and  $V_{gas}$  the volume of the gas mixture.

## 3. Biomass availability in Brazil and Mexico and potential analysis

Biomass is a renewable organic material that serves as a sustainable source of energy to produce electricity or other forms of power. Some of the drivers to utilize it are lowering fossil-fuel utilization, decreasing greenhouse gas (GHG) emissions, and promote economic development and agricultural development. The following sections briefly describe the potential of Brazil and Mexico for bioenergy production using agroforestry residues and MSW.

### 3.1 Brazil

Brazil has an electrical matrix of predominantly renewable origin with an emphasis on the water source. Renewable sources account for 82.9% of the domestic supply of electricity in Brazil, which is the result of the sum of the amounts referring to domestic production plus imports distributed as 64.9% hydro, 8.6% wind, 8.4% biomass, and 1% solar [49]. The energy production from fossil fuels accounted for 17.1% of the national total, which 2.0% oil products, 2.5% nuclear, 9.3% natural gas, and 3.3% charcoal. This distribution represents the structure of the domestic supply of electricity in Brazil in 2019 [53].

The energy needed to move the economy of a region in a period, Internal Energy Supply in 2019, was 294 million toe (tons of oil equivalent) or Mtoe. Looking specifically the renewable sources, they increased by 2.8% in 2019 compared to 2018, that was supported by a strong increase in the production of sugarcane products with 5.5% in ethanol, adding the increase of wind, solar, and biodiesel with 4.4% [54], as shown in **Table 6**.

The choice for the energy matrix also relates to the system costs and regional conditions. For agro-industrial regions, biomass can be a viable raw material to produce clean and renewable energy, at the same time is a form to minimize the environmental impacts of agro-industrial production. In the Brazilian energy matrix, the types of biomass most used are from sugar cane and its products, firewood, black liquor, and rice husks. Considering the energy matrix in Brazil, a general view of the installed potency is shown in **Table 7**, the installed capacity of electricity generation by source in MW, and the evolution from 2015 to 2019 [53].

#### 3.1.1 Forestry residues

Brazil is a forest country with hectares (59% of its territory) of natural and planted nearly 500 million forests [55], representing the second largest forest area in the world with 502,082.1 (1000 ha) [55], only surpassed by Russia [56]. The distribution area is 57.31% in natural forests and 1.16% in planted ones [56].

Brazil has around 10 million hectares of forest plantations, mainly with species of Eucalyptus and Pinus genera, which represent 96% of the total area. Forest

Description	Production (ktoe)		Increase or retraction %	Production (%)	
	2018	2019		2018	2019
Non-renewable	157,972	158,395	0.3	54.5	53.9
Petroleum and derivatives	99,627	101,051	1.4	34.4	34.4
Natural gas	35,905	35,909	0	12.4	12.2
Mineral coal and derivatives	16,418	15,480	-5.7	5.7	5.3
Uranium (u3o8) and derivatives	4174	4174	0	1.4	1.4
Other non-renewable <sup>a</sup>	1848	1780	-3.7	0.6	0.6
Renewable	131,898	135,642	2.8	45.5	46.1
Hydraulics and electricity	36,460	36,364	-0.3	12.6	12.4
Firewood and charcoal	25,511	25,725	0.8	8.8	8.7
Sugar cane derivatives	50,090	52,841	5.5	17.3	18
Other renewables <sup>b</sup>	19,837	20,712	4.4	6.8	7
TOTAL	289,870	294,036	1.4	100	100
of which fossils	153,798	154,221	0.3	53.1	

<sup>a</sup>Blast furnace, melt shop, and sulfur gas.  
<sup>b</sup>Black liquor, biodiesel, wind, solar, rice husk, biogas, wood waste, charcoal gas, and elephant grass.

**Table 6.**  
*Internal Energy Supply (OIE) [54].*

plantations amount to 1.2% of Brazil's area, and 2.0% of the total forest areas. The composition of forest plantations in 2018 was 7,401,334 ha of Eucalyptus, 2,030,419 ha of Pinus, and 407,933 ha of other species [56] including rubber, acacia, teak, and parica.

The industrial sector of forest plantations is based on the cultivation of trees for industrial purposes, generating a variety of products numbering nearly five thousand, including lumber, pulp, paper, flooring, wood panels, and charcoal [57]. **Figure 5** presents the area of planted trees in 2019, by state and by genus (in millions) [57].

According to the Food and Agriculture Organization of the United Nations, FAO, in 2019 the generated wood residues in Brazil were 19,140,000 m<sup>3</sup> [58]. Concerning the management of industrial and forest waste, the Brazilian planted tree sector has adopted sustainable practices to dispose of various types of domestic and urban waste generated during its production processes.

As shown in **Table 8**, in 2019 most of the waste from factories and forest companies was directed toward energy generation, approximately 67%. In the second place, 12% of waste was directed to other industrial sectors for reuse as a raw material. Of the total waste generated before consumption, 7.4% was kept in the field to protect and enrich the soil, 4.2% was sent to landfills, and 3.4% was recycled [57].

### 3.1.2 Agricultural residues

Agricultural occupation in Brazil is estimated at 65.91 million hectares, equivalent to 7.8% of the national territory [59], the numbers show that Brazil uses 7.57% of its territory for crops. This area also corresponds to only 3.41% of the cultivated area worldwide.

Agroindustry waste generation in Brazil is spread off in all the country states from North to South regions, is from various crops, varies with seasonality, and

<b>Plants in operation</b>		<b>2015</b>	<b>2016</b>	<b>2017</b>	<b>2018</b>	<b>2019</b>
UHE / Hydro		86.366	91.499	94.662	98.287	102.999
PCH / Hydro		4.886	4.941	5.020	5.157	5.291
CGH / Hydro		398	484	594	695	768
EOL / Wind		7.633	10.124	12.283	14.390	15.378
SOL / Solar		21	24	935	1.798	2.473
Termo	<b>Total</b>	39.564	41.275	41.537	40.523	41.219
	<b>Biomass</b>	13.257	14.147	14.505	14.790	14.978
	Bagasse	10.573	10.979	11.158	11.368	11.438
	Others	2.684	3.168	3.347	3.422	3.540
	Biogas	84	119	135	140	186
	Elephant Grass	32	66	32	32	32
	Charcoal	51	54	43	43	48
	Rice Peels	45	45	45	45	53
	Charcoal Gas	112	115	114	128	128
	Black-Liquor	1.923	2.333	2.543	2.556	2.544
	Vegetal Oil	27	4	4	4	4
	Wood Residue	409	432	431	474	544
	<b>Fossil</b>	24.961	25.550	25.453	24.127	24.642
	Steam Coal	3.389	3.389	3.324	2.858	3.228
	Refinery Gas	316	316	316	320	320
	Natural Gas	12.428	12.965	12.980	13.359	13.385
	Fuel Oil	3.197	4.020	4.056	3.363	3.316
	Diesel Oil	5.632	4.825	4.737	4.186	4.353
	Viscous Oil		—	—	—	—
	<b>Others<sup>1</sup></b>		35	41	41	40
	Industrial Effluent	1.346	1.578	1.579	1.606	1.599
	Gaseous Effluent <sup>2</sup>	160	176	172	172	66
	Sulfur	71	71	71	71	79
	Blast Furnace Gas	216	422	422	417	512
	Process Gas	674	654	658	721	715
	Steel Gas	225	255	255	225	226
	Unknown sources			92	—	—
Nuclear		1.990	1.990	1.990	1.990	1.990
<b>Total</b>		140.858	150.338	157.112	162.840	170.118

<sup>1</sup>Includes TAR.

<sup>2</sup>Includes heat of the process (Table in MW).

**Table 7.**  
Installed Capacity of Electricity Generation by Source [53].

represents a huge amount. The availability of the main selected products from agricultural residues, animal waste, and its respective analyses as to generation potential was determined [60]. The main selected products are analyzed from the



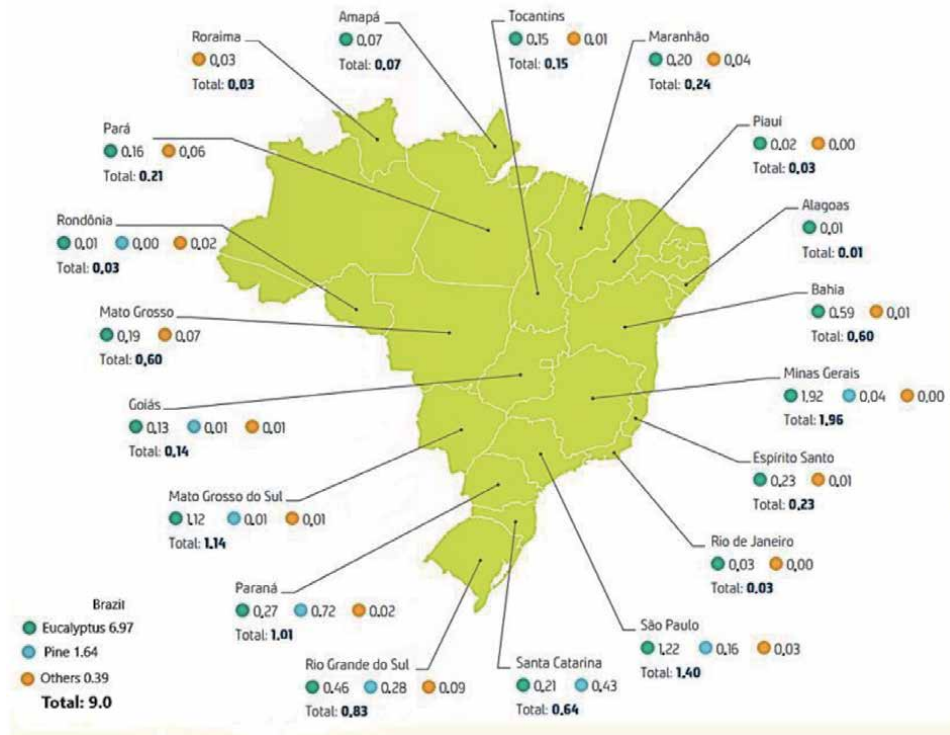


Figure 5. Area of Planted Trees in Brazil in 2019, by state and by genus (in millions) [56].

Waste generated during the production process	% of tons by type of waste, by destination	Final destination
Bark, branches, leaves, lime sludge, boiler ash, others	7.4%	kept in the fields to protect and fertilize the soil, composted
Drags and grits, sludge, ash, metal scrap, plastic, cardboard, etc.	3.4%	recycling
Bark, branches, leaves, woodchips, sawdust, black liquor	66.6%	energy generation
Sawdust, paper scraps, lime sludge, and boiler ash	0.7%	reused as raw materials by companies in the planted tree sector
Sawdust, paper scraps, lime sludge, and boiler ash	11.7%	reused as raw materials by other industrial sectors
Paper scraps, lime sludge, non-hazardous wastes, others	4.2%	sent to landfills
Bark, sawdust, sludge/filtrate from water treatment plants, knots, and rejects from fiber lines	0.7%	sold or shipped to various companies
Various types of waste already described above and other non-specified	5.3%	other destinations, including co-processing

Table 8. Solid Waste Generated by Type, According to Final Destination, in % of Total Waste [57].

point of view of Brazil's economy and about the necessary conditions for the rural producer to keep up with sustainable growth. **Table 9** presents the most common and produced agricultural residues [60].

Brazil stands out as a major biomass generator, the mass supply of biomass in 2005 was 558 million tons, with a projected growth to 1402 million tons in 2030 [53]. **Table 10** shows the evolution of mass supply per agricultural residue, agro-industrial, and forestry residues.

Biomass availability is a key aspect of bioenergy. The total bioenergy supply in 2019 was 93.9 Mtoe (1824 thousand bop/day), corresponding to 31.9% of the Brazilian energy matrix. Sugarcane products as bagasse and ethanol with 52.8 Mtoe,

Feedstock	Abbreviation	Generating potential index -GP <sup>a</sup> (tons/total residues - tons/total waste <sup>b</sup> )
Sugar cane	SC	0.22 t TR/SC
Soybean	SO	2.05 t TR/SO
Maize (corn)	MI	1.42 t TR/MI
Rice (straw)	RI	1.49 t TR/RI
Cotton (Perennial)	CO	2.95 t TR/CO
Orange - 100	OG	0.50 t TR/OG
Wheat -70	WH	1.42 t TR/WH
Cassava - 100	CA	0.20 t TR/CA
Tobacco	TO	0.75 t TR/TO

<sup>a</sup>Generating potential index GP (Tons/culture).  
<sup>b</sup>GP Index abbreviation: TR= Total Residue; TW= Total waste.

**Table 9.**  
Estimates of generating potential index (GP) for agricultural residues and animal waste in Brazil [60].

Residue	2005	2010	2015	2020	2030
Total	558	731	898	1058	1402
Agricultural Residues	478	633	768	904	1196
Soybean	185	251	302	359	482
Maize (corn)	176	251	304	361	485
Rice (straw)	57	59	62	66	69
sugar cane	60	73	100	119	160
Agro industrial waste	80	98	130	154	207
Bagasse sugar cane	58	70	97	115	154
Rice (Husk)	2	2	3	3	3
Black Liquor	13	17	21	25	34
Wood	6	8	10	12	16
Energy Forests	13	30	31	43	46
Super plus Wood	13	30	31	43	46

**Table 10.**  
Mass supply of biomass by agro-industrial agricultural waste and forestry (millions of tons) [61].

accounted for 56.3% of bioenergy and 18% of the matrix. Firewood, with 25.7 Mtoe, accounted for 27.4% of bioenergy and 8.7% of the matrix.

Other bioenergy (black liquor, biogas, wood residues, residues from agribusiness, and biodiesel), with 15.3 Mtoe, accounted for 16.3% of bioenergy and 5.2% of the matrix [49]. **Tables 11** and **12** show the energy supply and consumption by sugarcane products: sugarcane bagasse as input for electricity generation and sugarcane juice for alcohol production [50].

### 3.1.3 Municipal solid waste residues

Between 2010 and 2019, the generation of MSW in Brazil registered a considerable increase, going from 67 million to 79 million tons per year (in 2020). In Brazil, most of the collected MSW goes to disposal in landfills, having registered an increase of 10 million tons in a decade, going from 33 million tons per year to 43 million tons. On the other hand, the amount of waste that goes to inadequate units (dumps and controlled landfills) has also grown, from 25 million tons per year to just over 29 million tons per year [62].

It should be noted, in **Figure 6**, that the organic fraction remains the main component of MSW, with 45.3%. Dry recyclable waste, on the other hand, adds up to 35% being mainly composed of plastics (16.8%), paper and cardboard (10.4%), in addition to glass (2.7%), metals (2.3%), and multilayer packaging (1.4%) [58].

Flow	2015	2016	2017	2018	2019
Production	162.6	168.6	165.6	157.8	162.2
Total consumption	162.6	168.6	165.6	157.8	162.2
Transformation*	28.0	28.7	28.9	28.5	29.3
Final consumption	134.6	139.9	136.8	129.3	132.9
Final energy Consumption	134.6	139.9	136.8	129.3	132.9
Energy sector	61.8	57.5	56.0	67.1	71.1
Industrial	72.8	82.4	80.8	62.1	61.9
Chemical	0.0	0.0	0.0	0.0	0.0
Foods and beverages	72.7	82.3	80.6	62.0	61.7
Paper and pulp	128.0	141.0	146.0	157.0	147.0
Others	0.0	0.0	0.0	0.0	0.0

\*Input for alcohol production (Table in 10<sup>3</sup> ton).

**Table 11.**  
 Sugar Cane Bagasse [53].

Flow	2015	2016	2017	2018	2019
Production	209.3	183.7	179.9	243.1	260.5
Total Consumption	209.3	183.7	179.9	243.1	260.5
Transformation*	209.3	183.7	179.9	243.1	260.5

\*Input for alcohol production (Table in 10<sup>3</sup> ton).

**Table 12.**  
 Sugar Cane Juice [53].

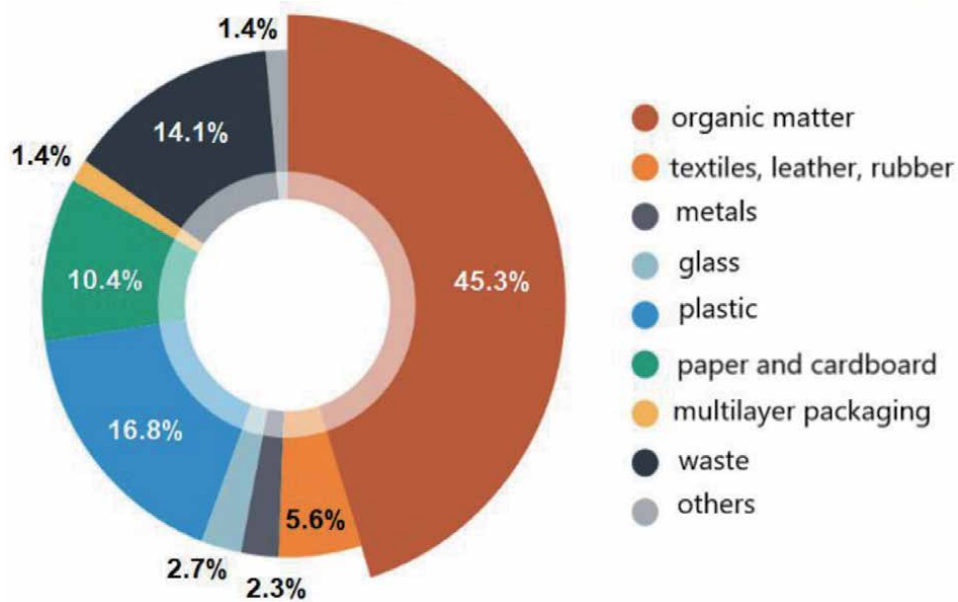


**Figure 6.**  
*Gravimetry of MSW in Brazil [62].*

The tailings, in turn, correspond to 14.1% of the total and mainly contemplate the sanitary materials. As for the other fractions, we have textile waste, leather, and rubber, with 5.6%, and other waste, also with 1.4%, which contemplate various materials theoretically reverse logistics objects [62].

The national gravimetry, in **Figure 6**, was estimated based on the weighted average of the total generation of MSW by income bracket of the municipalities and their respective gravimetry, considering the population and generation per capita.

It is possible to estimate the economic development of a country by analyzing the physical composition of its MSW. In general, the greater the income of a country the higher the consumption and, therefore, the amount of waste generated [63]. The physical compositions of MSW from towns in different regions of Brazil are shown in **Table 13** [63].

The National Solid Waste Policy (NSWP) was established by Federal Law n. 12,305 in August 2010, and it can be a milestone for waste management in Brazil [64]. The goals of this law are the reduction, reuse, recycling, treatment, and appropriate disposal of MSW, including energy recovery systems, to avoid damage to the environment and public health. This law prohibits the open dump disposal of MSW, and it is stipulated that all states and cities must have closed their open dumps by 2014. Nevertheless, the situation about MSW in Brazil has changed very little since the introduction of the NSWP [63].

### 3.1.4 Brazilian politics related to the bioenergy sector

In Brazil, the bioenergy sector is promoted by programs instituted by the federal government. In 2002 the Brazilian government launched the Incentive Program for Alternative Sources of Electric Energy (PROINFA), of the Ministry of Mines and Energy in response to the scarcity of energy in the country, in search of renewable sources [63].

As part of the incentive to biodiesel, the National Biodiesel Production and Use Program (PNPB) was launched in 2004 [65]. The PNPB's strategy is to make

Regions	North <sup>a</sup> (%)	North-east <sup>b</sup> (%)	Mid-west <sup>c</sup> (%)	South-east <sup>d</sup> (%)	South <sup>e</sup> (%)	Brazil <sup>f</sup> (%)
MSW						
Organic matter	54.68	57.00	54.02	52.00	57.27	51.4
Recyclables	27.46	10.31	29.72	41.70	26.87	31.9
Metal	1.09	1.74	3.64	1.66	1.46	2.9
Paper and cardboard	10.87	3.7	7.48	15.39	11.62	13.1
Plastic	14.67	3.86	16.73	21.15	11.23	13.5
Glass	0.83	1.01	1.87	3.50	2.56	2.4
Others	17.86	32.69	16.26	6.30	15.86	16.7
Total	100	100	100	100	100	100

<sup>a</sup>Prefeitura Municipal de Araguaína (2013).  
<sup>b</sup>Contrato Prefeitura Municipal de Cubatí (2013).  
<sup>c</sup>Prefeitura de Paranaíba (2014).  
<sup>d</sup>Prefeitura da Cidade do Rio de Janeiro (2015).  
<sup>e</sup>Prefeitura de Porto Alegre (2013).  
<sup>f</sup>Ministério do Meio Ambiente (2012).

**Table 13.**  
 Physical composition of MSW from towns in different regions of Brazil [63].

feasible the production and use of biodiesel in the country, with a focus on competitiveness, the quality of the biofuel produced, the guarantee of security of its supply, the diversification of raw materials, the social inclusion of family farmers and in strengthening the regional potential for the production of raw materials [66].

RenovaBio is the new National Biofuel Policy, instituted by Law 13,576/ 2017 [67], whose objective is to expand the production of biofuels in Brazil, based on predictability, environmental, economic, and social sustainability, and compatible with the growth of the market. Based on this expansion, the aim is to make an important contribution by biofuels in reducing greenhouse gas emissions in the country. The program will seek its performance based on four strategic axes: discussing the role of biofuels in the energy matrix; development based on environmental, economic, and financial sustainability; marketing rules and attention to new biofuels [68].

Regarding MSW and its destination to the bioenergy sector, in 2020, an association of four important sectorial entities - ABCP (portland cement), Abetre (waste and effluent treatment), Abiogás (production and use of biogas), and Abrelpe (public cleaning) - launched the FBRER (Brazil Front for Energy Recovery of Waste), which aims to boost energy capture from waste deposited in landfills. The signing of the Cooperation Agreement for Energy Recovery of Waste was signed by the entities and the Ministry of the Environment of the federal government [69].

The cooperation agreement will seek to coordinate efforts to remove regulatory barriers that hinder the more intense use of waste. Besides, it intends to make feasible projects for the energy recovery of solid waste and promote its integration into the clean and renewable energy market [69].

### 3.1.5 Limitations for implementing pyrolysis and gasification of biomass in Brazil

In Brazil, one of the challenges faced by biomass gasification projects is that the facilities are constructed and operated in the laboratory, and on a small scale, it was not possible managed to show viability on a large scale. The lack of

gasification plants in operation leads to the unreliability of the business, which alienates investors.

Another factor observed is the comparison between the technologies used to reduce MSW. Considering gasification, pyrolysis, and incineration, it is observed that for the gasification process, solid waste generally needs to have humidity lower than 30%, an average granulometry of 50 mm, and an average calorific value of 3500 kcal/kg [70], the solid waste must be prepared as fuels derived from municipal waste. Such treatment of waste to transform it into a good fuel requires an increase in the costs of production.

Likewise, in the pyrolysis process, waste also needs to be pre-treated. This pre-treatment raises the costs of the MSW energy plant. The pyrolysis process produces gases, oils, and solid waste (metals, oxides, and inert material), which need to be of high quality to identify markets for their absorption. Given these characteristics of gasification and pyrolysis process, energy reuse projects for solid waste end up using incineration technology.

There are several challenges for Brazil to achieve high levels of sustainability in the management of MSW as waste to energy through gasification or pyrolysis technologies. The biggest of these is related to the sale of energy that will be generated by plants using MSW, as it is the largest revenue of this enterprise since this market is not yet regulated.

### **3.2 México**

In contrast with Brazil, around 88.70% of the energy production in Mexico comes from fossil fuels, 3.17% charcoal, 1.16% Nuclear, and 6.97% renewable (3.79% biomass, 1.62% geothermal, hydropower 1.42%, solar and wind 0.14%). Regarding energy contribution to power generation, 78% comes from fossil fuels, 2.8% nuclear, biomass 9.30%, hydropower 3.70%, and 6% from others. As one may infer, energy production in Mexico relies mostly on fossil fuels [71]. Therefore, the potential of other resources such as biomass is not being exploited, preventing the strengthening of the agricultural sector and the reduction of GHG.

Mexico occupies 3rd place in LATAM and the Caribbean in terms of cropland area, after Brazil and Argentina. The cultivated area in 2007 was 21.7 million ha, producing 270 million tons. The residuals from these crops are currently used for animal feed and bedding, mulch, and burning to produce energy and compost. In fact, in 2012 bioenergy has an operational capacity of 645 MW installed, of which 598 MW are from bagasse and the rest from biogas. However, in 2019, it is registered that Mexico increased its capacity of bagasse to 791 MW, which means 32% more, or a 4.28% increase per year [71]. Although the production of energy from biomass has increased, the full potential is not being exploited. The following section presents the biomass availability in Mexico.

#### *3.2.1 Forestry residues*

Mexico has 138 million hectares of forest, equivalent to 70% of the national territory. The forests and jungles are an important part of these lands and cover 64.9 million hectares, of which it is estimated that 15 million hectares have the potential for commercial use. The available forest biomass is distributed in different areas of the country. However, the greatest potential is in the mountain ranges of and the Yucatan peninsula [72].

Forest biomass contributes 8% of primary energy demand, being used in residential firewood and small industries. However, it can be considered as an alternative source for renewable energy generation and provide multiple benefits [72].

Forest management, extraction, and industrialization activities generate a significant amount of residual forest biomass annually. Some studies have been carried out on the use of forest residues in the production of bioenergy, and the results indicate that Mexico generates around 703,323.6 (1,774,994.0 m<sup>3</sup>r, cubic meters of unbarked round timber) tons of dry base biomass, which come from forest residues of mainly pine, and oak. [72].

According to the production of forest biomass, 598,858.1 tons correspond to pine and 104,465.5 tons to oak. In terms of energy, this forest biomass represents a renewable energy resource of 12,827.8 TJ of which 11,425.4 TJ corresponds to pine and 1402.4 TJ to oak. [72]. In Mexico, the main industry supply forest basins have been identified (**Figure 7**), where a remarkable amount of sawmill waste is concentrated, which can be used as feedstock for integrated energy generation systems (thermal and electrical) [72]. The fact of integrating forest residues into energy generation is an opportunity for community forest companies, ejidos, and communities, to generate income that comes from forest biomass that is now used for waste or that has a minimal economic recovery.

### 3.2.2 Agricultural residues

Several studies have pointed out and assessed the potential of biomass energy production in Mexico, considering three main categories: wood & forestry residues, crop, and agro residues, and MSW [72]. Some estimates range from 3035 to 4550 PJ/y, where wood forestry residues share is 27–54%, crop and agro residues 26, and 0.6% from MSW. Other estimates more conservative said 626 PJ/y and 2228 PJ/y.

**Table 14** shows the main agricultural residues produced in Mexico, which considers the residue index (RI) of each crop. Maize primary residue has a 44% share of the main crop residues producing in Mexico. While sorghum primary

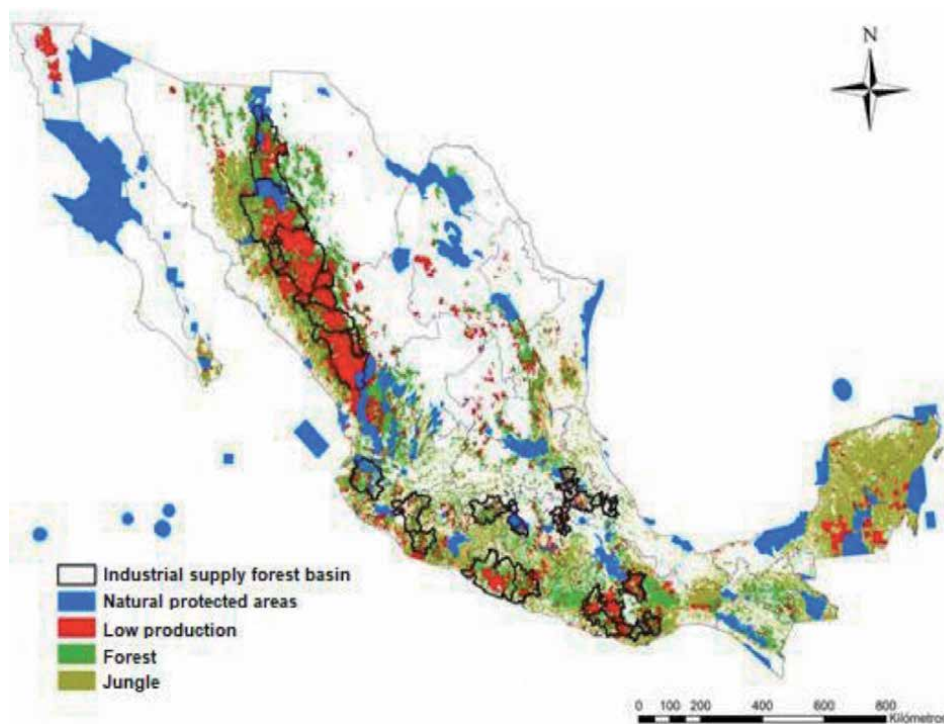


**Figure 7.**  
Main Industrial supply forest basin in Mexico adapted from [72].

Crop Information			Primary Residue					Secondary Residue							
Crop	Crop Production (kt/yr)	C.V. (%)	Residues Energy Potential (PJ/yr)	Residue Index	Production (kt/y)	Available Material* (kt/y)	HHV (MJ/kg)	Energy Potential (PJ/y)	Residue	Residue Index	Recovery Factor	Production (kt/yr)	Available Material* (kt/yr)	HHV (MJ/kg)	Energy Potential (PJ/yr)
Sugarcane	53,834.44	7.10	124.19	0.14	7536.82	3014.73	17.31	52.18	Bagasse	0.14	0.50	7536.82	3768.41	19.11	72.01
					Tops & leaves										
Maize	23,740.53	12.97	278.92	1.41	33,474.15	13,389.66	17.18	230.03	Cob	0.15	0.80	3561.08	2848.86	17.16	48.89
Sorghum	6127.56	17.85	174.93	3.90	23,897.48	9558.99	18.30	174.93	—	—	—	—	—	—	—
					Staw/stalk										
Wheat	3622.61	9.64	45.45	1.62	5868.63	2347.45	19.36	45.45	—	—	—	—	—	—	—
Coffee	1186.38	—	2.04	—	—	—	—	—	Pulp	0.10	0.90	118.64	106.77	19.10	2.04
Coffee	1186.38	—	0.84	—	—	—	—	—	Hull	0.04	0.90	47.46	42.71	19.59	0.84
Beans	1079.82	17.62	7.12	0.88	950.24	380.10	18.74	7.12	—	—	—	—	—	—	—
Barley	776.21	25.44	10.70	1.75	1358.37	543.35	18.45	10.02	Husk	0.10	0.50	77.62	38.81	17.50	0.68
Cotton	631.66	23.37	5.66	1.28	808.52	323.41	17.50	5.66	—	—	—	—	—	—	—
Soybean	268.04	49.09	3.01	1.60	428.86	171.55	17.52	3.01	—	—	—	—	—	—	—
Rice	233.53	14.43	2.67	1.61	375.98	150.39	15.37	2.31	Husk	0.20	0.50	46.71	23.35	15.36	0.36
Chickpea	159.22	32.86	1.96	1.70	270.67	108.27	18.10	1.96	—	—	—	—	—	—	—
Safflower	120.56	42.24	2.11	2.28	274.88	109.95	19.23	2.11	—	—	—	—	—	—	—
Oat	96.73	29.36	1.70	2.52	243.76	97.50	17.48	1.70	—	—	—	—	—	—	—
Groundnut	92.91	12.39	1.92	2.12	196.97	78.79	19.01	1.50	Shells	0.30	0.80	27.87	22.30	18.73	0.42
Sesame	45.10	21.29	1.20	3.80	171.38	68.55	17.47	1.20	—	—	—	—	—	—	—
Fava bean	27.72	30.69	0.26	1.43	39.64	15.86	16.31	0.26	—	—	—	—	—	—	—
Tobacco	12.97	25.64	0.48	5.00	64.85	25.94	18.52	0.48	—	—	—	—	—	—	—
Lentil	6.18	46.71	0.09	2.10	12.98	5.19	17.08	0.09	—	—	—	—	—	—	—



Crop Information			Primary Residue					Secondary Residue					
Crop	Crop Production (kt/yr)	C.V. (%)	Residues Energy Potential (PJ/yr)	Residue Index	Production (kt/y)	Available Material* (kt/y)	HHV (MJ/kg)	Energy Potential (PJ/y)	Residue Index	Production (kt/yr)	Available Material* (kt/yr)	HHV (MJ/kg)	Energy Potential (PJ/yr)
Sunflower	7.83	6.68	0.16	—	23.49	9.40	17.50	0.16	—	—	—	—	—
Agave (tequila)	1369.95	23.52	3.98	Leaves	273.99	109.60	17.50	1.92	Bagasse	164.39	131.52	16.35	2.15
Agave (mescal)	279.59	26.71	0.88	Leaves	55.92	22.37	18.84	0.42	Bagasse	33.55	26.84	16.09	0.43
Total	94,905.9		670.34					542.53					127.81

\* Recovery factor 0.4.

**Table 14.**  
 Agricultural Residues in Mexico [73].

residue is 31%. As forestry residues, the use of agro residues is an opportunity for agro communities and industries to generate income by a better valorization of residues.

### 3.2.3 Municipal solid waste residues

In Mexico, 102,895.00 tons of waste are generated daily, from which 83.93% are collected and 78.54% are disposed of in landfills or open-air dumps, recycling only 9.63% of the waste generated. That translates into an economic loss by diverting materials that are susceptible to rejoining the production system, reducing the demand and exploitation of new resources, unlike countries like Switzerland, the Netherlands, Germany, Belgium, Sweden, Austria, and Denmark, where the final disposal of waste is less than 5% in sanitary landfills [74].

Article 10 from the Mexican General Law for the Prevention and Comprehensive Management of Waste (LGPGIR) establishes municipalities oversee the integral management of MSW, which consists of the collection, transfer, treatment, and final disposal [75].

Municipalities encounter challenges that fall outside their technical and financial capacities due to the lack of trained personnel in acquiring or committing financial resources that give certainty to private sector investments. This situation is maybe because of the short time of the municipal administrations, which leads to the breaking of the learning curve, and therefore to a lack of continuity in actions and projects that guarantee integral management of urban solid waste [74]. Whatever the case, the reality is that MSW has become a big problem in Mexico, especially in big cities like Mexico City.

Mexico has 2203 areas (landfills or open-air dumps) for final MSW disposal. **Figure 8** shows the average composition of MSW in Mexico.

Food and garden waste and disposable diapers have a share of 48.98% of the total MSW in Mexico. While other MSW fractions like paper, paperboard, rags, and plastics represent around 25% of the total MSW in Mexico. Those fractions can be

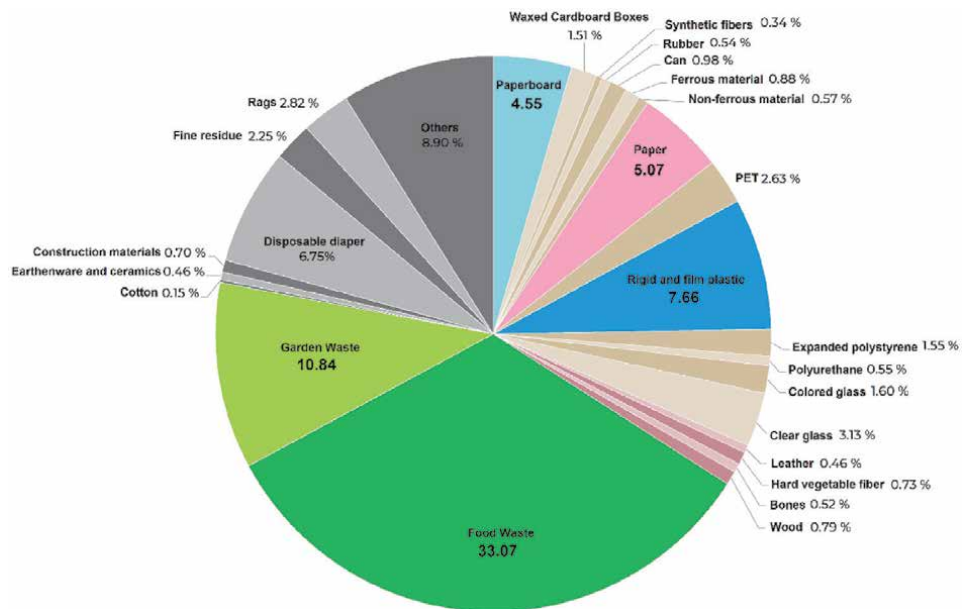


**Figure 8.** Mexican MSW Composition 2017 adapted from [76].

utilized to produce a refuse-derived fuel, which can be used as feedstock for gasification or pyrolysis processes, generating energy vectors and adding value to materials that did not have any other purpose than to be disposed of.

### *3.2.4 Mexican politics related to the bioenergy sector*

The law for the promotion and development of bioenergetics published in 2008 aims to promote and develop bioenergetics to contribute to energy diversification and sustainable development as conditions that allow guaranteeing the development of the agricultural sector [77].

Another law that is related to the bioenergy sector is the Mexican General Law on Climate Change published in 2012 and modified in 2018, which sets the rights and responsibilities of state governments to climate change mitigation and adaptation. Since then, state governments have made progress in developing specific policy instruments, provided in both the Law and the National Climate Change Strategy. However, little clarity regarding the current level of progress of these state efforts exists at the national level. In this sense, seventeen policy instruments (laws, regulations, plans, programs, among others) of the 32 states of Mexico were set [78]. Four of them are related to MSW management, which is potential biomass to produce bioenergy.

### *3.2.5 Limitations for implementing pyrolysis and gasification of biomass in Mexico*

Even though Mexico has a high potential for Renewable Energy Sources (RES) development, only a small amount of this energy has been utilized. This may be due to the following reasons:

- The lack of an energy plan that evaluates the RES feasibility in short term.
- Consume the cheapest energy source, usually fossil fuels, rather than sustainable and eco-friendly resources. This situation is preventing RES development.
- Complex supply-chains and vulnerable to fossil carbon inputs mainly associated with feedstock transport.
- Higher abatement CO<sub>2</sub> costs compared to actions in other sectors. For liquid biofuels, the estimated cost ranges from 7 to 12 US\$/tCO<sub>2</sub>e, while for biogas and upgraded wastewater treatment plants the cost is around 60 US\$/tCO<sub>2</sub>e.

Whether forestry agricultural residues or municipal solid waste, it exists a great potential to produce energy vectors in Mexico. However, socio-political factors have delayed their use. To overcome such limitations is vital to have a national plan for renewable energy in Mexico by the explicit establishment of RES participation, considering financial schemes that help small renewable energy producers as it was established in the law for the promotion and development of bioenergetics published in 2008. Another noteworthy point is the palletization of agroforestry residues or MSW to produce fuel pellets, also known as RDF, which is a more uniform fuel than MSW regarding particle size and heating value, and it is easy to transport.

Another important factor is to know beforehand the composition and yields of each technology's products, considering the available feedstocks in each country. Unfortunately, this would require major investments to produce experiential data.

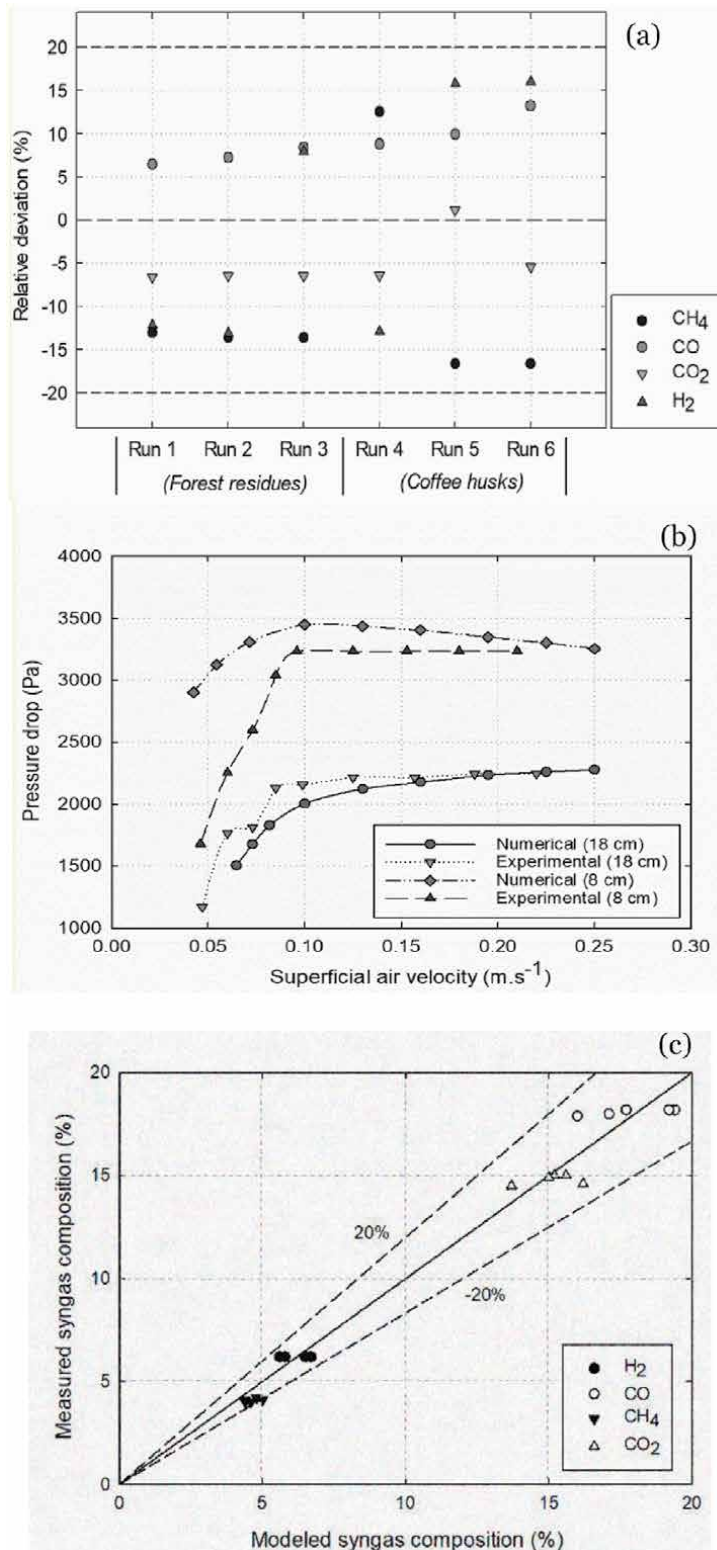


**Figure 9.** (a) Relative deviation between the experimental and numerical syngas composition produced in the 250 kWth gasifier using forest residues and coffee husks (b) Experimental and numerical fluidization curves gathered at 8 and 18 cm height from the 75 kWth reactors (c) Model gas composition of wood (adapted from [83, 84]).

Knowing this information can help decision-makers to decide which agroforestry residue is a priority, the type of technology to employ, and the use of the products. Fortunately, mathematical models of these technologies can help predict with certainty this information. The following chapter describes a mathematical model used for the gasification of wood residues, an important residue in Brazil and Mexico.

#### 4. Experimental and numerical analysis

Mathematical models reduce efforts, investments, and time, promoting a better perception of the physical and chemical mechanisms immerse in complex technologies like pyrolysis and gasification [79]. Modeling approaches can be as complex as the available software allows. However, the approach can also be simple, effective, and with an excellent degree of certainty. For example, equilibrium models are reliable and uncomplex [79]. Nevertheless, they do not deal with essential parameters such as hydrodynamics, transport process, or reaction kinetics. In contrast with kinetic models that consider reactions' kinetic, being much more accurate but computationally expensive [80].

Fortunately, the growth of computational power is leading to better software that is gradually replacing empirical or semi-empirical models for computational fluid dynamics. These models can provide relevant information on what is happening inside the reactor, which can lead to a better understanding of the technology as well as improvements in it. However, their extreme complexity means that these models are still in the development stage [81, 82].

Gasification and pyrolysis processes involve multiple phases, which makes them very complex. **Figure 9** summarize the validation of a model applied to two fluidized bed reactors with 250 kWth and the other 75 kWth, both operated by our research team. The relative deviation between the experimental and numerical syngas composition produced in the 250 kWth gasifier using forest residues and coffee husks is depicted in **Figure 9a**.

**Figure 9b** displays the deviation between the experimental and the numerical fluidization curves performed at two different bed heights (8 and 18 cm) in the 75 kWth reactors. Overall, the numerical curves successfully forecasted the slope of the experimental curve with acceptable precision. The broader deviations arose at the lowest velocities. This is due to the movement of the solid before fluidization occurred. It can be also due to the inefficiency of the mathematical model since it considers a low entropy.

The mathematical model effectively predicted the acquired experimental data trends with acceptable accuracy for both equipment at different validation points and experimental conditions. It is worth acknowledging that this model has already been extensively validated and submitted to constant improvements in dealing with different biomass substrates and the heterogeneity of MSW at distinct operating conditions, gasifying agents, and reactor scales. In this example, the gas composition of wood gasification could contain an excellent number of combustible gases, namely H<sub>2</sub>, CO, CH<sub>4</sub>, and CO<sub>2</sub> (see **Figure 9c**), which can be used to produce energy or heat in Brazil and Mexico.

#### 5. Feasibility

As it was discussed in Section 2, gasification and pyrolysis are already at full-scale, mostly in developed countries [85]. However, small-scale energy systems

demonstrated to be more advantageous and cost-effective to install in certain regions since this model offers mobility and simplicity [86].

These models can provide energy to decentralized areas or rural households communities, particularly in developing countries like Brazil and Mexico, delivering alternative electric power solutions to communities where connection to the central grid is economically unfeasible. Furthermore, blending biomass residues with other wastes, such as MSW (RDF included), is praised as a clever strategy to lessen exploration costs, boost plant production efficiency, and avoid biomass exploration excess and consequent disequilibrium of ecosystems [87]. In fact, small-scale biomass gasification systems became attractive for off-grid functions due to their cost-effectiveness and high plant load factor.

Biomass-based systems afford an important asset particularly in rural areas since agricultural and timber residues are easily accessible. Furthermore, biomass exploration affords a helping hand towards wildfire hazards reduction, promoting forest biomass harvesting and cleaning in overgrown areas [88]. These units have already proved their suitability for power generation in small towns, being already widely used for rural electrification solutions. In fact, small towns require low electrical load demand. Thus, biomass gasification systems are more cost-competitive than solar PV or even grid electrification for rural areas that are off-grid [89].

These factors could point to the feasibility of energy production through biomass in Brazil and Mexico because of their large amounts of biomass and regions that are not connected to the grid. Besides, the used small stations could be the step towards large-scale production using, for example, MSW, which has become a big problem in large cities such as Brasilia and Mexico City.

The feasibility of financial indicators is resolved by measuring their flexibility and assessing the project performance response to stressful scenarios, appointing either a favorable or unfavorable evolution of several variables simultaneously, where some variables may be more uncertain than others. Some of the variables that can affect the feasibility of a gasification or pyrolysis project are: (1) the initial investment, (2) the return of investment, (3) future costs and benefits, (4) electricity sales price (5) electricity production, (6) biomass cost, (7) governmental policies, etc. In short, sensitivity analysis allows assessing the project's risk by simulating several scenarios and forecasting their outcomes, assessing decision-making over uncertainty [90]. The World Bank Group has released a set of typical key financial benchmarks for success in biomass related energy projects, considering some financial indicators, namely Net Present Value (NPV) ought to be a positive value, International Rate of Return (IRR) above 10%, and a Payback Period (PBP) less than 10 years [91]. Some of these financial indicators might provide an idea of the benchmarks in the biomass to the energy sector. However, these financial indicators or models may not encompass all factors that can influence the success of a project. Some of these factors are the policy of a set country and its project-specific constraints. Yet, to the point, benchmarks allow standardizing decision-making by building trust within investors less willing to take risks.

## **6. Conclusions**

Latin American countries have one of the highest rates of urbanization in the world. Among the various problems caused by large urbanization, those that refer to mobility, safety, health, well-being, sanitation, and adequate management of MSW stand out. It is important to highlight that a waste energy recovery plant (WTE) is not exactly an energy generation undertaking, but essentially a sanitation agent whose energy input is a valuable by-product. This context is essential to

demonstrate to the authorities the nature and essentiality of WTE plants, especially in terms of cost and benefit, when compared to other sources of power generation. Biomass and MSW have the potential to become a major source in LATAM's primary energy sector, as presented in Section 3, with a survey of the availability of biomass and MSW found in Brazil and Mexico.

Implementing gasification and pyrolysis in these countries can offer benefits in terms of reducing the use of fossil fuels, reducing greenhouse gas emissions by preventing the extraction of virgin fossil fuels, and providing income diversification to farmers. However, the integration of these energy vectors on large scale should pass for a previous step, which is decentralized gasification and pyrolysis plants as was analyzed in the feasibility section. This is because many rural areas are not connected to the grid yet, in addition, the logistics of biomass is complicated in rural areas and involves an extra cost.

There is still a long way to go. However, the major urgency relies on real policy integration that enables a full converge of the different bioenergy actors. Therefore, catalyze the economic and environmental benefits that pyrolysis and gasification of biomass can provide.

## **Acknowledgements**

The authors would also like to express their gratitude to the Fundação para a Ciência e a Tecnologia (FCT) for the grant SFRH/BD/146155/2019, and the projects IF/01772/2014, FCT/CAPES 2018/2019, DMAIC-AGROGAS: 02/SAICT/2018. This work is also a result of the project "Apoio à Contratação de Recursos Humanos Altamente Qualificados" (Norte-06-3559-FSE-000045), supported by Norte Portugal Regional Operational Programme (NORTE 2020), under the PORTUGAL 2020 Partnership Agreement.

## **Conflict of interest**

The authors declare that they have no known competing financial interests or personal relationships that could have appeared to influence the work reported in this chapter.

## **Nomenclature**

BR	Brazil
MX	Mexico
VE	Venezuela
CO	Colombia
AR	Argentina
CL	Chile
PY	Paraguay
PE	Peru
EC	Ecuador
UY	Uruguay
BO	Bolivia
CAM*	Central America
Lat	Latin America
EU	European Union

W**	World
SE	Sweden
FI	Finland
CA	Canada
NL	Netherlands
USA	The United States
IE	Ireland
DE	Germany
CH	Switzerland
IN	India
LATAM	Latin America
CHP	Coal handling plant
EU	European Union
GHG	greenhouse gas
MSW	municipal solid waste
RDF	refuse-derived fuel
RES	Renewable Energy Sources
CGE	cold gas efficiency
$LHV_F$	lower heating value of the feed stream
$LHV_{gas}$	LHV of the gas
$LHV_i$	LHV of the component “i”
$LHV_{liquid}$	LHV of the liquid
$LHV_{solid}$	LHV of the solid
$m_F$	feedstock mass
$m_{gas}$	gas mass
$m_i$	mass of the component “i”
$m_{liquid}$	liquid mass
$m_{solid}$	solid mass
$y_{igas}$	mass fraction of the component “i” in the gas
$y_{iliquid}$	mass fraction of the component “i” in the liquid
$y_{isolid}$	mass fraction of the component “i” in the solid
$Y_{gas}$	gas yield
$y_{gas}$	gas Efficiency
$Y_{liquid}$	liquid yield
$Y_{solid}$	solid yield
$V_G$	Gas Volume



## Author details

José Antonio Mayoral Chavando<sup>1</sup>, Valter Silva<sup>1,2\*</sup>, Danielle Regina Da Silva Guerra<sup>3</sup>, Daniela Eusébio<sup>1</sup>, João Sousa Cardoso<sup>1,4</sup> and Luís A.C. Tarelho<sup>5</sup>

1 Polytechnic Institute of Portalegre, Portalegre, Portugal

2 ForestWise, Collaborative Laboratory for Integrated Forest and Fire Management, Vila Real, Portugal

3 Federal University of Pará, Belém, Pará, Brazil


4 Instituto Superior Técnico, Universidade de Lisboa, Lisboa, Portugal

5 Centre for Environmental and Marine Studies (CESAM), Department of Environment and Planning, University of Aveiro, Aveiro, Portugal

\*Address all correspondence to: [valter.silva@ipportalegre.pt](mailto:valter.silva@ipportalegre.pt);  
[valter.silva@forestwise.pt](mailto:valter.silva@forestwise.pt)

## IntechOpen

---

© 2021 The Author(s). Licensee IntechOpen. This chapter is distributed under the terms of the Creative Commons Attribution License (<http://creativecommons.org/licenses/by/3.0/>), which permits unrestricted use, distribution, and reproduction in any medium, provided the original work is properly cited. 

## References

- [1] IRENA, “Plan De Acción Regional: Acelerando El Despliegue De Energía Renovable En América Latina,” 2019. Accessed: Dec. 08, 2020. [Online]. Available: [https://www.irena.org/-/media/Files/IRENA/Agency/Regional-Group/Latin-America-and-the-Caribbean/IRENA\\_LatAm\\_plan\\_de\\_accion\\_2019\\_ES.PDF?la=en&hash=5DE35BAFD5941A43F110B7E6F0B88B5B5FC26C5D](https://www.irena.org/-/media/Files/IRENA/Agency/Regional-Group/Latin-America-and-the-Caribbean/IRENA_LatAm_plan_de_accion_2019_ES.PDF?la=en&hash=5DE35BAFD5941A43F110B7E6F0B88B5B5FC26C5D).
- [2] IRENA, *Renewable Energy Statistics 2020*. 2020.
- [3] OurWorldinData, “Share of electricity production from renewables, 2019,” 2020. <https://ourworldindata.org/grapher/share-electricity-renewables> (accessed Dec. 19, 2020).
- [4] EPE, “Plano Decenal de Expansão de Energia 2026,” 2020. <https://www.epe.gov.br/pt/publicacoes-dados-abertos/publicacoes/Plano-Decenal-de-Expansao-de-Energia-2026> (accessed Dec. 19, 2020).
- [5] T. Liu, L. J. Mickley, S. Singh, M. Jain, R. S. DeFries, and M. E. Marlier, “Crop residue burning practices across north India inferred from household survey data: Bridging gaps in satellite observations,” *Atmos. Environ. X*, vol. 8, p. 100091, Dec. 2020, doi: 10.1016/j.aea.2020.100091.
- [6] Y. H. Chan *et al.*, “An overview of biomass thermochemical conversion technologies in Malaysia,” *Sci. Total Environ.*, vol. 680, pp. 105–123, Aug. 2019, doi: 10.1016/j.scitotenv.2019.04.211.
- [7] W. Y. Chen, T. Suzuki, and M. Lackner, *Handbook of climate change mitigation and adaptation, second edition*, vol. 1–4. Springer International Publishing, 2016.
- [8] A. V. Bridgwater, “Catalysis in thermal biomass conversion,” *Appl. Catal. A, Gen.*, vol. 116, no. 1–2, pp. 5–47, Sep. 1994, doi: 10.1016/0926-860X(94)80278-5.
- [9] I. Y. Mohammed, Y. A. Abakr, and R. Mokaya, “Integrated biomass thermochemical conversion for clean energy production: Process design and economic analysis,” *J. Environ. Chem. Eng.*, vol. 7, no. 3, Jun. 2019, doi: 10.1016/j.jece.2019.103093.
- [10] H. Chen, “Lignocellulose biorefinery product engineering,” in *Lignocellulose Biorefinery Engineering*, Elsevier, 2015, pp. 125–165.
- [11] Green Fuel Nordic Oy, “Products,” 2020. <https://www.greenfuelnordic.fi/en/products> (accessed Dec. 13, 2020).
- [12] Green Fuel Nordic Oy, “Our Production Technologies,” 2020. <https://www.greenfuelnordic.fi/en/articles/our-production-technologies> (accessed Dec. 13, 2020).
- [13] IRENA, VTT, and MEAE, *Bioenergy from Finnish Forests*. 2018.
- [14] btgbioliquids, “Pyrocell - BTG Bioliquids,” 2020. <https://www.btg-bioliquids.com/plant/pyrocell-gavle-sweden/> (accessed Dec. 07, 2020).
- [15] Green Fuel Nordic Oy, “Green Fuel Nordic Oy,” 2020. <https://greenfuelnordic.fi/en/company> (accessed Dec. 07, 2020).
- [16] Green Fuel Nordic Oy, “Lieksa refinery begins bio-oil deliveries to customers,” Dec. 04, 2020. <https://greenfuelnordic.fi/en/articles/lieksa-refinery-begins-bio-oil-deliveries-customers> (accessed Dec. 07, 2020).
- [17] ENSYN, “CÔTE NORD - Port-Cartier, Quebec - Biocrude Expansion,” 2020. <http://www.ensyn>.

com/quebec.html (accessed Dec. 07, 2020).

[18] Twence, “BTG-BTL hands over Empyro to Twence,” Dec. 2018. <https://www.twence.nl/en/twence/news/2018/BTG-BTL-hands-over-Empyro-to-Twence.html> (accessed Dec. 07, 2020).

[19] ENSYN, “Georgia Project,” 2020. <http://www.ensyn.com/georgia.html> (accessed Dec. 07, 2020).

[20] D. Meier, C. Eusterbrock, and B. Gannon, “Ablative fast pyrolysis of biomass: A new demonstration project in California, USA,” *Pyroliq 2019 Pyrolysis Liq. Biomass Wastes*, Jun. 2019, Accessed: Dec. 07, 2020. [Online]. Available: [https://dc.engconfintl.org/pyroliq\\_2019/32](https://dc.engconfintl.org/pyroliq_2019/32).

[21] ENSYN, “Licensed Production - Ensyn - Renewable Fuels and Chemicals from Non-Food Biomass.,” 2020. <http://www.ensyn.com/licensed-production.html> (accessed Dec. 07, 2020).

[22] KIT, “bioliq - Flash Pyrolysis,” 2018. <https://www.bioliq.de/english/64.php> (accessed Dec. 07, 2020).

[23] S. Wijeyekoon, K. Torr, H. Corkran, and P. Bennett, “Commercial status of direct thermochemical liquefaction technologies,” Aug. 2020.

[24] VALMET, “Bio-oil,” 2015. <https://www.valmet.com/more-industries/bio/bio-oil/> (accessed Dec. 07, 2020).

[25] ENSYN, “Aracruz Project,” 2020. <http://www.ensyn.com/brazil.html> (accessed Dec. 07, 2020).

[26] W. Cai and R. Liu, “Performance of a commercial-scale biomass fast pyrolysis plant for bio-oil production,” *Fuel*, vol. 182, pp. 677–686, Oct. 2016, doi: 10.1016/j.fuel.2016.06.030.

[27] MASH Energy, “Turning unused resources into value.” <https://www.ma>

sh-energy.com/ (accessed Dec. 07, 2020).

[28] Fortum, “Fortum concludes the sale of its district heating business in Joensuu, Finland ,” Jan. 10, 2020. <https://www.fortum.com/media/2020/01/fortum-concludes-sale-its-district-heating-business-joensuu-finland> (accessed Dec. 21, 2020).

[29] F. Gao, “Pyrolysis of Waste Plastics into Fuels,” University of Canterbury, 2010.

[30] VALMET, “Valmet Gasifier for biomass and waste,” 2020. <https://www.valmet.com/energyproduction/gasification/> (accessed Dec. 07, 2020).

[31] VALMET, “Fuel conversion for power boilers: Vaskiluodon Voima Oy, Vaasa, Finland,” 2012. <https://www.valmet.com/media/articles/all-articles/fuel-conversion-for-power-boilers-vaskiluodon-voima-oy-vaasa-finland/> (accessed Dec. 07, 2020).

[32] Thyssenkrupp, “Uhde entrained-flow gasification,” 2020. Accessed: Dec. 14, 2020. [Online]. Available: [https://ucpcdn.thyssenkrupp.com/\\_binary/UCPthyssenkruppBAIS/en/products-and-services/chemical-plants-and-processes/gasification/link-TK\\_20\\_0770\\_uhde\\_Gasification\\_Broschuere\\_SCREEN.pdf](https://ucpcdn.thyssenkrupp.com/_binary/UCPthyssenkruppBAIS/en/products-and-services/chemical-plants-and-processes/gasification/link-TK_20_0770_uhde_Gasification_Broschuere_SCREEN.pdf).

[33] “Outotec Advanced Staged Gasifier,” 2020. <https://www.outotec.com/products-and-services/technologies/energy-production/advanced-staged-gasifier/> (accessed Dec. 07, 2020).

[34] N. P. Cheremisinoff and M. B. Haddadin, “Refining Operations and the Sources of Pollution,” in *Beyond Compliance*, Elsevier, 2006, pp. 1–77.

[35] C. Marsico, “ThyssenKrupp Uhde’s commercially proven PRENFLO® and HTW TM Gasification Technologies,” 2013. Accessed: Dec. 07, 2020. [Online]. Available: <http://ibi-wachstumskern.de/>

tl/tl\_files/PDF/symposium-2013/Marsic o.pdf.

[36] Sumitomo Heavy Industries, “Biomass Gasifiers,” 2020. <https://www.shi-fw.com/clean-energy-solutions/biomass-gasifiers/> (accessed Dec. 07, 2020).

[37] L. Sumitomo Heavy Industries, “NSE Biofuels Oy Ltd.” [https://www.shi-fw.com/all\\_projects/nse-biofuels-oy-ltd/](https://www.shi-fw.com/all_projects/nse-biofuels-oy-ltd/) (accessed Dec. 07, 2020).

[38] E. Kurkela, “Review of Finnish biomass gasification technologies,” 2002. [https://www.researchgate.net/publication/30482338\\_Review\\_of\\_Finnish\\_biomass\\_gasification\\_technologies](https://www.researchgate.net/publication/30482338_Review_of_Finnish_biomass_gasification_technologies) (accessed Dec. 07, 2020).

[39] Sumitomo, “High-value gasification solutions The power of sustainable energy solutions.”

[40] M. Dobrin, “Production of Biofuels using thyssenkrupp Gasification Technologies,” 2016. Accessed: Dec. 07, 2020. [Online]. Available: <https://missionenergy.org/Gasification2016/presentation/thyssenkrupp.pdf>.

[41] VALMET, “Highest electrical efficiency from waste: Lahti Energia, Lahti Finland,” 2012. <https://www.valmet.com/media/articles/all-articles/highest-electrical-efficiency-from-waste-lahti-energia-lahti-finland/> (accessed Dec. 07, 2020).

[42] RENUGAS, “RENUGAS ,” 1993. <https://www.gti.energy/renugas/> (accessed Dec. 07, 2020).

[43] VALMET, “Valmet-supplied gasification plant inaugurated at Göteborg Energi’s GoBiGas in Sweden,” 2014. <https://www.valmet.com/energyproduction/gasification/valmet-supplied-gasification-plant-inaugurated-at-goteborg-energis-gobigas-in-sweden/> (accessed Dec. 07, 2020).

[44] VALMET, “Biomass gasification eliminates fossil fuels in the pulp mill,” 2017. <https://www.valmet.com/energyproduction/gasification/biomass-gasification-eliminates-fossil-fuels-in-the-pulp-mill/> (accessed Dec. 07, 2020).

[45] Taylor Biomass Energy, “The Montgomery Project,” 2019. [http://www.taylorbiomassenergy.com/taylorbiomass04\\_mont\\_mn.html](http://www.taylorbiomassenergy.com/taylorbiomass04_mont_mn.html) (accessed Dec. 07, 2020).

[46] E. Voegelé, “Taylor Biomass Energy project receives RES approval in New York |,” Jan. 29, 2019. <http://biomassmagazine.com/articles/15912/taylor-biomass-energy-project-receives-res-approval-in-new-york> (accessed Dec. 07, 2020).

[47] Amec Foster Wheeler, “Amec Foster Wheeler,” 2020. <https://www.woodplc.com/investors/amec-foster-wheeler> (accessed Dec. 07, 2020).

[48] Amec Foster Wheeler, “VESTA methanation,” 2020. <https://www.woodplc.com/capabilities/consulting/technology-and-process-equipment/vesta-methanation> (accessed Dec. 07, 2020).

[49] Vaskiluodon Voima, “Pioneer of Biofuel Plants, Producer of Combined Heat and Power,” 2020.

[50] VALMET, “Turning Waste to Energy Efficiently,” 2020. <https://valmetsecure.force.com/solutionfinderweb/FilePreview?id=06958000001COcNAAW> (accessed Dec. 14, 2020).

[51] J. Fuchs, J. C. Schmid, S. Müller, A. M. Mauerhofer, F. Benedikt, and H. Hofbauer, “The impact of gasification temperature on the process characteristics of sorption enhanced reforming of biomass,” *Biomass Convers. Biorefinery*, vol. 10, no. 4, pp. 925–936, Dec. 2020, doi: 10.1007/s13399-019-00439-9.

- [52] P. Ponangrong and A. Chinsuwan, "An investigation of performance of a horizontal agitator gasification reactor," in *Energy Procedia*, Jan. 2019, vol. 157, pp. 683–690, doi: 10.1016/j.egypro.2018.11.234.
- [53] EPE and Ministerio de Minas e Energia, "Balanço Energético Nacional," 2020. Accessed: Jan. 05, 2021. [Online]. Available: [https://www.epe.gov.br/sites-pt/publicacoes-dados-abertos/publicacoes/PublicacoesArquivos/publicacao-479/topico-528/BEN2020\\_sp.pdf](https://www.epe.gov.br/sites-pt/publicacoes-dados-abertos/publicacoes/PublicacoesArquivos/publicacao-479/topico-528/BEN2020_sp.pdf).
- [54] Ministério de Minas E Energia, "Resenha Energética Brasileira 2020," May 2020. Accessed: Jan. 05, 2021. [Online]. Available: [www.mme.gov.br/Publica](http://www.mme.gov.br/Publica).
- [55] FAO, "FAO Country Profiles: Brazil," 2016. <http://www.fao.org/countryprofiles/index/en/?iso3=BRA> (accessed Jan. 05, 2021).
- [56] Ministry of Agriculture. and Livestock and Food Supply., "BRAZILIAN FORESTS at a glance 2019," 2019. Accessed: Jan. 10, 2021. [Online]. Available: <http://www.floresta.l.gov.br/documentos/publicacoes/4262-brazilian-forests-at-a-glance-2019/file>.
- [57] Indústria Brasileira de árvores, "Relatório 2019 Indústria Brasileira de árvores," 2019. <https://iba.org/datafiles/publicacoes/relatorios/iba-relatorioanua12019.pdf> (accessed Jan. 10, 2021).
- [58] FAOSTAT, "FAOSTAT: Forestry Production and Trade," 2019. <http://www.fao.org/faostat/en/#data/FO> (accessed Jan. 10, 2021).
- [59] Revista Globo Rural, "Nasa aponta que Brasil usa 7,6% do seu território com lavouras," Dec. 29, 2017. <https://revistagloborural.globo.com/Noticias/Agricultura/noticia/2017/12/nasa-aponta-que-brasil-usa-76-do-seu-territorio-com-lavouras.html> (accessed Jan. 05, 2021).
- [60] T. Forster-Carneiro, M. D. Berni, I. L. Dorileo, and M. A. Rostagno, "Biorefinery study of availability of agriculture residues and wastes for integrated biorefineries in Brazil," *Resour. Conserv. Recycl.*, vol. 77, pp. 78–88, Aug. 2013, doi: 10.1016/j.resconrec.2013.05.007.
- [61] S. L. de Moraes, C. P. Massola, E. M. Saccoccio, D. P. da Silva, and Y. B. T. Guimarães, "Cenário brasileiro da geração e uso de biomassa adensada," *Rev. IPT/Tecnol. e Inovação*, vol. 1, no. 4, pp. 58–73, 2017.
- [62] Abrelpe, "Panorama dos Resíduos Sólidos no Brasil," 2020. <https://abrelpe.org.br/panorama/> (accessed Jan. 10, 2021).
- [63] R. G. de S. M. Alfaia, A. M. Costa, and J. C. Campos, "Municipal solid waste in Brazil: A review," *Waste Management and Research*, vol. 35, no. 12. SAGE Publications Ltd, pp. 1195–1209, Dec. 01, 2017, doi: 10.1177/0734242X17735375.
- [64] Institui a Política Nacional de Resíduos Sólidos, "LEI N° 12.305," Aug. 02, 2010. [http://www.planalto.gov.br/ccivil\\_03/\\_ato2007-2010/2010/lei/l12305.htm](http://www.planalto.gov.br/ccivil_03/_ato2007-2010/2010/lei/l12305.htm) (accessed Jan. 28, 2021).
- [65] C. Nunes De Castro, "O Programa Nacional De Produção E Uso Do Biodiesel (Pnpb) E A Produção De Matéria-Prima De Óleo Vegetal No Norte E No Nordeste," 2011. Accessed: Jan. 28, 2021. [Online]. Available: [https://www.ipea.gov.br/portal/images/stories/PDFs/TDs/td\\_1613.pdf](https://www.ipea.gov.br/portal/images/stories/PDFs/TDs/td_1613.pdf).
- [66] Minist'erio da Agricultura Pecuária e Abastecimento., "Programa Nacional de Produção e Uso do Biodiesel (PNPB)," 2020. <https://www.gov.br/agricultura/pt-br/assuntos/agricultura-familiar/biodiesel/programa-nacional->

de-producao-e-uso-do-biodiesel-pnpb (accessed Jan. 10, 2021).

[67] Ubrabio, “Política Nacional de Biocombustíveis (RenovaBio) - Lei nº 13.576/2017,” 2017. <https://ubrabio.com.br/2017/12/26/lei-no-13-576-2017/> (accessed Jan. 28, 2021).

[68] RenovaBio.org, “RenovaBio.org,” 2020. <https://www.renovabio.org/> (accessed Jan. 10, 2021).

[69] ABCP, “Frente Brasil de Recuperação Energética de Resíduos,” 2020. <https://abcp.org.br/imprensa/criada-a-fbrer-frente-brasil-de-recuperacao-energetica-de-residuos/> (accessed Jan. 10, 2021).

[70] ABEGÁS, “WEG aposta na gaseificação do lixo para geração,” 2020. <https://www.abegas.org.br/arquivos/74019> (accessed Jan. 10, 2021).

[71] E. J. F. Dallemand, J. A. Hilbert, and F. Monforti, *Bioenergy and Latin America: A Multi-Country Perspective*. 2015.

[72] PRONADEN, “Programa Nacional de Dendroenergía,” 2018. Accessed: Dec. 17, 2020. [Online]. Available: [https://www.gob.mx/cms/uploads/attachment/file/281088/Programa\\_Nacional\\_de\\_Dendroenergia\\_2016-2018.pdf](https://www.gob.mx/cms/uploads/attachment/file/281088/Programa_Nacional_de_Dendroenergia_2016-2018.pdf).

[73] J. A. Honorato-Salazar and J. Sadhukhan, “Annual biomass variation of agriculture crops and forestry residues, and seasonality of crop residues for energy production in Mexico,” *Food Bioprod. Process.*, vol. 119, pp. 1–19, Jan. 2020, doi: 10.1016/j.fbp.2019.10.005.

[74] SEMARNAT, “Residuos Sólidos Urbanos (RSU),” 2020. <https://www.gob.mx/semarnat/acciones-y-programas/residuos-solidos-urbanos-rsu> (accessed Dec. 18, 2020).

[75] SEMARNAT, “Prevención y gestión integral de los residuos.” <https://www.gob.mx/semarnat/acciones-y-programas/prevencion-y-gestion-integral-de-los-residuos> (accessed Jan. 25, 2021).

[gob.mx/semarnat/acciones-y-programas/prevencion-y-gestion-integral-de-los-residuos](https://www.gob.mx/semarnat/acciones-y-programas/prevencion-y-gestion-integral-de-los-residuos) (accessed Jan. 25, 2021).

[76] DBGIR, “Diagnóstico Básico para la Gestión Integral de los Residuos,” May 2020. Accessed: Dec. 26, 2020. [Online]. Available: <https://www.gob.mx/cms/uploads/attachment/file/554385/DBGIR-15-mayo-2020.pdf>.

[77] Camara de diputados Mexico, “Ley de promoción y desarrollo de los bioenergéticos,” Feb. 2008. Accessed: Dec. 27, 2020. [Online]. Available: <http://www.diputados.gob.mx/LeyesBiblio/pdf/LPDB.pdf>.

[78] INECC, “Análisis de la incorporación de la política climática en instrumentos de planeación estatales | Instituto Nacional de Ecología y Cambio Climático,” 2020. <https://www.gob.mx/inecc/documentos/analisis-de-la-vinculacion-de-instrumentos-normativos-de-planeacion-y-programaticos-de-temas-estrategicos-con-la-politica-nacional-de-cambi> (accessed Dec. 27, 2020).

[79] T. K. Patra and P. N. Sheth, “Biomass gasification models for downdraft gasifier: A state-of-the-art review,” *Renewable and Sustainable Energy Reviews*, vol. 50. Elsevier Ltd, pp. 583–593, May 30, 2015, doi: 10.1016/j.rser.2015.05.012.

[80] C. Loha, S. Gu, J. De Wilde, P. Mahanta, and P. K. Chatterjee, “Advances in mathematical modeling of fluidized bed gasification,” *Renewable and Sustainable Energy Reviews*, vol. 40. Elsevier Ltd, pp. 688–715, 2014, doi: 10.1016/j.rser.2014.07.199.

[81] R. I. Singh, A. Brink, and M. Hupa, “CFD modeling to study fluidized bed combustion and gasification,” *Applied Thermal Engineering*, vol. 52, no. 2. Elsevier Ltd, pp. 585–614, 2013, doi: 10.1016/j.applthermaleng.2012.12.017.

- [82] V. Silva *et al.*, “Multi-stage optimization in a pilot scale gasification plant,” *Int. J. Hydrogen Energy*, vol. 42, no. 37, pp. 23878–23890, 2017, doi: 10.1016/j.ijhydene.2017.04.261.
- [83] V. B. R. E. Silva and J. Cardoso, “Overview of biomass gasification modeling: Detailed analysis and case study,” in *Computational Fluid Dynamics Applied to Waste-To-energy-processes*, Elsevier, 2020, pp. 123–149.
- [84] V. Silva *et al.*, “Multi-stage optimization in a pilot scale gasification plant,” *Int. J. Hydrogen Energy*, vol. 42, no. 37, pp. 23878–23890, Sep. 2017, doi: 10.1016/j.ijhydene.2017.04.261.
- [85] P. Bajpai, “Biomass energy projects worldwide,” in *Biomass to Energy Conversion Technologies*, Elsevier, 2020, pp. 175–188.
- [86] R. L. Fosgitt, “Small-scale Gasification for Biomass and Waste-to-Energy for Military and Commercial CHP Applications,” 2015.
- [87] S. Ciuta, D. Tsiamis, and M. J. Castaldi, “Field scale developments,” in *Gasification of Waste Materials: Technologies for Generating Energy, Gas, and Chemicals from Municipal Solid Waste, Biomass, Nonrecycled Plastics, Sludges, and Wet Solid Wastes*, Elsevier, 2017, pp. 65–91.
- [88] J. Cardoso, V. Silva, and D. Eusébio, “Techno-economic analysis of a biomass gasification power plant dealing with forestry residues blends for electricity production in Portugal,” *J. Clean. Prod.*, vol. 212, pp. 741–753, Mar. 2019, doi: 10.1016/j.jclepro.2018.12.054.
- [89] S. Mahapatra and S. Dasappa, “Rural electrification: Optimising the choice between decentralised renewable energy sources and grid extension,” *Energy Sustain. Dev.*, vol. 16, no. 2, pp. 146–154, Jun. 2012, doi: 10.1016/j.esd.2012.01.006.
- [90] J. A. Ramirez and T. J. Rainey, “Comparative techno-economic analysis of biofuel production through gasification, thermal liquefaction and pyrolysis of sugarcane bagasse,” *J. Clean. Prod.*, vol. 229, pp. 513–527, Aug. 2019, doi: 10.1016/j.jclepro.2019.05.017.
- [91] I. F. Corporation, “Converting Biomass to Energy A Guide for Developers and Investors,” Washington, DC, 2017. Accessed: Apr. 22, 2021. [Online]. Available: <https://openknowledge.worldbank.org/handle/10986/28305>.





# Two-Stage Pyrolytic Conversion of Biomass

*Oleg Aleksandrovich Ivanin, Viktor Zaichenko Mikhailovich,  
Georgy Aleksandrovich Sytchev,  
Vladimir Aleksandrovich Sinelshchikov,  
Vladimir Aleksandrovich Lavrenov and  
Olga Mihailovna Larina*

## Abstract

The widespread adoption of biomass as an energy fuel is hindered by a number of its significant drawbacks, such as low heating value, low ash melting point, low bulk density etc. Technological solutions that allow to fully overcome these shortcomings and ensure high economic performance have not yet been proposed, although there is a significant demand for them. A new technology for thermal processing of biomass into gas fuel, based on the pyrolysis process, has been developed at the Joint Institute for High Temperatures of the Russian Academy of Sciences (JIHT RAS). The degree of energy conversion of the processed raw materials in the proposed technology is about 75%. The gas fuel yield is  $\sim 1.3 \text{ m}^3/\text{kg}$  of biomass, and its heating value, on average, is  $11 \text{ MJ}/\text{m}^3$ . The content of the liquid phase in the energy gas obtained by the developed technology is not more than  $50 \text{ mg}/\text{m}^3$ . The gas produced by the technology under consideration on average consists of 90% hydrogen and carbon monoxide. According to existing standards, this gas can be used as a fuel for mini-CHP with gas-piston engines. A promising direction for using this gas is the production of liquid motor fuels.

**Keywords:** synthesis gas, pyrolysis, biomass processing, two-stage thermal conversion process, liquid fuel, biochar

## 1. Introduction

The development of distributed generation and the gradual decline in the share of traditional hydrocarbon energy sources in the global energy balance are sustainable trends of the 21st century. The decision to gradually refuse fossil fuels made by world's leading economies is caused by depletion of deposits cheap in the exploitation. The desire to reduce the environmental burden and to improve the energy security through the use of local energy resources also matters. Biomass has a number of advantages over other types of renewable energy resources as an alternative to fossil hydrocarbons (availability, all-seasonality), which is directly reflected in its contribution to energy production: 12.4% of world consumption in 2017 [1]. However, biomass also has a number of obvious disadvantages: low specific heating value, high hygroscopicity, low bulk density. Some types of

biomass are characterized by a low ash melting point, which makes it difficult for direct combustion in industrial plants. In addition, one of the most economically efficient way of converting thermal energy from solid biomass combustion into electrical energy for power plants with a capacity of less than 2 MW is the use of turbine CHP operating according to the Rankine cycle using a low-boiling coolant (ORC) and having an electrical efficiency of no more than 18% [2]. All these disadvantages can be largely overcome by converting biomass into liquid or gaseous fuels [3, 4]. Gasification is one of the most efficient and commercially viable methods of such processing used in industry today [5, 6]. At the same time, syngas obtained in air-blown gasifier is, firstly, strongly ballasted with nitrogen, which leads to a significant decrease in its higher heating value (4–6 MJ/m<sup>3</sup>), and secondly, it contains a significant amount of high molecular weight organic compounds (the so-called “tar”) [7]. With oxygen or steam gasification, which makes it possible to increase the heating value of the resulting gas mixture, an air separation unit or a steam generator must be provided in the technological chain, which leads to a significant increase in the cost of the final product. As concerned tar there are rather severe restrictions on its content in the gas mixtures receiving by biomass gasification and using as gaseous fuel. Presence of tar leads to fouling process equipments such as internal combustion engines and turbines. Various methods of tar removal are used both directly at the gasification stage and at the stage of purification of the resulting gas mixtures [8, 9]. The need for gas cleaning and its high cost are among the obstacles to the widespread introduction of gasification technologies.

A two-stage pyrolytic conversion is proposed as a method for producing pure mid-calorific synthesis gas. Two-stage pyrolytic conversion is a process that combines pyrolysis and subsequent high-temperature heterogeneous cracking of volatiles on biomass coke (**Figure 1**). As a result of this conversion, a high efficiency of energy conversion of raw materials (more than 70%) is achieved in comparison with conventional pyrolysis and gasification. In addition, a sufficiently high heating value of the resulting gas is provided (11–12 MJ/m<sup>3</sup>) due to a decrease in the proportion of non-combustible components (for example, nitrogen, which is an integral component of the gas mixture obtained during air gasification).

The idea of using heterogeneous cracking as an additional stage in the processing of biomass into gaseous fuel in order to reduce the tar content was expressed in [10] and, later, was developed and used in the works of the Joint Institute for High Temperatures RAS (JIHT RAS) [11, 12] in relation to processing of wood, peat and straw. Similar approach was also implemented in the Viking gasifier developed at the Danish Technical University [13]. The proposed technology of two-stage pyrolytic conversion differs from the process implemented by “Viking” due to the absence of an oxidant supply to the reactor, which allows achieving the maximum heating value of the obtained synthesis gas. In the works of JIHT RAS, which will be discussed below, the process of converting biomass into gas was completely allothermal – the heat necessary for its implementation came from outside.

This chapter provides an overview of the results obtained in laboratory conditions for justification of the new technology conversion of biomass into synthesis gas and a description and characteristics of a pilot plant implementing the technology under consideration. The chapter has been designed so that the reader can get a comprehensive understanding of the two-stage pyrolytic conversion process, its effectiveness, features of practical realization and possible applications:

- Section 2 explains the nature of the process and contains recommendations regarding the selection of the main operating parameters noted in **Figure 1**.
- Section 3 contains characteristics of synthesis gas obtained by the method of two-stage pyrolytic conversion from 6 different types of biomass, as well as

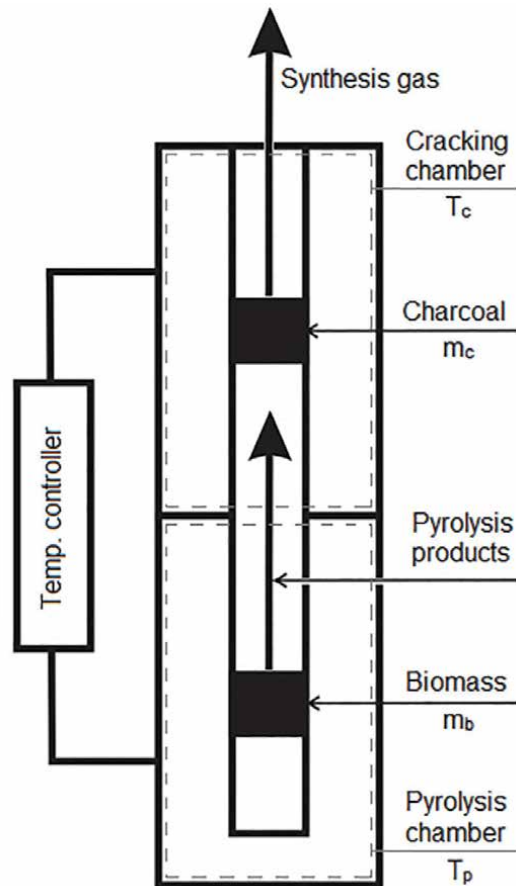


**Figure 1.** Schematic diagram of the two-stage pyrolytic conversion process.  $T_p$  – Temperature in the pyrolysis chamber;  $T_c$  – Temperature in the cracking chamber;  $m_b$  – Mass of feedstock loaded into the reactor;  $m_c$  – Mass of charcoal loaded into the cracking chamber.

characteristics of product gas obtained from the same types of biomass by the method of traditional pyrolysis.

- Section 4 contains a description of the pilot installation for two-stage pyrolytic conversion, designed and built at the Joint Institute for High Temperatures RAS, and the characteristics of the gas produced by it. The section also includes an assessment of the energy efficiency of this installation and an analysis of technical solutions that can improve the efficiency of its operation.
- Section 5 describes the possible applications of gas produced by the two-stage pyrolytic conversion method.

## 2. Features of the two-stage pyrolytic conversion process and recommended operating parameters

### 2.1 The mass ratio of the coke residue in the cracking zone and the initial biomass

The condensing fraction of the pyrolysis products of woody biomass is a complex mixture of pyrogenetic moisture, acetic, formic and lactic acids, methanol,

furfural, levoglucosan, compounds of various classes (aldehydes, ketones, esters), etc. [14]. Heating pyrolysis products when passing through a porous coke residue leads to thermal decomposition of high-molecular substances (heterogeneous cracking), mainly with the formation of carbon monoxide and hydrogen. In addition, non-condensable pyrolysis products and pyrogenetic moisture vapor interact with the carbon of the coke residue with the formation of CO and H<sub>2</sub>, which leads to a decrease in the mass of the coke residue. Obviously, the ratio of the masses of the feedstock and coke residue fed into the reactor of two-stage pyrolytic conversion should affect the yield of conversion products. The influence of this ratio was studied in detail experimentally by the authors in [15] for coniferous wood pellets, while in [16] later studies for dry oak sawdust are also included. The results of these experiments are shown in **Figure 2**. In both cases, the heating rate in the pyrolysis zone was 10 °C/min until the temperature reached 1000 °C.

The points in **Figure 2** correspond to the experimental data, while the lines are plotted by approximation. In accordance with the experimental results, the maximum yield of non-condensable gases in both cases corresponds to the mass ratio of the coke residue and the biomass sample  $m_c/m_b = 0.67$ . This ratio can be considered optimal for the given experimental conditions. With an increase in the rate of the feedstock heating, the optimal ratio  $m_c/m_b$  increases due to an increase of the mass flow rate of volatiles through the coke residue, and with a decrease in the rate of heating, it decreases. It is important to note that the weight loss of the coke residue in the experiments did not exceed some dozens of percent of the newly formed residue mass; therefore, the use of heterogeneous cracking does not require additional costs for the production or purchase of the coke residue.

## 2.2 The temperatures in the pyrolysis and cracking zones

In biomass processing by the two-stage pyrolytic conversion method, the first stage is conventional pyrolysis. The main change in the mass of raw materials and an increase in the volume of non-condensable gases formed as a result of the process occurs at a temperature in the pyrolysis zone  $T_p = 250\text{--}500$  °C, corresponding to the range of formation of the liquid fraction [17]. However,  $T_p = 700$  °C can be chosen

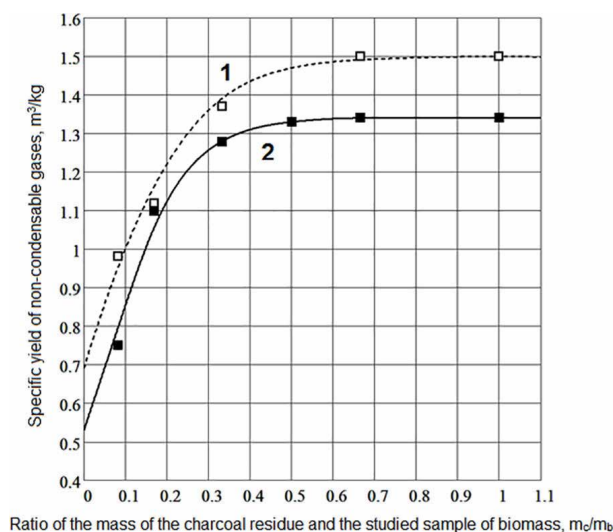
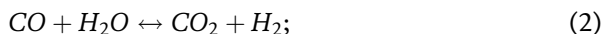


**Figure 2.** Dependence of the specific yield of non-condensable gases ( $m^3/kg$ ) on the ratio of the mass of the charcoal residue and the studied sample of biomass ( $m_c/m_b$ ) for pellets from coniferous wood (1) and oak sawdust (2).

as the maximum pyrolysis temperature, which, according to [18], is the upper temperature limit for the formation of primary tar. With further heating, the formation of tar does not occur due to thermal destruction of biomass, but only from primary tar.

The dependence of the specific yield of non-condensable product gases on the temperature in the pyrolysis zone for woody biomass is shown in **Figure 3**.

In the process of two-stage conversion when the biomass pyrolysis stage is carried out in the temperature range of  $T_p = 250\text{--}500\text{ }^\circ\text{C}$ , formation of gas has two main mechanisms: decomposition of vapors of condensable high-molecular compounds and three reactions proceeding in the forward direction:



where (Eq. (1)) is the reaction of steam gasification of carbon on the coke residue, (Eq. (2)) is the water-gas shift reaction, (Eq. (3)) is the Boudouard reaction. In the temperature range of  $T_p = 500\text{--}700\text{ }^\circ\text{C}$ , a further, relatively small increase in the volume of produced gases occurs, mainly due to the release of hydrogen from the carbonized feedstock in the pyrolysis zone.

The temperature in the cracking zone significantly affects the yield of non-condensable gases. Of greatest interest is temperature  $T_c = 1000\text{ }^\circ\text{C}$ , since it was shown in [12] that at a temperature of  $T_c = 1000\text{ }^\circ\text{C}$  and an interaction time of about 4 seconds in the cracking zone, almost complete conversion of condensing pyrolysis products into gas occurs, and  $CO_2$  is almost completely converted to  $CO$  due to the developed surface and high reactivity of the coke residue. The experimentally obtained dependences of the yield of non-condensable gases on the temperature in the pyrolysis zone for different temperatures in the cracking zone [17] are shown in **Figure 4**. It can be seen from the figure that with an increase in  $T_c$  from  $850\text{ }^\circ\text{C}$  to  $950\text{ }^\circ\text{C}$  the increase of the gas yield is  $0.285\text{ m}^3/\text{kg}$ , and with an increase in  $T_c$  from  $950\text{ }^\circ\text{C}$  to  $1000\text{ }^\circ\text{C}$  the volume of produced non-condensable gases is increased by another  $0.227\text{ m}^3/\text{kg}$ . At the same time, as the temperature in the cracking zone

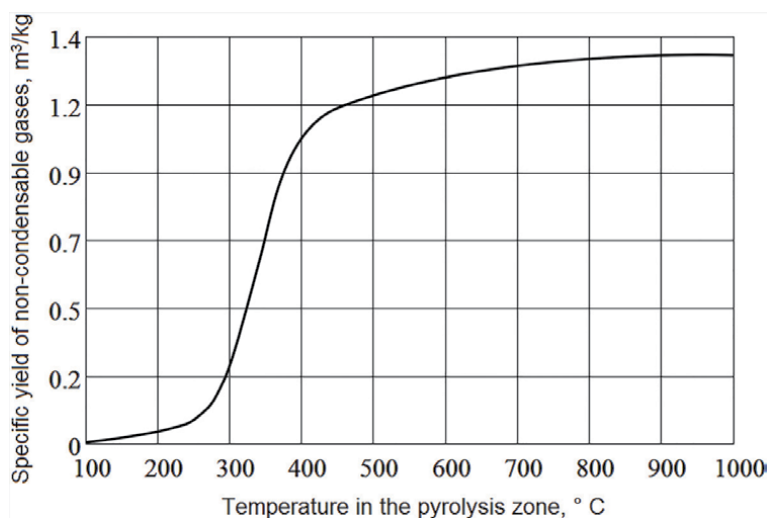


**Figure 3.** Dependence of the specific yield of non-condensable gases ( $m^3/\text{kg}$ ) on the temperature in the pyrolysis zone at a fixed temperature in the cracking zone  $T_c = 1000\text{ }^\circ\text{C}$ .

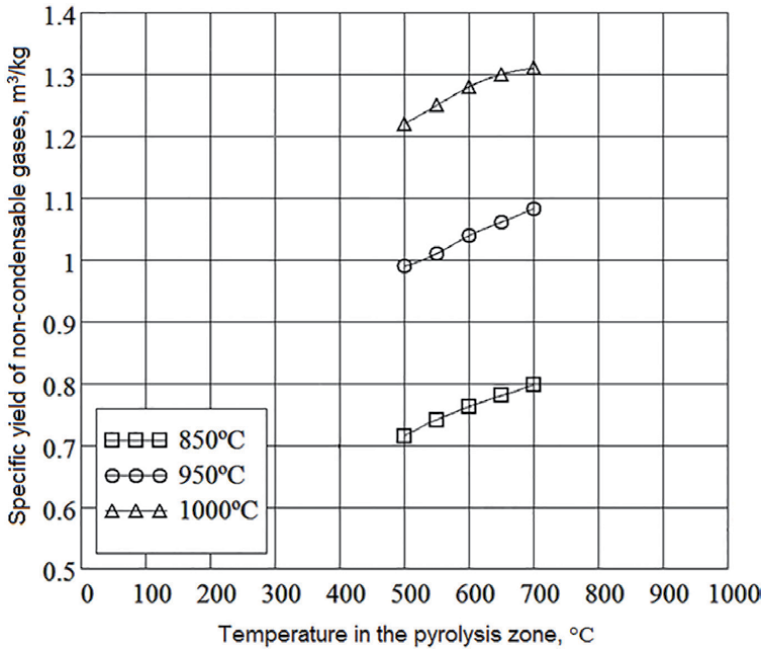


**Figure 4.** Specific yield of non-condensable gases for different temperatures in the cracking zone (850 °C, 950 °C, 1000 °C) depending on the temperature in the pyrolysis zone.

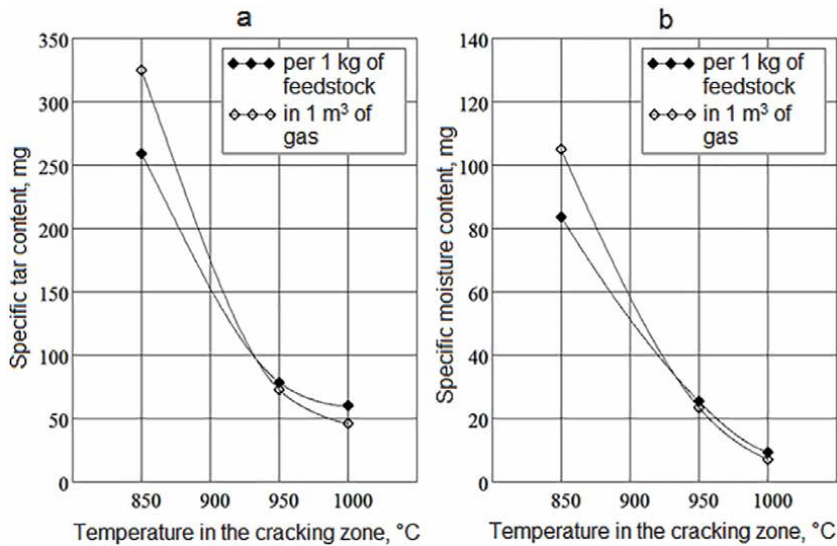


**Figure 5.** Dependences of the specific content of tar (a) and moisture (b) in gas on temperature in the cracking zone  $T_c$ .

risers, a decrease in the content of tar and moisture in the resulting synthesis gas is also observed (Figure 5).

The tar content is an important characteristic of synthesis gas, since it largely determines the possibility of its use in internal combustion engines. The issue of the maximum permissible tar content remains controversial due to the small number of tests on engines operating on gas contaminated with tars. However, most of the authors of the works cited in [19] agree that a specific tar content of less than 100 mg/m<sup>3</sup> is acceptable, and less than 50 mg/m<sup>3</sup> is preferable for long-term engine

operation. Based on the dependences shown in **Figure 5**, it can be concluded that the content of tar in the gas obtained by the method of two-stage pyrolytic conversion will correspond to the permissible and preferable values in modes with  $T_c \geq 930$  °C and  $T_c \geq 985$  °C, respectively.

### 3. Characteristics of the synthesis gas obtained from various types of biomass and comparison of two-stage pyrolytic conversion with conventional pyrolysis

The process characteristics described in the previous section are derived from experiments carried out on woody biomass. However, the possibilities of processing other types of biomass are of great interest. This section is devoted to a brief description of the results of experiments on processing by the method of two-stage pyrolytic conversion of six types of biomass: wood pellets, peat pellets, straw pellets, sunflower husk pellets, pellets from poultry litter and wastewater sludge (WWS). These results are presented in more detail in [20].

**Table 1** shows the characteristics of the considered types of biomass. The data on the elemental composition of pellets from sunflower husks were borrowed from [21].

The experimental setup had structure corresponding to the diagram shown in **Figure 1**. During the experiments, the temperature in the pyrolysis section gradually increased to 1000 °C with a heating rate of 10 °C/min. The temperature in the cracking section was 1000 °C during the entire experiment, and the time of passage of pyrolysis vapors and gases through it was no less than 4 s. The characteristics of the synthesis gas obtained as a result of a series of experiments are shown in **Table 2**. It should be noted that the synthesis gas obtained during the processing of wastewater sludge contains the largest amount of hydrogen, which makes this type of waste the most suitable raw material for the subsequent production of synthetic aviation fuel.

To compare the two-stage pyrolytic conversion with conventional pyrolysis, a series of experiments in which the temperature inside the cracking did not exceed 100 °C was carried out. Thus, the treatment was reduced to conventional pyrolysis. The characteristics of the gas mixture obtained as a result of these experiments are presented in **Table 3**.

Raw material	Moisture, wt %	Ash cont., wt %	Volatile fraction, wt %	Elemental composition, wt %					Higher heating value, MJ/kg	
				dry state			dry ash-free state		$Q_H^{exp}$	$Q_H^{cal}$
				W	A	$M_{vp}$	C	H		
Wood pellets	8.0	0.8	83.6	50.3	6.0	0.4	43.3	<0.05	20.6	19.8
Peat pellets	8.0	3.3	64.1	55.7	6.9	1.7	35.7	<0.05	21.9	23.6
Straw pellets	6.0	6.8	79.4	47.8	6.2	0.6	45.4	<0.05	19.6	19.0
Sunflower husk pellets	7.4	6.4	79.1	51.7	6.3		42.0		21.4	20.8
Litter pellets	16	13.8	82.6	48.0	6.4	5.9	39.0	0.7	20.4	20.1
WWS	2.7	22.7	89.1	51.7	7.5	8.5	26.0	1.5	25.0	25.9

**Table 1.** Characteristics of the raw materials. The 'exp' index denotes the experimentally measured heating value, while the 'cal' index denotes the value obtained by calculation on the base of elemental composition data.

Raw material		Wood pellets	Peat pellets	Straw pellets	Sunflower husk pellets	Litter pellets	WWS	
Syngas yield m <sup>3</sup> /kg	exp	Initial state	1.39	1.39	1.35	1.39	1.3	1.04
		Dry ash-free state	1.3	1.34	1.37	1.39	1.25	1.29
	cal	Dry ash free state	1.28	1.29	1.33	1.29	1.31	1.27
Volume fraction of combustible components		H <sub>2</sub>	0.46	0.49	0.4	0.43	0.46	0.53
		CO	0.46	0.41	0.38	0.37	0.37	0.27
		C <sub>n</sub> H <sub>m</sub>	0.00	0.01	0.00	0.00	0.01	0.05
Heating value, MJ/m <sup>3</sup>		higher	11.7	11.8	9.9	10.2	10.9	12.2
		lower	10.8	10.8	9.1	9.3	10.0	10.9
Energy conversion degree		0.74	0.72	0.69	0.66	0.67	0.63	
Adiabatic temperature of combustion, °C		2040	2030	2000	2010	2020	1970	
Crackling section filter		Wood charcoal	Carbon residue from peat pyrolysis	Carbon residue from straw pyrolysis	Carbon residue from sunflower husk pyrolysis	Wood charcoal	Wood charcoal	

**Table 2.**  
*Characteristics of synthesis gas obtained by two-stage pyrolytic processing from different types of biomass.*

Raw material		Wood pellets	Peat pellets	Straw pellets	Sunflower husk pellets	Litter pellets	WWS
Syngas yield, m <sup>3</sup> /kg (exp)	Initial state	0.26	0.29	0.26	0.38	0.26	0.22
	Dry ash-free state	0.28	0.33	0.30	0.44	0.36	0.29
Volume fraction of combustible components	H <sub>2</sub>	0.28	0.23	0.20	0.18	0.20	0.24
	CO	0.26	0.19	0.17	0.16	0.23	0.07
	C <sub>n</sub> H <sub>m</sub>	0.16	0.13	0.11	0.09	0.06	0.18
Heating value, MJ/m <sup>3</sup>	higher	13.2	10.5	9.1	7.9	7.8	11.1
	lower	12.0	9.5	8.2	7.2	7.2	9.9
Energy conversion degree		0.18	0.16	0.14	0.16	0.14	0.13
Adiabatic temperature of combustion, °C		1860	1730	1720	1640	1710	1770

**Table 3.**  
*Characteristics of product gas obtained in conventional pyrolysis from different types of biomass.*

Comparison of conventional pyrolysis with two-stage pyrolytic conversion in terms of the generated gas volume and the degree of energy conversion is shown in **Figure 6**. It is important to note that the degree of energy conversion was estimated exclusively for gaseous pyrolysis products.

From the presented data, it follows that the method of two-stage pyrolytic conversion makes it possible to efficiently process biomass of various types into synthesis gas with a calorific value of about 10–12 MJ/m<sup>3</sup>. The gas productivity of the process is several times higher than the gas productivity of conventional



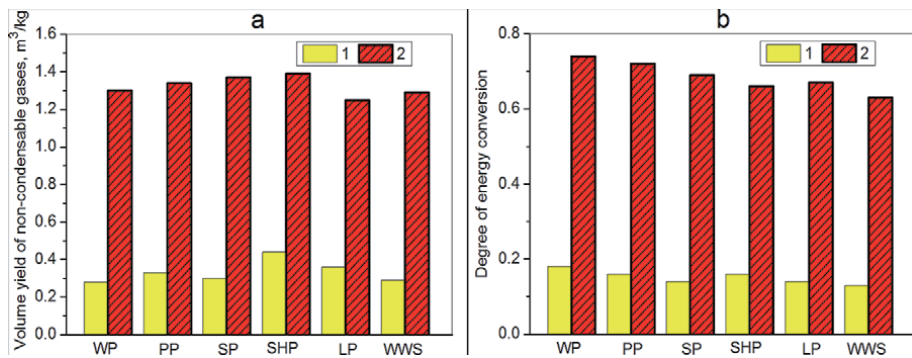


**Figure 6.** Volume yield of gas per 1 kg of combustible mass of the feedstock (a) and the degree of energy conversion (b) at conventional (1) and two-stage pyrolytic processing (2) of different types of biomass: WP – Wood pellets, PP – Peat pellets, SP – Straw pellets, SHP – Sunflower husk pellets, LP – Litter pellets.

pyrolysis. The ratio of volume contents of hydrogen to carbon monoxide in the produced synthesis gas varies from 1:1 to 1:2 depending on the type of biomass. Moreover, the synthesis gas does not contain volatile pyrolysis products of high molecular weight, which makes this fuel cleaner than pyrolytic.

#### 4. An experimental installation for the implementation of the two-stage pyrolytic conversion process and the results of its testing

**Figure 7** shows a schematic diagram of a two-stage pyrolytic conversion module designed at the JIHT RAS.

The thermochemical conversion module operates in the following way. Wood biomass (sawdust, shavings) from the feedstock storage is fed in portions to the pyrolysis reactor using a reciprocating piston; the role of the lift mechanism is performed by a hydraulic cylinder connected to the pumping station through a hydraulic valve with electromagnetic control. At the entrance to the pyrolysis reactor, the biomass is compacted under the action of the force applied from the piston,

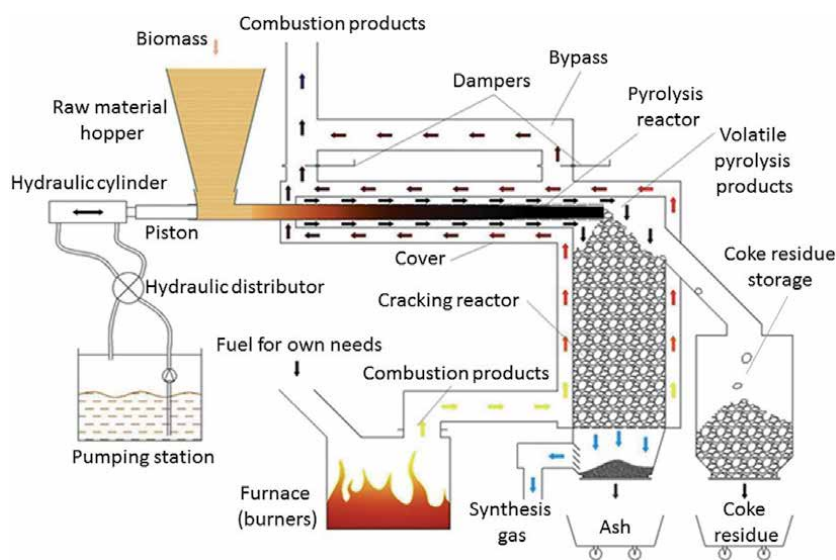


**Figure 7.** Schematic diagram of a two-stage pyrolytic biomass conversion module.

creating an air-tight briquette that prevents the release of gaseous products to the outside, and then, in the form of a compressed briquette, moves through the pyrolysis reactor due to the arrival of new portions. Heat is supplied to the compacted biomass through the wall from the hot combustion products formed in the furnace or burner. To ensure the supply of the amount of thermal energy required to maintain the conversion process, any available fuel is burned, for example, natural gas or propane (used in experiments on separate modules of the installation), the initial biomass or coke residue of the processed biomass. In the pyrolysis reactor, the biomass is gradually warmed up to a temperature of about 500–700 °C, accompanied by the release of volatiles, which, through perforation in the wall of the pyrolysis reactor, enter the gas collectors, along which they move into a vertically located retort filled with coke residue of the processed biomass - a cracking reactor. The temperature of the coke residue in the cracking reactor can be maintained by supplying heat through the wall from the combustion products at a level of 1000 °C. Pyrolysis gases and vapors pass through a fixed high-temperature layer of coke residue, in which gases and high-molecular compounds (including tar) are converted into synthesis gas, which is then removed for cleaning, cooling and further use. As a result of chemical reactions, the coke residue in the cracking reactor is consumed, but is constantly replenished with coke residue coming from the pyrolysis reactor. The mass loss of coke residue in the cracking reactor is less than the mass of the newly formed coke residue. Therefore, a coke storage is provided in the thermochemical reactor, which can be periodically unloaded. The excess of the resulting coke residue can be used both in the process itself (to provide for own needs in thermal energy), and for other purposes. The outer casing of the thermochemical conversion module has a bypass and dampers that allow regulating the flow of combustion products in the pyrolysis zone, thereby ensuring the ability to maintain the required reactor temperature.

The pilot installation for two-stage pyrolytic conversion was implemented as a structure of 4 modules. The scheme of the module and the photograph of the installation are shown in **Figure 8**.

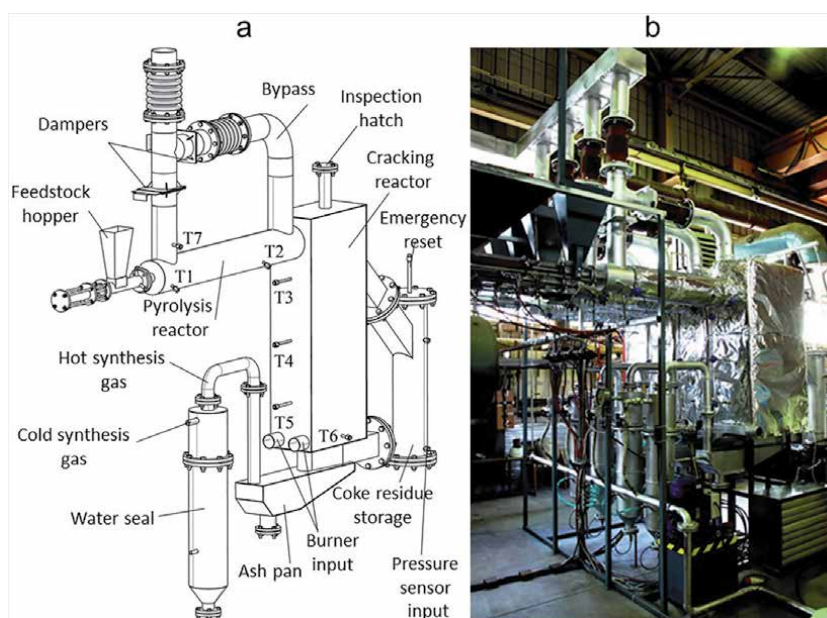


**Figure 8.** Diagram of a thermochemical conversion module (a) and a photograph of an installation consisting of four modules (b).

The unit was tested for two modes of operation (mode A, mode B). The parameters characterizing the operating modes of the unit are presented in **Table 4**. The characteristics of woody biomass and coal residue obtained during the tests are presented in **Table 5**, and the characteristics of the resulting synthesis gas are presented in **Table 6**. Data on the calorific value of raw materials and two-stage conversion products obtained in mode A are presented in **Table 7**.

The energy balance of the installation can be calculated from the test results. The energy flows diagram of the installation is shown in **Figure 9**.

The general energy balance equation is as follows:

$$P_{BM} + P_{CP} - P_L = P_{SP}^{ch} + P_{SP}^{ph} + P_{GP}^{ch} + P_{GP}^{ph}, \quad (4)$$

where the superscript “ch” refers to chemical heat and the superscript “ph” refers to the physical heat of solid and gaseous products of the process. The results of calculating the components of the energy balance are shown in **Table 8**.

The degree of energy conversion of the installation was determined as follows:

$$\eta_{ec} = \frac{g_{SG} \cdot Q_{SG}^{net}}{Q_{BM}^{net}}, \quad (5)$$

where  $Q_{SG}^{net}$  is the lower heating value of synthesis gas, MJ/m<sup>3</sup>;  $g_{SG}$  is the specific productivity of the unit for synthesis gas per 1 kg of feedstock, m<sup>3</sup>/kg. According to the results of calculations, the degree of energy conversion was 79,8%.

Parameter	Dimen-sion	Mode	
		A	B
<b>Mode symbol</b>		<b>A</b>	<b>B</b>
Biomass type		Oak sawdust	Pine shavings
Biomass consumption	kg/h	6,0	5,0
The mass of the coke residue in the cracking reactor	kg	8,6	8,6
Fuel type for own needs		Natural gas	Propane
Working value of gas pressure	bar	0,1 – 0,4(0,45)	0,4 – 2,0(2,2)
Fuel consumption for own needs in steady mode	m <sup>3</sup> /h	3,22	1,08
Thermal power of burners in steady mode	kWt	30,0	27,4
Pumping station power	kWt	2,26	
Temperature parameters of pyrolysis and cracking reactors:			
At the entrance to the pyrolysis reactor (T1)	°C	300	250
At the outlet of the pyrolysis reactor (T2)	°C	660	500
At the entrance to the cracking reactor (T3)	°C	950	870
In the middle of a cracking reactor (T4)	°C	980	910
At the outlet of the cracking reactor (T5)	°C	1000	950
Combustion products inlet (T6)	°C	1100	1100
Combustion products outlet (T7)	°C	600	570

**Table 4.**  
 Operating parameters of the pilot installation during tests.

Parameter	Mass fraction, %	
	Oak sawdust	Pine shavings
Biomass parameters		
Total moisture	5,50 / - / -	8,80 / - / -
Ash content	0,50 / 0,53 / -	0,48 / 0,53 / -
Total carbon	46,96 / 49,69 / 49,95	47,68 / 52,28 / 52,56
Organic hydrogen	5,42 / 5,73 / 5,77	5,54 / 6,07 / 6,10
Oxygen	41,47 / 43,89 / 44,12	37,43 / 41,04 / 41,26
Nitrogen	0,14 / 0,15 / 0,15	0,05 / 0,06 / 0,06
Combustible sulfur	0,01 / 0,01 / 0,01	0,02 / 0,02 / 0,02
The release of volatile substances at 700°C	81,1 / 80,0 / 80,4	84,5 / 83,0 / 83,4
The release of volatile substances at 1000°C	83,6 / 82,7 / 83,1	87,9 / 86,8 / 87,3
Coke residue parameters		
Specific yield (per 1 kg of feedstock)	0,163	0,156
Ash content	3,05 / 3,05 / 0	4,01 / 4,01 / 0
Total carbon	94,39 / 94,39 / 97,36	92,48 / 92,48 / 96,34
Organic hydrogen	0,99 / 0,99 / 1,02	0,85 / 0,85 / 0,88
Oxygen	0,89 / 0,89 / 0,91	2,09 / 2,09 / 2,17
Nitrogen	0,68 / 0,68 / 0,70	0,56 / 0,56 / 0,58
Combustible sulfur	0,01 / 0,01 / 0,01	0,02 / 0,02 / 0,02

**Table 5.** Characteristics of woody biomass and coke residue. \* In terms of working/ dry/dry ash-free condition.

Parameter	Dimension	Parameter value	
		Oak sawdust (A)	Pine shavings (B)
Synthesis gas volumetric flow	m <sup>3</sup> /h	7,66	6,50
Specific yield of the obtained synthesis gas	m <sup>3</sup> /kg	1,28	1,30
Synthesis gas chemical composition			
Hydrogen (H <sub>2</sub> )	% vol.	50,4	49,2
Carbon monoxide (CO)		40,8	40,8
Carbon dioxide (CO <sub>2</sub> )		5,5	5,0
Nitrogen (N <sub>2</sub> )		1,5	1,8
Oxygen (O <sub>2</sub> )		0,0	0,0
Hydrocarbons (C <sub>n</sub> H <sub>m</sub> ), among them:		1,8	3,2
- methane (CH <sub>4</sub> )	% of the total vol. of C <sub>n</sub> H <sub>m</sub>	90,7	91,8
- ethane (C <sub>2</sub> H <sub>6</sub> )		1,2	0,7
- ethene (C <sub>2</sub> H <sub>4</sub> )		1,1	0,8
- propane (C <sub>3</sub> H <sub>8</sub> )		4,2	2,7
- propene (C <sub>3</sub> H <sub>6</sub> )		0,2	0,1

Parameter	Dimension	Parameter value	
		Oak sawdust (A)	Pine shavings (B)
- i-butane (C <sub>4</sub> H <sub>10</sub> )		1,1	1,0
- n-butane (C <sub>4</sub> H <sub>10</sub> )		0,6	1,0
- i-pentane (C <sub>5</sub> H <sub>12</sub> )		0,2	0,4
- n-pentane (C <sub>5</sub> H <sub>12</sub> )		0,7	1,5

**Table 6.**  
 Characteristics of synthesis gas obtained as a result of tests.

Parameter	Dimension	Value
Lower heating value of biomass	MJ/kg	16,9
Higher heating value of biomass	MJ/kg	18,2
Lower heating value of coke residue	MJ/kg	33,0
Higher heating value of coke residue	MJ/kg	33,2
Lower heating value of synthesis gas	MJ/ m <sup>3</sup>	10,5
	MJ/kg	16,0
Higher heating value of synthesis gas	MJ/ m <sup>3</sup>	11,5
	MJ/kg	17,5

**Table 7.**  
 Heating value of raw materials, coke residue and synthesis gas obtained as a result of tests in mode a.

The efficiency of the installation was calculated as follows:

$$\eta_{\Sigma} = \frac{G_{BM} \cdot g_{SG} \cdot Q_{SG}^{net}}{G_{BM} \cdot Q_{BM}^{net} + N_{PS} + G_{NG} \cdot Q_{NG}^{net}}, \quad (6)$$

where  $G_{BM}$  is the consumption of biomass, kg/s;  $N_{PS}$  is the power of the pump station, MW;  $G_{NG}$  – consumption of natural gas burned in the furnace, m<sup>3</sup>/s;  $Q_{NG}^{net}$  – lower heating value of natural gas, MJ/m<sup>3</sup>. According to the results of calculations, the efficiency was 37.1%.

Thus, the designed unit has a high efficiency of energy conversion of woody biomass into synthesis gas, but it has a low thermal efficiency. The main ways to increase efficiency are to increase the degree of using biomass energy and reduce heat losses with the flue gases [22, 23]. The problem of reducing heat losses with the flue gases can be solved both by increasing the efficiency of heat exchange processes inside the unit (improving the flow parts of heat exchangers by using developed fins and optimizing the geometry of the coolant channels), and by recuperating part of the thermal energy of flue gases for heating air, which then goes into the solid fuel furnace for combustion. The disadvantage of the latter solution is also the complication of the installation and an increase in electricity consumption due to the appearance of a heat exchanger and an air blower. A schematic diagram, including the proposed areas of modernization, is shown in **Figure 10**.

It is shown in [12] that when solving the problem of finding the optimal operating parameters of a modernized installation, its efficiency can be increased to 69.5%, but the efficiency of energy conversion of raw materials will decrease to 70.3%.

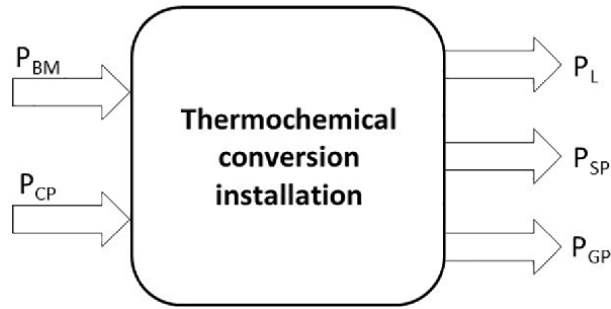


**Figure 9.** Energy flows diagram of a thermochemical conversion installation.  $P_{BM}$  – Energy of biomass processed per unit of time;  $P_{CP}$  – Thermal power introduced by natural gas combustion products;  $P_L$  – Total heat losses of the installation;  $P_{SP}$  – Energy corresponding to the heat content of solid products produced per unit of time;  $P_{GP}$  – Energy corresponding to the heat content of gaseous products produced per unit of time.

Parameter	Designation	Quantity, kWt
Energy corresponding to the heat content of the biomass processed per unit of time	$P_{BM}$	30,3
Thermal power brought in by natural gas combustion products	$P_{CP}$	14,7
Thermal power of losses into the environment through the thermally insulated walls of pyrolysis and cracking reactors	$P_L$	8,1
Energy corresponding to the heat content of solid and gaseous products formed per unit of time (chemical and physical heat):		
• solid products, chemical heat	$P_{SP}^{ch}$	9,0
• solid products, physical heat	$P_{SP}^{ph}$	0,2
• gaseous products, chemical heat	$P_{GP}^{ch}$	24,5
• gaseous products, physical heat	$P_{GP}^{ph}$	2,8
Energy balance discrepancy	$\Delta P$	0,4

**Table 8.** Energy balance of the pilot plant.

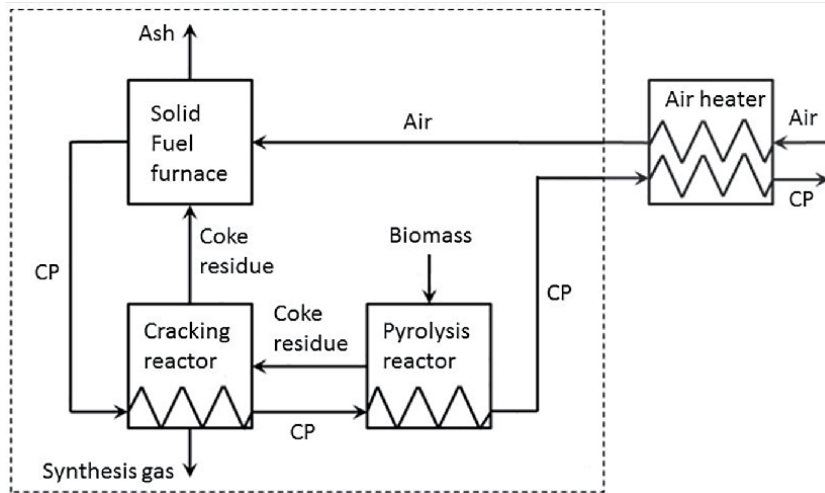


**Figure 10.** Schematic diagram of the modernized installation. CP – Combustion products.

## 5. Potential application areas for two-stage pyrolytic conversion

### 5.1 Cogeneration complex based on a gas piston engine

The schematic diagram of an autonomous cogeneration complex is shown in **Figure 11**. The diagram assumes parallel operation of 4 thermochemical conversion modules. The capacity of each module is 10–12 kg/h for the initial biomass or 12.8–15.4 m<sup>3</sup>/h for the synthesis gas.

The synthesis gas produced during the conversion of biomass is cleaned of solid particles (cleaning from tar is not required) in the filter and through the receiver enters the gas-piston engine (GPE). The rated power of the generator connected to the GPE is 75 kW. The combustion products of the GPE are cooled in a shell-and-tube heat exchanger to a temperature of 50 °C, after which they are removed into the atmosphere. In the same heat exchanger water is heated, which is then cooled in a heater (heat load up to 100 kW). The heater can be replaced by any other heat consumer.

The parameters of the energy complex are chosen in such a way as to ensure the possibility of testing it at the JIHT RAS stand. In the course of the tests carried out, the thermochemical conversion module was brought to the operating temperature mode, then the elastic gas tank was filled with synthesis gas, after which the GPE was started in the mode of the minimum load, which increased stepwise to 30 and then to 50 kW. During the tests, for each mode, we measured the flow rate of synthesis gas at the engine inlet, temperatures, pressures, and parameters of the electric generator. The engine running time at each load was 10 minutes. The results of measurements and calculations are presented in **Table 9**.

The tests carried out with one thermochemical conversion module have shown the possibility of implementing an autonomous cogeneration complex. The data obtained indicate that with the capacity of one module (in terms of feedstock – 12 kg/h), four thermochemical conversion modules will be able to provide gas to a power plant with a capacity of up to 50 kW. The thermal power in the cogeneration mode will be 54.4 kW.

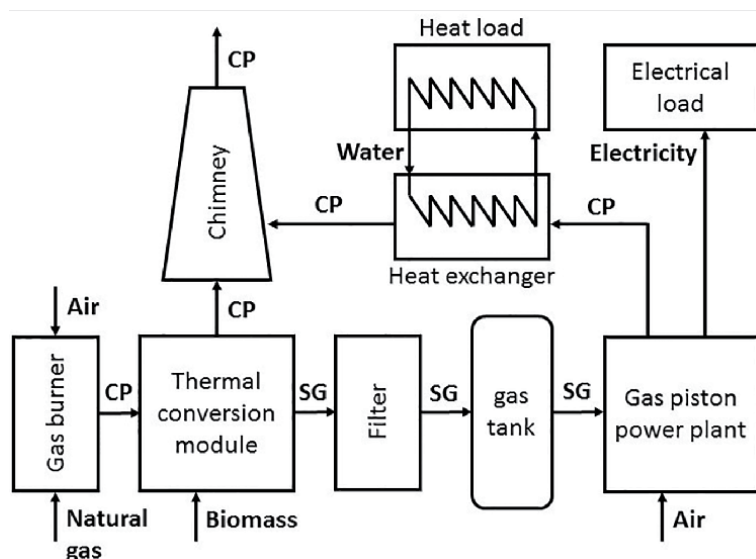


**Figure 11.** Schematic diagram of a cogeneration energy-technological complex based on a gas piston unit. SG – Synthesis gas; CP – Combustion products.

No	Load current, A	Voltage, V	Electric Power, kW	Frequency Hz	Syngas consumption, m <sup>3</sup> /h	Thermal power, kW
1	133,9	224	30	50	39,1	35,3
2	219,3	228	50	50	56,2	54,4

**Table 9.**  
*Test results of the power engineering complex.*

### 5.2 Substitution of liquid fuel in existing liquid fuel boilers

The synthesis gas obtained in the process of two-stage pyrolytic conversion can be used for partial replacement of diesel fuel in liquid fuel boilers. To study the co-firing of syngas and diesel fuel, a thermochemical conversion module was installed next to the boiler house. The schematic diagram of the heating complex is shown in **Figure 12**.

The heating complex uses a floor-standing cast iron boiler “RIELLO RTT 93” with an installed oil burner “CUENOD NC12H101”. The nominal heat output of the boiler is 100 kW. The schematic diagram is provided for two modules for thermochemical conversion of biomass, which allow replacing up to 90% of diesel fuel with synthesis gas during continuous operation of the boiler at rated power. At the time of testing, one module and one elastic gas tank with a volume of 10 m<sup>3</sup> were installed, which made it possible to carry out preliminary tests and evaluate the possibility of replacing liquid fuel with synthesis gas, since in fact the boiler operated in intermittent mode: after heating the direct supply water to the set temperature, the burner automatically turned off and remained off until the temperature of the direct supply water reached the lower threshold value, after which the burner re-ignited and the cycle was repeated.

For the co-combustion of diesel fuel and synthesis gas, a special nozzle was made on the flame head of a liquid fuel burner, which consists of two main elements - a supply pipe and a gas manifold with outlets after the air swirler (**Figure 13**). This

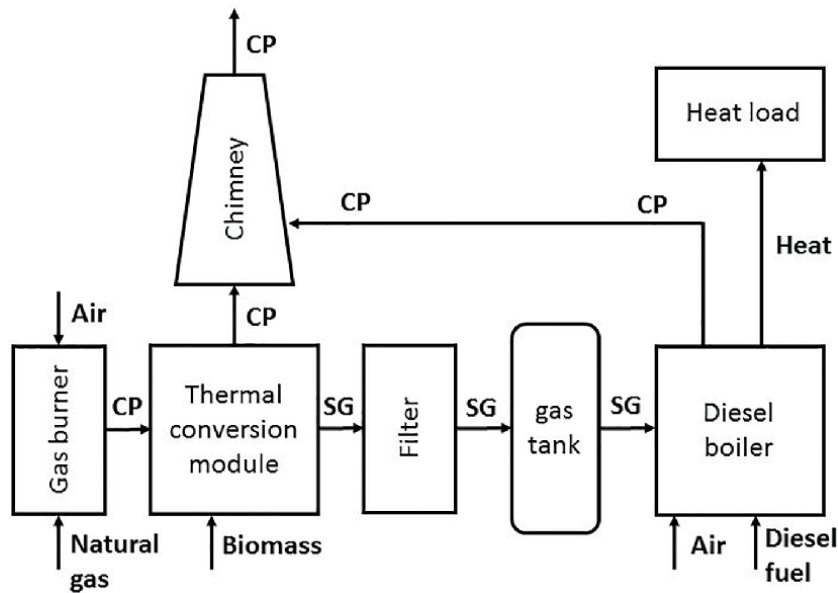


**Figure 12.**  
*Schematic diagram of the heating complex.*





**Figure 13.**  
*Flame head of liquid fuel burner with nozzle for co-combustion of gaseous fuel.*

allows synthesis gas to be fed into a turbulized air stream, which results in good mixing of gas and air. When it enters the boiler combustion chamber, the gas-air mixture burns out, while the liquid-fuel part of the burner, the power of which can be reduced to 10% of the nominal due to the installation of a low-flow nozzle, ensures guaranteed ignition of the mixture, preventing the occurrence of explosive situations. The total area of the openings for the gas outlet was selected experimentally (by measuring the gas flow rate) in such a way as to ensure the required gas performance of the burner in the operating range of excess pressures (5–30 mbar).

Heating complex tests included the following stages:

1. Bringing the thermochemical conversion module to the operating mode.
2. Filling an elastic gas tank with synthesis gas with subsequent determination of the composition of the syngas in the tank.
3. Start-up and subsequent operation of the boiler only on diesel fuel.
4. Boiler operation in the mode of combined combustion of diesel fuel and synthesis gas.

During testing of the heating complex, the temperature of the direct supply water was set on the boiler control panel and amounted to 58–62 °C. The tests were carried out for five modes of operation: three modes of operation on diesel fuel and two modes of co-combustion of diesel fuel and synthesis gas. Pine sawdust was used as the initial biofuel. The operating time in each mode was 10–15 minutes. Data on fuel consumption and parameters of combustion products in each mode are presented in **Table 10**.

Based on the data obtained as a result of the tests, the power and efficiency of the boiler were calculated in five operating modes (**Table 11**).

As tests have shown, the efficiency of the boiler in operating modes 4 and 5 turns out to be practically equal to the efficiency corresponding to the operation in the nominal mode, which indicates that there are no significant changes in the combustion conditions when diesel fuel is partially replaced by synthesis gas. Thus, the tests confirm the possibility of replacing liquid fuel in boiler houses with gaseous fuel obtained by the method of two-stage pyrolytic conversion.

Parameter	Dimension	Operating mode number				
		1	2	3	4	5
DF to SG ratio	% / %	100 / 0	100 / 0	100 / 0	90 / 10	80 / 20
Parameters of the oil part of the burner:						
Pressure of DF	Bar	11	9	7	9	7
DF consumption	kg/h	8,76	7,92	6,98	7,92	6,98
Parameters of the gas part of the burner:						
SG consumption	m <sup>3</sup> /h <sup>4</sup>	0	0	0	3,6	7,4
	kg/h	0	0	0	2,29	4,72
Parameters of combustion products behind the boiler:						
Temperature	°C	297	292	286	299	303
O <sub>2</sub> content	% vol.	3,2	4,74	6,20	3,12	3,08
Air excess ratio	—	1,20	1,32	1,46	1,19	1,19

**Table 10.**

*Fuel consumption and parameters of combustion products during testing of the heating complex. DF – Diesel fuel; SG – Synthesis gas.*

Parameter	Dimension	Operating mode number				
		1	2	3	4	5
Thermal power	kW	90,4	80,9	70,5	90,7	90,4
Efficiency	%	87,2	86,3	85,3	87,2	87,1

**Table 11.**

*Power and efficiency of the boiler at different operating modes.*

The efficiency of the heating complex can be increased if the combustion products formed in the boiler are sent to the thermochemical conversion module. In a similar way, the efficiency of the energy technology complex shown in **Figure 11** can be increased by using the combustion products generated in the GPE in the thermochemical conversion module.

### 5.3 Production of synthetic aviation fuel

The authors of [24, 25] have shown that synthesis gas obtained by two-stage thermal conversion of woody biomass during experiments can be used to synthesize dimethyl ether (DME) and methanol, which serve as the basis for the production of the base component of aviation fuel. Studies have shown that the synthesis of DME and methanol from lean synthesis gas with an H<sub>2</sub>:CO ratio of 0.95–1.25 can be efficiently carried out with a two-layer loading of a methanol catalyst and  $\gamma$ -Al<sub>2</sub>O<sub>3</sub>.

The volumetric content of individual gases, as well as various inclusions in the composition of the synthesis gas used for the production of DME and methanol, have a significant impact on both the efficiency of synthesis and the quality of the products obtained. Tar, moisture, solid particles, nitrogen and sulfur compounds in synthesis gas are undesirable impurities that reduce the catalyst life and deteriorate the quality of synthesis products. In the production of synthesis gas from woody feedstock by the method of two-stage pyrolytic conversion, gas purification is significantly simplified in comparison with the gas obtained from air gasification.

## 6. Conclusions

Two-stage pyrolytic conversion is a method for obtaining gaseous fuel with a calorific value of about 11 MJ/m<sup>3</sup> from biomass. The process includes two stages: pyrolysis of the feedstock and subsequent heterogeneous cracking of pyrolysis products when they are passed through a carbon packing. As a result, synthesis gas is formed, as well as a coal residue, which can be further used in the coal packing in the cracking reactor, as a fuel for own heat demand or for other applications.

The optimum (in terms of the specific yield of non-condensable gases) temperature in the pyrolysis zone is 500–700 °C, while the optimum temperature in the cracking zone is 1000 °C. The minimum mass of coal in the cracking reactor to achieve the maximum yield of non-condensable gases should be at least 67% of the mass of the feedstock fed to the pyrolysis reactor, provided that the heating rate in the pyrolysis reactor is 10 °C/min.

Experiments on the processing of six types of biomass (pellets from wood, peat, straw, sunflower husks and poultry litter, as well as wastewater sludge) by the method of two-stage pyrolytic conversion showed that each of the considered types of biomass can be used as raw material for synthesis gas production. The gas productivity of the process is several times higher than the gas productivity of conventional pyrolysis. The ratio of volumes of hydrogen to carbon monoxide in the produced synthesis gas varies from 1:1 to 1:2 depending on the type of biomass, while it does not contain volatile pyrolysis products with high molecular weight, which makes it possible to use it as fuel for internal combustion engines.

An experimental installation was built at the JIHT RAS, which implements the process of two-stage pyrolytic conversion. The unit provides the degree of energy conversion of the initial biomass into synthesis gas up to 79.8%. However, it has a low thermal efficiency: only 37.1%. This characteristic can be increased up to 69.5% with the heat recovery from flue gases.

Tests have confirmed that the synthesis gas obtained in the process of two-stage pyrolytic conversion can be used as motor fuel for internal combustion engines, as well as for partial replacement of diesel fuel in liquid fuel boilers. Moreover, it can be used as a raw material for the production of liquid aviation fuel. The best suited for this is the synthesis gas obtained during the processing of wastewater sludge due to its high hydrogen content.

## Acknowledgements

The authors are grateful to colleagues who took part in the development and study of the two-stage pyrolytic conversion process, as well as in the preparation of the materials published in this chapter: Kosov V.F., Kosov V.V., Markov A.V., Morozov A.V., Pchelkin M.D., Suslov V.A., Faleeva Yu.M., Tsyplakov A.I.

## Nomenclature

CHP	combined heat and power (plant);
ORC	organic Rankine cycle;
WWS	wastewater sludge;
SG	synthesis gas;
CP	combustion products;
GPE	gas piston engine;
DF	diesel fuel;
DME	dimethyl ether.

## **Author details**

Oleg Aleksandrovich Ivanin\*, Viktor Zaichenko Mikhailovich,  
Georgy Aleksandrovich Sytchev, Vladimir Aleksandrovich Sinelshchikov,  
Vladimir Aleksandrovich Lavrenov and Olga Mihailovna Larina  
Joint Institute for High Temperatures of the Russian Academy of Sciences  
(JIHT RAS), Moscow, Russia

\*Address all correspondence to: oleggin2006@yandex.ru

## **IntechOpen**

---

© 2021 The Author(s). Licensee IntechOpen. This chapter is distributed under the terms of the Creative Commons Attribution License (<http://creativecommons.org/licenses/by/3.0>), which permits unrestricted use, distribution, and reproduction in any medium, provided the original work is properly cited. 

## References

- [1] Renewables 2019 Global Status Report [Internet]. 2020. Available from: <https://www.ren21.net/gsr-2019/> [Accessed: 2020-12-01]
- [2] Quoilina S., Van Den Broek M., Declaye S. et al. Techno-economic survey of Organic Rankine Cycle (ORC) systems. *Renewable and Sustainable Energy Reviews*. 2013;22: 168–186. DOI: 10.1016/j.rser.2013.01.028
- [3] Sikarwar V. S., Zhao M., Fennel P.S. et al. Progress in biofuel production from gasification. *Progress in Energy and Combustion Science*. 2017;61:189–248. DOI: 10.1016/j.pecs.2017.04.001
- [4] Molino A., Larocca V., Chianese S., Musmarra D. Biofuels Production by Biomass Gasification: A Review. *Energies*. 2018;11:811–842. DOI: 10.3390/en1104081
- [5] Wang L., Weller C.L., Jones D.D., Hanna M.A. Contemporary issues in thermal gasification of biomass and its application to electricity and fuel production. *Biomass and Bioenergy*. 2008;32:573–581. DOI: 10.1016/j.biombioe.2007.12.007
- [6] Sikarwar V. S., Zhao M., Clough P. et al. An overview of advances in biomass gasification. *Energy & Environmental Science*. 2016;9 (10):2927–3304. DOI: 10.1039/C6EE00935B
- [7] Geletuha G.G., ZHeleznaya T.A. Obzor tekhnologij gazifikacii biomassy (Review of biomass gasification technologies). *Ekotekhnologii i resursosberezhenie*. 1998;2:21–29.
- [8] Neubauer Y. Strategies for Tar Reduction in Fuel-Gases and Synthesis-Gases from Biomass Gasification. *Journal of Sustainable Energy & Environment Special Issue*. 2011:67–71.
- [9] Rios M.L.V., Gonzalez A.M., Lora E. E.S., Almazan del Olmo O.A. Reduction of tar generated during biomass gasification: A review. *Biomass and Bioenergy*. 2018;108:345–370. DOI: 10.1016/j.biombioe.2017.12.002
- [10] Chembukulam S.K et al. Smokeless fuel from carbonized sawdust. *Ind. Eng. Chem. Prod. Res. Dev.* 1981, 20, 4, 714–719. DOI: 10.1021/i300004a024
- [11] Batenin V.M. et al. Thermal Methods of Reprocessing Wood and Peat for Power Engineering Purposes. *Thermal Engineering*. 2010;57(11):946–952. DOI: 10.1134/S0040601510110066
- [12] Batenin V.M., Zaichenko V.M., Kosov V.F., and Sinel'shchikov V.A. Pyrolytic Conversion of Biomass to Gaseous Fuel. *Doklady Chemistry*. 2012; 446(1):196–199. DOI: 10.1134/S0012500812090030
- [13] Henriksen U. et al. The Design, Construction and Operation of a 75 kW Two-Stage Gasifier. *Energy*. 2006;31 (10–11):1542–1553. DOI: 10.1016/j.energy.2005.05.031
- [14] Bajus M. Pyrolysis of woody material. *Petroleum & Coal*. 2010;52(3): 207–214.
- [15] Kosov V.F., Kosov V.V., Zaichenko V.M. Investigation of a two-stage process of biomass gasification. *Chemical Engineering Transactions*. 2015;43:457–462. DOI: 10.3303/CET1543077
- [16] Lavrenov V.A. Eksperimental'noe issledovanie processa dvuhstadijnoj termicheskoy konversii drevesnoj biomassy v sintez-gaz (Experimental study of the process of two-stage thermal conversion of woody biomass into synthesis gas) [thesis]. Moscow: Joint Institute for High Temperatures RAS; 2016.

- [17] Zaitchenko V.M., Lavrenov V.A., Sinelshchikov V.A. Study of characteristics of gaseous fuel produced by two-stage pyrolytic conversion of wood waste. *Alternative Energy and Ecology (ISJAEE)*. 2016;(23–24):42–50. (In Russ.) DOI: 10.15518/isjaee.2016.23-24.042-050
- [18] Morf P., Hasler P., Nussbaumer T. Mechanisms and kinetics of homogeneous secondary reactions of tar from continuous pyrolysis of wood chips. *Fuel*. 2002;81:843–853. DOI: 0.1016/S0016–2361(01)00216–2
- [19] Liu K., Song C., Subramani V. *Hydrogen and Syngas Production and Purification Technologies*. Hoboken, New Jersey: John Wiley & Sons, Inc.; 2010. 533 p.
- [20] Lavrenov V.A., Larina O.M., Sinelshchikov V.A., and Sytchev G.A. Two-Stage Pyrolytic Conversion of Different Types of Biomass into Synthesis Gas. *High Temperature*. 2016; 54(6):892–898. DOI: 10.1134/S0018151X16060092
- [21] Kollerov L.K., *Gazifikatsionnye kharakteristiki rastitel'nykh otkhodov (Gasification Characteristics of Plant Waste)*, Nikiforov V.V., Ed. Leningrad: Mashgiz; 1950.
- [22] Zaitchenko V.M., Kosov V.F., Lavrenov V.A. Razrabotka sposobov uvelicheniya effektivnosti pererabotki biomassy v sintez gaz metodom dvuhstadijnoj termicheskoy konversii (Development of ways to increase the efficiency of biomass processing into synthesis gas by the method of two-stage thermal conversion). In: *Proceedings of the IV International Conference 'Renewable Energy: Problems and Prospects'*; 21–24 September 2015; Makhachkala. Makhachkala; 2015;2:150–153.
- [23] Kosov V.F., Lavrenov V.A., Zaitchenko V.M. Simulation of a process for the two-stage thermal conversion of biomass into the synthesis gas. *Journal of Physics: Conference Series*. 2015;653(1):012031. DOI: 10.1088/1742-6596/653/1/012031
- [24] Kachalov V.V., Lavrenov V.A., Lishchiner I.I. et al. Scientific bases of biomass processing into basic component of aviation fuel. *Journal of Physics: Conference Series*. 2016;774(1): 012136. DOI: 10.1088/1742-6596/774/1/012136
- [25] Ershov M.A., Zaitchenko V.M., Kachalov V.V. et al. Synthesis of the base component of aviation gasoline from synthesis gas obtained from biomass. *Ecology and Industry of Russia*. 2016;20(12):25–29. (In Russ.) DOI: 10.18412/1816-0395-2016-12-25-29

# Co-Pyrolysis of Biomass Solid Waste and Aquatic Plants

*Md. Emdadul Hoque and Fazlur Rashid*

## Abstract

Reduction of conventional fuel has encouraged to find new sources of renewable energy. Oil produced from the pyrolysis method using biomass is considered as an emerging source of renewable energy. Pyrolytic oil produced in pyrolysis needs to be upgraded to produce bio-oil that can be used with conventional fuel. However, pyrolytic oil contains high amounts of oxygen that lower the calorific value of fuel, creates corrosion, and makes the operation unstable. On the other hand, the up-gradation process of pyrolytic oil involves solvent and catalyst material that requires a high cost. In this regard, the co-pyrolysis method can be used to upgrade the pyrolytic oil where two or more feedstock materials are involved. The calorific value and oil yield in the co-pyrolysis method are higher than pyrolytic oil. Also, the upgraded oil in the co-pyrolysis method contains low water that can improve the fuel property. Therefore, the co-pyrolysis of biomass waste is an emerging source of energy. Among different biomasses, solid waste and aquatic plants are significantly used as feedstock in the co-pyrolysis method. As a consequence, pressure on conventional fuel can be reduced to fulfill the demand for global energy. Moreover, the associated operating and production cost of the co-pyrolysis method is comparatively low. This method also reduces environmental pollution.

**Keywords:** co-pyrolysis, pyrolytic oil, biomass solid waste, aquatic plants, conventional fuel

## 1. Introduction

The reduction of conventional fuel sources such as coal, natural gas, and petroleum encourages to search for new sources of renewable energy. Previous literature predicts that coal would be the sole fossil fuel after 2042 [1]. On the other hand, the increase in fossil fuel prices and sustainable effects on the environment are the primary reasons for the use of alternate renewable energy [2–4]. A number of different ways are now underway to search for alternate sources of energy that are environmentally-friendly. However, environmental impact is more apparent after an environmental summit of the earth [5]. Therefore, to reduce environmental warming and pollution, it is required to control emissions produced by fossil fuels. The effective way of reducing environmental pollution and dependency on conventional fuel is to use renewable sources of energy [3, 6, 7].

There are a number of different alternative sources of available energy that can be utilized to substitute conventional sources of energy. The selection of effective and efficient alternative sources of energy is important. In general, an alternate source of energy is suggested to select based on cost, availability, and

environmental impact [4]. In this case, biomass is a prospective source of future energy that is abundant in nature, less costly, and environmental-friendly. Biomass is a significant source of bioenergy that can be utilized to generate energy and used to reduce environmental warming [8]. Biomass energy source is significant because it is the only available renewable resources that can be used to produce all three types of fuels, such as solid (char), liquid (oil), and gas ( $\text{CH}_4$ ) [9]. By comparing different biomass conversion methods, such as composting, incineration, landfill, and pyrolysis, it is found that pyrolysis is an effective biomass conversion process [10]. Pyrolysis method can be used to process biomass solids and produce solid, liquid, and gaseous fuel. The pyrolysis method can be used to process biomass solids and produce solid, liquid, and gaseous fuel. This process can also be able to produce the highest quantity of yield in liquid form (~75 wt.%) at a moderate level of temperature (~550 °C) [9]. The remaining quantity of yield can be reduced by changing different operating parameters in the pyrolysis process. The liquid yield produced from the pyrolysis method is called pyrolytic oil and it can be used directly to operate engines, boilers, furnaces, and turbines [11]. Moreover, pyrolytic oil reduces the environmental emissions and global warming [12].

However, pyrolytic oil generated from the pyrolysis method is less efficient on the basis of fuel combustion when compared to conventional fuels, such as diesel, petrol, etc. This is due to the reason that pyrolytic oil usually contains a high quantity of oxygen that creates unnecessary combustion problems. In different previous research, it was found that pyrolytic oil contained approximately 30–60 wt. % of oxygen in the form of water molecules [11, 13–15]. In addition, high oxygen contents in pyrolytic oil cause lower calorific value and instability of operation. As a consequence, it is required to upgrade and improve pyrolytic oil generated in the pyrolysis process.

To improve the quality of pyrolytic oil, it is required to reduce the quantity of dissolved oxygen. It is possible to reduce the dissolved oxygen from pyrolytic oil by catalytic cracking, co-pyrolysis, and catalytic cracking and hydrodeoxygenation (HDO) process.

In the catalytic cracking and hydrodeoxygenation (HDO) method, external catalysts are added in the pyrolysis process. However, the addition of catalysts increases the operating cost of the pyrolysis process. It also increases the number of solid materials at disposal [16]. Overall, this process is costly, complex, and require higher pressure during operation. In contrast, the co-pyrolysis method is an effective and efficient process that can improve the quality of pyrolytic oil.

Therefore, this chapter presents the co-pyrolysis method of biomass feedstocks. This chapter also presents the generation of liquid fuel from solid waste (wood, plastic) and aquatic plants (water hyacinth) using the co-pyrolysis method. Additionally, by using biomass solid wastes (plastic, wood) as feedstock material, the co-pyrolysis method can reduce environmental pollution and help the global waste management system. This method also uses invasive aquatic plants (water hyacinth) as feedstock material and reduces the negative effects of water hyacinth on aquatic flora, fauna. Hence, solid and aquatic plant biomass would be a potential source of energy that produces less impact on the environment.

The outcomes of this chapter will help to decrease the pressure on conventional fuel. On the other hand, the majority of the recent literature shows the use of rice straw, pinewood, and plastic material as feedstocks in the co-pyrolysis method. However, this chapter shows the generation of product yield for two different combinations of feedstocks and compares the performance of them at a different proportion that is rare in previous research. By effectively maintaining the required proportion of biomass feedstock materials, it is possible to generate a significant quantity of solid, liquid, and gas yield. As a consequence, biomass feedstocks would be a feasible option to fulfill the global energy demand.



## 2. Biomass conversion techniques

Biomass can be converted in a number of different ways. The most significant ways are pyrolysis, gasification, combustion, and liquefaction, as shown in **Figure 1**. On the other hand, all biomass conversion techniques are performed using three major process technologies, as depicted in **Figure 2**.

### 2.1 Pyrolysis

Pyrolysis is defined as the method of heating organic biomass in absence of oxygen. This is due to the reason that without oxygen, there is no combustion occurred in biomass materials. However, applying heat decomposes the chemical components of biomass materials such as lignin, cellulose, and hemicellulose and produce charcoal and combustible gases [17].

In the pyrolysis method, the produced combustible gases are condensed to a combustible liquid called pyrolytic oil. The other products of the pyrolysis method are CO<sub>2</sub>, CO, H<sub>2</sub>, and HC. Therefore, the pyrolysis method generates three types of products, such as solid (charcoal), liquid (bio-oil/pyrolytic oil), and gas (synthetic gas). **Figure 3** presents the overall schematic diagram of the pyrolysis method that generates pyrolytic oil.

Moreover, in pyrolysis method, biomass feedstock materials are decomposed in pyrolytic oil by the following reaction mechanism Equations [18]:

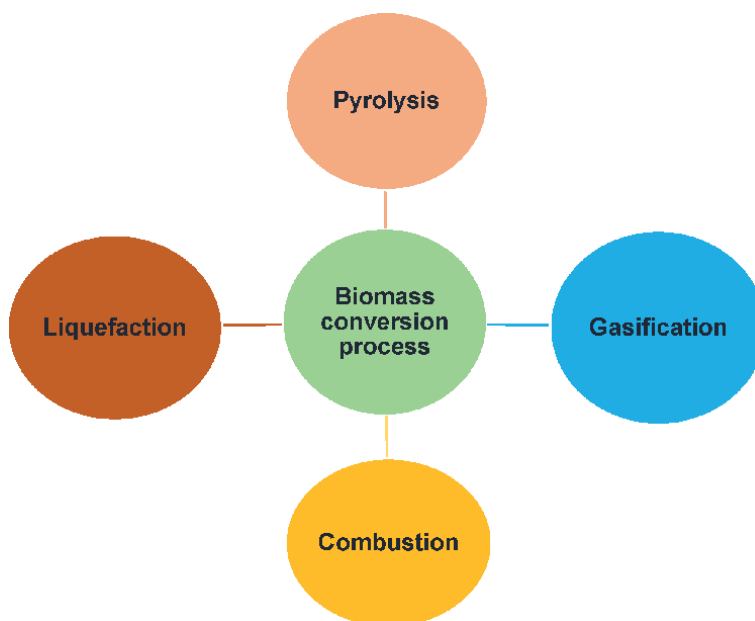
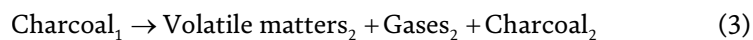
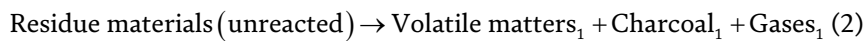
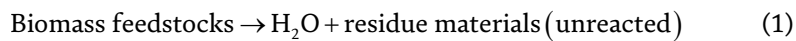


**Figure 1.**  
*Biomass conversion techniques.*

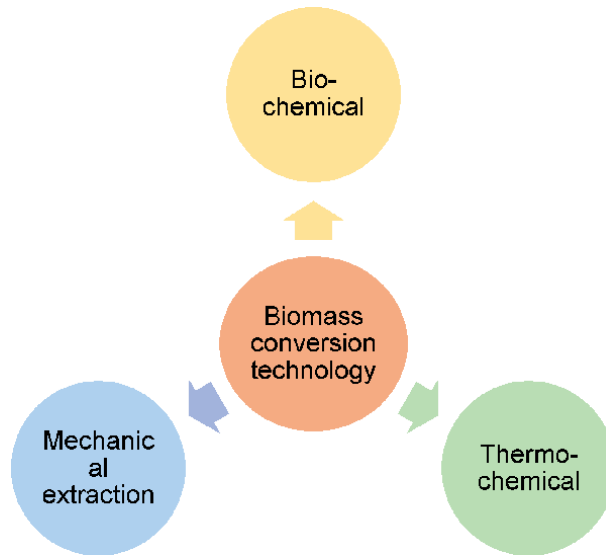


**Figure 2.**  
*Flow diagram of the pyrolysis process.*

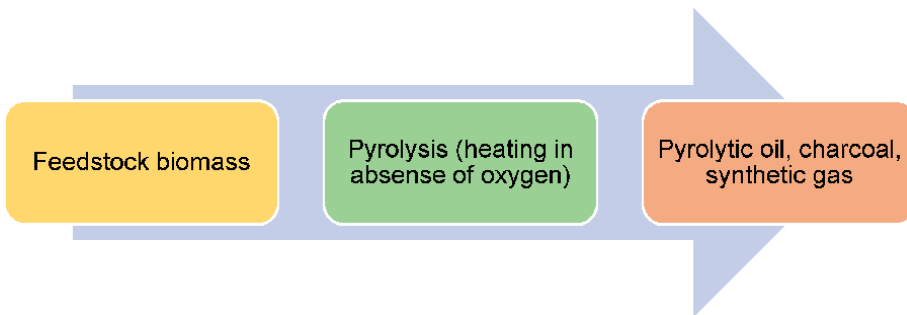


**Figure 3.**  
*Biomass conversion process technologies [17].*

Therefore, in the biomass pyrolysis method, firstly, moisture contents, and volatile matters are lost as presents by Eq. (1). Secondly, unreacted residue materials are transformed into volatile matters, as shown in Eq. (2). Finally, charcoal material is re-arranged at a slower step, as shown in Eq. (3).

Depending on the reaction temperature, residence time, and rate of heating, the pyrolysis process can be classified as fast, slow, and flash pyrolysis. Pyrolysis process usually occurs in a fixed bed, fluidized bed, moving bed, suspended bed reactors.

However, the generated pyrolytic oil in the pyrolysis process contains a higher quantity of oxygen that decreases internal combustion engines' efficiency. Therefore, up-gradation of pyrolytic oil generated from the pyrolysis method is necessary. The pyrolytic oil generated from the pyrolysis method can be upgraded by esterification, emulsification, or catalytic cracking. All these up-gradation methods include extra operating costs for the pyrolysis process and they are rather costly. The other effective method of producing high-quality pyrolytic oil is the co-pyrolysis method that can produce high-quality pyrolytic oil with less quantity of oxygen.

**Figure 4** shows the upgradation methods of pyrolytic oil generated from biomass pyrolysis method.

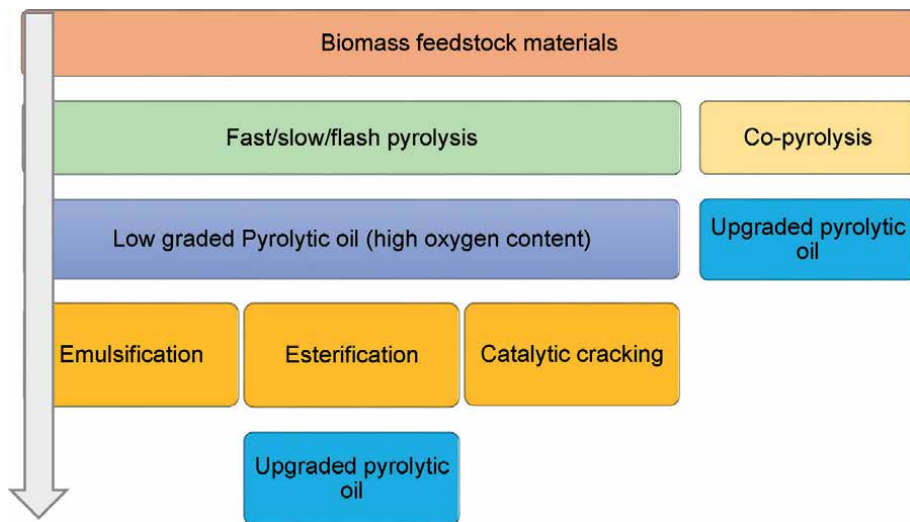


**Figure 4.**  
 Upgradation methods of pyrolytic oil [19].

## 2.2 Co-pyrolysis

Co-pyrolysis is the process where two or more feedstock materials include to improve the quality of pyrolytic oil in absence of oxygen at a moderate temperature (~500 °C). Effectiveness and simplicity are two important characteristics of the co-pyrolysis process. **Figure 5** shows the overall process of co-pyrolysis.

It is seen from **Figure 5** that, in the co-pyrolysis method, two or more feedstock materials are dried and ground to prepare feedstock material. After that inert gases are required to add to the reactor. Inert gases use to speed up the sweeping vapors of feedstock materials from the pyrolysis region to the condenser region. Nitrogen gas is used as an inert gas in the co-pyrolysis process due to its low cost. Initially, charcoal and combustible gases are produced. After condensation, combustible gases generate upgraded pyrolytic oil. Therefore, the co-pyrolysis method requires three steps for the generation of pyrolytic oil, such as preparation of feedstock materials, co-pyrolysis, and condensation.

Drying of feedstock material can be done using the oven method at a higher temperature (~105 °C) for 1 day. The drying process is required to remove the

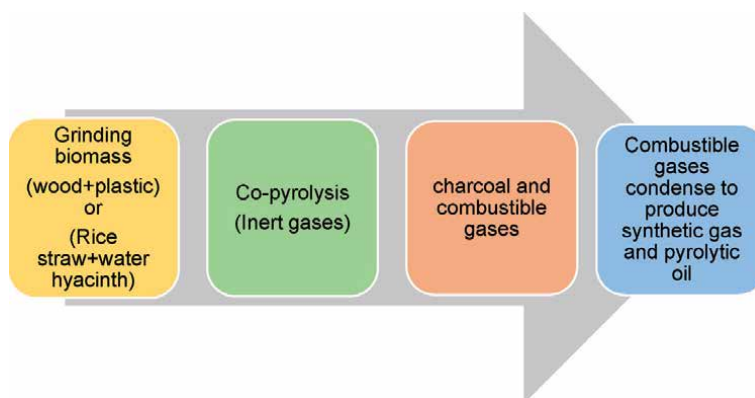


**Figure 5.**  
 Overall process of co-pyrolysis [9].

Feedstock materials	Temperature(°C)	Inert gas	Pyrolytic oil (wt.%)
Wood, plastic, rice husk, rice straw, water hyacinth	300 ~ 500	N <sub>2</sub>	45-75

**Table 1.**  
*Optimum operating conditions of co-pyrolysis method [9].*

moisture contents in the feedstock material. However, for industrial purposes, the amount of required heat is higher than lab-scale. Hence, process integration is used to heat feedstock materials [9].

The optimum temperature of the co-pyrolysis process is considered as 400 ~ 600 °C. At this temperature, approximately 45 wt. % of pyrolytic oil is usually produced from feedstock material [9]. **Table 1** presents the optimum operating conditions of co-pyrolysis method for different feedstock materials.

In this chapter, pinewood with plastic material, and rice straw with water hyacinth material is considered as feedstock materials for the co-pyrolysis process. Pinewood [20, 21] and waste plastic [22, 23] materials are commonly available in environment that can create environmental pollution.

### 3. Reaction parameters of co-pyrolysis process

Reactions of the co-pyrolysis method are complex and it includes a number of different co-pyrolysis reactions. The biomass co-pyrolysis process and their reactions depend on different parameters, such as the effect of feedstock materials, blending ratio, rate of heat, temperature, reactor type, etc. This section of the chapter presents the effect of different parameters on the co-pyrolysis method.

#### 3.1 Effect of different feedstocks

Biomass feed materials consist of lignin, cellulose, and hemicellulose [24]. These components generate synergistic effects on the thermal behavior of biomass. It is considered that the cracking of biomass depends on the H and OH radicals release during biomass pyrolysis [25, 26]. On the other hand, hemicellulose components serve effects of promotion on biomass conversion during co-pyrolysis process [27].

**Table 2** shows the characteristics of different biomass materials.

#### 3.2 Effect of blending ratio

The blending ratio is defined as the proportion of biomass in the blend of feedstock materials during co-pyrolysis. In the co-pyrolysis method, the

Feedstock materials	Lignin (wt. %)	Cellulose (wt. %)	Hemicellulose (wt. %)
Pinewood	24 [28]	42 [28]	23 [28]
Water hyacinth	3 ~ 28 [29]	~30 [30]	~25 [30]
Rice straw	16.5 [31]	29.8 [31]	33.3 [31]
Waste plastic (polystyrene)	10 ~ 15 [32]	35 ~ 55 [32]	20 ~ 40 [32]

**Table 2.**  
*Characteristics of different biomass materials.*

generated quantity of gas, liquid, and solid materials depends on the blending ratio of feedstock material [33]. It was found that increasing biomass blending ratio reduces the solid charcoal generation, while liquid and gas production increases [34]. The blending ratio of biomass materials can also influence the degree of synergistic effect.

### **3.3 Effect of rate of heat**

The rate of heating is a significant factor that can affect the biomass co-pyrolysis process. The biomass co-pyrolysis process can be distinguished if the rate of heat is low. At a low heating rate, only additive behavior of biomass materials occurs. On the other hand, the devolatilization process of biomass materials becomes slower with the increase in the heating rate.

Synergism of biomass feedstock materials is favored by the increased heating rate of feedstock material [27, 35, 36]. It was found that low heating rate caused lack of synergies. Moreover, a high rate of heat during co-pyrolysis generally produces higher volatile yields [37].

### **3.4 Effect of temperature**

The temperature in the co-pyrolysis process is an important factor for the generation of solid (charcoal), liquid (pyrolytic oil), and gas. By increasing the temperature inside the co-pyrolysis reactor, it is possible to decrease the production of charcoal from biomass co-pyrolysis. As a consequence, the overall efficiency of the co-pyrolysis method can be increased by increasing the temperature [38, 39].

### **3.5 Effect of types of reactor**

Different types of reactors, such as fixed bed, fluidized bed, TG, drop style, auger are commonly used in pyrolysis and co-pyrolysis process. In this chapter, the fixed bed reactor is considered for biomass feedstock materials. However, the TG reactor is most commonly used during the co-pyrolysis method.

In a fixed bed pyrolysis reactor, a large quantity of feedstock materials provides intimate contact between fuel particles and their generated volatiles. Due to this phenomena, synergistic effect is occurred for gas and pyrolysis product yield [40]. Fluidized bed and drop style type reactors are fast pyrolysis reactors that can be used to carry the co-pyrolysis process. Auger reactor is more effective than fixed-bed reactor for co-pyrolysis process. Auger type reactor usually generates higher liquid product yield than fixed-bed reactor [41].

## **4. Sample preparation and feedstocks for co-pyrolysis**

Availability is one of the important factors for the selection of alternative energy sources. With respect to this condition, biomass is considered a potential energy source all over the world. It can be generated from the forest (wood), agriculture (rice husk, rice straw), solid waste (plastic), aquatic plants (water hyacinth), etc. In this work, rice straw, plastic, water hyacinth, and pinewood are considered as feedstock material.

Biomass feedstock materials are required to collect from the local market. They contain moisture and volatile matters that can reduce the overall efficiency of the pyrolysis process. To overcome this problem, biomass materials are dried using the oven for lab-scale operation and process heat through industrial applications. After

drying, biomass feedstock materials are crushed and sieved to a particle size of 0.5 ~ 2 mm [42]. Thermogravimetric analysis (TGA) can be carried out to find the measurement of moisture content, thermal degradation, fixed, and volatile carbons in biomass feedstock materials.

Characterizing of biomass feed materials is significant because it provides C, H, N, S, moisture, ash, fixed carbon, and volatiles. **Table 3** shows the ultimate analysis and **Table 4** presents a proximate analysis of rice straw, water hyacinth, pinewood, and plastic biomass materials.

The heating value of biomass feedstock materials is another significant property that can affect the overall efficiency of the co-pyrolysis method. **Table 5** presents the heating value of rice straw, water hyacinth, pinewood, and waste plastic materials.

It is seen from **Table 5** that plastic material generates the highest quantity of heat when combusts. On the other hand, they are available as waste material in the natural environment.

The co-pyrolysis method can use two or more feedstock materials, therefore, this chapter presents and compares the performance of pinewood and waste plastic biomass with rice straw and water hyacinth aquatic plants.

In the co-pyrolysis process, rice straw, water hyacinth, pinewood, and waste plastic material was used to perform the experiment in a fixed bed reactor, as shown in **Figure 6**. The feedstock materials were prepared with a nominal size of 5 mm. All the biomass feedstock materials were added in the fixed bed reactor and nitrogen was used as the carrier gas. An external electrical heater was used to externally heat up the reactor during the co-pyrolysis process. The heater increased the reactor temperature to around 60 °C per minute. The final reactor temperature during the co-pyrolysis process was 550 °C. The overall reaction time for the biomass co-pyrolysis process was ~30 min. The solid and liquid product yields were collected by

Feedstock materials	Carbon (C) (wt.%)	Hydrogen (H <sub>2</sub> ) (wt.%)	Nitrogen (N <sub>2</sub> ) (wt.%)	Sulfur (S) (wt.%)
Pinewood [43]	47.5	6.50	0.095	~0.13
Water hyacinth [42]	34.85	6.50	0.8	1.5
Rice straw [42]	36.1	5.20	0.6	0.30
Waste plastic (polystyrene) [44]	90.40	8.60	0.070	0.080

**Table 3.**  
*Ultimate analysis of biomass feedstock materials.*

Feedstock materials	Fixed carbon (wt.%)	Moisture (wt.%)	Volatile matters (wt.%)	Ash (wt.%)
Pinewood [43]	17.90	14.2	67.70	45
Water hyacinth [42]	4.90	13.15	69.2	25.50
Rice straw [42]	6.90	11.7	78.1	15.2
Waste plastic (polystyrene) [44]	~0.7–12	0.20	99.31	0.50

**Table 4.**  
*Proximate analysis of biomass feedstock materials.*

Feedstock materials	Heating value (MJ/kg)
Pinewood	18–21.5
Water hyacinth	14.6
Rice straw	14–15.1
Waste plastic (polystyrene)	40

**Table 5.**  
 Heating value of biomass feedstock materials.

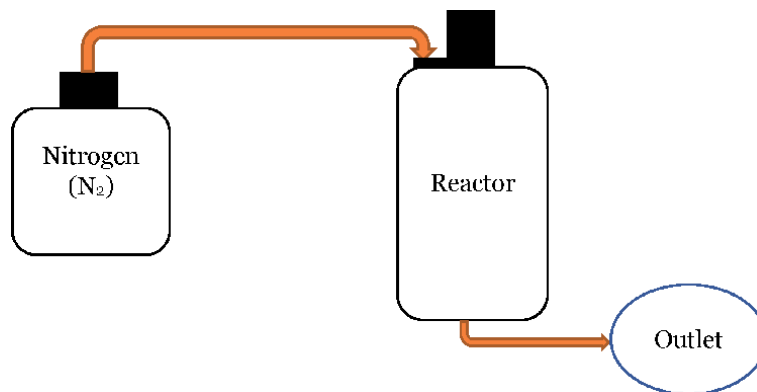


**Figure 6.**  
 Schematic diagram of the co-pyrolysis process of rice straw, water hyacinth, pinewood, and plastic biomass.

weight basis, while gas yields collected in a gas reservoir bag. After that, a gas analyzer was required to analyze the composition of gas yield generated in co-pyrolysis of rice straw, water hyacinth, pinewood, and plastic materials.

## 5. Co-pyrolysis using biomass solids and aquatic plants

Co-pyrolysis of pinewood and waste plastic feedstock material is a potential source of energy. On the other hand, rice straw and water hyacinth is another significant source of biomass energy that can be used as feedstocks in the co-pyrolysis process. Individually rice straw, plastic, water hyacinth, and pinewood biomass materials, when used in the pyrolysis process, produce less efficient pyrolytic oil that creates unnecessary combustion problems due to high oxygen contents. As a consequence, different proportions of two or more feedstock materials are usually used in the co-pyrolysis method that can provide better performance. This section of the chapter presents the performance analysis of pinewood with waste plastic and rice straw with water hyacinth biomass feedstock materials during the co-pyrolysis method at different proportions of feedstock materials. The product yields were solid (charcoal), liquid (pyrolytic oil), and gas. Likewise, the co-pyrolysis of rice straw, water hyacinth, pinewood, and plastic materials provide product yield of charcoal, pyrolytic oil, and gas.

In pinewood and waste plastic feedstocks, the products of charcoal production do not depend on the addition of waste plastics. It was also found that very little quantity of charcoal produced from the co-pyrolysis of waste plastic [45, 46]. While, in the co-pyrolysis of rice straw and water hyacinth feedstocks, the production of bio-oils depends on the reactor temperature, and with the increase of reactor temperature up to 400 °C, the pyrolytic oil production is also increased. After that, above temperature 400 °C, generation of pyrolytic oil decreases [42].

## 5.1 Performance analysis

In the co-pyrolysis method of pinewood-waste plastic and rice straw-water hyacinth, it was observed that liquid yield generation was higher in pinewood-waste plastic feedstocks than rice straw-water hyacinth feedstocks. This is due to the higher heating value of pinewood and plastic material than water hyacinth. The porosity of water hyacinth feedstocks can also negatively affect the generation of product yield during the co-pyrolysis process. In addition, the density of rice straw and water hyacinth is lower than the density of pinewood and waste plastic that can negatively influence the generation of pyrolytic oil for the co-pyrolysis method.

In this process, initially pinewood with waste plastic (polystyrene) and rice straw with water hyacinth materials were added in a 1: 1 ratio.

**Figure 7** presents the generation of liquid yield from the co-pyrolysis process for pinewood-plastic (polystyrene) and rice straw-water hyacinth feedstock materials. It is seen from **Figure 7** that the liquid yield (pyrolytic oil) of pinewood with plastic (polystyrene) feedstocks in co-pyrolysis was higher than rice straw with water hyacinth feedstock materials at 400 °C temperature [9, 42].

In the co-pyrolysis method, the amount of solid, liquid, and gas yield depends on the type of biomass feedstocks and the proportion at which they are added in the co-pyrolysis process. In this chapter, three different ratios of feedstocks have been considered to analyze the performance of co-pyrolysis.

The co-pyrolysis of rice straw with water hyacinth feedstock materials produced the highest yield of liquid (pyrolytic oil) than solid (charcoal) and gas yield at an equal proportion of rice straw and water hyacinth (1:1). It was also found that with the increase of water hyacinth proportion with rice straw, the liquid (pyrolytic oil) yield was decreased but solid (charcoal) yield increased, while gas yield remained almost same [42]. This trends were statistically significant. On the other hand, a high proportion of rice straw with water hyacinth reduced the liquid yield from the liquid yield of an equal amount of rice straw and water hyacinth, as shown in **Figure 8**.

**Figure 9** presents the mean and standard deviation of the product yield wt. % for three different compositions of rice straw and water hyacinth. It is seen from **Figure 9** that the variation of solid yield (charcoal) with the change of composition of rice husk and water hyacinth was lower than liquid (pyrolytic oil) and gas yield.

**Figure 10** shows the product yield of co-pyrolysis for different proportions of pinewood and waste plastic (polystyrene) biomass materials. It was found that



**Figure 7.** Pyrolytic oil generation from biomass co-pyrolysis process at 400 °C [9, 42].



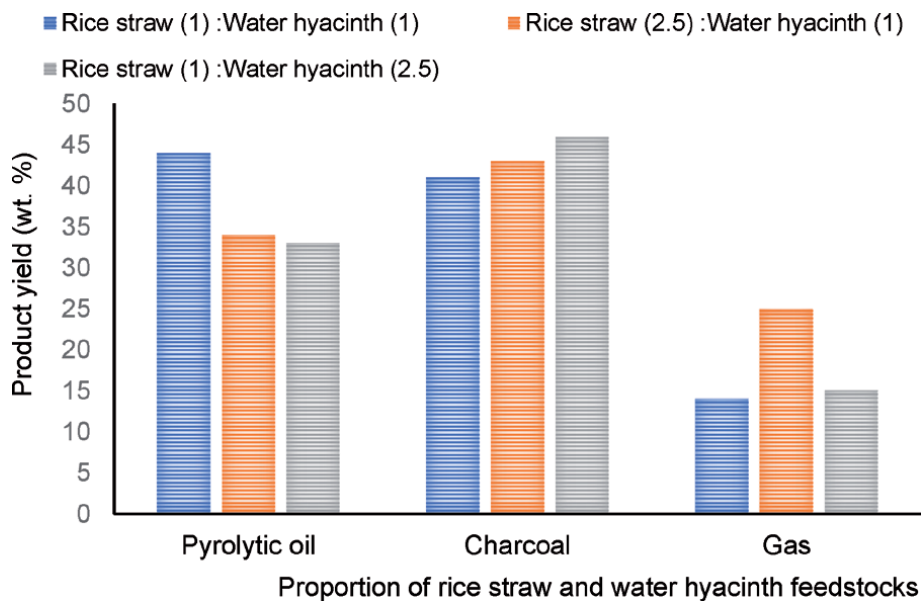


**Figure 8.** Product yield generation from different proportion of rice straw and water hyacinth in co-pyrolysis process [42].

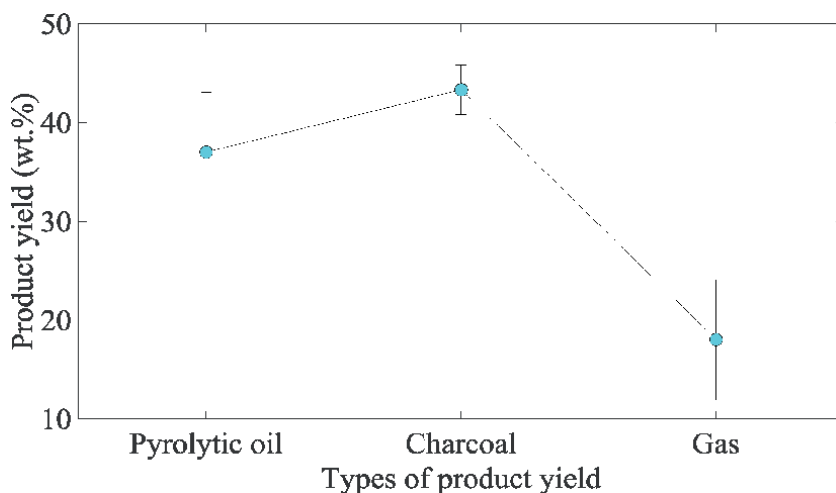


**Figure 9.** Statistical analysis of product yield generation from the different proportion of rice straw and water hyacinth feedstocks (rice straw (1): Water hyacinth (1), rice straw (2.5): Water hyacinth (1), and rice straw (1): Water hyacinth (2.5)) in co-pyrolysis process.

co-pyrolysis of pinewood with waste plastic (polystyrene) feedstock materials produced the highest yield of liquid (pyrolytic oil) than solid (charcoal) and gas yield at an equal proportion of pinewood and waste plastic (polystyrene) (1:1). It was also found that with the increase of waste plastic (polystyrene) proportion with pinewood, the liquid (pyrolytic oil) yield was increased but solid (charcoal) yield decreased [47]. This trends were statistically significant. On the other hand, a high proportion of pinewood with waste plastic (polystyrene) reduced the liquid yield from the liquid yield of an equal amount of pinewood with waste plastic (polystyrene), as shown in **Figure 10**.

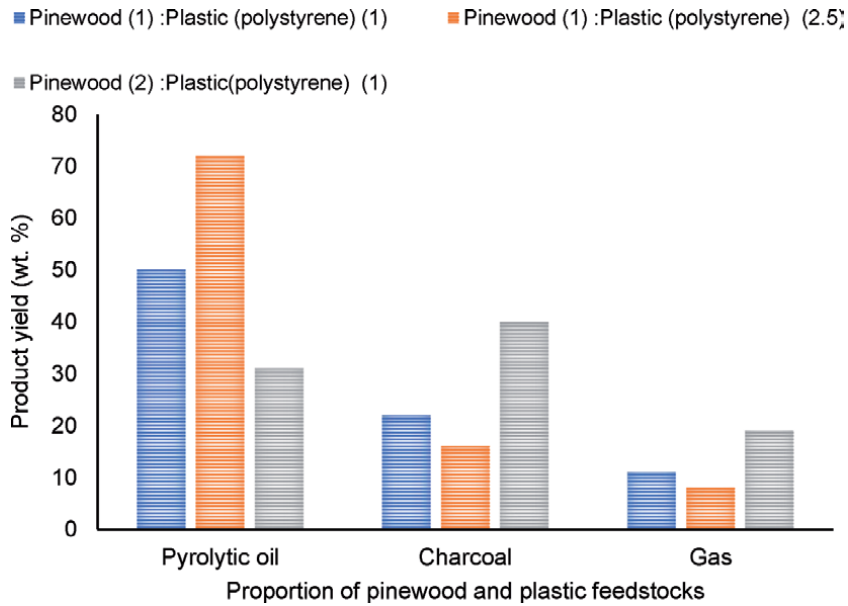


**Figure 10.** Product yield generation from different proportion of pinewood and waste plastic (polystyrene) in co-pyrolysis process [47].

**Figure 11** presents the mean and standard deviation of the product yield wt. % for three different compositions of pinewood and plastic (polystyrene) feedstocks. It is seen from **Figure 11** that the variation of a gas yield with the change of composition of pinewood and plastic (polystyrene) was lower than liquid (pyrolytic oil) and solid yield (charcoal) yield.

### 5.2 Characteristics analysis

In the co-pyrolysis process, the quality of the generated pyrolytic oil is better than the pyrolysis process. As a consequence, the oxygen content in the pyrolytic

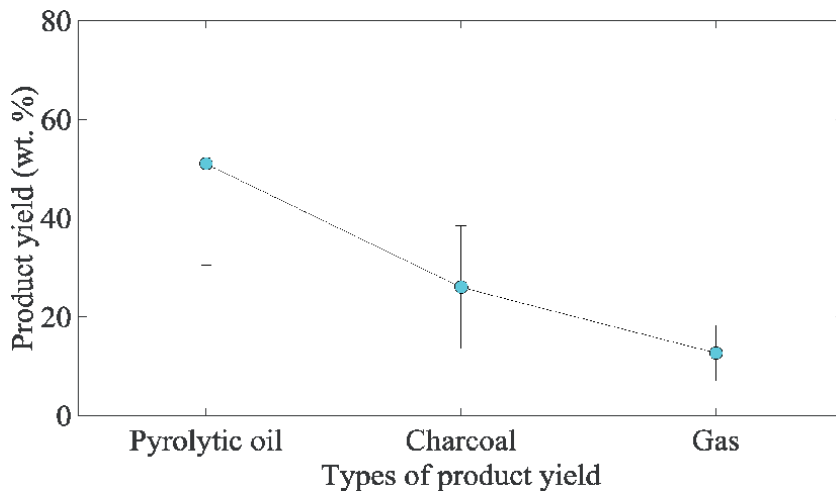


**Figure 11.** Statistical analysis of product yield generation from the different proportion of pinewood and plastic (polystyrene) feedstocks (pinewood (1): Plastic (polystyrene) (1), pinewood (1): Plastic (polystyrene) (2.5), and pinewood (2): Plastic (polystyrene) (1)) in co-pyrolysis process.

Feedstock materials	Calorific value (MJ/kg) of solids	Calorific value (MJ/kg) of liquids	Calorific value (MJ/kg) of Diesel
Pinewood- plastic (polystyrene) [47]	33 ~ 45	32 ~ 45	45.5
Rice straw-water hyacinth [48]	32 ~ 42	33 ~ 42	45.5

**Table 6.**  
*Calorific value of product yield of co-pyrolysis process.*

oil generated from the co-pyrolysis method is lower than the pyrolysis process. However, to improve or upgrade pyrolytic oil in the pyrolysis method requires an intermediate process that increases the complexity and cost. Hence, this chapter considers only the co-pyrolysis process of biomass feedstock materials and their related characteristics.

However, the calorific value of pyrolytic oil and gas generated in the co-pyrolysis process for pinewood-waste plastic or rice straw-water hyacinth was higher than the calorific value of product yield when used only pinewood or rice straw or water hyacinth feedstock biomass. **Table 6** presents the calorific value of different feedstock materials in pyrolysis and co-pyrolysis process.

Overall, the generation of liquid yield (pyrolytic oil) and solid yield (charcoal) in the co-pyrolysis method increases with the increase of temperature of the pyrolysis reactor. However, the required temperature of the co-pyrolysis process (300–450 °C) is lower than the temperature required for the pyrolysis process (550–750 °C).

## 6. Conclusion

Biomass is a bio-renewable source of energy. It can be used to generate energy through the pyrolysis and co-pyrolysis process. The generated liquid and gas yield in the pyrolysis and co-pyrolysis method can be used with conventional fuel. However, due to higher dissolved oxygen in pyrolytic oil produced in the pyrolysis process, they are required to be improved or upgraded that makes the process complex and costly. Therefore, the co-pyrolysis process is used that can generate better quality and, upgraded liquid and gas yield. The co-pyrolysis process requires a lower reactor temperature than the pyrolysis process. In this study, co-pyrolysis of rice straw with water hyacinth and pinewood with waste plastic feedstock materials have been analyzed. It is seen that with the increase of pyrolysis reactor temperature, the liquid yield (pyrolytic oil) production also increases. However, if the reactor temperature exceeds 400 °C then the generation of liquid yield decreases. On the other hand, the generation of solid (charcoal), liquid (pyrolytic oil), and gas yield depend on the proportion of feedstock biomasses in the co-pyrolysis process. The calorific value of product yield in the co-pyrolysis process is higher than the pyrolysis process and comparable with conventional fuel, such as diesel. Therefore, the biomass co-pyrolysis process would be a potential source of bio-renewable energy that can fulfill the global energy demand with conventional fuel.

## Acknowledgements

Authors would like to acknowledge the department of Mechanical Engineering, Rajshahi University of Engineering & Technology, Bangladesh for the support of accessing the laboratory facilities to study the pyrolysis and co-pyrolysis process.

## **Author details**

Md. Emdadul Hoque\* and Fazlur Rashid  
Department of Mechanical Engineering, Rajshahi University of Engineering and  
Technology, Rajshahi, Bangladesh

\*Address all correspondence to: emdadulhoque@gmail.com

## **IntechOpen**

---

© 2021 The Author(s). Licensee IntechOpen. This chapter is distributed under the terms of the Creative Commons Attribution License (<http://creativecommons.org/licenses/by/3.0>), which permits unrestricted use, distribution, and reproduction in any medium, provided the original work is properly cited. 

## References

- [1] Shafiee, S. and E. Topal, When will fossil fuel reserves be diminished? Energy policy, 2009. 37(1): p. 181-189.
- [2] Hoque, M.E., Rashid, F., M. Prodhan, and A. Arman. Analysis of Energy Consumption and Efficiency to Reduce Power Losses in Industrial Equipment. in International Conference on Mechanical Engineering, BUET, 18-20 December, 2017, Bangladesh.
- [3] Hoque, M. E., Biswas, A., Rashid, F., Saad, A.M., and Bir, P.K., production of electricity from renewable energy sources for home appliances and nano-grid, in Proceedings of the International Conference on Mechanical Engineering and Renewable Energy, 26-29 November 2015, CUET, Bangladesh.
- [4] Rashid, F., Hoque, M.E., K. Peash, and F. Faisal, performance analysis and investigation for the development of energy efficient building, in Proceedings of the International Conference on Mechanical Engineering and Renewable Energy, 18-20 December 2017, CUET, Bangladesh.
- [5] Agarwal, A.K., Biofuels (alcohols and biodiesel) applications as fuels for internal combustion engines. Progress in energy and combustion science, 2007. 33(3): p. 233-271.
- [6] Manzano-Agugliaro, F., A. Alcayde, F.G. Montoya, A. Zapata-Sierra, and C. Gil, Scientific production of renewable energies worldwide: An overview. Renewable and Sustainable Energy Reviews, 2013. 18: p. 134-143.
- [7] Uddin, M.S., Islam M.S., Rashid F., I.M. Habibulla, and N. Haque, Energy and Carbon Footprint Analysis of University Vehicles in Bangladesh, in Proceedings of the International Conference on Mechanical, Industrial and Materials Engineering, 28-30 December 2017, RUET, Bangladesh.
- [8] Key world energy statistics. 2007: International Energy Agency Paris.
- [9] Abnisa, F. and W.M.A.W. Daud, A review on co-pyrolysis of biomass: an optional technique to obtain a high-grade pyrolysis oil. Energy Conversion and Management, 2014. 87: p. 71-85.
- [10] Wang, C., H. Bi, Q. Lin, X. Jiang, and C. Jiang, Co-pyrolysis of sewage sludge and rice husk by TG-FTIR-MS: Pyrolysis behavior, kinetics, and condensable/non-condensable gases characteristics. Renewable Energy, 2020. 160: p. 1048-1066.
- [11] Bridgwater, A., D. Meier, and D. Radlein, An overview of fast pyrolysis of biomass. Organic geochemistry, 1999. 30(12): p. 1479-1493.
- [12] Vitolo, S., M. Seggiani, P. Frediani, G. Ambrosini, and L. Politi, Catalytic upgrading of pyrolytic oils to fuel over different zeolites. Fuel, 1999. 78(10): p. 1147-1159.
- [13] Guillain, M., K. Fairouz, S.R. Mar, F. Monique, and L. Jacques, Attrition-free pyrolysis to produce bio-oil and char. Bioresource technology, 2009. 100(23): p. 6069-6075.
- [14] Oasmaa, A. and S. Czernik, Fuel oil quality of biomass pyrolysis oils state of the art for the end users. Energy & Fuels, 1999. 13(4): p. 914-921.
- [15] Parihar, M., M. Kamil, H. Goyal, A. Gupta, and A. Bhatnagar, An experimental study on pyrolysis of biomass. Process Safety and Environmental Protection, 2007. 85(5): p. 458-465.
- [16] Zhang, Q., J. Chang, T. Wang, and Y. Xu, Review of biomass pyrolysis oil properties and upgrading research. Energy conversion and management, 2007. 48(1): p. 87-92.

- [17] Pourkarimi, S., A. Hallajisani, A. Alizadehdakhel, and A. Nouralishahi, Biofuel production through micro- and macroalgae pyrolysis—a review of pyrolysis methods and process parameters. *Journal of Analytical and Applied Pyrolysis*, 2019. 142: p. 104599.
- [18] Demirbas, A., Effects of temperature and particle size on bio-char yield from pyrolysis of agricultural residues. *Journal of analytical and applied pyrolysis*, 2004. 72(2): p. 243-248.
- [19] Uzoejinwa, B.B., X. He, S. Wang, A.E.-F. Abomohra, Y. Hu, and Q. Wang, Co-pyrolysis of biomass and waste plastics as a thermochemical conversion technology for high-grade biofuel production: Recent progress and future directions elsewhere worldwide. *Energy conversion and management*, 2018. 163: p. 468-492.
- [20] Sharypov, V., N. Marin, N. Beregovtsova, S. Baryshnikov, B. Kuznetsov, V. Cebolla, and J. Weber, Co-pyrolysis of wood biomass and synthetic polymer mixtures. Part I: influence of experimental conditions on the evolution of solids, liquids and gases. *Journal of analytical and applied pyrolysis*, 2002. 64(1): p. 15-28.
- [21] Sharypov, V., N. Beregovtsova, B. Kuznetsov, L. Membrado, V. Cebolla, N. Marin, and J. Weber, Co-pyrolysis of wood biomass and synthetic polymers mixtures. Part III: Characterisation of heavy products. *Journal of analytical and applied pyrolysis*, 2003. 67(2): p. 325-340.
- [22] Mahari, W.A.W., C.T. Chong, W.H. Lam, T.N.S.T. Anuar, N.L. Ma, M.D. Ibrahim, and S.S. Lam, Microwave co-pyrolysis of waste polyolefins and waste cooking oil: influence of N<sub>2</sub> atmosphere versus vacuum environment. *Energy Conversion and Management*, 2018. 171: p. 1292-1301.
- [23] Mourshed, M., M.H. Masud, F. Rashid, and M.U.H. Joardder, Towards the effective plastic waste management in Bangladesh: a review. *Environmental Science and Pollution Research*, 2017. 24(35): p. 27021-27046.
- [24] Gates, B.C., G.W. Huber, C.L. Marshall, P.N. Ross, J. Siirola, and Y. Wang, Catalysts for emerging energy applications. *MRS bulletin*, 2008. 33(4): p. 429-435.
- [25] Sonobe, T., N. Worasuwannarak, and S. Pipatmanomai, Synergies in co-pyrolysis of Thai lignite and corncob. *Fuel processing technology*, 2008. 89(12): p. 1371-1378.
- [26] Blesa, M., J. Miranda, R. Moliner, M. Izquierdo, and J. Palacios, Low-temperature co-pyrolysis of a low-rank coal and biomass to prepare smokeless fuel briquettes. *Journal of Analytical and Applied Pyrolysis*, 2003. 70(2): p. 665-677.
- [27] Yuan, S., X.-l. Chen, W.-f. Li, H.-f. Liu, and F.-c. Wang, Nitrogen conversion under rapid pyrolysis of two types of aquatic biomass and corresponding blends with coal. *Bioresource technology*, 2011. 102(21): p. 10124-10130.
- [28] Anoop, E., V. Ajayghosh, J. Nijil, and C. Jijeesh, Evaluation of pulp wood quality of selected tropical pines raised in the high ranges of Idukki District, Kerala. *Journal of Tropical Agriculture*, 2014. 52(1): p. 59-66.
- [29] Mukaratirwa-Muchanyereyi, N., J. Kugara, and M.F. Zaranyika, Surface composition and surface properties of water hyacinth (*Eichhornia crassipes*) root biomass: Effect of mineral acid and organic solvent treatment. *African Journal of Biotechnology*, 2016. 15(21): p. 891-896.
- [30] Soetaredjo, F.E., Y.-H. Ju, and S. Ismadji, conversion of water hyacinth

*Eichhornia crassipes* into biofuel intermediate: combination subcritical water and zeolite based catalyst processes, special issue, Renewable energy, 64-69, 2016

[31] Shawky, B.T., M.G. Mahmoud, E.A. Ghazy, M.M. Asker, and G.S. Ibrahim, Enzymatic hydrolysis of rice straw and corn stalks for monosugars production. Journal of Genetic Engineering and Biotechnology, 2011. 9(1): p. 59-63.

[32] Yang, J., Y.C. Ching, and C.H. Chuah, Applications of lignocellulosic fibers and lignin in bioplastics: A review. Polymers, 2019. 11(5): p. 751.

[33] Aboyade, A.O., M. Carrier, E.L. Meyer, H. Knoetze, and J.F. Görgens, Slow and pressurized co-pyrolysis of coal and agricultural residues. Energy Conversion and Management, 2013. 65: p. 198-207.

[34] Quan, C., S. Xu, Y. An, and X. Liu, Co-pyrolysis of biomass and coal blend by TG and in a free fall reactor. Journal of Thermal Analysis and Calorimetry, 2014. 117(2): p. 817-823.

[35] Zhang, L., S. Xu, W. Zhao, and S. Liu, Co-pyrolysis of biomass and coal in a free fall reactor. Fuel, 2007. 86(3): p. 353-359.

[36] Yuan, S., Z.-j. Zhou, J. Li, X.-l. Chen, and F.-c. Wang, HCN and NH<sub>3</sub> released from biomass and soybean cake under rapid pyrolysis. Energy & fuels, 2010. 24(11): p. 6166-6171.

[37] Demirbas, A., Pyrolysis of ground beech wood in irregular heating rate conditions. Journal of Analytical and Applied Pyrolysis, 2005. 73(1): p. 39-43.

[38] Park, D.K., S.D. Kim, S.H. Lee, and J.G. Lee, Co-pyrolysis characteristics of sawdust and coal blend in TGA and a fixed bed reactor. Bioresource technology, 2010. 101(15): p. 6151-6156.

[39] Onay, Ö., E. Bayram, and Ö.M. Koçkar, Copyrolysis of seytömer–lignite and safflower seed: influence of the blending ratio and pyrolysis temperature on product yields and oil characterization. Energy & fuels, 2007. 21(5): p. 3049-3056.

[40] Fei, J., J. Zhang, F. Wang, and J. Wang, Synergistic effects on co-pyrolysis of lignite and high-sulfur swelling coal. Journal of Analytical and Applied Pyrolysis, 2012. 95: p. 61-67.

[41] Martínez, J.D., A. Veses, A.M. Mastral, R. Murillo, M.V. Navarro, N. Puy, A. Artigues, J. Bartrolí, and T. García, Co-pyrolysis of biomass with waste tyres: Upgrading of liquid bio-fuel. Fuel Processing Technology, 2014. 119: p. 263-271.

[42] Jin, X., N. Chen-yang, Z. Deng-yin, G. Yan-hui, H. Qi-min, and X. Yu-hong, Co-pyrolysis of rice straw and water hyacinth: Characterization of products, yields and biomass interaction effect. Biomass and Bioenergy, 2019. 127: p. 105281.

[43] Nwokolo, N., S. Mamphweli, and G. Makaka, Analytical and thermal evaluation of carbon particles recovered at the cyclone of a downdraft biomass gasification system. Sustainability, 2017. 9(4): p. 645.

[44] Yao, D., H. Yang, H. Chen, and P.T. Williams, Co-precipitation, impregnation and so-gel preparation of Ni catalysts for pyrolysis-catalytic steam reforming of waste plastics. Applied Catalysis B: Environmental, 2018. 239: p. 565-577.

[45] Bernardo, M., N. Lapa, M. Gonçalves, B. Mendes, F. Pinto, I. Fonseca, and H. Lopes, Physico-chemical properties of chars obtained in the co-pyrolysis of waste mixtures. Journal of Hazardous Materials, 2012. 219: p. 196-202.

[46] López, A., I. De Marco, B. Caballero, M. Laresgoiti, and A. Adrados, Dechlorination of fuels in pyrolysis of PVC containing plastic wastes. *Fuel Processing Technology*, 2011. 92(2): p. 253-260.

[47] Paradela, F., F. Pinto, I. Gulyurtlu, I. Cabrita, and N. Lapa, Study of the co-pyrolysis of biomass and plastic wastes. *Clean Technologies and Environmental Policy*, 2009. 11(1): p. 115-122.

[48] Huang, L., C. Xie, J. Liu, X. Zhang, K. Chang, J. Kuo, J. Sun, W. Xie, L. Zheng, and S. Sun, Influence of catalysts on co-combustion of sewage sludge and water hyacinth blends as determined by TG-MS analysis. *Bioresource technology*, 2018. 247: p. 217-225.



---

Section 2

# Gasification

---



# Chemical Carbon and Hydrogen Recycle through Waste Gasification: The Methanol Route

*Alessia Borgogna, Gaetano Iaquaniello, Annarita Salladini,  
Emanuela Agostini and Mirko Boccacci*

## Abstract

A large amount of valuable Carbon and Hydrogen is lost in the disposal of the non-recyclable fraction of Municipal Solid Waste (MSW) – particularly unsorted waste fraction and plastics residue from mechanical recycle process. The waste-to-chemical technology allows to exploit the components entrapped in the non-recyclable waste by converting it into new chemicals. The core of waste-to-chemical technology is the gasification process, which is designed to convert waste into a valuable syngas to be used as example for methanol production. Waste to methanol schemes allow to achieve significant environmental and economic benefits, which can be further intensified within the scenario of increasing share of renewable energy.

**Keywords:** Waste gasification, carbon recycle, methanol, hydrogen

## 1. Introduction

By now, it is undeniable the (negative) impact that human activities have on environmental and climate conditions. The concentration of CO<sub>2</sub> in the atmosphere has reached 415 ppm [1]; a value which has no comparison throughout mankind history, and even before [2].

The discrepancy between the rate at which humans consume fossil resources and the earth's capability of absorbing emitted carbon and reproducing natural carbon resources is glaring [3]; and it represents the rationale behind the climate change issue. Therefore, this is today the problem to tackle.

To such end, three conceptual typologies of intervention can be identified. Reducing the emissions deriving from human activities; resorting to different (renewable) carbon sources; directly helping the planet absorb CO<sub>2</sub> in excess. These three interventions do not exclude one another – i.e., they can be deployed simultaneously. As a matter of fact, every kind of contributions may result essential to avoiding reaching the point of no return in relation to earth's climate change.

As for the first type of intervention, emissions can be abated by directly reducing our consumption. This can be achieved by limiting the use of throwaway material; by applying sharing and sustainable mobility [4]; by increasing environmental efficiency of each productive process – i.e., limiting the emissions of CO<sub>2</sub> per unity of product achieved.

Second type of intervention – which has a lower impact on our habits and lifestyle. Using a source of carbon which could be timely reproduced – algae represent one of the most recent examples thereof [5]. However, attention must be paid to the compatibility of the source exploitation with other environmental and social constraints, water usage and food production competition. Indeed, European Commission adds to the criteria for environmental evaluation of biofuels the Indirect Land Usage Change (ILUC) factors [6].

Third and final type of intervention. Technology and innovation should also serve the ambitious aim of finding systems able to remove the CO<sub>2</sub> excess already present in the atmosphere. An example thereof is direct capture of CO<sub>2</sub> from air, which, however, is far from being economically competitive. As a matter of fact, by 2019 only 15 plant with an overall capacity of about 9 ktCO<sub>2</sub> captured per year have been implemented [7]. This value is quite far from 30 Gton/y of CO<sub>2</sub> which is the reduction of emissions estimated to be required for limiting the global warming below 2°C [8].

Conversion of waste into a chemical encompasses both the first and the second type of intervention. In this way, waste is utilized as a source of carbon and hydrogen, thus representing a renewable source which is produced at a sufficiently high rate directly through the community, thus being (quite) proportional distributed and available, without any geographical restriction. About 2 billion Mtons per year of waste are globally produced. By 2050 it is foreseen to reach 3.4 billion of Mtons, due to the expected increase of population and GDP, which both influence waste production value per year [9]. Further, this source does not imply indirect usage of land, on the contrary it is a clever alternative to landfill.

As a matter of fact, both chemical production and waste disposal imply high greenhouse gases (GHG) emissions. Integration of these two processes into one allows to significantly reduce overall emissions.

What described above is only one of the successful aspects of the waste-to-chemical process. Economical aspect is also a favorable factor of a kind of process able to simultaneously convert waste and produce chemicals. Differently from what has been commonly seen till now, regarding chemical production economics, the main sources of income are two: - the usual one, the selling of the product; – the unconventional one, a gate fee for the feedstock, i.e. a payment for the disposal of the waste.

The waste fractions which are taken into account as sources in the waste-to-chemical process are indeed fractions which alternatively would have been disposed through – at worst – landfilling or – at best – incineration with energy recovery. While, the waste-to-chemical process allows carbon and hydrogen recovery, i.e. contextually material and energy recovery.

Refuse Derived Fuel (RDF), dry fraction of unsorted fraction of Municipal Solid Waste (MSW), and unrecycled fraction of plastic sorted waste, are kind of waste eligible for the waste-to-chemical process. It is worth noting that these fractions come from social and technological constraints relating to the practical recyclability of MSW.

The waste-to-chemical process allows to convert the mentioned kinds of waste thank to its core section, a high temperature melting gasifier. Here, due to the high temperature reached, the combustible part of the feed is converted into valuable syngas, meanwhile the inorganic part is melted and then vitrified. A completely inert residue is produced. Further, it can be also used for rockwool production or as inert filling in the civil sector material. Thus, zero residue from MSW can be reached, by integrating the waste-to-chemical process with technologies for material recycle available by now.

The syngas produced can be applied for methanol production, after tailored syngas purification. The chapter includes a technical, economic and environmental

assessment of the overall technology, from waste conversion to methanol production. Two possible schemes are exposed, the second one integrates a base waste to methanol process with electrolysis, showing how waste to chemical is a feasible technology able to accompany process industry in the pathway of energy transition.

## 2. High temperature gasification for waste valorization

As already mentioned, waste feedstock like Municipal solid Waste, Refuse Derived Fuel (RDF) and plastics residues, due to the high content of carbon and hydrogen, may be considered a sort of alternative and sustainable feedstock. Typical compositions for the above-mentioned waste are reported in the **Table 1**. As shown by the elementary composition, carbon content varies in the range 30–60%w while hydrogen in the range 4–7%w.

If properly converted, these kinds of wastes may be used in substitution of conventional fossil feedstock building a new chemistry pathway allowing to produce conventional chemicals in a more sustainable way [10].

Under this scenario technology plays a major role in the fully implementation of circular economy around the concept of waste as feedstock for industrial processes. This paradigm implies a robust and reliable technology able to manage the heterogeneous nature of waste as well as their pollutants content.

The proposed technology allowing to convert waste into chemicals, is based on a high temperature gasification process carried out under pure oxygen environment. A schematic view of gasifier reactor allowing to perform such conversion is shown in **Figure 1**.

The gasifier reactor consists of three sections: the melting zone (1600°C), where exothermic reactions and melting of inert compounds take place; the gasification zone (600–800 C°), where low oxygen-content brings to partial oxidation reactions; the stabilization zone, where a further introduction of auxiliary fuel and oxygen lead to an increase of temperature (1100°C) ensuring tar degradation, full decomposition of the long chain organic molecules and inhibition of dioxins formation.

Multiple injection of oxygen and auxiliary fuel along the reactor, take temperature in order of 1600–2000°C in the bottom, 600–800°C in the middle up to 1100–1200°C on the top. Such temperature profile assures a full conversion of waste into

Component	Value	RDF	PW
Wet basis			
C	% weight	33–38	47–61
H	% weight	4–5	5–7
O	% weight	16–18	14–20
N	% weight	0.2–1.0	0.2–0.5
S	% weight	0.02–0.15	0.02–0.3
Cl	% weight	0.8–1.5	0.8–1.5
Moisture	% weight	17–21	5–9
Inert	% weight	17–25	7–20
LHV <sub>wet</sub>	MJ/kg	14–16	21–24

**Table 1.**  
*Typical elementary composition of PW and RDF and relevant LHV values.*

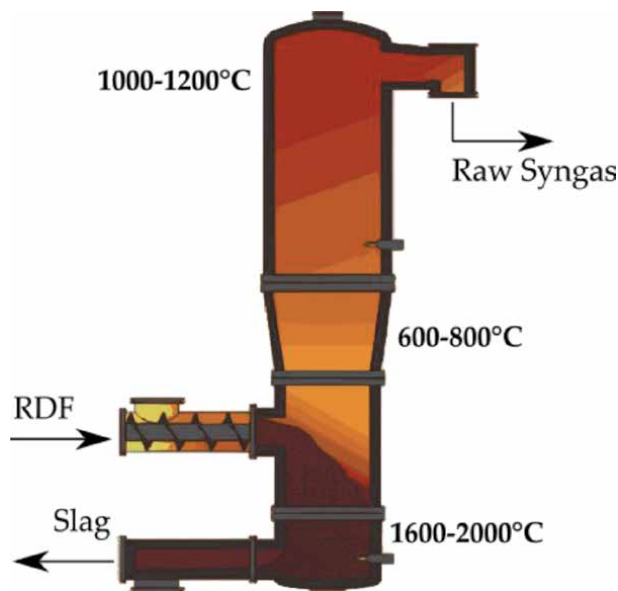


**Figure 1.**  
*High temperature gasification reactor.*

two products: a high valuable syngas rich in  $H_2$ , CO and free of char, tar, dioxin and furans (Iaquaniello et al. 2018) discharged from the top of reactor and an inert vitrified material discharged on the bottom [11]. The high temperature held on the melting zone allows to discharge the inert components of waste (mineral and metals), in a granulated and vitrified state ideally carbon free. Depending on local legislation, such material can be valorized into cement or construction industry otherwise disposed as standard waste.

As reported by Salladini et al. [12], the syngas yield and relevant composition, are mainly affected by the LHV value and C/O ratio. On the overall higher LHV results into higher syngas yield as well as higher content in terms of CO and  $H_2$  and lower concentration of  $CO_2$ . Produced syngas contains as major components CO,  $H_2$ ,  $CO_2$  and under minor content volatile metals and any particles up drafted with the syngas. **Figure 2** reports a block diagram of the gasification section, preliminary cleaning and syngas purification section.

As first step the hot gas is routed to an evaporative quench where temperature is abruptly reduced down to  $85\text{--}90^\circ\text{C}$  by direct injection of water. Although there is a loss of high temperature heat, this rapid cooling freezes chemical composition achieved at high temperature avoiding any undesired reaction. The two-phase mixture at the bottom exit of quench is routed to a sedimentation tank. This unit allows to collect on the bottom the sludge, continuously removed from the system, and clarified water reused as cooling water in the quench. The Sedimentation works under low pH condition (1.5–3) in order to promote the migration of volatile metals in liquid phase. The syngas exiting the sedimentation tank is routed to an acidic column that further promote the metal removal.

Syngas exiting from the acidic columns of each gasification line is collected and sent to a common section based on alkaline scrubbing column, wet electrostatic precipitators (WESP) and subcooling column. Water stream collected from the bottom of the washing columns due to the potential content of pollutants are routed to the WasteWater Treatment unit.

Gasifier works under quite atmospheric pressure achieving at the end of cleaning section pressure in order of few mbar above the atmospheric pressure. It

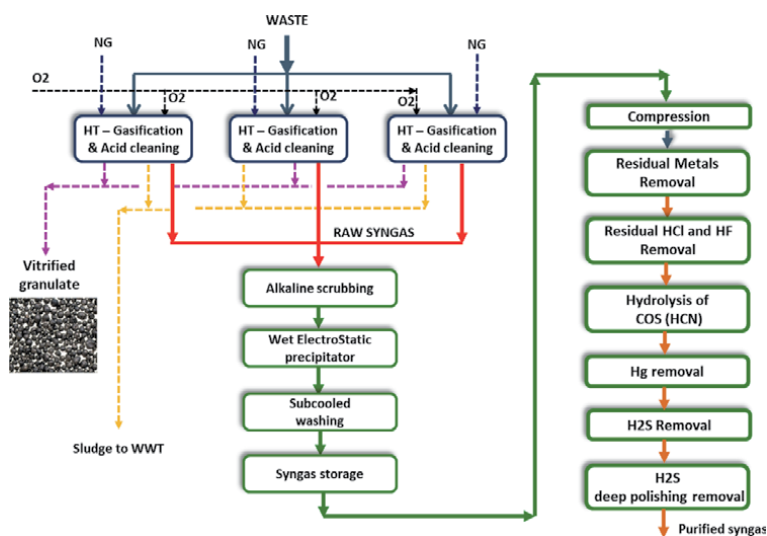


**Figure 2.**  
 Block scheme: Gasification and syngas primary gas cleaning.

derives that a compression section is needed before routing the syngas to downstream section. In order to assure stable condition in terms of syngas pressure and flowrate at suction of compressors, a gas holder is installed between the gasification section and compression.

The cleaned syngas still contains sulfur compounds mainly in the form of  $H_2S$  and COS together with residual chlorine, HCN and trace of Hg. Once compressed, syngas is routed to the purification section involving the following step: removal of residual dust and metals, removal of HCl, hydrolysis of the COS and HCN,  $H_2S$  removal through an oxy-reduction system and a final polishing step based on zinc oxide absorbents in order to reduce sulfur content down to ppb as required by catalyst adopted for downstream synthesis.

The high temperature regime and the use of a waste as feedstock, requires dedicated maintenance work around the gasifier aiming at preventing damages on refractory materials and avoiding excessive fouling along the quench wall and sedimentation. On this regard a plant architecture based on multiple gasification lines working in parallel is foreseen in order to assure plant availability during maintenance operation: when a gasification line is kept shut down for maintenance service, the other lines are kept under maximum capacity to assure a continuous syngas production with a minimum reduction of productivity.

The purification procedure described above, delivers a syngas suitable to be fed to catalyst-based synthesis. Depending on selected end product, a conditioning step aiming at adjustment of  $H_2$  and CO content is required [13, 14].

### 3. Waste to methanol scheme

The proposed waste to methanol case study will be developed around a waste feedstock having an average composition describing a mixture of 75% RDF and 25% plastic residues. Resulting mixture composition is reported in **Table 2**.

By applying the process scheme depicted in **Figure 2**, resulting syngas composition at the end of syngas cleaning (inlet compression) and downstream the purification step is reported in **Table 3**. A very low level of contaminants are achieved

Component	U.m.	Value
Wet basis		
C	% weight	38.9
H	% weight	5.3
O	% weight	21.5
N	% weight	0.85
S	% weight	0.20
Cl	% weight	0.94
Moisture	% weight	15.7
Inert	% weight	16.5
LHV	MJ/kg	16.0

**Table 2.**  
Waste used for the case study (mixture 75% RDF-25% plastics).

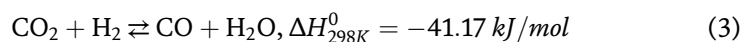
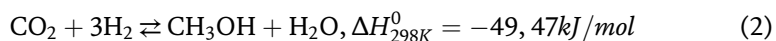
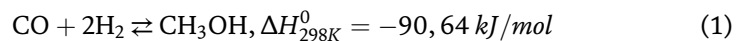
Component	Downstream cleaning section		Downstream purification section
	u.m.	Value	Value
H <sub>2</sub>	%mol	37.6	39.1
CO	%mol	41.0	42.6
CO <sub>2</sub>	%mol	12.4	12.8
H <sub>2</sub> O	%mol	4.0	0.4
N <sub>2</sub>	%mol	4.6	4.8
CH <sub>4</sub>	%mol	0.21	0.21
Arg	%mol	0.03	
H <sub>2</sub> S	ppm	930	0.01
COS	ppm	45	0.1
HCN	ppm	10	0.1
HCl	ppm	4.1	0.1
Hg	ppm	0.02	—
PM	ppm	0.3	—

**Table 3.**  
Syngas composition.

through the proposed architecture thus accounting for a syngas to be used as building block for downstream synthesis.

To proper design the condition section, it is necessary to understand constraint required on syngas composition.

Methanol synthesis is based on the following catalytic reactions where only two are linearly independent:





According to the stoichiometry of reactions involved (1)–(3), a proper content of H<sub>2</sub>, CO and CO<sub>2</sub> has to be assured in the gas mixture fed to methanol loop. Such content is controlled by introducing the following parameter named Methanol Module (MM) is defined:  $MM = (H_2 - CO_2)/(CO + CO_2)$ .

The stoichiometric MM is equal to 2, thus a value of MM around 2.0–2.4, is generally recommended in the industrial plant [15].

As reported in **Table 3**, resulting syngas is characterized by a low value of MM (0.47) meaning that an excess of carbon or rather a deficit of hydrogen exists. In order to achieve required composition for methanol synthesis, two different approaches may be adopted. One option is to increase the hydrogen content through water gas shift reaction and reduce the resulting excess carbon in the form of pure CO<sub>2</sub> while another option is to add an external source of H<sub>2</sub> to balance the deficit. Such H<sub>2</sub> would be preferably produced from water electrolysis powered from renewable source in order to avoid any indirect fossil CO<sub>2</sub> emissions.

### 3.1 Waste to methanol scheme with internal hydrogen production

The process architecture for methanol production from waste based on internal hydrogen production, is depicted in **Figure 3**. As introduced above, without foresee any additional external source of Hydrogen, to comply the methanol module it is necessary to increase the internal H<sub>2</sub> content through water gas shift reaction by reacting CO and H<sub>2</sub>O to produce CO<sub>2</sub> and H<sub>2</sub>.



To promote shift reaction, medium steam is mixed at the inlet of the shift reactor, operating with a steam/dry-syngas ratio at least of 1.5 in order to manage the shift exit temperature below 480°C. As shown by the stoichiometry, the shift reaction accounts for an increase of hydrogen content but does not allow any variation in the MM therefore a CO<sub>2</sub> removal system is required to achieve proper composition as per methanol module. To achieve a MM in order of 2.1, only a fraction of purified syngas has to be routed to the conditioning section based on shift reaction and CO<sub>2</sub> removal system [16]. The higher the fraction of syngas

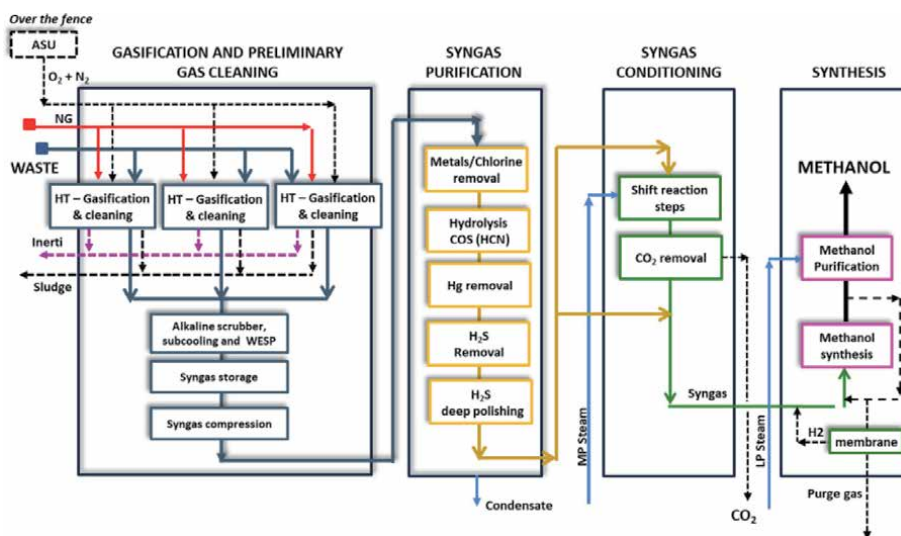


**Figure 3.** Waste to methanol scheme with internal H<sub>2</sub> production (scenario a).

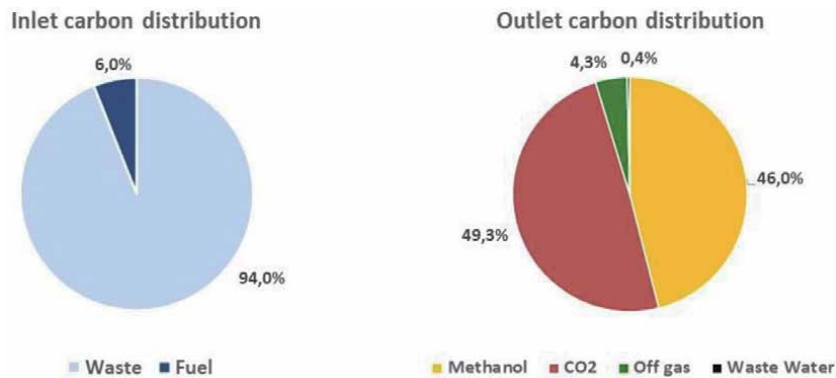


**Figure 4.** Carbon distribution of the waste to methanol scheme with internal H<sub>2</sub> production. Scenario A.

conditioned, the higher is the carbon converted into CO<sub>2</sub> that means a lower fraction converted into final product. The sweet syngas coming from CO<sub>2</sub> removal system is reconnected with fresh syngas. To increase carbon utilization, a recovery of pure hydrogen through a membrane separation is applied on the bleed stream coming from methanol loop normally routed to combustion. The target value of MM = 2.1 at the inlet of methanol section, is thus achieved through the addition of H<sub>2</sub> recovered from methanol loop.

The resulting conditioned syngas is compressed and routed to the methanol synthesis reactor. The raw methanol is recovered by condensation and then purified via distillation in order to fulfill the required grade.

In the proposed architecture three gasification lines are adopted with an overall capacity of about 192.000 ton/y of waste and around 98.000 ton/y of methanol. As described above, the excess carbon contained in the waste is discharged as pure CO<sub>2</sub> to battery limits. It derives that it can be reused for any application ranging from food industry or other industrial application. Without any external H<sub>2</sub> addition, the proposed scheme based on feedstock reported in **Table 2**, allows to fix around 46% of incoming carbon into the methanol and to deliver at battery limits around 49% of carbon as pure CO<sub>2</sub> as shown by carbon distribution graph in **Figure 4**. The residual is discharged into the atmosphere as diluted flue gas. Such distribution accounts for a production of 1.07 ton pure CO<sub>2</sub>/ton MeOH and around 0,094 ton diluted CO<sub>2</sub>/ton MeOH as flue gas. A conventional methanol production scheme based on fossil feedstock performs higher direct CO<sub>2</sub> emission in the form of flue gas ranging from 0.52–0.70 ton CO<sub>2</sub>/ton MeOH once based on natural gas steam reforming, up to 1.4 ton CO<sub>2</sub>/ton MeOH once the reference scheme is partial oxidation of fossil oil [17].

Heat and material balance around the proposed scheme have been performed through Aspen Plus Process simulator. Main results in terms of products and by-product production as well as utilities consumption are reported in **Table 4**.

As shown in Block diagram depicted in **Figure 3**, a purge gas stream suitable to be used as fuel is delivered to battery limits. To take care of its residual calorific value, it was calculated the equivalent natural gas saving and properly considered in the OPEX evaluation.

### 3.2 Waste to methanol scheme with addition of external hydrogen

As discussed above, a different approach in managing the syngas composition characterized by an excess of carbon may be adopted. The latter consist into an

Feed/Product/bioproduct	Quantity per year	U.m.
Waste feedstock	192.000	ton/y
Methanol production	98.000	ton/y
Granulated	31872	t/y
Sludge	7520	t/y
Utilities	Quantity per year	U.m.
Electric Power	110720	MWh/y
Well water	256800	m <sup>3</sup> /y
Demi water	5600	m <sup>3</sup> /y
BFW	149037	m <sup>3</sup> /y
Medium Pressure (MP) steam	81936	ton/y
Low Pressure (LP) steam	126304	ton/y
Natural Gas	6456	ton/y
Instrument Air	10104000	Nm <sup>3</sup> /y
Nitrogen	12800000	Nm <sup>3</sup> /y
Oxygen	75840000	Nm <sup>3</sup> /y
Cooling water	23656000	m <sup>3</sup> /y
NG saving through off-gas energy recovery	2800	ton/y

**Table 4.**  
 Heat and material balance scenario a.

external addition of hydrogen in order to achieve a better carbon utilization. An overall simplification of process scheme is obtained considering that shift reaction and carbon removal system are no more required.

On this regards the conditioning section results into a mixing between the external Hydrogen stream and the purified syngas. Source of external hydrogen would be preferably derived from water electrolysis in order to benefit of the oxygen coproduced by the electrolysis.

Corresponding process scheme is reported in **Figure 5**.

In this scenario for the same overall waste capacity of about 192.000 ton/y, the Methanol productivity is quite doubled reaching a value of around 196.000 ton/y. Such architecture allows to fix around 92.5% of carbon in the final end-product thus reducing to around 7% the amount lost in the off gas (**Figure 6**). The resulting direct emission factor is equal to 0.075 ton diluted CO<sub>2</sub>/ton MeOH with a consistent reduction in comparison to conventional routes. In terms of direct CO<sub>2</sub> emissions, the Scenario B allows for a better valorization of carbon contained in the waste increasing the fraction transferred into the product.

Of course, looking at indirect CO<sub>2</sub> emission, the overall environmental performance of this configuration will be directly related to emission of the electric energy source in terms of ton CO<sub>2</sub>/MWh.

Main results of Heat and material balance around the H<sub>2</sub> assisted Waste to Methanol scheme is reported in the **Table 5**.

Due to the high electric energy consumption associated to the use of electrolysis, this figure becomes feasible from economic and environmental point of view under low electric energy price and high sharing of renewables into the electric energy system.

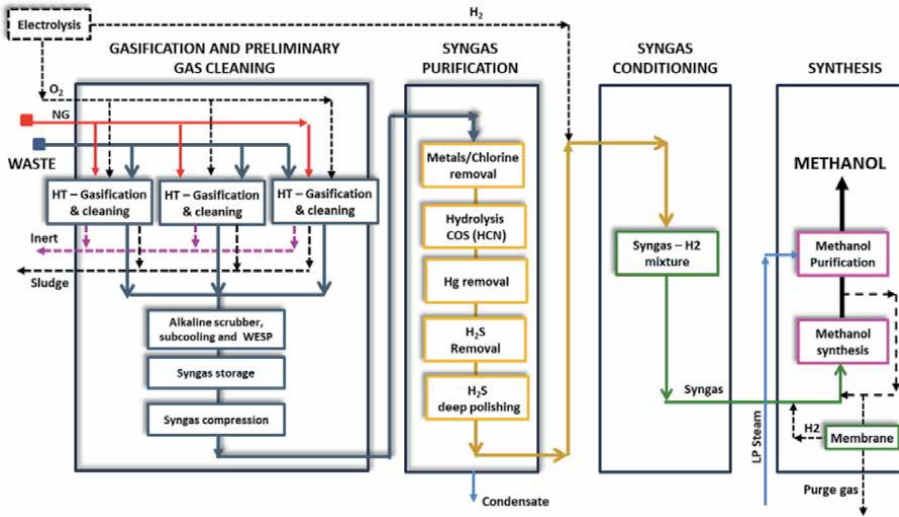


Figure 5. Waste to methanol scheme with external H<sub>2</sub> addition (scenario B).

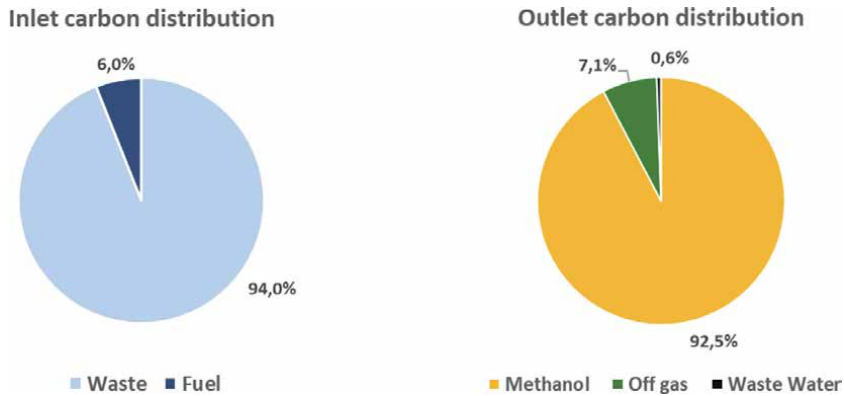


Figure 6. Carbon distribution of the waste to methanol scheme with external H<sub>2</sub> addition.

#### 4. Evaluation of methanol cost of production

In order to assess the economic feasibility of the waste to methanol technology, an economical evaluation has been carried out based on Capital EXpenditures (CAPEX) and OPERating EXpenditures (OPEX) around the above-described schemes: the scenario A where syngas conditioning is performed by internal hydrogen production at the expense of CO, and scenario B where syngas conditioning is achieved through external H<sub>2</sub> addition.

The overall CAPEX has been evaluated starting from the cost of equipment and applying proper multiplying factor to take into account all cost contribution to the CAPEX (erection, civil work, engineering activities etc.) (Table 6) [18].

In order to evaluate OPEX and related methanol cost of production, the following assumptions in terms of specific cost of utilities has been adopted (Table 7).

On the basis of utilities consumption derived from heat and material balance (Tables 4 and 5), OPEX for the two scenarios have been estimated as reported in Table 8.

Feed/Product/bioproduct	Quantity per year	U.m.
Waste feedstock	192.000	Ton/y
Methanol production	196.000	ton/y
Granulated	31872	t/y
Sludge	7520	t/y
Sulfur cake	680	t/y
Waste water	88000	t/y
Utilities	Quantity per year	U.m.
Electric Power process consumption	165798	MWh/y
Electric Power electrolysis	936000	MWh/y
Well water	503328	m <sup>3</sup> /y
Demi water	176189	m <sup>3</sup> /y
BFW	292113	m <sup>3</sup> /y
MP steam	0	ton/y
LP steam	126304	ton/y
Natural Gas	6456	ton/y
Instrument Air	10104000	Nm <sup>3</sup> /y
Nitrogen	12840000	Nm <sup>3</sup> /y
Oxygen	0	Nm <sup>3</sup> /y
Cooling water	45404820	m <sup>3</sup> /y
NG saving through off-gas energy recovery	1021	ton/y

**Table 5.**  
 Heat and material balance scenario B.

	Scenario A	Scenario B
	M€	M€
CAPEX ISBL	193	214
ELECTROLYSYS	—	128
CAPEX OSBL	35	40
Contingency (10%)	22	38
<b>TOTAL</b>	<b>250</b>	<b>420</b>

**Table 6.**  
 CAPEX estimation for methanol case study.

Taking into account a capital structure based on 30% equity and residual 70% as bank loan, the corresponding methanol Cost of Production (COP) results into 243 €/ton and 522 €/ton for the scenario A and B respectively.

By considering a market price of grey methanol currently estimated in order of 390€/ton for the European Market [19] a minimum conservative price of 400 €/ton has been considered as market price for the *circular* methanol. On such basis the Internal rate of Return (IRR) has been estimated as a function of main parameters.

For the Scenario A, IRR has been evaluated as a function of methanol market price and waste gate fee (**Figure 7**). The base case performs a project IRR around 11% thus assessing a reasonable profitability.

Cost component	Value
Waste treatment ton/year (three gasification lines)	192000
Vitrified granulate produced ton/year	32000
Concentrated sludge produced ton/year	7500
Maintenance cost as % of the CAPEX	2%
Depreciation	0.0872
Equity (20 year and 6% interest rate)	0.0672
Bank loan (12 year and 3% interest rate)	
Personnel (at company cost) M€ per year	1.75
7 people per shift (7x5) = 35 people	0.24
3 specialist all over the working day	0.12
1 Manager	
RDF-Plastics price € per ton	150
Electric energy cost € per MWh	70
Natural gas price, € per Sm <sup>3</sup>	0.24
MP steam cost, € per ton	28.3
LP steam cost, € per ton	24.2
O <sub>2</sub> cost, € per Nm <sup>3</sup>	0.078
N <sub>2</sub> cost, € per Nm <sup>3</sup>	0.078
Instrument air, € per Nm <sup>3</sup>	0.028
Raw water, € per m <sup>3</sup>	0.08
Cooling water, € per m <sup>3</sup>	0.014
Demi water, € per m <sup>3</sup>	0.43
Cost slag disposal € per ton	40
Cost concentrated sludge disposal € per ton	200
Electrolytic H <sub>2</sub> consumption, kWh per Nm <sup>3</sup>	4.5
Electrolytic cost € per kWh	1100

**Table 7.**  
*Assumption list for economic evaluation.*

To properly assess the impact of methanol price and gate fee, sensitivities analysis has been carried out varying the Methanol market price in the range 400–500 €/ton and the waste gate fee in the range 130–160 €/ton.

For the scenario B, due to the high impact on power consumption, project IRR has been estimated as function of electric energy price.

As shown in **Figure 8**, electric energy cost in order of 30 €/MWh allows to achieve project IRR comparable with those obtained with the Scenario A.

## 5. Estimation of CO<sub>2</sub> emission for the waste to methanol technology

For a better understanding of potential carbon footprint reduction of the proposed Waste to Methanol technology, a simplified LCA analysis has been performed.

The use of waste as feedstock for chemical synthesis allows to fulfill at the same time two different services: from one side the disposal of waste and from the other the synthesis of a chemical in this case methanol. It derives that such system compared with conventional route of waste disposal represented by incinerator and

Utility	M€	M€
Electric Power	7.86	11.77
Electric power electrolysis	—	66.46
Well water	0.02	0.04
Demi water	0.002	0.076
BFW	0.22	0.44
MP steam	2.32	—
LP steam	3.06	3.06
Natural Gas	2.13	2.13
Instrument Air	0.28	0.20
Nitrogen	1.00	1.93
Oxygen	5.95	—
Cooling water	0.33	0.33
Granulated	1.27	1.27
Sludge	1.50	1.50
Chemicals	0.50	0.50
Others	1.00	1.00
NG saving through off-gas energy recovery	-0.93	-0.34
<b>Variable cost subtotal</b>	<b>28.21</b>	<b>90.37</b>
Maintenance	4.60	7.65
Labor cost	2.01	2.28
<b>TOTAL OPEX</b>	<b>34.78</b>	<b>100.30</b>
Depreciation (Equity)	6.54	12.20
Bank loan repayment	11.76	18.82
<b>TOTAL COST + DEPRECIATION + BANK LOAN</b>	<b>53.08</b>	<b>131.06</b>
<b>REVENUES</b>		
From WASTE gate fee	28.80	28.80
<b>COP (€/ton)</b>	<b>243</b>	<b>522</b>

**Table 8.**  
*OPEX and COP estimation.*

chemical synthesis from fossil feedstock, allows for a better exploitation of carbon and at the end for a saving in terms of CO<sub>2</sub> emissions. The below evaluation is referred to the entire life of products that means taking into account also emission related to the use of methanol. The proper estimate the CO<sub>2</sub> saving of the waste to chemical approach, the following formulation has been adopted:

$$CO_2 \text{ saving} = \frac{(CO_{2Conv.methanol}) - (CO_{2Waste to Methanol} - CO_{2Incinerator})}{CO_{2Conv. methanol}} \quad (5)$$

### 5.1 Emission of conventional methanol production

The estimation of CO<sub>2</sub> emission for conventional methanol production, takes into consideration that equivalent emission for feed and fuel is around 75% of the

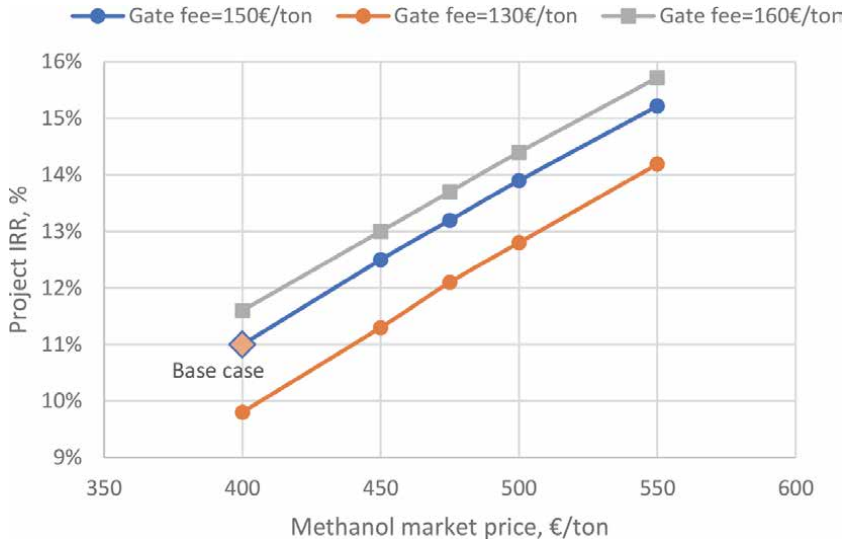


**Figure 7.**  
Project IRR evaluation vs. methanol price and gate fee.

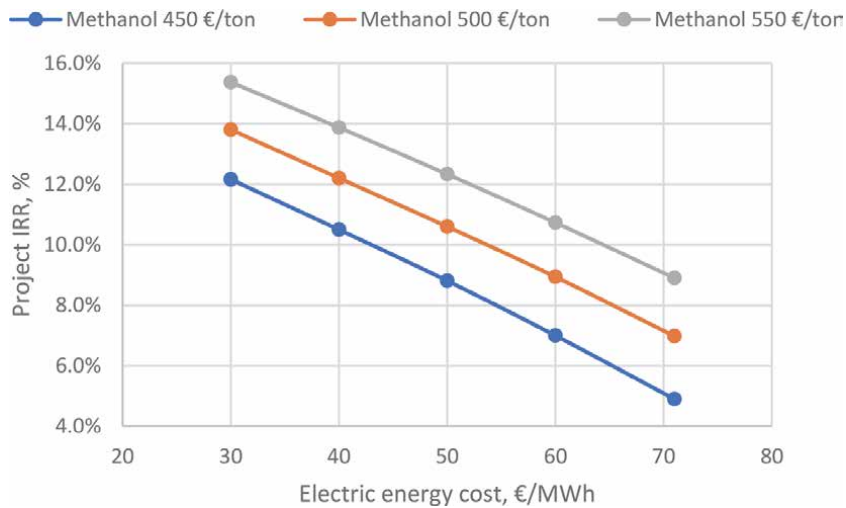


**Figure 8.**  
Project IRR evaluation vs. electric energy price and methanol market price. SCENARIO B.

overall LCA emission. An average feed & fuel consumption for conventional methanol plant equal to 32,7Gcal/ton methanol has been assumed [20]. The resulting specific emission to be taken into account for the above-mentioned criteria is around 2.5 tonCO<sub>2</sub>/ton MeOH.

## 5.2 Emission of incinerator

For the incinerator it is adopted the reference value of around 2tonCO<sub>2</sub>/tonWaste. To proper account for the equivalent CO<sub>2</sub> emission deriving from electric power no more produced from waste and needed to be replaced from the grid, it is assumed an electric energy efficiency of 28%. It derives that 24 t/h of waste having a calorific value of 16MJ/kg, considering also a combustion assisted with natural gas in



order of 2% of energetic content of waste can produced 30.5 MWe. This electric power no more produced from waste needs to be replaced by electric energy from the grid.

### 5.3 Emission of waste to methanol

For the waste to methanol plant the following contribution have been taken into account:

C1 = CO<sub>2</sub> emission derived from all carbon contained in the waste which along the process is converted into CO<sub>2</sub>. Considering the reference waste composition, this contribution is in order of 2.8 tonCO<sub>2</sub>/ton Methanol distributed into methanol, flue gas and concentrated CO<sub>2</sub>.

C2 = CO<sub>2</sub> emission derived from fuel consumption. This contribution considers not only the direct fuel consumption but also the equivalent consumption for steam used along the process. The overall consumption is in order of 0.257 ton CO<sub>2</sub>/ton Methanol).

C3 = CO<sub>2</sub> emission derived from fugitive emission of natural gas used along the project calculated as 2,5% of natural gas consumption [21] with a Methane GWP equal to 28 [22]; the resulting value is in order of 0.061 tonCO<sub>2</sub>/ton Methanol.

C4 = Equivalent CO<sub>2</sub> emission to replace electric energy no more produced from waste incinerator. Resulting amount of equivalent CO<sub>2</sub> is in order of 0.61 tonCO<sub>2</sub>/ton Methanol on the basis of a grid electric emission factor of 0.245 kgCO<sub>2</sub>/kWh.

C5 = Indirect CO<sub>2</sub> emission for electric energy absorbed along the process; resulting value is in order of 0.43 ton CO<sub>2</sub>/ton methanol according to a grid emission factor of 0.245 kgCO<sub>2</sub>/kWh.

C6 = Equivalent CO<sub>2</sub> emission derived from transport of Waste from production facility assuming a distance between gasifier and waste facility of around 100 km. resulting specific consumption is 0.017 ton CO<sub>2</sub>/ton methanol.

Taking into account the above contribution, the overall CO<sub>2</sub> emission for the waste to methanol plant is in order of 4.17 ton CO<sub>2</sub>/ton methanol.

As shown in **Figure 9**, main contribution of CO<sub>2</sub> emission for the waste to methanol approach, without considering Carbon contained in the waste and released as flue gas, pure CO<sub>2</sub> and product, is addressed to electric energy. The latter accounts for electric energy consumed by the process and that replacing the electric

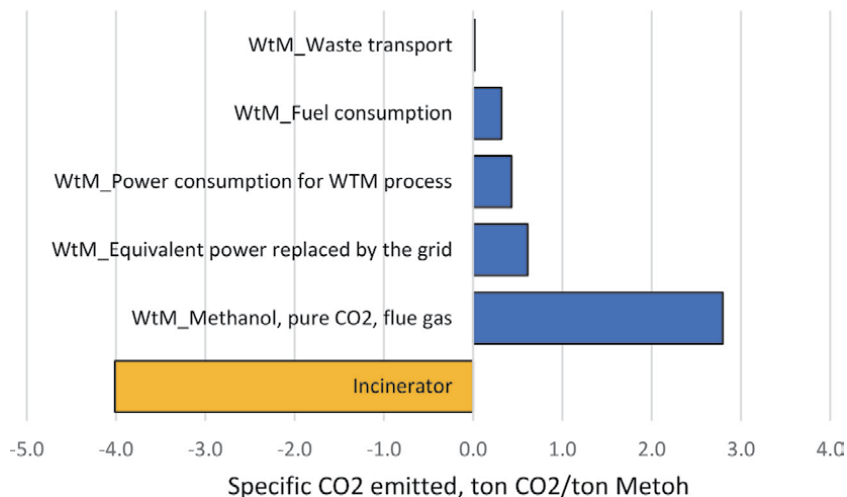


**Figure 9.**  
Net LCA CO<sub>2</sub> emission of the waste to methanol scheme (SCENARIO B).

energy no more produced from waste. Under a scenario where it is expected an increasing share of renewables into the global energetic system, the CO<sub>2</sub> saving of the Waste to Chemicals approach has the potential to be further increased. The overall saving achieved by the waste to methanol plant, according to a simplified LCA analysis, is in order of 94% corresponding to around 229.000 tCO<sub>2</sub>/year.

## **6. Conclusion**

Waste like RDF, Municipal Solid Waste and residue plastics, once properly converted into syngas, may be used as feedstock for the synthesis of wide range of chemicals. This approach fulfills the hierarchy of waste management being addressed to waste no more recyclable and normally routed to incinerator or land-fill. The key step allowing for a reasonable use of waste as alternative feedstock, is the primary conversion step based on a high temperature gasification carried out under pure oxygen environment and with a temperature profile assuring certain characteristics for produced syngas.

The case study here analyzed based on methanol production from waste, resulted in a feasible solution from technical, economic and environmental point of view. Competitive cost of production may be achieved with the scenario A under Gate fee in order of 140–150€/ton. Scenario based on external hydrogen addition as per Scenario B, although accounting for a strongly reduction of direct CO<sub>2</sub> emission, needs of a cheap electric energy cost, in order of 30€/MWh, to be competitive.

The simplified LCA analysis performed around the waste to methanol scenario, shows the consistent benefit of proposed solution in terms of CO<sub>2</sub> emission. The waste to Methanol scheme fulfills two different service: from one side the disposal of a waste and from the other the synthesis of a chemical. Under this scenario, once compared with conventional methanol production based on fossil feedstock, a saving of CO<sub>2</sub> emission in order of 94% may be achieve. The latter, for the reference capacity accounts for an avoidance of around 229.000 tCO<sub>2</sub>/y.

Taking into account the increasing sharing of renewable expected for the future, the CO<sub>2</sub> avoidance of the Waste methanol scheme may be further increased.

## **Acknowledgements**

We kindly acknowledge Maire Tecnimont Group for support to the research and development in the field of Waste to Chemical area.

## Author details

Alessia Borgogna<sup>1\*</sup>, Gaetano Iaquaniello<sup>2</sup>, Annarita Salladini<sup>1</sup>, Emanuela Agostini<sup>1</sup>  
and Mirko Boccacci<sup>1</sup>


1 Nextchem S.p.A., Rome, Italy

2 KT S.p.A., Roma, Italy

\*Address all correspondence to: [a.borgogna@nextchem.it](mailto:a.borgogna@nextchem.it)

## IntechOpen

---

© 2021 The Author(s). Licensee IntechOpen. This chapter is distributed under the terms of the Creative Commons Attribution License (<http://creativecommons.org/licenses/by/3.0>), which permits unrestricted use, distribution, and reproduction in any medium, provided the original work is properly cited. 

## References

- [1] Nasa. Globale Climate Change. Vital Sign of the Planet. [Internet]. Available from: <https://climate.nasa.gov/vital-signs/carbon-dioxide/> [Accessed: 2021-01-25]
- [2] Bereiter, B., Eggleston, S., Schmitt, J., Nehrbass-Ahles, C., Stocker, T. F., Fischer, H., ... & Chappellaz, J. (2015). Revision of the EPICA Dome C CO<sub>2</sub> record from 800 to 600 kyr before present. *Geophysical Research Letters*, 42(2), 542-549.
- [3] Prentice, I. C., Farquhar, G. D., Fasham, M. J. R., Goulden, M. L., Heimann, M., Jaramillo, V. J., ... & Wallace, D. W. (2001). *The carbon cycle and atmospheric carbon dioxide*. Cambridge University Press.
- [4] Gallo, M., & Marinelli, M. (2020). Sustainable mobility: A review of possible actions and policies. *Sustainability*, 12(18), 7499.
- [5] Laurens, L. M. L. (2017). *State of Technology Review—Algae Bioenergy*. Golden: IEA Bioenergy.
- [6] European Commission. Indirect Land Usage Change. [Internet]. Available from: [https://ec.europa.eu/commission/presscorner/detail/en/MEMO\\_12\\_787](https://ec.europa.eu/commission/presscorner/detail/en/MEMO_12_787) [Accessed: 2021-01-27]
- [7] International energy agency. Direct air capture. [Internet]. Available from: <https://www.iea.org/reports/direct-air-capture> [Accessed: 2021-01-27]
- [8] Mac Dowell, N., Fennell, P. S., Shah, N., & Maitland, G. C. (2017). The role of CO<sub>2</sub> capture and utilization in mitigating climate change. *Nature Climate Change*, 7(4), 243-249.
- [9] World Data Bank. What a waste. [Internet]. Available from: [https://datatopics.worldbank.org/what-a-waste/trends\\_in\\_solid\\_waste\\_management.html](https://datatopics.worldbank.org/what-a-waste/trends_in_solid_waste_management.html) [Accessed: 2021-01-27]
- [10] G. Iaquaniello, G. Centi, A. Salladini, E. Palo, S. Perathoner, Waste to Chemicals for a Circular Economy. *Chemistry A European Journal*. DOI: 10.1002/chem.201802903
- [11] Iaquaniello G., L. Spadacini, A. Salladini, E. Antonetti (2018), Method and equipment to produce a syngas from wastes, preferably industrial or municipal wastes and their deliverables. WO 2018/066013 A1.
- [12] Salladini, A., Borgogna, A., Spadacini, L., Pitrelli, A., Annesini, M. and Iaquaniello, G., 2018. Methanol production from Refuse Derived Fuel: A preliminary analysis on the influence of the RDF composition on process yield. Available at: [http://uest.ntua.gr/athens2017/proceedings/pdfs/Athens2017\\_Salladini\\_Borgogna\\_Spadacini\\_Pitrelli\\_Annesini\\_Iaquaniello.pdf](http://uest.ntua.gr/athens2017/proceedings/pdfs/Athens2017_Salladini_Borgogna_Spadacini_Pitrelli_Annesini_Iaquaniello.pdf).
- [13] E. Antonetti, G. Iaquaniello, A. Salladini. A carbon neutral process and relating apparatus to produce urea from municipal or industrial wastes with zero emissions. WO 2017/134691.
- [14] G. Iaquaniello, A. Salladini, E. Antonetti. A process and relating apparatus to make pure hydrogen from syngas originated from wastes gasification. In corso di replica alle osservazioni. WO 2018/078661.
- [15] F. Maréchal, G.H., B. Kalitventzeff, Energy savings in methanol synthesis: Use of heat integration techniques and simulation tools. *Computers & Chemical Engineering*, 1997, 20 May. 21 (Supplement): p. S511-S516.
- [16] G. Iaquaniello, A. Salladini. A process and relating apparatus to make pure bio-methanol from a syngas originated from wastes gasification. WO 2018/134853.
- [17] M. Pérez-Fortes, J. C. Schöneberger, A. Boulamanti, E. Tzimas, Methanol

synthesis using captured CO<sub>2</sub> as raw material. *Applied Energy* 161 (2016) 718–732.

[18] M. Peters, K. Timmerhaus, R. West. *Plant Design and Economics for Chemical Engineers*. McGraw-Hill Education, 2003.

[19] Metanex. <https://www.methanex.com/our-business/pricing>. Accessed February 2021.

[20] H-J. Althaus, R. Hischier, A. Primas, *Life Cycle Inventories of Chemicals*. Ecoinvent Centre. FData v2.0 (2007)

[21] R. W. Howarth, Methane emissions and climatic warming risk from hydraulic fracturing and shale gas development: implications for policy, *Energy and Emission Control technologies*, 2015.

[22] Green House Gas Protocol. Global Warming Potential Values. Available at Microsoft Word - Global-Warming-Potential-Values.docx (ghg protocol.org). Accessed February 2019



# Dioxin and Furan Emissions from Gasification

*Seyedeh Masoumeh Safavi, Christiaan Richter  
and Runar Unnthorsson*

## Abstract

PCDD/Fs are a 75-member family of toxic chemicals that include congeners (members) that have serious health effects including congeners that are classified group 1 carcinogens, endocrine disruptors and weakening or damage to the immune system. Municipal solid waste (MSW) incinerations had historically been implicated as the major source of PCDD/Fs distributed by air. As a result of awareness and legislation most European MSW incinerators were either shut down or equipped with modern air pollution control systems necessary to achieve MSW incineration with PCDD/F emissions within regulatory limits set by national and international laws (typically  $<0.1$  ng TEQ/Nm<sup>3</sup>). There is a common belief that gasification of waste and/or biomass, unlike incineration, inherently and always achieve emission below regulatory and detectable limits. However, a review of the literature suggests that the belief that the substitution of incineration with gasification would always, or necessarily, reduce PCDD/Fs emissions to acceptable levels is overly simplistic. This chapter discusses the mechanisms of PCDD/Fs formation, the operational measures and parameter ranges that can be controlled during gasification to minimize PCDD/Fs formation, and methods for post-formation PCDD/F removal are reviewed. The purpose of this chapter is to assist researchers and practitioners in formulating waste management policies and strategies, and in conducting relevant research and environmental impact studies.

**Keywords:** gasification, dioxins, furans, dioxin formation mechanism, PCDD/F removal technologies

## 1. Introduction

Due to industrialization and improved living standards, global energy consumption is on the rise. Simultaneous population growth and per capita energy demand led to increased fossil fuel production and consumption accounting for about 80% of world energy consumption, while nuclear, biomass, and hydroelectric energy accounting for the remaining 20%. This trend of fossil fuel use as the largest portion of the growing global energy mix results in a steady increase in CO<sub>2</sub>, NO<sub>2</sub> and SO<sub>2</sub> emissions, leading to environmental threats. Therefore, seeking sustainable solutions is urgent. Biomass is defined as biological and carbon-containing material derived from living or recently living organisms. Biomass is one of the biggest sources of energy and is a renewable, possibly efficient, and an attractive alternative to fossil fuels. Biomass when compared to fossil fuels contains much less

carbon, more oxygen, and less heat in the range of 12–16 MJ/kg [1]. Its average net greenhouse gas emissions are lower than fossil fuels, an environmental advantage that may be a key driver for biomass and waste energy extraction. Biomass is the predominant source of energy in many developing countries, but in some industrialized ones it also plays an important role. Biomass-based options for energy production are widely researched and developed to replace fossil fuels in heat and electricity production, chemicals formation, agriculture, moving towards sustainability, regional economic and social development in order to alleviate the emission of greenhouse gas [2].

### **1.1 General overview: thermochemical biomass conversion methods**

Through biochemical, chemical, and thermochemical conversion techniques, the chemical energy that is contained in biomass is converted to heat, electricity or fuel. Biochemical and chemical methods can only convert selected biomass to biogas, biodiesel, etc., while most biomass materials can be thermochemically converted. Thermochemical biomass conversion is one of the most energy-efficient, flexible, and high-energy yield methods for extraction of energy from biomass and organic waste, and therefore one of the most promising pathways with many environmental benefits. This thermal treatment can be divided into different processes depending on the supply of oxygen: (1) combustion; direct biomass burning using excess oxygen, (2) gasification; biomass burning with a limited oxygen supply, and (3) pyrolysis; biomass burning without oxygen [3], where gasification is the most efficient energy extraction process [4, 5].

Given its economic and environmental benefits, gasification has attracted worldwide attention. Many agricultural and industrial waste streams that are currently problematic can be used sustainably through gasification. Industrial waste (e.g., from the food and pulp and wood industries), municipal waste (e.g., household waste), or agricultural waste (e.g., gardening and animal manure) [6] and energy products can be all converted into a mixture of non-combustible gas in a gasifier (producer gas) via gasification. Gasification is the conversion of solid carbon to a gas under a limited oxygen supply at high temperatures (400–1000°C [7]). Producer gas is a mixture of CO, H<sub>2</sub>, CH<sub>4</sub>, slight amounts of other light hydrocarbons, steam, CO<sub>2</sub>, N<sub>2</sub>, in addition to impurities like char, ash, tar, and oil particles. The producer gas can simply be stored and combusted at a later time to produce heat and/or steam. The producer gas can also produce electricity when used in gas turbines or to power and engine-generator combo. Syngas is the purified producer gas that can be used as fuel or as feedstock to produce higher value fuel or chemicals [8].

Although the main feedstock for gasification can be any hydrocarbons; the acceptable range of feedstock properties is practically very narrow for most existing real world gasifiers. This is a major disadvantage compared to incineration. The reaction chemistry and fluid-dynamics within gasifiers tend to be highly sensitive to changes in the composition of raw materials, their reactivity, density, particle size, moisture, and ash content. The beneficial output in combustion plants is power and possibly heat, while the output in gasification can also be chemicals, liquid fuels or hydrogen in addition to power and heat. Due to the presence of acid gases, tar particles, and other impurities that exist in the gas produced by the gasifier, the producer gas should be treated properly for optimal production of chemicals, liquid or hydrogen fuels and internally-fired cycles (internal combustion engines, gas turbines) [8].

Biomass conversion efficiency varies based on the gasifier itself, purpose of use, type of treated material, its particle shape and size, and the gas flow. The process



of gasification which occurs in gasifiers can be divided into five groups: (1) the calorific heat of the producer gas is high when it is between 10 to 40 MJ/Nm<sup>3</sup>; it is medium if it is between 5 to 10 MJ/Nm<sup>3</sup>; and it is low when below 5 MJ/Nm<sup>3</sup>; (2) nature of gasification agents (air, O<sub>2</sub>, steam, H<sub>2</sub>); (3) the direction in which consuming material and gasifying agents move (updraft, downdraft; cross draft or fluidized bed); (4) operating pressure (atmospheric or high pressures of up to 6 MPa); (5) type of feedstock (municipal solid waste (MSW), industrial waste, biomass/wood). There are only a few processes that do not fall into these categories, namely molten iron bath gasification, in situ gasification (underground gasification), plasma gasification or hydrogasification and rotary kiln gasification [8, 9].

## 1.2 Gasification vs. combustion

Combustion has been a viable method for waste management with drawbacks such as harmful process residues and hazardous emissions. Gasification has come up to tackle these issues and improve energy efficiency. Gasification reduces corrosion and emission by preserving alkali and heavy metals (excluding Hg and Cd), sulfur and chlorine in the process residues, greatly inhibiting dibenzo-p-dioxins (PCDDs) and chlorinated dibenzofluorans (PCDFs) formation and decrease the formation of thermal nitrogen oxides (NO<sub>x</sub>) owing to lower temperatures and reducing conditions [10]. Slag gasification can destruct dangerous compounds, however, S and Cl species such as H<sub>2</sub>S and HCl might remain present in the producer gas. When producer gas volume is small, lower dimensioned gas cleanups is needed. This can save the cost of investment while using O<sub>2</sub> raises both the costs and the producer gas calorific value. Producer gas can be used in different applications energetically or as raw material which has a higher efficiency [9, 11]. Some of the potential benefits of gasification versus combustion and their corresponding potential drawbacks are summarized in **Figure 1**, using reference [12] with the permission of Elsevier.

PCDD/Fs are a group of unwanted by-products and pollutants coming from thermal and combustion processes. The toxicological and chemical properties of compounds of this sort depend on the number and position of the chlorine atoms that are bound to the two aromatic rings [13]. PCDDs and PCDFs are composed of 75 and 135 homologs, respectively. Specific isomers of PCDD/F have been recognized for their toxicological properties that have serious carcinogens [14]. They are highly toxic and cause severe bronchitis, asthma, and strangulation of the lungs in

Potential advantages of gasification vs. combustion	Related issues that hinder the benefits of gasification
<ul style="list-style-type: none"> <li>the combustible gas generated by gasification is easier to handle, meter and control than waste</li> <li>the homogenous, gas-phase combustion of syngas can be carried out under conditions more favorable than those achievable with waste</li> </ul> <p>The reducing conditions in the gasifier:</p> <ul style="list-style-type: none"> <li>improve the quality of solid residues, particularly metals</li> <li>reduce the generation of some pollutants (dioxins, furans and NO<sub>x</sub>)</li> </ul> <p>Syngas can be used, after proper treatment, in highly efficient internally-fired cycles</p> <p>Syngas can be used, after proper treatment, to generate high-quality fuels (diesel fuel, gasoline or hydrogen) or chemicals</p> <p>Gasification at high pressure enhances the opportunities to increase energy conversion efficiency and reduce costs gasification</p>	<ul style="list-style-type: none"> <li>since syngas is highly toxic and explosive, its presence raises major security concerns and requires sophisticated control equipment</li> <li>since feedstock is oxidized/converted in two steps (gasification + syngas combustion/conversion) plants tend to be more complex and costly, more difficult to operate and maintain, less reliable</li> </ul> <p>The actual production of pollutants depends on how syngas is processed downstream of the gasifier; if syngas is eventually oxidized, dioxins, furans and NO<sub>x</sub> may still be an issue</p> <ul style="list-style-type: none"> <li>Required syngas treatment is costly and causes significant energy consumption/losses</li> <li>Due to the consumption/losses of gasification and syngas clean-up, overall energy conversion efficiency is typically lower than that of combustion plants</li> <li>At the small scale typical of waste treatment plants, efficiency of internally-fired systems are low (especially if gas turbine-based)</li> <li>Required syngas treatment very demanding and costly</li> <li>At the small scale typical of waste treatment plants, synthesizing quality fuels or chemicals can entail prohibitive costs</li> </ul> <p>Pressurized waste gasification poses formidable challenges and has not been attempted by any technology developer</p>

**Figure 1.**  
 Comparison of waste gasification and combustion.

humans. Agricultural lands and livestock in the vicinity of incinerators can also be affected by dioxin that infects meat, dairy products, and so on. Consuming these products may destroy the human immune system, thyroid function, hormone dysfunction, and causes cancer. It has negative health condition in infants because of dioxin exposure through breast milk and uterine exposure. Scientists have conducted numerous experimental studies on experimental animals (rats and mice) to investigate the effects of dioxin contamination that lead to carcinogenicity, liver toxicity, and immune toxicity. 2,3,7,8-tetrachlorodibenzo-p-dioxin (TCDD), considered to be very toxic and assigned a toxic equivalence factor (TEF) value of 1 [10, 15, 16], and commonly used as a test substance in toxicity tests. In immunotoxicity experiments, 2,3,7,8-TCDD caused thyroid atrophy, cellular and humoral immune abnormalities, constrained host resistance to viral infections, and inhibited antibody formation [17].

In 1977, the release of PCDD/F from incineration processes was first observed. Since then, researchers have evaluated emission of this compound by a series of thermal processes that include integrated combustion and gasification [16]. The main reason for the negative environmental reputation of waste incineration is the emission of PCDD/F and other pollutants during the process [18], especially for MSW incineration [19–21]. After PCDD/F enters the atmosphere, they are exposed to chemical, physical, and biological changes and eventually contaminate soil, body and sediment [22].

The purpose of this chapter is to shed more light on PCDD/F formation and their sources in combustion. The main objective is to review the PCDD/F formation in gasification as there is no review on formation and emission of dioxins from processes based on gasification know-hows. This chapter highlights the likelihood of reducing the emission of PCDD/Fs to well below regulatory limits or even detection limits, by using gasification technology. We have done a thorough study of all the accessible articles came into existence over the last 30 years in literature to be able to frame this review which is really felt missing in the field.

## 2. Dioxin formation

In the 1950s and 1960s, incinerating organic waste from chemical plants and releasing greenhouse gases into the atmosphere became common practice. Its extension to incineration of solid waste, especially MSW, increased during the 1960s and 1970s and enabled these processes to recover the energy generated by waste incineration, reduce the waste by 80–90% of volume, and consequently decrease the areas required for landfilling. Nonetheless, the release of very toxic organic compounds from waste incineration, recognized as dioxins, was not known back then [23]. Actually, the toxic effects of PCDD/F were not materialized until around the end of 1980s. Due to maximum enforcement of available control technology regulations, the release of “toxic equivalent” dioxin (TEQ) from US power plants was lessened by three orders of magnitude to less than 12 g of TEQ per year by 1987 [24]. It has been widely acknowledged that combustion processes lead to the formation or emission of by-products such as NO<sub>x</sub>, SO<sub>x</sub>, HCl, TOC, CO, HF, and CO<sub>2</sub> into the atmosphere. Moreover, small quantities of toxic substances such as metals and PCDD/F are released into the atmosphere [23]. **Figure 2** shows the structure of PCDD/Fs [25].

### 2.1 Dioxin formation during combustion

The formation and emission of dioxin - group of chlorinated poly-nuclear aromatic compounds - from waste combustion is of prodigious public concern.

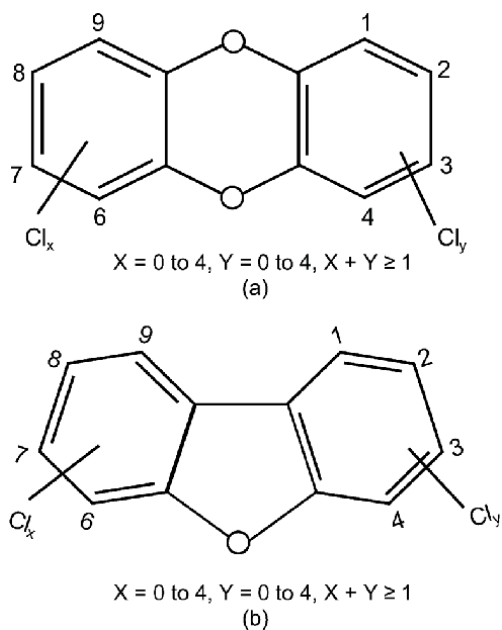


**Figure 2.** Molecular structure of polychlorinated dibenzo-*p*-dioxins (a) and dibenzofurans (b). Reprinted from [25] with the permission of Elsevier.

Dioxin is released in small quantities from combustion sources mainly in the process of municipal waste incineration, which is one of the most important sources of PCDD/Fs formation in the environment. Therefore, dioxin control measurement from combustion sources has become vital and the mechanisms of dioxin formation have been comprehensively investigated because of its carcinogenic and mutagenic effects.

### 2.1.1 Mechanism of PCDD/F formation

PCDD/Fs can be formed when reaction of hydrocarbons and chlorine takes place in vicinity of O<sub>2</sub> and metals like Cu at high temperatures of 200 to 800°C. There are many theories regarding the mechanism of dioxin formation. PCDD/F formation proceed via: (1) homogeneous (gas phase) reactions at high temperatures (500 to 800°C), and the main mechanism of the reaction process is via chlorination precursors like chlorophenol (CP) and chlorobenzene (CB) in the gas phase. This high-temperature homogeneous path is known as “precursor route” in which a smaller subset of PCDD/Fs is formed in the gas phase. (2) heterogeneous (surface-catalyzed) reactions at lower temperatures (200 to 400°C) in the post-combustion zone [21, 26]. This low temperature heterogeneous path is called the “de novo route” (for the PCDD/Fs subset of carbon, oxygen, hydrogen and chlorine in the cooling flue gas). In the heterogeneous mechanism, the formed PCDD/Fs may also come from CPs or CBs or from carbon in fly ash. The catalytic effect of fly ash or soot is the main factor in the latter case, and this is a well-known example of a de novo process. It is said that the two pathways of dioxin formation occur simultaneously and independently. It is still debated whether the carbon in the heterogeneous PCDD/F mainly comes from gas precursors or from carbon in fly ash [25, 27]. Dickson et al. [28] disclosed that under similar conditions, the rate of PCDD/Fs precursor formation is 72–99000 times higher than the rate of carbon formation in fly ash. Luijk et al. [29] thought that the formation of PCDD/Fs from

precursors was about 3,000 times faster than the de novo process of activated carbon. The precursors were found to be the major source of PCDD/Fs formation by Tuppurainen et al. [30]. **Figure 3** is a stylized illustration of the mechanisms by which PCDD/F is formed in combustion systems. The surface shows a particle of ash, and the arrows depict both the reaction and absorption processes. Thick arrows indicate the relative importance of pathways in the formation of PCDD/F.

The emission of PCDD/Fs is directly related to the amount of carbon used. Along with CP, CBs, polycyclic aromatic hydrocarbons (PAHs), and residual carbon, there are also key elements that influence the formation of PCDD/Fs including residence time, precursors, combustion temperature, PCDD and chlorine in the feed, feed processing, supplemental fuel and oxygen availability [31, 32].

Dioxin formation happens in a temperature range of 200 to 800°C with a maximum reaction rate reached between 350 to 400°C [33]. Data from the literature show that the rate is very slow in the range of 200 to 250°C. Under optimum combustion conditions (such as adequate oxygen, mixing, and airflow), virtually all organic compounds including PCDD/F are destroyed above 800°C. However, PCDD/F is formable at high temperatures, but under less optimum conditions like insufficient oxygen [34]. Dioxin formation correlates well with access to organic precursors, CO, unburned carbon or combustion products (even soot particles), metal salts and hydrogen chloride/chlorine. Dioxins are formed during the cooling cycles of the flue gas in combustion systems. This formation process goes via one of the two mechanisms mentioned above [21, 35]. The main mechanism of dioxin formation in combustion systems appears to be de novo synthesis where morphology of the carbon from deteriorated graphical configuration is critical for dioxin formation. Therefore, such carbon morphologies have been investigated. It was found that the soot particles from gas phase combustion reactions including deteriorated graphical configurations are a potential source of de novo dioxins synthesis.

The formation of PCDD/F in combustion processes can be described in a two-step route: (1) formation of carbon: carbon particles comprised of deteriorated graphical configurations in the combustion region. (2) oxidation of carbon: the

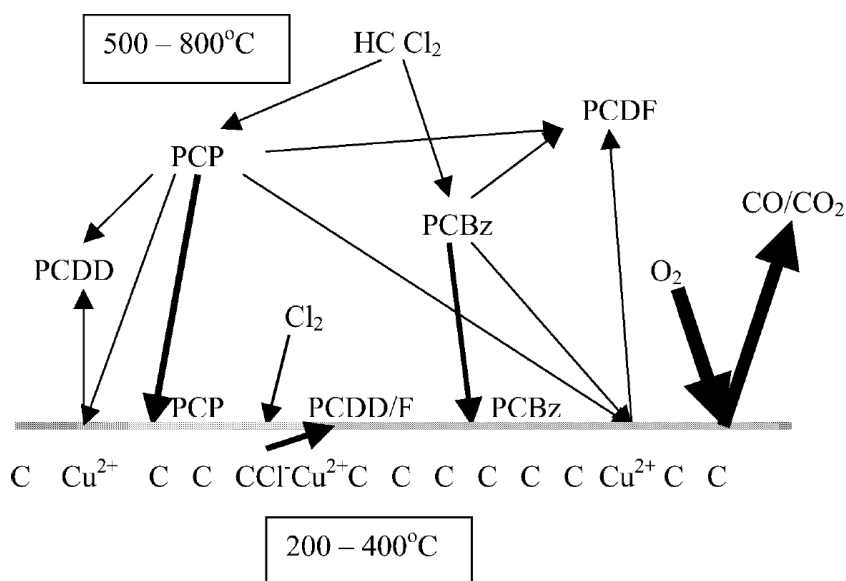


**Figure 3.** The pathway for formation of PCDD/F is illustrated in this diagram. Reprinted from [25] with the permission of Elsevier.

carbon particles that have not been properly burnt can still be oxidized in low temperatures after combustion. PCDD/Fs are by-products of oxidative degradation of the graphical structure of carbon particles. There are several steps and chemical reactions involved in these routes. Here are at least three known steps for carbon formation: nucleation, agglomeration and particle growth. Here are four steps involved in carbon oxidation: oxidant adsorption, complex intermediate formation with metal ion catalysts, interaction with graphitic carbon structure, and product desorption. The nature of these chemical reactions is complex and heterogeneous [21].

Since the reactants for the formation of PCDD/Fs are inadequate during combustion, the combustion conditions are likely to have a major influence on the formation of PCDD/F. There are some conditions in the combustion process that can cause a favorable formation of PCDD/F. These conditions are: low combustion temperature, poor turbulence in the combustion chamber, short residence time in the combustion zone, low O<sub>2</sub> content resulting in deficient combustion, sluggish flue gas cooling process in the critical temperature range [23]. Moreover, existence of metals (Cu, Fe, Pb and Zn) [35] in fly ash catalytically increase formation of PCDD/F. Also in presence of these metals, PCDD/F can react with chloride and unburned carbon and contribute to the so-called *de novo* synthesis of PCDD/F [35–37].

Chlorine content in raw materials is one reason for PCDD/Fs formation during combustion [21, 38]. When combusting wood, for example, presence of phenol, lignin or carbon and chlorine particles can contribute to emission of PCDD/Fs [39]. Since the concentration of chlorine in uncoated natural wood is low [40], the combustion of this feedstock yields a much lower emission rate of PCDD/Fs compared to when combusting straw, coal, and sewage sludge [41]. Contrarily, during combustion of wood, PCDD/Fs compounds can remain on the surface and thus be removed by fly ash particles. Thus, primary and secondary emission control measurements are vital to effectively mitigate this part of the PCDD/FS emission in the flue gas. Some example of these control measurements are: usage of high quality wood fuel, optimizing combustion conditions, and try to precipitate the fly ash at low temperatures (less than 200°C) [42].

There is a review on dioxin emission from wood combustion by Lavric et al. [19] emphasizing on the fact that the combustion conditions and fuel properties are the most dominant considerations on the dioxin release rate. They concluded that using flue gas cleaning systems when combusting non-contaminated natural wood, lowers the level of dioxin emission below the legitimate levels. The minimum concentration of dioxin in greenhouse gas emissions prescribed by most current European legislation is 0.1 ng m<sup>3</sup> expressed in I-TEQ units [43].

## **2.2 Dioxin formation in gasification**

The formation of harmful chemicals, especially PCDD/Fs, is the most serious problem. It is important to reduce the formation of polychlorinated compounds and increase their capture due to their environmental emissions. Although there is an increasing trend of well-designed gasifiers with a broad range of raw materials that are essentially used in gasifiers, not all materials should necessarily be gasified in a given setup. Processed plastic, rubber, and tanned leather [44] as well as various animal biomasses (such as food waste) and sewage sludge [45] contain large amounts of chlorine.

Solid waste segment is commonly treated at incinerators. Energy generation via waste incineration has become an effective way of managing combustible waste, because it reduces the volume and mass of waste. Nevertheless, perilous

emissions and detrimental process residues are among the drawbacks of incineration. Incineration causes fly and bottom ashes, and thus release leachable toxic heavy metals, PCDD/Fs, and volatile organic compounds. Therefore, it is possible to replace incinerators with gasifiers. Incinerators emit PCDD/Fs and their concentration often exceeds the legal limit, which calls for a different technology for waste treatment. Gasification processes usually emit PCDD/Fs within acceptable limits as determined by national and international organizations [35]. The amount of pollutants in producer gas can be lower than that of the flue gas of an incinerator [46], and it is because of partial oxidation of waste with limited oxygen supply [47]. Gasification benefits from numerous advantages in comparison of traditional waste combustion. It occurs in a low oxygen environment (where the equivalence ratio varies between 0.25 to 0.50) which limits the formation of PCDD/Fs and large amounts of SO<sub>x</sub> and NO<sub>x</sub> [48]. Gasification reduces the emission of acidic gases due to higher temperatures and reduction conditions [49]. However, small amounts of PCDD/Fs can result from deficient destruction of the PCDD/Fs present in the waste itself or from the existence of organic chlorinated compounds in the reactor [50, 51].

It is evident that the mechanisms of dioxin formation and its related amounts to producer gas correlate well with tar formation, and is therefore a relatively comparable parameter for all gasifiers in which tar is partly converted to producer gas [52]. Zwart et al. scrutinized the formation of dioxin from refuse derived fuel (RDF), sewage sludge, and untreated wood pellets gasification in an extensive range of temperatures. The outcome revealed that the level of dioxins was very different in terms of gasification temperature and feedstock quality (chlorine content). Their conclusion was that high amounts of chlorine in the feedstock cause dioxin formation, especially at temperatures below 800°C. At temperatures above 800°C, dioxins levels are drastically reduced, along with corresponding tar levels. At temperatures above 850°C, the PCDD/Fs concentration in the producer gas was within the range of 0.5 ng TEQ/Nm<sup>3</sup> for clean wood pellets and sewage sludge. However, PCDD/Fs concentrations became lower in higher temperatures for RDF, it was still above the allowed limit [52].

### **3. PCDD/Fs removal**

Assessing the environmental impacts of gasification know-how is vital to ensure the practicality of the process. An occasional misconception that gasification plants are only minor variations of incinerators is the cause of gasification processes to still face environmental community resistance. One important distinction is that gasification can be an intermediary process for the production of producer gas in a broad range of applications. Utilizing syngas to generate on-site electrical and thermal energy is the most dominant process in gasification, however, the production of chemicals and fuel may be the ideal goal for the near future. Gasification contributes to air pollution control and make it less complex and costly compared to that needed for incineration. Although cleaning exhaust gases from non-combustion thermochemical conversion processes could be simpler than that of incineration, proper design and emission control systems are critical to satisfy health and safety requirements. Products of gasifiers must be controlled before discharging into the air as they can comprise several air pollutants. These include particles, hydrocarbons, CO, tars, N<sub>2</sub>, SO<sub>x</sub>, and small amounts of PCDD/Fs.

Lonati et al. [53] evaluated the risk of human carcinogenicity owing to the release of PCDD/Fs and Cd from a waste gasification plant using a probabilistic method. Probability density functions were used to define emission rates and risk model parameters of pollutants via Monte Carlo simulations. This gave a probability

distribution estimation with involvement of epistemic uncertainty and aleatory variability. The results showed that Cd emissions are much higher than PCDD/Fs despite their higher toxicity. PCDD/Fs concentrations were well below the current permissible limit of 0.1 ngTEQ m<sup>-3</sup>. They indicated that 95% of carcinogenic risk is due to Cd exposure.

To control greenhouse gas emissions from gasification processes different strategies can be adapted, depending on plant configuration, the requirements of specific energy conversion equipment or reactors and catalysts for downstream fuel synthesis. In any case, there is the advantage that it can be possible to control the air pollution of the reactor and the exhaust gas output in numerous cases using a combined method [9]. Coal filters were the first dioxin-reducing technologies, which were installed in the backend of an air pollution control system in many wastes to energy plants, in the late 1980s.

Filters also helped to absorb other organic compounds and mercury, but their bulky volume and probability of ignition were their pitfalls. For the sake of safety, inorganic sorbents such as zeolites were used for monitoring and inertisation of CO [54]. It was also found in the 1980s that oxidative catalysts have high degradation potential for dioxins [55]. Those catalysts were initially operational at 300 to 350°C, and then they were further developed to reach higher destruction efficiency of 99% at temperatures of about 230°C [56].

The high operating temperature (> 1000°C) along with oxygen deficiency eliminates any PCDD/Fs that may be present in the raw material and eradicates potential formation of PCDD/Fs. Thus, operating the gasification process at high temperature or maximizing the conversion of hydrocarbons that are being produced in pyrolysis are possible approaches to reduce the formation of dioxins [57]. For example, high-temperature gasification lowers dioxin formation when high-chlorine content fuels are used [57]. Another effective and easily applicable measure is the rapid cooling of the syngas by a water immersion that inhibits the synthesis of PCDD/Fs [58]. The capture of PCDD/Fs by a special multi-step absorption filter is the most effective method of removing dioxins from the residual burst stage and/or the gas or cooling effluent, regardless of technology used. Volatile organic compounds such as PCDD/F and other organics are effectively eliminated in the gaseous and liquid phases due to the high temperature reactor and shock cooling [35, 59].

As an example, Andersson et al. who got inspired by Griffin's theory [60] were successful to lower the concentration of dioxins [61]. They increased the concentration of SO<sub>2</sub> in the flue gas and adjusted the Cl/S ratio in a way that lowered the concentration of dioxin to around 0.1 ng(Te)/m<sup>3</sup> in the raw gas. As another example, Pařízek et al. applied the REMEDIA technology in a MSW incinerator, and they varied the operational temperature from 180–260°C. They saw that the degradation efficiency can be extended to 99–97% while dioxin emission can be lowered below 0.1 ng. (TEQ)/m<sup>3</sup> [62]. REMEDIA technology benefits from catalytic substrates that are overlaid on a two-layer polytetrafluoroethylene (PTFE) membraned material to filter and eliminate PCDD/F.

Off-gas cleaning system is vital for both incineration and gasification processes in thermal waste treatment plants, as it keeps the amount of pollutants being released into the environment lower than that legislated. PCDD/F can be cleaned using DeNO<sub>x</sub>/DeDiO<sub>x</sub> technologies such as sodium bicarbonate or PCDD/F removal using catalytic filtration or adsorption materials such as activated carbon [63].

### **3.1 Catalytic filtration of PCDD/F**

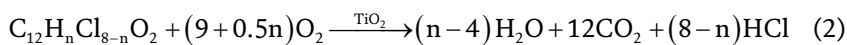
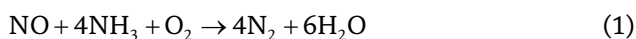
On the basis of applied applications it has been found that the method of dioxin removal by catalytic filtration REMEDIA [64] is highly effective. A GORE-TEX is

a special fabric filter bags usually used in catalytic filtration by which particles of solid fly ash are well separated via instantaneous removal of dioxins in flue gases. The filtration efficiency of the gas can be elevated to around 96.6% due to a PTFE-type membrane used in the external filtration layer. This refined gas is then driven inward the internal filtration layer comprised of catalytically active compounds that can eliminate dioxins further to reach 98.8% efficiency. The external filtration layer is periodically revived with the help of a usual pulse jet cleaning system. In the gasification process, catalytic filtration is usually placed immediately after a mechanical cleaning of the flue gases [65].

The Japanese government enforced the guideline of dioxin emission via Waste Management and General Purification Act (WMGPA) in 1997. After this WMGPA enforcement, the industrial sector was obliged to install catalytic reactors and bag filters in the new facilities. Following this enforcement, not only the adjusted values for the combustion temperature, the cooling temperature of the exhaust gas from the furnace, and the CO concentration in the exhaust gas from the stack were satisfactory at almost all facilities, but also the concentration of dioxin, acidic gases, and NO<sub>x</sub> in the discharged gases was significantly lower than those made before 1997 [66].

### 3.2 Technology DeNO<sub>x</sub>/DeDio<sub>x</sub>

One proficient approach to remove Dioxin is to combine its catalytic degradation with selective reduction of NO<sub>x</sub> according to the following stoichiometric equations [67]:



In order to selectively reduce NO<sub>x</sub>, ammonia can be injected prior to the catalytic reactor. Simultaneous removal of NO<sub>x</sub> and dioxins (DeNO<sub>x</sub>/DeDio<sub>x</sub>) can be carried out in a catalytic reactor at 200 to 300°C [56]. Although the NO<sub>x</sub> and dioxins removal via this method is a highly efficient process, catalyst poisoning is one of the main detriments. In addition to mechanical and chemical cleaning, the reactor in this setup needs to be installed after dust removal from flue gases (**Figure 4**). This means that re-heating of the flue gases to 200–300°C is required [68].

Parizek et al. [69] analyzed the economical balance of catalytic filtration versus DeNO<sub>x</sub>/DeDiox technology. They used a computer-based system for simulation calculations making solution more approachable. The annual economic balance of the operation of the catalytic filtration REMEDIA is composed of: cost of the filtration bags (for this study the guaranteed lifespan and real lifespan of the filtration tube was 4 and 8 years, respectively), energy cost of the fan drive, cost required to spray the flue gases before entering the filter. Also the annual economic balance of the operation of DeNO<sub>x</sub>/DeDiox technology is composed of: catalyst costs (a 4-year life-time operation was considered), energy costs of the fan drive, and cost for heating of flue gases. Results showed that the operating cost of the DeNO<sub>x</sub>/DeDiox technology rises due to the reheating of flue gases to the required temperature of the reaction and the cost was linked with the increased pressure drop. Catalytic filtration does not require heating of flue gases and the cost of the filtration bags falls due to their real lifespan.



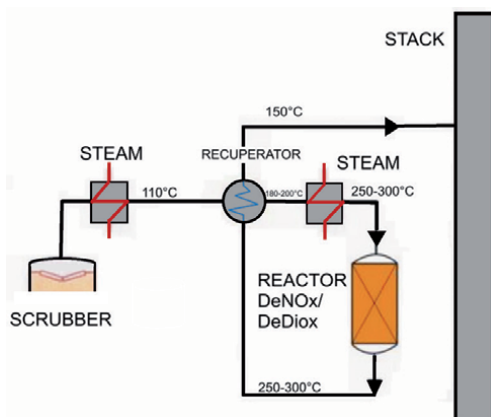


**Figure 4.**  
Scheme of DeNOx/DeDiox technology [69].

#### 4. Experimental evidence of PCDD/Fs in gasification and reliable mitigation

In an upcoming article [70] we will publish an extensive review of experimental measurements and evidence of PCDD/F emissions from gasifiers of various types and sizes, varying operating conditions and feedstocks.

The main findings are:

- Although PCDD/F emissions from gasification are in general lower than those from incinerators without modern emission control of the same feedstock it is not correct to assume that PCDD/F emission from a gasifier will *necessarily* be safe or below regulatory limits. PCDD/F can be produced in gasification above safe and regulatory limits.
- The two main factors that can widely and reliably reduce PCDD/F emissions to very low levels in gasification are
  1. peak operating temperature ( $> 1000^{\circ}\text{C}$ ) in the combustion and cracking zone together with oxygen deprivation
  2. rapid cooling of syngas by for example a water quench which prevents de novo synthesis
  3. high amounts of chlorine in the feedstock cause dioxin formation, especially at temperatures below  $800^{\circ}\text{C}$ . At temperatures above  $800^{\circ}\text{C}$ , dioxins levels are drastically reduced.

#### 5. Future work or guidelines

The main purpose of this chapter is to assist researchers in making primed decisions when adopting waste management policies and conducting relevant research and environmental impact studies. There is a need to establish more information on PCDD/F formation in gasification by experimentation of different feedstock when using different operational parameters and removal technologies;

in order to be able to choose an appropriate PCCD/F mitigation method when gasifying different waste streams.

## 6. Conclusions

Dioxin formation and emission from the incineration of waste have been reduced in Europe and North America by either decommissioning plants or otherwise installing of air pollution control systems [71–73]. However, given the severity of the health impacts and continued unknowns (like emissions during start-up, shut-down and other peak events) the topic continues to be of great public concern both in Europe and North America [73–75] and the developing world [73, 76, 77]. Gasification can offer a substitute approach for waste treatment and energy generation that may indeed more consistently achieve lower toxic PCDD/F emission levels compared to combustion.

All combustion processes can result in formation of PCDD/F at temperature range of 200 to 600°C in case organic carbon, oxygen, and chlorine become accessible. The formation of dioxins is effectively reduced due to the high temperature reactor (in special cases >1000°C) and shock cooling of gases combined, with an absence of available oxygen.

## Acknowledgements

Financial support was provided by the Rannís Technology Development Fund (project 175326-0611), the Icelandic Research Fund (grant 196458-051), and the Northern Periphery and Arctic program (project H-CHP 176).

## Conflict of interest

The authors declare no conflict of interest.

## Nomenclature

PCDDs	Polychlorinated dibenzo-p-dioxins
PCDFs	Polychlorinated dibenzofurans
TCDD	2,3,7,8-tetrachlorodibenzo-p-dioxin
PCBs	Polychlorinated biphenyls
TEF	Toxic equivalence factor
TEQ	Toxic equivalent
CPs	Chlorophenols
CBs	Chlorobenzenes
PAHs	Polycyclic aromatic hydrocarbons
SO <sub>x</sub>	Sulfur oxides
NO <sub>x</sub>	Nitrogen oxides
DeNO <sub>x</sub> /DeDiox	Removal of nitrogen oxides and dioxins
RDF	Refuse derived fuel
MSW	Municipal solid waste
WEEE	Waste electrical and electronic equipment
PVC	Polyvinyl chloride
BR	Cogasified biofermenting residue

iGCLC	In-situ gasification chemical looping
GEK	Gasifier's experimenter's kit
LHV	Low heating value (MJ/m <sup>3</sup> )
HHV	High heating value (MJ/m <sup>3</sup> )

## Author details

Seyedeh Masoumeh Safavi\*, Christiaan Richter and Runar Unnthorsson  
School of Engineering and Natural Sciences, University of Iceland, VR-II,  
Hjardarhaga, Reykjavik, Iceland

\*Address all correspondence to: [seyedeh.m.safavi@gmail.com](mailto:seyedeh.m.safavi@gmail.com)

## IntechOpen

© 2021 The Author(s). Licensee IntechOpen. This chapter is distributed under the terms of the Creative Commons Attribution License (<http://creativecommons.org/licenses/by/3.0>), which permits unrestricted use, distribution, and reproduction in any medium, provided the original work is properly cited. 

## References

- [1] Chopra S, Jain A. A review of fixed bed gasification systems for biomass. *Agric Eng Int CIGR Ejournal* 2007;IX:1-23. doi:http://hdl.handle.net/1813/10671.
- [2] Demirbas AH, Demirbas I. Importance of rural bioenergy for developing countries. *Energy Convers Manag* 2007;48:2386-2398. doi:10.1016/j.enconman.2007.03.005.
- [3] Pollex A, Ortwein A, Kaltschmitt M. Thermo-chemical conversion of solid biofuels. *Biomass Convers Biorefinery* 2012;2:21-39. doi:10.1007/s13399-011-0025-z.
- [4] Susastriawan AAP, Saptoadi H, Purnomo. Small-scale downdraft gasifiers for biomass gasification: A review. *Renew Sustain Energy Rev* 2017;76:989-1003. doi:10.1016/j.rser.2017.03.112.
- [5] Purohit P. Economic potential of biomass gasification projects under clean development mechanism in India. *J Clean Prod* 2009;17:181-193. doi:10.1016/j.jclepro.2008.04.004.
- [6] Basu P. Biomass gasification, pyrolysis and torrefaction practical design and theory. 2nd ed. Elsevier; 2013.
- [7] Briesemeister L, Kremling M, Fendt S, Spliethoff H. Air-Blown Entrained-Flow Gasification of Biomass: Influence of Operating Conditions on Tar Generation. *Energy and Fuels* 2017;31:10924-10932. doi:10.1021/acs.energyfuels.7b01801.
- [8] Knoef H, Ahrenfeldt J. Handbook biomass gasification. BTG biomass technology group; 2005.
- [9] Arena U. Process and technological aspects of municipal solid waste gasification. A review. *Waste Manag* 2012;32:625-639. doi:10.1016/j.wasman.2011.09.025.
- [10] Mukherjee A, Debnath B, Ghosh SK. A Review on Technologies of Removal of Dioxins and Furans from Incinerator Flue Gas. *Procedia Environ Sci* 2016;35:528-540. doi:10.1016/j.proenv.2016.07.037.
- [11] Malkow T. Novel and innovative pyrolysis and gasification technologies for energy efficient and environmentally sound MSW disposal. *Waste Manag* 2004;24:53-79. doi:10.1016/S0956-053X(03)00038-2.
- [12] Consonni S, Viganò F. Waste gasification vs. conventional Waste-To-Energy: A comparative evaluation of two commercial technologies. *Waste Manag* 2012;32:653-666. doi:10.1016/j.wasman.2011.12.019.
- [13] Altarawneh M, Długogorski BZ, Kennedy EM, Mackie JC. Mechanisms for formation, chlorination, dechlorination and destruction of polychlorinated dibenzo- p -dioxins and dibenzofurans (PCDD/Fs). *Prog Energy Combust Sci* 2009;35:245-274. doi:10.1016/j.peccs.2008.12.001.
- [14] Paladino O, Massabò M. Health risk assessment as an approach to manage an old landfill and to propose integrated solid waste treatment: A case study in Italy. *Waste Manag* 2017. doi:10.1016/j.wasman.2017.07.021.
- [15] Zhou H, Meng A, Long Y, Li Q, Zhang Y. A review of dioxin-related substances during municipal solid waste incineration. *Waste Manag* 2015;36:106-118. doi:10.1016/j.wasman.2014.11.011.
- [16] Huang H, Buekens A. De novo synthesis of polychlorinated dibenzo- p -dioxins and dibenzofurans. Proposal of a mechanistic scheme.

Sci Total Environ 1996. doi:10.1016/S0048-9697(96)05330-2.

[17] Environment Agency (Japan), Ministry of Health and Welfare (Japan). Report on Tolerable Daily Intake (TDI) of Dioxins and Related Compounds. 1999.

[18] Cunliffe AM, Williams PT. De-novo formation of dioxins and furans and the memory effect in waste incineration flue gases 2009;29:739-748. doi:10.1016/j.wasman.2008.04.004.

[19] Lavric ED, Konnov AA, De Ruyck J. Dioxin levels in wood combustion - A review. Biomass and Bioenergy 2004;26:115-145. doi:10.1016/S0961-9534(03)00104-1.

[20] Environment Australia. Incineration and Dioxins Review of Formation Processes A consultancy funded by Environment Australia Department of the Environment and Heritage 1999:42.

[21] Huang H, Buekens A. On the mechanisms of dioxin formation in combustion processes. Chemosphere 1995;31:4099-4117. doi:10.1016/0045-6535(95)80011-9.

[22] Martens D, Balta-Brouma K, Brotsack R, Michalke B, Schramel P, Klimm C, et al. Chemical impact of uncontrolled solid waste combustion to the vicinity of the Kouroupitos Ravine, Crete, Greece 1998;36:2855-2866.

[23] Cheung WH, Lee VKC, McKay G. Minimizing dioxin emissions from integrated MSW thermal treatment. Environ Sci Technol 2007;41:2001-2007. doi:10.1021/es061989d.

[24] Psomopoulos CS, Bourka A, Themelis NJ. Waste-to-energy: A review of the status and benefits in USA. Waste Manag 2009;29:1718-1724. doi:10.1016/j.wasman.2008.11.020.

[25] Stanmore BR. The formation of dioxins in combustion

systems. Combust Flame 2004;136:398-427. doi:10.1016/j.combustflame.2003.11.004.

[26] Zhang M, Buekens A, Li X. Brominated flame retardants and the formation of dioxins and furans in fires and combustion. J Hazard Mater 2016;304:26-39. doi:10.1016/j.jhazmat.2015.10.014.

[27] Environmental and Safety Services. Incineration and Dioxins Review of Formation Processes 1999:42.

[28] Dickson LC, Lenoir D, Hutzinger O. Quantitative comparison of de novo and precursor formation of polychlorinated dibenzo-p-dioxins under simulated municipal solid waste incinerator postcombustion conditions. Environ Sci Technol 1992;26:1822-1828. doi:10.1021/es00033a017.

[29] Luijk R, Akkerman DM, Slot P, Olie K, Kapteijn F. Mechanism of formation of polychlorinated dibenzo-p-dioxins and dibenzofurans in the catalyzed combustion of carbon. Environ Sci Technol 1994;28:312-321. doi:10.1021/es00051a019.

[30] Tuppurainen K, Halonen I, Ruokojärvi P, Tarhanen J, Ruuskanen J. Formation of PCDDs and PCDFs in municipal waste incineration and its inhibition mechanisms: A review. Chemosphere 1998;36:1493-1511. doi:10.1016/S0045-6535(97)10048-0.

[31] McKay G. Dioxin characterisation, formation and minimisation during municipal solid waste (MSW) incineration: review. Chem Eng J 2002;86:343-368. doi:10.1016/S1385-8947(01)00228-5.

[32] Tame NW, Dlugogorski BZ, Kennedy EM. Formation of dioxins and furans during combustion of treated wood. Prog Energy Combust Sci 2007;33:384-408. doi:10.1016/j.pecc.2007.01.001.

- [33] Ddwel. Simultaneous sampling of PCDD/PCDF inside the combustion chamber and on four boiler levels of a waste incineration plant. A-to-Z Guid to Thermodyn Heat Mass Transf Fluids Eng 1990;C:1-3. doi:10.1615/AtoZ.c.combustion\_chamber.
- [34] Walker. literature review of formation and release of PCDD/Fs from gas manufacturing 1997;35:1409-22.
- [35] Lopes EJ, Okamura LA, Yamamoto CI. FORMATION OF DIOXINS AND FURANS DURING MUNICIPAL SOLID WASTE GASIFICATION. Brazilian J Chem Eng 2015;32:87-97. doi:10.1590/0104-6632.20150321s00003163.
- [36] Baumgärtel G. The Siemens Thermal Waste Recycling Process - a modern technology for converting waste into usable products. J Anal Appl Pyrolysis 1993;27:15-23. doi:10.1016/0165-2370(93)80019-V.
- [37] Schubert R, Stahlberg R. Advanced Continuous In-line Gasification and Vitrification of Solid Waste. Sustain Dev Int 1999;1:37-40.
- [38] Sippula O, Lind T, Jokiniemi J. Effects of chlorine and sulphur on particle formation in wood combustion performed in a laboratory scale reactor. Fuel 2008;87:2425-2436. doi:10.1016/j.fuel.2008.02.004.
- [39] Chagger H., Kendall A, McDonald A, Pourkashanian M, Williams A. Formation of dioxins and other semi-volatile organic compounds in biomass combustion. Appl Energy 1998;60:101-114. doi:10.1016/S0306-2619(98)00020-8.
- [40] Schatowitz B, Brandt G, Gafner F, Schlumpf E, Bühler R, Hasler P, et al. Dioxin emissions from wood combustion. Chemosphere 1994;29:2005-2013. doi:10.1016/0045-6535(94)90367-0.
- [41] Salthammer T, Klipp H, Peek R-D, Marutzky R. Formation of polychlorinated dibenzo-p-dioxins (PCDD) and polychlorinated dibenzofurans (PCDF) during the combustion of impregnated wood. Chemosphere 1995;30:2051-2060. doi:10.1016/0045-6535(95)00083-K.
- [42] Lind T, Kauppinen EI, Hokkinen J, Jokiniemi JK, Orjala M, Aurela M, et al. Effect of Chlorine and Sulfur on Fine Particle Formation in Pilot-Scale CFBC of Biomass. Energy & Fuels 2006;20:61-68. doi:10.1021/ef050122i.
- [43] Ferraz MCMA, Afonso SA V. Dioxin Emission Factors for the Incineration of Different Medical Waste Types. Environ Contam Toxicol n.d. doi:10.1007/s00244-022-2033-2.
- [44] Wang J, Zhao H. Evaluation of CaO-decorated Fe<sub>2</sub>O<sub>3</sub>/Al<sub>2</sub>O<sub>3</sub> as an oxygen carrier for in-situ gasification chemical looping combustion of plastic wastes. Fuel 2016. doi:10.1016/j.fuel.2015.10.020.
- [45] Tillman D. The combuston of solid fuels and wastes. San Diego: Academic Press Inc.; 1991.
- [46] Panepinto D, Tedesco V, Brizio E, Genon G. Environmental Performances and Energy Efficiency for MSW Gasification Treatment. Waste and Biomass Valorization 2014;6:123-135. doi:10.1007/s12649-014-9322-7.
- [47] Thakare S, Nandi S. Study on Potential of Gasification Technology for Municipal Solid Waste (MSW) in Pune City. Energy Procedia 2015;90:509-517. doi:10.1016/j.egypro.2016.11.218.
- [48] Klein A. Gasification: an alternative process for energy recovery and disposal of municipal solid wastes. New York 2002:1-50.
- [49] Xu P, Jin Y, Cheng Y. Thermodynamic Analysis of the

Gasification of Municipal Solid Waste. *Engineering* 2017;3:416-422. doi:10.1016/J.ENG.2017.03.004.

[50] Seggiani M, Puccini M, Raggio G, Vitolo S. Effect of sewage sludge content on gas quality and solid residues produced by cogasification in an updraft gasifier. *Waste Manag* 2012;32:1826-1834. doi:10.1016/j.wasman.2012.04.018.

[51] Werther J, Ogada T. Sewage sludge combustion. *Prog Energy Combust Sci* 1999;25:55-116. doi:10.1016/S0360-1285(98)00020-3.

[52] Zwart RWR, Van der Drift A, Bos A, Visser HJM, Cieplik MK, Könemann HWJ. Oil-based gas washing-Flexible tar removal for high-efficient production of clean heat and power as well as sustainable fuels and chemicals. *Environ Prog Sustain Energy* 2009;28:324-335. doi:10.1002/ep.10383.

[53] Lonati G, Zanoni F. Probabilistic health risk assessment of carcinogenic emissions from a MSW gasification plant. *Environ Int* 2012. doi:10.1016/j.envint.2012.01.013.

[54] Dannecker W, Hemschemeier H. Level of activated-coke technology for flue gas dust collection behind refuse destruction plants looking at the problem from the special aspects of dioxin separation. *Organohalogen Compd* 1990.

[55] Hiraoka M, Takizawa Y, Masuda Y, Takeshita R, Yagome K, Tanaka M, et al. Investigation on generation of dioxins and related compounds from municipal incinerators in Japan. *Chemosphere* 1987;16:1901-1906. doi:10.1016/0045-6535(87)90185-8.

[56] Goemans M, Clarysse P, Joannès J, De Clercq P, Lenaerts S, Matthys K, et al. Catalytic NO<sub>x</sub> reduction with simultaneous dioxin and furan oxidation.

*Chemosphere* 2003;50:489-497. doi:10.1016/S0045-6535(02)00554-4.

[57] Kamińska-Pietrzak N, Smoliński A. Selected Environmental Aspects of Gasification and Co-Gasification of Various Types of Waste. *J Sustain Min* 2013;12:6-13. doi:10.7424/jsm130402.

[58] Diego Mauricio Yepes Maya, Angie Lizeth Espinosa Sarmiento, Cristina Aparecida Vilas Boas de Sales Oliveira, Electo Eduardo Silva Lora, Rubenildo Vieira Andrade. Gasification of Municipal Solid Waste for Power Generation in Brazil, a Review of Available Technologies and Their Environmental Benefits. *J Chem Chem Eng* 2016;10:249-255. doi:10.17265/1934-7375/2016.06.001.

[59] Kwak T-H, Lee S, Park J-W, Maken S, Yoo YD, Lee S-H. Gasification of municipal solid waste in a pilot plant and its impact on environment. *Korean J Chem Eng* 2006;23:954-960. doi:10.1007/s11814-006-0014-2.

[60] Griffin RD. A new theory of dioxin formation in municipal solid waste combustion. *Chemosphere* 1986;15:1987-1990. doi:10.1016/0045-6535(86)90498-4.

[61] Andersson S, Karlsson M, Hunsinger H. Sulphur recirculation for lowcorrosion waste-to-energy. *Int. Solid Waste Assoc. World Congr., Hamburg*: 2010.

[62] Pařízek T, Bébar L, Stehlík P. Persistent pollutants emission abatement in waste-to-energy systems. *Clean Technol Environ Policy* 2008;10:147-153. doi:10.1007/s10098-007-0135-2.

[63] Kojima N, Mitomo A, Itaya Y, Mori S, Yoshida S. Adsorption removal of pollutants by active cokes produced from sludge in the energy recycle process of wastes. *Waste Manag* 2002. doi:10.1016/S0956-053X(02)00022-3.

- [64] Pranghofer G. FK. Destruction of polychlorinated dibenzo-p-dioxins and dibenzofurans on fabric filters: recent experiences with catalytic filter system. Recent Exp. with Catal. filter Syst. 3rd Int. Symp. Inciner. Flue Gas Treat. Technol., Brussels, Belgium: 2001.
- [65] Bonte JL, Fritsky KJ, Plinke MA, Wilken M. Catalytic destruction of PCDD/F in a fabric filter: experience at a municipal waste incinerator in Belgium. Waste Manag 2002;22:421-426. doi:10.1016/S0956-053X(02)00025-9.
- [66] Inoue K, Yasuda K, Kawamoto K. Report: Atmospheric pollutants discharged from municipal solid waste incineration and gasification-melting facilities in Japan. Waste Manag Res 2009;27:617-622. doi:10.1177/0734242X08096530.
- [67] Fino D., Russo N., Solaro S., Sarraco G., Comaro U., Bassetti A. S V. Low temperature SCR catalysts for the simultaneous destruction of NOx and dioxins. 4th Eur. Congr. Chem. Eng., Granada, Spain: 2003.
- [68] Dvořák R, Pařízek T, Bébar L, Stehlík P. Incineration and gasification technologies completed with up-to-date off-gas cleaning system for meeting environmental limits. Clean Technol Environ Policy 2009;11:95-105. doi:10.1007/s10098-008-0170-7.
- [69] Parizek T, Bebar L, Oral J, Stehlik P. Emissions abatement in Waste-to-Energy Systems. 17th Eur. Symp. Comput. Aided Process Eng., 2007, p. 1-6.
- [70] Safavi SM, Richter C, Unnthorsson R. A review of dioxin formation in biomass gasification. Submitted n.d.
- [71] Quaß U, Fermann M, Bröker G. The European Dioxin Air Emission Inventory Project - Final Results. Chemosphere 2004;54:1319-1327. doi:10.1016/S0045-6535(03)00251-0.
- [72] Nzihou A, Themelis NJ, Kemiha M, Benhamou Y. Dioxin emissions from municipal solid waste incinerators (MSWIs) in France. Waste Manag 2012;32:2273-2277. doi:10.1016/j.wasman.2012.06.016.
- [73] Dopico M, Gómez A. Review of the current state and main sources of dioxins around the world. J Air Waste Manag Assoc 2015;65:1033-1049. doi:10.1080/10962247.2015.1058869.
- [74] Abel Arkenbout. Hidden emissions : A story from the Netherlands. 2018.
- [75] Domingo JL, Marquès M, Mari M, Schuhmacher M. Adverse health effects for populations living near waste incinerators with special attention to hazardous waste incinerators. A review of the scientific literature. Environ Res 2020;187:109631. doi:10.1016/j.envres.2020.109631.
- [76] Rathna R, Varjani S, Nakkeeran E. Recent developments and prospects of dioxins and furans remediation. J Environ Manage 2018;223:797-806. doi:10.1016/j.jenvman.2018.06.095.
- [77] Zhang T, Fiedler H, Yu G, Ochoa GS, Carroll WF, Gullett BK, et al. Emissions of unintentional persistent organic pollutants from open burning of municipal solid waste from developing countries. Chemosphere 2011;84:994-1001. doi:10.1016/j.chemosphere.2011.04.070.



# Solid Waste Gasification: Comparison of Single- and Multi-Staged Reactors

*Xianhui Zhao, Kai Li, Meghan E. Lamm, Serdar Celik,  
Lin Wei and Soydan Ozcan*

## Abstract

Interest in converting waste into renewable energy has increased recently due to concerns about sustainability and climate change. This solid waste is mainly derived from municipal solid waste (MSW), biomass residue, plastic waste, and their mixtures. Gasification is one commonly applied technology that can convert solid waste into usable gases, including H<sub>2</sub>, CO, CH<sub>4</sub>, and CO<sub>2</sub>. Single- and multi-staged reactors have been utilized for solid waste gasification. Comparison in reactor dimensions, operating factors (e.g., gasification agent, temperature, and feed composition), performance (e.g., syngas yield and selectivity), advantages, and disadvantages are discussed and summarized. Additionally, discussion will include economic and advanced catalysts which have been developed for use in solid waste gasification. The multi-staged reactor can not only be applied for gasification, but also for pyrolysis and torrefaction.

**Keywords:** solid waste, gasification, single-staged reactor, multi-staged reactor, syngas, catalyst

## 1. Introduction

Solid waste can be derived from municipal solid waste (MSW), biomass residue, plastic waste, and their mixtures. For example, MSW management has become a big challenge all over the world. Based on a World Bank report [1], the world generates 0.74 kg of waste per capita per day, and the total MSW production is projected to grow to 3.40 billion tons by 2050. 37% of this MSW ends up in landfills and 33% is openly dumped worldwide [1]. Only 19% undergoes material recovery through recycling and composting, while the remaining 11% is treated through modern incineration. This creates serious environmental problems and a huge energy waste. One sustainable strategy for waste management is to reduce landfill disposal, thus minimizing the environmental impact. Meanwhile, utilizing solid waste resources to create value-added products has become one of the most attracting topics. The top 3 components of MSW are food and green waste (44%), paper and cardboard (17%), and rubber and leather (12%) [1]. Therefore, MSW contains a high content of organic material, which can be recovered through biochemical [2] and thermochemical processes [3]. Thermochemical processes are promising for dealing with a large quantity of MSW, especially from unsorted waste streams, as it can significantly reduce the waste in both

mass (about 70–80%) and volume (about 80–90%) with a high conversion rate. Other detailed advantages can be found in Arena's review on thermochemical processes [4].

Various thermochemical processes, such as incineration, pyrolysis, and gasification, have been developed to recover energy from the organic fraction in MSW [5]. Incineration is a full oxidation of the combustible materials in the waste and generates energy in the form of heat. Incineration has been traditionally used to treat waste. However, due to the production of flue gases ( $\text{CO}_2$ ,  $\text{H}_2\text{O}$ ,  $\text{O}_2$ ,  $\text{N}_2$ ) during the process and legislation enforcement regarding gas emission, new development of incineration is needed to reduce the environmental impact. Pyrolysis is the thermal degradation of waste, under a limit or total absence of an oxidizing agent. Pyrolysis can recover part of the organic fraction as liquid fuels (e.g., hydrocarbons, alcohols), while also generating a small amount of synthesis gas (syngas, a mixture of  $\text{CO}$ ,  $\text{H}_2$ ,  $\text{CO}_2$ ,  $\text{CH}_4$ , etc.) and biochar. The generated syngas can be used to power gas engines or turbines to generate electricity. Although there may be some differences in yield, proportion, and exact composition, gasification is a partial oxidation of organic compounds and mainly produces syngas. Syngas can be converted into value products through processes such as the Fischer-Tropsch synthesis [6, 7], or used as a fuel for electricity and heat generation. Therefore, gasification can produce energy, energy carriers (such as  $\text{H}_2$ ) and chemicals from the solid waste [8], all of which creates lots of research interest. Additionally, gasification has advantages including no limitations on the size and type of waste, different applications of the gaseous fuels, and a decrease in overall pollution.

Gasification of solid waste is a complex process, including different chemical and physical transformations at high temperature (e.g.,  $>600\text{ }^\circ\text{C}$ ). Based on the oxidation medium, gasification can be classified into partial oxidation with air, oxygen-enriched air, pure oxygen, steam, and plasma gasification. Different gasification processes generate different gas compositions, heating values and byproduct yields. In general, there are four steps in gasification: vaporization, devolatilization/pyrolysis, secondary cracking of tars, and reactions/reduction/gasification [9]. Vaporization involves heating the waste at low temperature (ca.  $160\text{ }^\circ\text{C}$ ) to remove water from the solid waste. Devolatilization/pyrolysis occurs at a higher temperature and generates char and volatiles, which include long chain hydrocarbon liquids and a small fraction of gases. Secondary cracking of tars (a mixture of condensable hydrocarbons) is used to further crack the tars and involves several homogeneous reactions in the gas phase and heterogeneous ones at the surface of the solid fuel or char particles. Reactions/reduction/gasification is used to react the char with a gas species using heterogeneous reactions. The reactions which occur during gasification are complex, making it difficult to optimize the processing parameters to obtain the best quality and yield of syngas. These parameters include equivalence ratio, reactor temperature, residence time of gases and waste, waste composition and physical properties, and composition and inlet temperature of the gasifying medium. Park et al. [10] performed a two-staged gasification of high-density polyethylene (HDPE) and biomass blends, comprised of an oxidative pyrolysis reactor and a thermal plasma reactor. They found that, for higher biomass fractions, enhanced  $\text{CO}_2$  yields were produced and reversely, an increased HDPE fraction yielded a higher content of hydrocarbons.

Different reactors, including single-staged and multi-staged gasifiers, have been developed for gasification [5]. For a single-staged reactor, the pyrolysis and gasification zones are packed into one reactor (**Figure 1a**). A single-staged gasifier includes a fixed bed gasifier [11, 12], fluidized bed gasifier [13, 14], and entrained flow gasifier [15, 16]. A multi-staged reactor system is configured in two ways: a single reactor with separate, controlled pyrolysis and gasification zones, and separate pyrolysis and gasification reactors connected in series (**Figure 1b**). The multi-staged gasification technology allows for optimization of reaction conditions

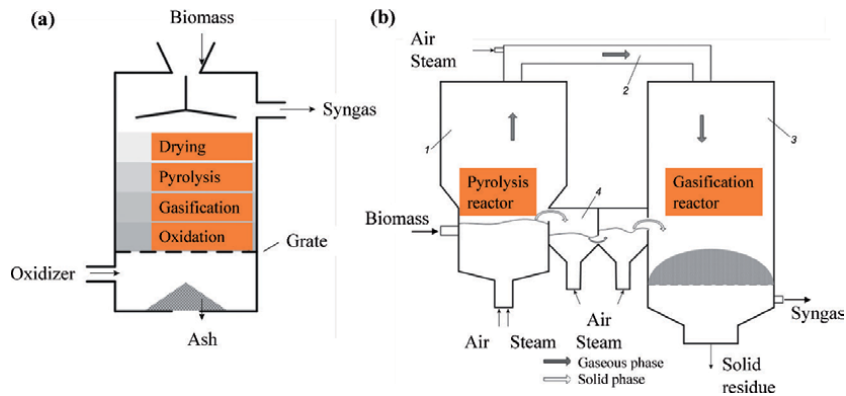


**Figure 1.** Schematic of a single-staged reactor (a, fixed bed gasifier) and multi-staged reactor (b, 1: first stage [pyrolysis], 2: second stage [thermal decomposition of tar], 3: third stage [gasification], 4: fluidized bed) [17]. Reproduced with permission from [17].

for the conversion of biomass at every separate stage. Both single- and multi-staged reactors have been utilized for solid waste gasification. Single- and multi-staged reactors are illustrated in **Figure 1**. Chan et al. [18] studied the single-staged gasification of MSW, finding that the tar content in syngas could reach  $7.8 \text{ g/Nm}^3$ . Bhoi et al. [19] investigated the co-gasification of a MSW and switchgrass mixture in a single-staged reactor, producing  $9.9\text{--}26 \text{ g/Nm}^3$  of tar. Compared with a single-staged reactor, a multi-staged reactor system can reduce the tar yield, which is beneficial because generated tar can cause failure of gasification projects [20]. Gómez-Barea et al. [21] developed a three-staged, fluidized bed based gasification reactor and found that this three-staged system depicted a higher gasification efficiency (14%) and lower tar content, compared to a regular single-staged fluidized bed reactor. However, literature providing a comparison between single- and multi-staged reactors for solid waste gasification remains sparse. The analysis of reactor dimensions, operating factors, and performance of these reactors has not been studied systematically. It is the goal of this review to present current literature comparing these reactor types and analyzing their relevant processing parameters.

This chapter focuses on the comparison of single- and multi-staged reactors used for solid waste gasification. Solid waste resources such as MSW, biomass residue, plastic waste, and their mixtures are discussed. The reactor dimensions, operating factors (e.g., temperature, gasification agent, and feed composition), performance (e.g., syngas yield), advantages, and disadvantages of single- and multi-staged reactors are discussed and summarized. Additionally, discussion includes economic and advanced catalysts (e.g., Ni-CaO-C and Ni/Al<sub>2</sub>O<sub>3</sub>) which have been developed for use in solid waste gasification. These Ni based catalysts are promising for solid waste gasification at high conversion efficiency. The multi-staged reactor can not only be applied for gasification, but also for pyrolysis and torrefaction.

## 2. Solid waste gasification

### 2.1 Single-staged reactor

#### 2.1.1 Reactor dimensions

Different reactor scales, including bench, lab, and pilot scale, have been developed for solid waste gasification. The inside diameter and length of the reactor

are typically in the range of 3–800 mm and 200–3500 mm, respectively, as shown in **Table 1**. Selection of the appropriate reactor dimensions is helpful for the solid waste gasification performance. For example, Xiong et al. [38] found that the reactor diameter had a negligible effect on gasification performance, but an increase in bed height (0.6–1.2 m) caused an increased heating value and carbon conversion efficiency. Basha et al. [39] found that a difference in the hydrocarbon content and methane concentration of the product gas depends on the reactor size and design. Larger reactors can increase the residence time of the product gas in the reactor, so that lighter hydrocarbons have more time to decompose or undergo oxidation into smaller molecules such as H<sub>2</sub> and CO [39]. There are various types of reactors developed for solid waste gasification, including bubbling fluidized bed, downdraft fluidized bed, updraft fluidized bed, downdraft fixed bed, updraft fixed bed, batch, and entrained-flow reactors, some of which are shown in **Figures 2–4**. Different types of reactors are applicable for specific types of solid waste. For example, steam gasification of waste with a high moisture content occurs well in a bubbling fluidized bed reactor.

Other designs, such as adding a stirrer or using sorbents, have been developed to improve the solid waste gasification performance. In a study, Indrawan et al. [32] utilized a stirrer in a downdraft reactor system to create a uniform mixing feed and prevent bridging inside the reactor; a rotating ash scrapper to unload ash from the reactor and prevent ash accumulation inside the reactor; and an inclined ash screw conveyor to transport the ash into the ash drum. Pinto et al. [30] used water to cool the feeding system and avoid clogging inside, which can arise from the feedstock pyrolysis (prior to entry into the reactor). N<sub>2</sub> was blown through the feeding system to help transfer the feedstock smoothly, avoid plugging, and prevent gas backflow. Lastly, the gas product passed through a cyclone to remove particulates [30]. Salaudeen et al. [42] used calcined eggshell as the bed material and CO<sub>2</sub> sorbent for the steam gasification of sawdust, in a bubbling fluidized bed reactor, to improve the hydrogen content in the syngas. The sorbent-enhanced gasification enabled the reactor operation at comparatively lower temperatures, and required less equipment [42]. In summary, the reactor design and size (inside diameter of 3–800 mm and length of 200–3500 mm) need to be optimized to maximize the solid waste gasification performance.

### 2.1.2 Operating factors and performance

During the solid waste gasification process, many parameters such as temperature, feed composition, gasification agent, and reaction time are investigated. **Table 2** shows the syngas yield (typically 1.2–2.2 Nm<sup>3</sup>/kg) obtained from gasification under varying conditions. Temperature is a significant parameter that can affect the gasification performance and is usually in the range of 600–900 °C. For example, Bai et al. [34] studied the gasification of PP at 23 MPa and 500–800 °C, finding that an increase in temperature improved the gasification efficiency. Bai et al. [43] also studied the supercritical water gasification of polyethylene terephthalate (PET), finding that the gasification efficiency increased with an increase in temperature from 500 to 800 °C. The PET gasification reaction increased slowly with the temperature (500–700 °C). Based on the kinetics, the PET gasification reaction was complex and intense in the initial stage of gasification. Most active components gasified quickly, while inert components reacted slowly in the later stage of gasification [43]. Peng et al. [44] studied the gasification at various gasification temperatures (750, 825, and 900 °C), finding that high temperature (900 °C) was favorable for tar cracking. Xiong et al. [38] studied gasification at 400–800 °C, finding that an increase in temperature affected the heating value and improved the gasifier

Waste	Reactor type	Reactor dimension	Other	Ref.
MSW	Lab scale fixed bed	Inside diameter = 48 mm, length = 500 mm	—	[22]
Landfill waste	Lab-scale horizontal tube	Inside diameter = 25 mm, length = 1000 mm	—	[23]
Lignite coal and plastic mixture	Sealed quartz	Inside diameter = 3 mm, length = 200 mm	Plastic: PP <sup>a</sup> , PE <sup>b</sup> , or PC <sup>c</sup>	[24]
Poplar wood chips	Stainless steel batch (autoclave)	—	Supercritical water gasification	[25]
Rice husk	Bubbling fluidized bed	Diameter = 0.08 and 0.8 m, bed height = 0.6–1.2 m	—	[38]
MSW	Fixed bed	Outside diameter = 219 mm, length = 600 mm	—	[26]
Chicken manure and wood chip mixture	Fixed bed downdraft	—	Feedstock flow rate: 10 kg/h	[27]
Rural solid waste	Fixed bed updraft	—	Feedstock main composition: paper, plastic, and kitchen waste	[28]
Biomass	Fixed bed reverse downdraft	Inside diameter = 54 mm, length = 1.25 m	—	[29]
Rice production waste mixture	Bench scale bubbling fluidized bed	Inside diameter = 80 mm, length = 1.5 m	Feedstock flow rate: 5 g/min	[30]
Biomass	Fluidized bed	Outside diameter = 120 mm, length = 610 mm	—	[31]
MSW and switchgrass mixture	Downdraft	Length = 3.2 m	Feedstock flow rate: 100 kg/h	[32]
Food waste	Batch	Reactor volume = 200 mL	Supercritical water gasification; maximum operation temperature: 600 °C, maximum operation pressure: 35 MPa	[33]
PP	Quartz tube	Inside diameter = 3 mm, length = 200 mm	—	[34]
MSW	Drop quartz tube	Inside diameter = 19 mm, length = 1.8 m	Feedstock flow rate: 0.78 g/min	[35]
MSW and biomass mixture	Pilot-scale bubbling fluidized bed	Inside diameter = 0.25 m, length = 2.3 m	—	[36]
Sawdust	Pilot scale bubbling fluidized	Inside diameter = 0.2 m, length = 3.5 m	Reactor capacity: 50 kg/h	[37]

<sup>a</sup>Polypropylene (PP).

<sup>b</sup>Polyethylene (PE).

<sup>c</sup>Polycarbonate (PC).

**Table 1.**  
 The solid waste gasification, single-staged reactor type, and dimension.

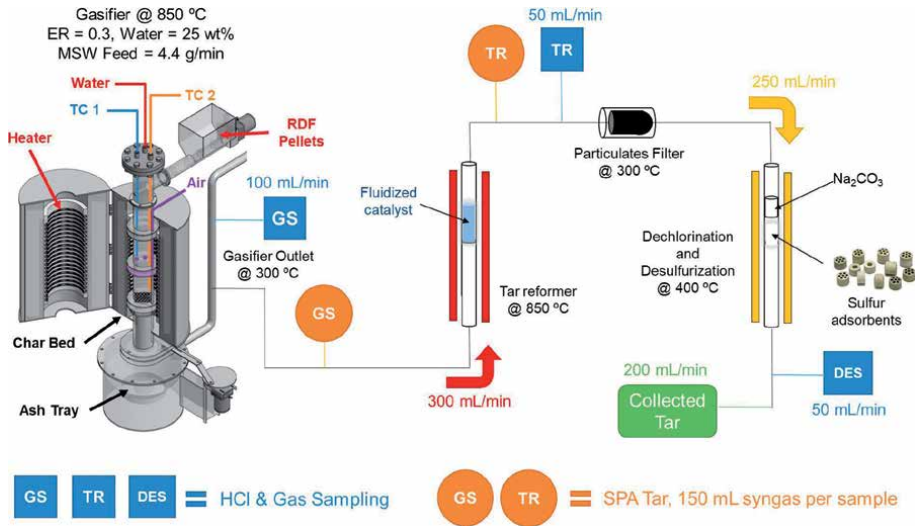


**Figure 2.** Illustration of the downdraft gasification of MSW integrated with a hot syngas purification system. RDF pellets were gasified to produce syngas. Some of the syngas passed through a purification system (including a tar reformer, particulate filter, and dechlorination/desulfurization reactor) to remove impurities (tar, particulates, HCl, and sulfur species). (ER: equivalence air ratio, TC1: thermocouple 1, TC2: thermocouple 2, RDF: refuse derived fuel, TR: tar reformer, DES: desulfurization reactor, GS: gasifier, SPA: solid phase adsorption) [18]. Reproduced with permission from [18].

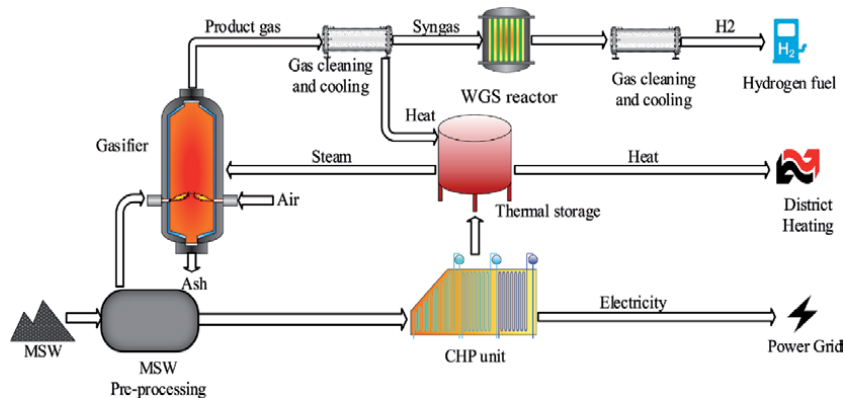


**Figure 3.** Schematic diagram of an H<sub>2</sub> production plant with gasification of MSW. MSW was pre-processed and then gasified to produce syngas, which passed through a WGS reactor to produce H<sub>2</sub>. Partial MSW combustion provided heat for district heating and power grid. (WGS: water gas shift, CHP: combined heat and power) [40]. Reproduced with permission from [40].

efficiency. Xiang et al. [26] studied the steam gasification at temperatures of 600–1000 °C, finding that the increase in temperature increased the total volume fraction of H<sub>2</sub> and CO from 56% to 66%. From all the above studies, an appropriate temperature (e.g., 800–900 °C) should be selected for solid waste gasification based on high gasification performance and low energy consumption.

Feed composition is also a significant parameter for gasification. For example, Pio et al. [36] studied gasification using a refuse-derived fuel (from MSW) and biomass (pine chips or pine pellets) mixture. 0, 10, 20, 50, and 100 wt% of refuse-derived fuel content in the mixture was studied. An increase in the refuse-derived fuel content increased both the CH<sub>4</sub> concentration and lower heating value (LHV) of the product gas. Therefore, the addition of refuse-derived fuel to biomass may improve

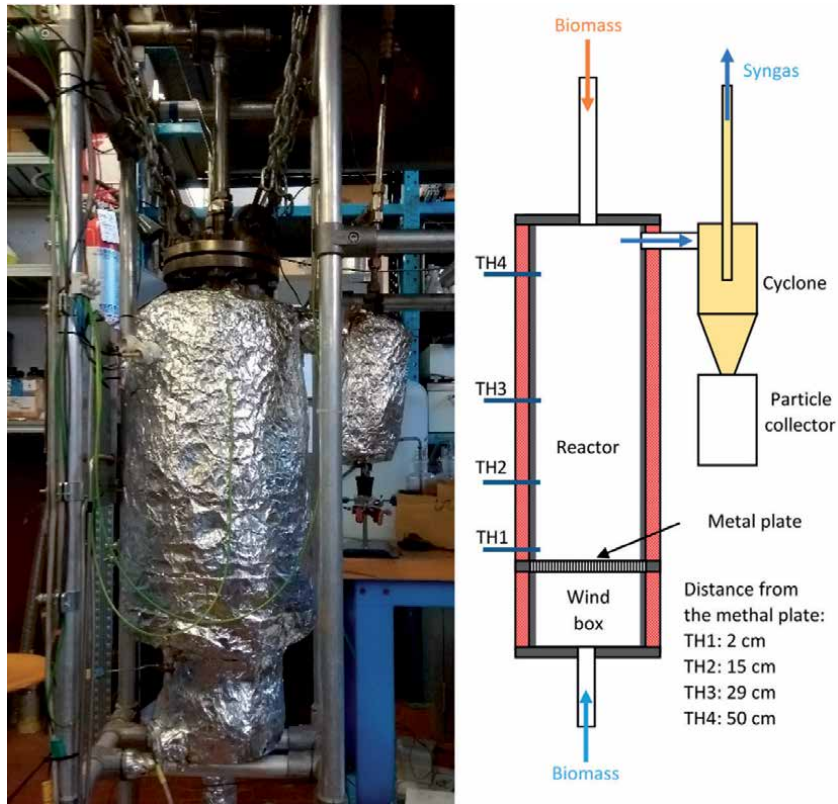


**Figure 4.** An updraft gasification reactor (left) and a schematic diagram of the reactor interior (right). The reactor consisted of a stainless-steel cylinder with a height of 59 cm and a diameter of 8.3 cm. Biomass was transported through a feeding cochlea at the top. Four thermocouples (TH1–TH4) were used to monitor the temperature evolution during the gasification process. A perforated metal plate was used as a support for the gasification bed to allow the oxidant to flow through. A wind box was used to preheat the oxidant agent. The produced syngas was cleaned using a cyclone and a ceramic filter for particle removal. Reproduced with permission from [41].

the economic viability and environmental benefits for gasification plants. There was no agglomeration, slag, or defluidization observed during the experiment [36]. Ng et al. [27] studied the gasification of a chicken manure and wood chip mixture. The co-gasification of this chicken manure and wood chip mixture (30 wt% chicken manure) produced a syngas of similar quality (in terms of LHV) compared to that of gasification of pure wood chip. The chicken manure was found to be a compatible feedstock for gasification in the presence of wood chips [27]. Su et al. [45] studied the gasification of food waste at a food waste concentration of 10–30 wt%. When the food waste concentration increased from 10 to 30 wt%, the  $H_2$  yield largely decreased from 1.1 to 0.6 mol/kg, while the  $CH_4$  yield increased. However, higher food waste concentrations may cause the reactor to plug and catalyst to deactivate [45].

More researchers have studied the effect of feed composition on gasification performance. For example, Bian et al. [24] studied the supercritical water co-gasification of a lignite coal and plastic (PP, PE, or PC) mixture at concentrations of 5–35 wt%. The co-gasification of lignite coal and plastic improved the gasification efficiency of each other, indicating a synergistic effect. This was also observed in other studies. Zaini et al. [23] studied the gasification of landfill waste and a landfill waste and biochar mixture. Co-gasification of landfill waste with biochar was beneficial to improve the  $H_2$  concentration in the syngas. At 800 °C, the addition of 35 wt% biochar enhanced the  $H_2$  concentration from 38 to 54 vol%, and reduced the tar yield from 0.05 to 0.01 g/g-fuel-daf (daf: dry-ash-free weight basis) [23]. It was

Waste	Reactor type	Reaction conditions	Performance	Other	Ref.
MSW	Downdraft fixed-bed	850 °C, equivalence air ratio of 0.3	Syngas yield: ~12 L/min	MSW feed rate: 4.4 g/min; MSW moisture content: 25 wt%	[18]
Food waste	Batch	420 °C, 23 MPa, reaction time of 30 min	Gas yield: 8.4 mol/kg; H <sub>2</sub> yield: 3.1 mol/kg	Reactor volume: 200 mL; heat rate: 10 °C/min	[46]
Biomass	Bubbling fluidized bed	700–854 °C, equivalence ratio of 0.17–0.36	Syngas yield: 1.2–2.2 Nm <sup>3</sup> /kg; carbon conversion efficiency: 60–88%	Biomass feed rate: 7–15 kg/h	[13]
MSW and switchgrass mixture	Fixed bed downdraft	~800 °C	Syngas yield: 1.5 Nm <sup>3</sup> /kg	20% MSW in the feed mixture	[19]
Palm kernel shell and PS <sup>a</sup> mixture	Downdraft	800 °C, air flow rate of 2.5 L/min	Solid yield: ~17 wt%; liquid yield: ~18 wt%; tar yield: ~5 wt%; gas yield: ~60 wt%	20 wt% PS in the feed mixture	[39]
PE and soda lignin mixture	Batch	700 °C, reaction time of 30 min	Gas yield: 75 mol/kg	Internal volume: 10 mL; 50% PE in the feed mixture	[47]
MSW	Drop-tube	900 °C	Syngas yield: 17.5 mol/kg	CO <sub>2</sub> gasification; MSW feed rate: 0.8 g/min	[48]
PET	Quartz tube	800 °C, reaction time of 10 min	Carbon conversion: 98 wt%	Supercritical water gasification	[43]

<sup>a</sup>Polystyrene (PS).

**Table 2.**

*The solid waste single-staged gasification factor and performance.*

also determined that an increase in feedstock concentration could cause problems with reactor operations, such as reactor plugging and damage, thus reducing the gasification efficiency. A suitable feedstock concentration should be selected to balance the gasification efficiency and industrial application [24].

During solid waste gasification, different gasification agents such as O<sub>2</sub> and air can be used. For example, Pinto et al. [30] studied the gasification of rice husk, rice straw and PE at ~850 °C using different gasification agents, such as a mixture of steam, air, oxygen, and CO<sub>2</sub>. At this temperature, the heavier gaseous hydrocarbons and tar contents can be minimized, while steam can promote steam reforming reactions, thus resulting in a gas enriched in H<sub>2</sub> and lower tar content. The use of steam and O<sub>2</sub> was also a good gasification agent option, especially since it lacked N<sub>2</sub> and prevented any diluting effects. The combination produces a larger gas HHV (around 42% higher) and greater energy conversion than those obtained when air was used instead of O<sub>2</sub>. However, the cost of O<sub>2</sub> is still a disadvantage and limits its use [30].



Meng et al. [37] studied the effect of gasifying agents such as air, air–steam, oxygen–steam, and oxygen-enriched air, on sawdust gasification. Compared to sawdust gasification using air, oxygen-enriched air increased LHV due to a reduction in N<sub>2</sub> dilution, while air–steam favored H<sub>2</sub> production due to water gas shift reaction enhancement [37]. Zheng et al. [35] studied the steam gasification of MSW using recycled CO<sub>2</sub> at 1000 °C with a CO<sub>2</sub>/steam ratio of 0.5–3.0, and found that increasing the CO<sub>2</sub>/steam ratio from 0.5 to 2.5 increased both H<sub>2</sub> and CO molar yields.

In order to further improve the gasification performance, various catalysts have been developed and explored. For example, Wang et al. [49] studied the CO<sub>2</sub>-assisted gasification of PP at 900 °C, and discovered the catalytic (Ni/Al<sub>2</sub>O<sub>3</sub> catalyst) gasification improved the gas evolution rate and syngas yield significantly compared to non-catalytic gasification. Irfan et al. [22] studied the catalytic gasification of MSW at 1 atm, finding that the use of waste marble powder as a catalyst was helpful to increase the H<sub>2</sub> concentration and decrease the CO<sub>2</sub> concentration in the gas product, compared to non-catalytic tests. Tian et al. [31] studied the gasification at 800–1000 °C, finding that the use of a catalyst (olivine) enhanced the syngas yield and reduced the cracked tar content. Peng et al. [44] studied gasification over a Ni/CeO<sub>2</sub>/Al<sub>2</sub>O<sub>3</sub> catalyst at different Ni loadings (20, 30, and 40%), finding that a high catalyst loading (40%) was favorable for high-purity H<sub>2</sub> production and tar cracking. The above research demonstrates that the use of an appropriate catalyst can improve product yield and selectivity.

Other parameters such as reaction time, waste pretreatment, and feed dimension have also been investigated for their influence on gasification performance. For example, Bai et al. [34] studied the gasification of PP at a reaction time of 2–60 min, finding that an increase in reaction time had a positive effect on the gasification efficiency. In another study, Bai et al. [43] studied the supercritical water gasification of PET, finding that gasification efficiency increased with the increase in reaction time from 2 to 60 min. Bai et al. [43] also found that the reaction pressure (21–29 MPa) had little impact on the gasification efficiency because the properties of the supercritical water did not change significantly at these different pressures. Su et al. [33] found that waste sorting is helpful to improve the H<sub>2</sub>-rich syngas production (or syngas yield) and gasification efficiency compared to unsorted waste. Xiang et al. [26] studied the steam gasification of MSW with two different MSW particle sizes (20 < diameter < 30 mm and 80 < diameter < 100 mm), finding that the increase of particle size decreased the total volume fraction of H<sub>2</sub> and CO from 52% to 50%. Basha et al. [39] selected a feedstock size of 2–4 mm because a larger particle size prevented a compact fuel bed, while a smaller particle size blocked the reactor and plugged the gas outlet.

### *2.1.3 Advantages and disadvantages*

In single-staged reactor systems, different types of reactors have been utilized based on their advantages and disadvantages. The common reactors used for solid waste gasification include fixed bed, fluidized bed, and entrained flow reactors [50]. A fixed bed reactor has simple construction and operation. However, a fixed bed reactor is typically used for small size reactions with limited loading/processing flexibility because of the poor adaptability for heterogeneous materials. A fluidized bed reactor can provide high mixing and solid–gas contact, promote heat and mass transfer, increase the reaction rate and conversion efficiency, and improve the process flexibility, compared to a fixed bed reactor. However, for both fixed bed and fluidized bed reactors, tar formation is a major problem, while entrained flow reactors have a high cost and poor biomass adaptability [50].

Indrawan et al. [32] studied the gasification of a MSW and switchgrass mixture, finding that the downdraft reactor (patented design) system design was selected due

to low tar content ( $< 0.5 \text{ g/Nm}^3$ ), compared to a circulating fluidized bed (up to  $12 \text{ g/Nm}^3$ ), fluidized bed (up to  $40 \text{ g/Nm}^3$ ), and updraft fixed-bed reactor (up to  $150 \text{ g/Nm}^3$ ). Bian et al. [24] used a sealed quartz reactor system in their study and determined that a fluidized bed reactor might be better for enhancing the mass transfer of the reactant and reducing reactor plugging problems. The fluidized bed gasifier has excellent solid–gas contact efficiency, uniform and controllable temperature distribution, and broad feedstock feasibility [51]. Based on this data, the downdraft fluidized bed is a promising reactor choice for solid waste gasification.

## 2.2 Multi-staged reactor

### 2.2.1 Reactor dimensions

The inside diameter and length of a multi-staged reactor is typically in the range of 3–750 mm and 150–3500 mm, respectively, shown in **Table 3**. These dimensions are similar to those of the single-staged reactor. Likewise, selection of appropriate reactor dimensions will be helpful for the solid waste gasification performance in a multi-staged reactor. There are multiple stages in a multi-staged reactor system such as pyrolysis, reforming, tar cracking, and water-gas shift. **Figure 5** shows a diagram of a two-staged gasification process. Different stages are developed for specified reactions. Parameters in each stage can be operated individually for optimization. In addition, using high temperatures in the tar cracking stage can be helpful to largely reduce tar [50].

Kuba and Hofbauer [62] studied the gasification in a dual fluid bed gasifier, where heat is supplied by the bed material circulating between the gasifier and the combustion reactor. The reactor design and the fluidization nozzle position had a significant effect on the tar formation and reduction. For example, an increase in the bed height of the gasifier can increase the residence time, leading to an overall decrease in tar. Additional fluidization nozzles in the inclined wall, located in the bubbling bed where the feedstock enters the gasifier via a conveyer screw, can improve the mixing of feedstock and bed material. A moving bed section above the inclined wall (no fluidization) can be used to reduce the tar formation. Additional fluidization nozzles can also be installed to reduce the influence of the inclined wall [62]. Chai et al. [63] studied the two-staged gasification of a mixture of LDPE and pine sawdust over catalysts, finding that  $\text{N}_2$  can be introduced into the gasifier to prevent oxidation of the catalyst in the bottom stage.

### 2.2.2 Operating factors and performance

**Table 4** shows the syngas yield (typically  $0.7\text{--}3.0 \text{ Nm}^3/\text{kg}$ ) obtained from different gasification processes, depending on feedstock species, reactor types, and operating conditions. Temperature is one operating parameter that has a significant influence on the solid waste gasification performance in a multi-staged reactor. For example, Bai et al. [52] studied the two-staged gasification kinetics of PC in supercritical water at different temperatures ( $500\text{--}800 \text{ }^\circ\text{C}$ ). An increase in temperature improved the free radical and cracking reactions of PC. The gasification reaction of PC was intense and underwent a cracking reaction, forming gas phase products and many small molecular fragments in the first stage. The gasification reaction was slow, but kept increasing in the second phase [52]. Xiao et al. [54] found the pyrolysis/gasification of pine sawdust was largely improved by increasing the reactor temperature from  $700$  to  $850 \text{ }^\circ\text{C}$ . Prasertcharoensuk et al. [56] found that pyrolysis temperature significantly influenced char properties, specifically, the surface area and pore size increased with an increase in temperature from  $600$  to  $900 \text{ }^\circ\text{C}$ . Liu et al. [59] studied the gasification at temperatures of  $600\text{--}800 \text{ }^\circ\text{C}$ , finding that a higher temperature was helpful

Waste	Reactor type	Reactor configuration	Other	Ref.
PC	Quartz two-staged tube	Inside diameter = 3 mm, length = 200 mm	Two stages: 500–700 °C, and 700–800 °C	[52]
Oat hull pellet	Two-staged fixed bed	—	Steam gasification	[53]
LDPE <sup>a</sup> and pine sawdust mixture	Two-staged fixed bed	Central diameter = 30 mm, length = 150 mm	Pyrolysis (feedstock loaded, 700 °C) and gasification (catalyst loaded, 600 °C)	[63]
Pine sawdust	Three-staged	First stage: inside diameter = 80 mm, length = 200 mm, second stage: inside diameter = 136 mm, length = 400 mm, and third stage: inside diameter = 26 mm, length = 2500 mm	First stage: pyrolysis/gasification, second stage: reformer for tar cracked, and third stage: combustor with air	[54]
Olive oil mill residue	Two-staged	Inside diameter = 0.75 m, length = 2 m	Pyrolysis and char gasification	[55]
Waste biomass	Two-staged fixed bed	Center diameter = 33 mm, length = 830 mm	—	[56]
Biomass	—	Inside diameter = 22 mm, length = 160 mm	—	[57]
Rice husk and PE mixture	Bench-scale two-staged fixed bed	First stage: diameter = 38 mm, length = 300 mm, and second stage: diameter = 25 mm, length = 300 mm	First stage: pyrolysis at 600 °C, and second stage: reforming at 800 °C	[58]
Rice husk	Two-staged downdraft fixed bed	First stage: inside diameter = 44 mm, length = 250 mm; second stage: inside diameter = 44 mm, length = 530 mm	First stage: pyrolysis, and second stage: tar cracking	[20]
Rice straw	Two-staged bubbling fluidized bed	Inside diameter = 50 mm, length = 1.2 m	—	[59]
Wood pellet or manure	Dual fluidized bed	Inside diameter = 150 mm, length = 3.5 m	—	[60]

<sup>a</sup>Low-density polyethylene (LDPE).

**Table 3.**  
*The solid waste gasification, multi-staged reactor type, and dimension.*

to enhance gasification performance. Khonde and Chaurasia [20] studied the two-staged gasification at different second-stage temperatures (700–900 °C). The tar yield decreased with increasing temperature, while tar cracking at higher temperatures led to hydrogen rich syngas production (or gas yield) [20].

Feed concentration and catalyst are important factors that have been investigated for solid waste gasification. For example, Bai et al. [52] studied the gasification kinetics of PC in supercritical water at different PC concentrations (5–25 wt%), finding that a decrease in PC concentration improved the gasification level of the unit feedstock. Chai et al. [63] studied the two-staged gasification of a mixture of

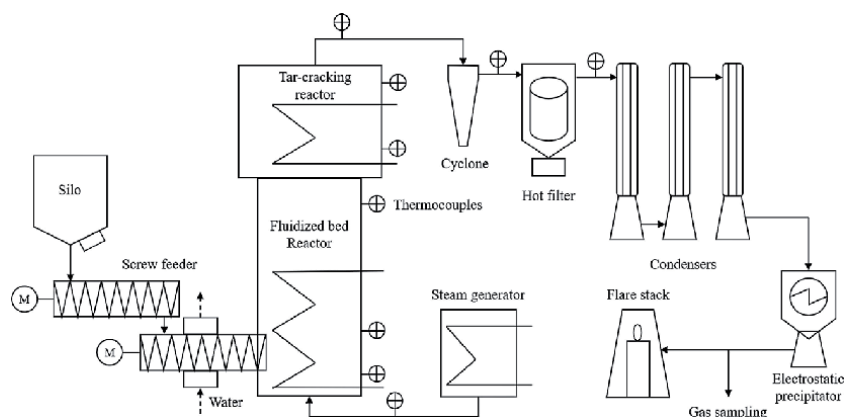


**Figure 5.** Diagram of a two-staged gasification process, which mainly consists of a feeding system, two reaction zones (fluidized bed reactor and tar-cracking reactor), a char separation system (cyclone and hot filter), and a quenching system (water-cooled condensers) [61]. Reproduced with permission from [61].

Waste	Reactor type	Conditions	Performance	Other	Ref.
Biomass briquette	Two-staged (fluidized bed and swirl-melting furnace)	First stage: 695 °C; second stage: 1280 °C	Gas yield: ~1.5 Nm <sup>3</sup> /kg	Biomass contains rice straw, plastic and paper; Biomass feed rate: 25 kg/h	[50]
Pine sawdust	Three-staged (pyrolyzer, reformer, and combustor)	Pyrolyzer: 700 °C; reformer: 850 °C; combustor: 850 °C	Gas yield: 1.6 Nm <sup>3</sup> /kg; tar yield: 1.0 g/kg	Biomass feed rate: 200 g/h	[64]
Pine sawdust	Three-staged (pyrolysis/gasification, reformer, and combustor)	Pyrolysis/gasification: 800 °C; reformer: 850 °C; combustor: 850 °C	Gas yield: 1.0 Nm <sup>3</sup> /kg	Biomass feed rate: 200 g/h	[54]
Wood sawdust and HDPE mixture	Two-staged (plasma gasification and folded plate)	Input power of 18 kW	Gas yield: ~2.2 Nm <sup>3</sup> /kg	40 wt% HDPE in the feed mixture	[65]
MSW	Two-staged (gasification and reforming)	Gasification: 850 °C; reforming: 850 °C	Syngas yield: 0.7 m <sup>3</sup> /kg	—	[66]
PE	Two-staged (fluidized bed gasifying and tar cracking)	Gasifying: 792 °C; cracking: 852 °C	Syngas yield: 3 Nm <sup>3</sup> /kg; char yield: 271 g/kg; tar yield: 68 g/kg	Steam gasification	[61]

**Table 4.** The solid waste multi-staged gasification factor and performance.

LDPE and pine sawdust, finding that the use of a Ni-CaO-C catalyst was helpful to improve the gas yield, compared with non-catalyst. Additionally, it was determined that the heat recovered from the catalyst regeneration can be used for heating

feedstocks in the reactor [63]. Al-Rahbi and Williams [57] studied a two-staged pyrolysis-reforming gasification, finding that the H<sub>2</sub> production increased largely with the use of a tyre pyrolysis char as the catalyst, compared to non-catalytic test.

Other parameters such as reaction time and pressure have also been investigated for gasification. For example, Bai et al. [52] studied the gasification kinetic of PC in supercritical water at different reaction time (5–60 min), finding that the increase in reaction time improved the gasification efficiency. Bai et al. [52] also studied the gasification at different pressures (21–29 MPa), finding that the pressure had no significant impact on gasification. This is likely because the properties of the supercritical water do not change significantly at these different pressures.

### *2.2.3 Advantages and disadvantages*

Compared to single-staged reactor systems, the use of multi-staged reactor systems for solid waste gasification has some advantages and disadvantages. A two-staged reactor system is convenient to investigate the specific effect of temperature at different stages [63]. The multi-staged reactor tends to be more promising and reliable in technique development [50]. For example, Al-Rahbi and Williams [57] studied two-staged pyrolysis-reforming gasification. The first stage was pyrolysis at 500 °C, and the second stage was reforming at 700–900 °C. The two-staged pyrolysis-reforming reactor was found to increase the total gas yield, compared to a single-staged reactor. One aim of this combination approach of pyrolysis and reforming is to improve the gas yield and obtain an optimum syngas ratio via shifting the reaction from exothermic to endothermic [57].

In a single reactor, it is difficult to control the different gasification reactions, such as pyrolysis, char gasification, tar cracking, and water-gas shift reaction, individually [64]. Multiple reactions can occur in one reactor, making it difficult to correlate feedstock properties and downstream utilization of the gas product. Multi-staged reactors can be helpful to improve gasification performance [64]. In a three-staged reactor system, the reactions can be optimized, individually, under appropriate conditions. This can also achieve efficient tar removal [54]. However, the multi-staged reactor is significantly more complex and has a higher capital cost, compared to a single-staged reactor [67]. Furthermore, a long and steady gasification operation needs to be developed for commercial scale H<sub>2</sub> production [61].

### *2.2.4 Applications of a multi-staged reactor*

Multi-staged reactors have some advantages, as discussed previously. They have been applied not only in gasification, but also in other technologies such as pyrolysis and torrefaction. For example, we previously studied the pyrolysis of alkali lignin to biofuel using a two-staged reactor (pyrolysis and catalytic reactor) [68]. The alkali lignin and catalyst were individually loaded into the pyrolysis and catalytic reactor, respectively. The alkali lignin was successfully converted into biofuel at a biofuel yield of 28 wt% [68]. Guzelciftci et al. [69] studied the pyrolysis of wood using a two-staged reactor system (auger and fluidized bed reactors). The auger reactor temperature varied between room temperature and 290 °C, while the fluidized bed reactor temperature varied between 500 and 700 °C. The obtained bio-oil yield varied largely between 24 and 52 wt% [69].

Granados et al. [70] used a two-staged rotary reactor system for torrefaction of poplar wood residues. The two-staged rotary reactor system consists of two in-series rotary drums for continuous drying (115 °C) and torrefaction (300 °C) processes. The HHV of the torrefied poplar wood residues reached 26 MJ/kg, which

was a much higher value than that of the raw poplar wood residues (18 MJ/kg) [70]. Nhuchhen et al. [71] studied the torrefaction of yellow poplar in a two-staged reactor system at an angular speed of 4 rpm. Three different torrefaction temperatures (260, 290, and 320 °C) were investigated. An increase in the torrefaction temperature resulted in a decrease in solid mass yield from 93 wt% to 81 wt%. The HHV of the torrefied poplar increased from 20 to 23 MJ/kg with an increase in the torrefaction temperature from 260 to 320 °C [71]. However, further torrefaction studies on the comparison of single- and multi-staged reactors will be needed.

### **3. Conclusion**

Solid waste, including MSW, biomass residue, plastic waste, and their mixtures, has accumulated fast in recent years, leading to solid waste gasification gaining great attention. However, no systematic study has been performed to compare single-staged and multi-staged reactors. This book chapter systematically reviewed state-of-the-art research for both single- and multi-staged reactors. Discussion included analysis of the reactor dimensions, operating factors and performance, advantages, and disadvantages of these reactors. The yield of syngas generated from solid waste gasification is mainly in the range of 0.7–3.0 Nm<sup>3</sup>/kg. Multi-staged reactors are a convenient approach to investigate the specific effect of parameters at different stages, and the reactions can be optimized individually under appropriate conditions. Additionally, a multi-staged reactor can be helpful to improve gasification performance, but is more complex and has higher capital cost, compared to a single-staged reactor.

Solid waste gasification is affected by several factors including temperature, reaction time, feed composition, and catalyst activity. An appropriate temperature (e.g., 800–900 °C) can be selected for solid waste gasification based on the elevated gasification performance and low energy consumption. A suitable feedstock concentration and reaction time should be selected to balance gasification efficiency and industrial application. Higher feedstock concentration can cause the reactor to plug and subsequent catalyst deactivation, while a longer reaction time may cause greater energy consumption. The use of a steam and O<sub>2</sub> mixture as the gasification agent is helpful for gasification efficiency because it produces steam reforming reactions and has a lack of N<sub>2</sub> dilution. Waste sorting is helpful to improve the gasification efficiency compared to unsorted waste. Moreover, an appropriate waste feed size should be selected because larger feed size can cause a loose bed and smaller feed size can lead to reactor blockage. The co-gasification of waste mixtures over Ni based catalysts is a promising technology due to the improved gasification efficiency derived from the synergistic effect of the feed mixture.

Additionally, multi-staged reactors have many unique advantages, which make them useful in other applications such as pyrolysis and torrefaction. However, reducing the processing cost of converting solid waste to syngas remains a major technical challenge. Pretreating solid waste, such as MSW, to remove the impurities, high energy consumption at elevated temperatures, and the use of catalysts remain the most expensive aspects of this process. In the future, a better understanding of the gasification reactions, reactor design, and catalyst development needs to be investigated to improve syngas yield and avoid tar formation.

### **Acknowledgements**

The authors acknowledge the support from the US Department of Energy (DOE), Office of Energy Efficiency and Renewable Energy, Advanced

Manufacturing Office, under CPS Agreement 36863. This book chapter was authored in part by UT-Battelle LLC under contract DE-AC05-00OR22725 with DOE. The US government retains and the publisher, by accepting the article for publication, acknowledges that the US government retains a nonexclusive, paid-up, irrevocable, worldwide license to publish or reproduce the published form of this book chapter, or allow others to do so, for US government purposes. DOE will provide public access to these results of federally sponsored research in accordance with the DOE Public Access Plan (<http://energy.gov/downloads/doe-public-access-plan>).

### **Conflict of interest**

The authors declare no conflict of interest.

### **Appendices and nomenclature**

MSW	Municipal solid waste
HDPE	High density polyethylene
PP	Polypropylene
PC	Polycarbonate
PE	Polyethylene
HHV	Higher heating value
LHV	Lower heating value
S/C	Steam to carbon ratio
ER	Equivalence air ratio
TC1	Thermocouple 1
TC2	Thermocouple 2
RDF	Refuse derived fuel
TR	Tar reformer
DES	Desulfurization reactor
GS	Gasifier
SPA	Solid phase adsorption
WGS	Water gas shift
CHP	Combined heat and power

## **Author details**

Xianhui Zhao<sup>1\*</sup>, Kai Li<sup>2</sup>, Meghan E. Lamm<sup>1</sup>, Serdar Celik<sup>3</sup>, Lin Wei<sup>4</sup>  
and Soydan Ozcan<sup>1\*</sup>

1 Manufacturing Science Division, Oak Ridge National Laboratory,  
Knoxville, Tennessee, United States

2 Chemical Sciences Division, Oak Ridge National Laboratory,  
Oak Ridge, Tennessee, United States


3 Department of Mechanical and Mechatronics Engineering, Southern Illinois  
University, Edwardsville, Illinois, United States

4 Agricultural and Biosystems Engineering Department, South Dakota State  
University, Brookings, South Dakota, United States

\*Address all correspondence to: zhaox@ornl.gov and ozcans@ornl.gov

## **IntechOpen**

---

© 2021 The Author(s). Licensee IntechOpen. This chapter is distributed under the terms of the Creative Commons Attribution License (<http://creativecommons.org/licenses/by/3.0>), which permits unrestricted use, distribution, and reproduction in any medium, provided the original work is properly cited. 



## References

- [1] S. Kaza, L. Yao, P. Bhada-Tata, F. Van Woerden, What a waste 2.0: a global snapshot of solid waste management to 2050, The World Bank 2018.
- [2] L.F. Pearse, J.P. Hettiaratchi, S. Kumar, Towards developing a representative biochemical methane potential (BMP) assay for landfilled municipal solid waste—A review, *Bioresource technology*, 254 (2018) 312-324.
- [3] S.S.A. Syed-Hassan, Y. Wang, S. Hu, S. Su, J. Xiang, Thermochemical processing of sewage sludge to energy and fuel: Fundamentals, challenges and considerations, *Renewable and Sustainable Energy Reviews*, 80 (2017) 888-913.
- [4] U. Arena, Process and technological aspects of municipal solid waste gasification. A review, *Waste management*, 32 (2012) 625-639.
- [5] A. Bosmans, I. Vanderreydt, D. Geysen, L. Helsen, The crucial role of Waste-to-Energy technologies in enhanced landfill mining: a technology review, *Journal of Cleaner Production*, 55 (2013) 10-23.
- [6] X. Zhao, A. Naqi, D.M. Walker, T. Roberge, M. Kastelic, B. Joseph, J.N. Kuhn, Conversion of landfill gas to liquid fuels through a TriFTS (tri-reforming and Fischer–Tropsch synthesis) process: a feasibility study, *Sustain Energy Fuels*, 3 (2019) 539-549.
- [7] X. Zhao, B. Joseph, J. Kuhn, S. Ozcan, Biogas Reforming to Syngas: A Review, *iScience*, 23 (2020) 101082.
- [8] S. Sansaniwal, K. Pal, M. Rosen, S. Tyagi, Recent advances in the development of biomass gasification technology: A comprehensive review, *Renewable and sustainable energy reviews*, 72 (2017) 363-384.
- [9] E.R. Widjaya, G.N. Chen, L. Bowtell, C. Hills, Gasification of non-woody biomass: A literature review, *Renewable & Sustainable Energy Reviews*, 89 (2018) 184-193.
- [10] J.H. Park, H.-W. Park, S. Choi, D.-W. Park, Effects of blend ratio between high density polyethylene and biomass on co-gasification behavior in a two-stage gasification system, *International Journal of Hydrogen Energy*, 41 (2016) 16813-16822.
- [11] T.K. Patra, P.N. Sheth, Biomass gasification models for downdraft gasifier: A state-of-the-art review, *Renewable and Sustainable Energy Reviews*, 50 (2015) 583-593.
- [12] A. Anukam, S. Mamphweli, P. Reddy, E. Meyer, O. Okoh, Pre-processing of sugarcane bagasse for gasification in a downdraft biomass gasifier system: A comprehensive review, *Renewable and Sustainable Energy Reviews*, 66 (2016) 775-801.
- [13] D.T. Pio, L.A.C. Tarelho, M.A.A. Matos, Characteristics of the gas produced during biomass direct gasification in an autothermal pilot-scale bubbling fluidized bed reactor, *Energy*, 120 (2017) 915-928.
- [14] S.L. Yang, H. Wang, Y.G. Wei, J.H. Hu, J.W. Chew, Eulerian-Lagrangian simulation of air-steam biomass gasification in a three-dimensional bubbling fluidized gasifier, *Energy*, 181 (2019) 1075-1093.
- [15] J. Schneider, C. Grube, A. Herrmann, S. Rönsch, Atmospheric entrained-flow gasification of biomass and lignite for decentralized applications, *Fuel Processing Technology*, 152 (2016) 72-82.
- [16] X. Gao, Y. Zhang, B. Li, X. Yu, Model development for biomass

- gasification in an entrained flow gasifier using intrinsic reaction rate submodel, *Energy Conversion and Management*, 108 (2016) 120-131.
- [17] A. Mednikov, A Review of Technologies for Multistage Wood Biomass Gasification, *Thermal Engineering*, 65 (2018) 531-546.
- [18] W.P. Chan, A. Veksha, J. Lei, W.-D. Oh, X. Dou, A. Giannis, G. Lisak, T.-T. Lim, A hot syngas purification system integrated with downdraft gasification of municipal solid waste, *Appl Energ*, 237 (2019) 227-240.
- [19] P.R. Bhoi, R.L. Huhnke, A. Kumar, N. Indrawan, S. Thapa, Co-gasification of municipal solid waste and biomass in a commercial scale downdraft gasifier, *Energy*, 163 (2018) 513-518.
- [20] R. Khonde, A. Chaurasia, Rice husk gasification in a two-stage fixed-bed gasifier: Production of hydrogen rich syngas and kinetics, *Int J Hydrogen Energ*, 41 (2016) 8793-8802.
- [21] A. Gómez-Barea, B. Leckner, A.V. Perales, S. Nilsson, D.F. Cano, Improving the performance of fluidized bed biomass/waste gasifiers for distributed electricity: a new three-stage gasification system, *Applied Thermal Engineering*, 50 (2013) 1453-1462.
- [22] M. Irfan, A. Li, L. Zhang, M. Wang, C. Chen, S. Khushk, Production of hydrogen enriched syngas from municipal solid waste gasification with waste marble powder as a catalyst, *Int J Hydrogen Energ*, 44 (2019) 8051-8061.
- [23] I.N. Zaini, Y. Gomez-Rueda, C. García López, D.K. Ratnasari, L. Helsen, T. Pretz, P.G. Jönsson, W. Yang, Production of H<sub>2</sub>-rich syngas from excavated landfill waste through steam co-gasification with biochar, *Energy*, 207 (2020) 118208.
- [24] C. Bian, R. Zhang, L. Dong, B. Bai, W. Li, H. Jin, C. Cao, Hydrogen/ Methane Production from Supercritical Water Gasification of Lignite Coal with Plastic Waste Blends, *Energy Fuel*, 34 (2020) 11165-11174.
- [25] D. Selvi Gökkaya, T. Çokkuvvetli, M. Sağlam, M. Yüksel, L. Ballice, Hydrothermal gasification of poplar wood chips with alkali, mineral, and metal impregnated activated carbon catalysts, *The Journal of Supercritical Fluids*, 152 (2019) 104542.
- [26] Y.L. Xiang, Q. Lin, L. Cai, Y. Guan, J. Lu, W. Liu, Study of the effect mechanism of municipal solid waste gasification conditions on the production of H<sub>2</sub> and CO using modelling technique, *J Environ Manage*, 230 (2019) 301-310.
- [27] W.C. Ng, S. You, R. Ling, K.Y.-H. Gin, Y. Dai, C.-H. Wang, Co-gasification of woody biomass and chicken manure: Syngas production, biochar reutilization, and cost-benefit analysis, *Energy*, 139 (2017) 732-742.
- [28] M. Lei, J. Hai, J. Cheng, J. Lu, J. Zhang, T. You, Variation of toxic pollutants emission during a feeding cycle from an updraft fixed bed gasifier for disposing rural solid waste, *Chinese Journal of Chemical Engineering*, 26 (2018) 608-613.
- [29] D. Antolini, S.S. Ail, F. Patuzzi, M. Grigante, M. Baratieri, Experimental investigations of air-CO<sub>2</sub> biomass gasification in reversed downdraft gasifier, *Fuel*, 253 (2019) 1473-1481.
- [30] F. Pinto, R. André, M. Miranda, D. Neves, F. Varela, J. Santos, Effect of gasification agent on co-gasification of rice production wastes mixtures, *Fuel*, 180 (2016) 407-416.
- [31] Y. Tian, X. Zhou, S. Lin, X. Ji, J. Bai, M. Xu, Syngas production from air-steam gasification of biomass with

natural catalysts, *Sci Total Environ*, 645 (2018) 518-523.

[32] N. Indrawan, S. Thapa, P.R. Bhoi, R.L. Huhnke, A. Kumar, Electricity power generation from co-gasification of municipal solid wastes and biomass: Generation and emission performance, *Energy*, 162 (2018) 764-775.

[33] H. Su, E. Kanchanatip, D. Wang, R. Zheng, Z. Huang, Y. Chen, I. Mubeen, M. Yan, Production of H<sub>2</sub>-rich syngas from gasification of unsorted food waste in supercritical water, *Waste Manag*, 102 (2020) 520-527.

[34] B. Bai, W. Wang, H. Jin, Experimental study on gasification performance of polypropylene (PP) plastics in supercritical water, *Energy*, 191 (2020) 116527.

[35] X. Zheng, Z. Ying, B. Wang, C. Chen, Hydrogen and syngas production from municipal solid waste (MSW) gasification via reusing CO<sub>2</sub>, *Appl Therm Eng*, 144 (2018) 242-247.

[36] D.T. Pio, L.A.C. Tarelho, A.M.A. Tavares, M.A.A. Matos, V. Silva, Co-gasification of refused derived fuel and biomass in a pilot-scale bubbling fluidized bed reactor, *Energ Convers Manage*, 206 (2020) 112476.

[37] F. Meng, Q. Ma, H. Wang, Y. Liu, D. Wang, Effect of gasifying agents on sawdust gasification in a novel pilot scale bubbling fluidized bed system, *Fuel*, 249 (2019) 112-118.

[38] Q. Xiong, M.M. Yeganeh, E. Yaghoubi, A. Asadi, M.H. Doranehgard, K. Hong, Parametric investigation on biomass gasification in a fluidized bed gasifier and conceptual design of gasifier, *Chemical Engineering and Processing - Process Intensification*, 127 (2018) 271-291.

[39] M.H. Basha, S.A. Sulaiman, Y. Uemura, Co-gasification of palm kernel

shell and polystyrene plastic: Effect of different operating conditions, *J Energy Inst*, 93 (2020) 1045-1052.

[40] S. Rudra, Y.K. Tesfagaber, Future district heating plant integrated with municipal solid waste (MSW) gasification for hydrogen production, *Energy*, 180 (2019) 881-892.

[41] F. Gallucci, R. Liberatore, L. Sapegno, E. Volponi, P. Venturini, F. Rispoli, E. Paris, M. Carnevale, A. Colantoni, Influence of oxidant agent on syngas composition: Gasification of hazelnut shells through an updraft reactor, *Energies*, 13 (2020) 102.

[42] S.A. Salaudeen, B. Acharya, M. Heidari, S.M. Al-Salem, A. Dutta, Hydrogen-Rich Gas Stream from Steam Gasification of Biomass: Eggshell as a CO<sub>2</sub> Sorbent, *Energ Fuel*, 34 (2020) 4828-4836.

[43] B. Bai, Y. Liu, H. Zhang, F. Zhou, X. Han, Q. Wang, H. Jin, Experimental investigation on gasification characteristics of polyethylene terephthalate (PET) microplastics in supercritical water, *Fuel*, 262 (2020) 116630.

[44] W.X. Peng, L.S. Wang, M. Mirzaee, H. Ahmadi, M.J. Esfahani, S. Fremaux, Hydrogen and syngas production by catalytic biomass gasification, *Energ Convers Manage*, 135 (2017) 270-273.

[45] H. Su, D. Hantoko, M. Yan, Y. Cai, E. Kanchanatip, J. Liu, X. Zhou, S. Zhang, Evaluation of catalytic subcritical water gasification of food waste for hydrogen production: Effect of process conditions and different types of catalyst loading, *Int J Hydrogen Energ*, 44 (2019) 21451-21463.

[46] H. Su, W. Liao, J. Wang, D. Hantoko, Z. Zhou, H. Feng, J. Jiang, M. Yan, Assessment of supercritical water gasification of food waste under the background of waste sorting: Influences

- of plastic waste contents, *Int J Hydrogen Energ*, 45 (2020) 21138-21147.
- [47] C. Cao, C. Bian, G. Wang, B. Bai, Y. Xie, H. Jin, Co-gasification of plastic wastes and soda lignin in supercritical water, *Chem Eng J*, 388 (2020) 124277.
- [48] X. Zheng, Z. Ying, B. Wang, C. Chen, CO<sub>2</sub> Gasification of Municipal Solid Waste in a Drop-Tube Reactor: Experimental Study and Thermodynamic Analysis of Syngas, *Energ Fuel*, 32 (2018) 5302-5312.
- [49] Z. Wang, X. Liu, K.G. Burra, J. Li, M. Zhang, T. Lei, A.K. Gupta, Towards enhanced catalytic reactivity in CO<sub>2</sub>-assisted gasification of polypropylene, *Fuel*, 284 (2021) 119076.
- [50] M. Niu, Y. Huang, B. Jin, S. Liang, Q. Dong, H. Gu, R. Sun, A novel two-stage enriched air biomass gasification for producing low-tar high heating value fuel gas: Pilot verification and performance analysis, *Energy*, 173 (2019) 511-522.
- [51] Z. Wan, S. Yang, Y. Sun, Y. Wei, J. Hu, H. Wang, Distribution and particle-scale thermochemical property of biomass in the gasifier of a dual fluidized bed, *Energ Convers Manage*, 209 (2020) 112672.
- [52] B. Bai, Y. Liu, X. Meng, C. Liu, H. Zhang, W. Zhang, H. Jin, Experimental investigation on gasification characteristics of polycarbonate (PC) microplastics in supercritical water, *J Energy Inst*, 93 (2020) 624-633.
- [53] A. Abedi, A.K. Dalai, Steam gasification of oat hull pellets over Ni-based catalysts: Syngas yield and tar reduction, *Fuel*, 254 (2019) 115585.
- [54] Y. Xiao, S. Xu, Y. Song, Y. Shan, C. Wang, G. Wang, Biomass steam gasification for hydrogen-rich gas production in a decoupled dual loop gasification system, *Fuel Process Technol*, 165 (2017) 54-61.
- [55] M. Lajili, C. Guizani, F.J. Escudero Sanz, M. Jeguirim, Fast pyrolysis and steam gasification of pellets prepared from olive oil mill residues, *Energy*, 150 (2018) 61-68.
- [56] P. Prasertcharoensuk, S.J. Bull, A.N. Phan, Gasification of waste biomass for hydrogen production: Effects of pyrolysis parameters, *Renew Energ*, 143 (2019) 112-120.
- [57] A.S. Al-Rahbi, P.T. Williams, Hydrogen-rich syngas production and tar removal from biomass gasification using sacrificial tyre pyrolysis char, *Appl Energ*, 190 (2017) 501-509.
- [58] D. Xu, Y. Xiong, J. Ye, Y. Su, Q. Dong, S. Zhang, Performances of syngas production and deposited coke regulation during co-gasification of biomass and plastic wastes over Ni/ $\gamma$ -Al<sub>2</sub>O<sub>3</sub> catalyst: Role of biomass to plastic ratio in feedstock, *Chem Eng J*, 392 (2020) 123728.
- [59] L. Liu, Y. Huang, J. Cao, C. Liu, L. Dong, L. Xu, J. Zha, Experimental study of biomass gasification with oxygen-enriched air in fluidized bed gasifier, *Science of The Total Environment*, 626 (2018) 423-433.
- [60] D. Schweitzer, A. Gredinger, M. Schmid, G. Waizmann, M. Beirrow, R. Spörl, G. Scheffknecht, Steam gasification of wood pellets, sewage sludge and manure: Gasification performance and concentration of impurities, *Biomass Bioenerg*, 111 (2018) 308-319.
- [61] Y.-S. Jeong, K.-B. Park, J.-S. Kim, Hydrogen production from steam gasification of polyethylene using a two-stage gasifier and active carbon, *Appl Energ*, 262 (2020) 114495.

- [62] M. Kuba, H. Hofbauer, Experimental parametric study on product gas and tar composition in dual fluid bed gasification of woody biomass, *Biomass Bioenergy*, 115 (2018) 35-44.
- [63] Y. Chai, N. Gao, M. Wang, C. Wu, H<sub>2</sub> production from co-pyrolysis/gasification of waste plastics and biomass under novel catalyst Ni-CaO-C, *Chem Eng J*, 382 (2020) 122947.
- [64] Y. Tursun, S. Xu, A. Abulikemu, T. Dilinuer, Biomass gasification for hydrogen rich gas in a decoupled triple bed gasifier with olivine and NiO/olivine, *Bioresour Technol*, 272 (2019) 241-248.
- [65] W. Ma, C. Chu, P. Wang, Z. Guo, B. Liu, G. Chen, Characterization of tar evolution during DC thermal plasma steam gasification from biomass and plastic mixtures: Parametric optimization via response surface methodology, *Energ Convers Manage*, 225 (2020) 113407.
- [66] L. Zhang, W. Wu, Y. Zhang, X. Zhou, Clean synthesis gas production from municipal solid waste via catalytic gasification and reforming technology, *Catal Today*, 318 (2018) 39-45.
- [67] V.S. Sikarwar, M. Zhao, P. Clough, J. Yao, X. Zhong, M.Z. Memon, N. Shah, E.J. Anthony, P.S. Fennell, An overview of advances in biomass gasification, *Energy & Environmental Science*, 9 (2016) 2939-2977.
- [68] S. Cheng, L. Wei, X. Zhao, J. Julson, E. Kadis, Converting alkali lignin to biofuels over NiO/HZSM-5 catalysts using a two-stage reactor, *Chem Eng Technol*, 40 (2017) 1069-1077.
- [69] B. Guzelciftci, K.-B. Park, J.-S. Kim, Production of phenol-rich bio-oil via a two-stage pyrolysis of wood, *Energy*, 200 (2020) 117536.
- [70] D.A. Granados, P. Basu, F. Chejne, Biomass Torrefaction in a Two-Stage Rotary Reactor: Modeling and Experimental Validation, *Energ Fuel*, 31 (2017) 5701-5709.
- [71] D.R. Nhuchhen, P. Basu, B. Acharya, Torrefaction of Poplar in a Continuous Two-Stage, Indirectly Heated Rotary Torrefier, *Energ Fuel*, 30 (2016) 1027-1038.



# Gasification Process Using Downdraft Fixed-Bed Gasifier for Different Feedstock

*Md. Emdadul Hoque and Fazlur Rashid*

## Abstract

The use of conventional fuels is decreasing globally due to its limited reserves and negative impact on the environment. The associated cost of conventional fuels is increasing owing to the higher demand for conventional fuels. Hence, utilization methods of biomass to generate energy are of growing interest. Among different biomass feedstocks, rice husks, waste plastics, and sawdust are significantly available in the global environment. The annual generation amount of rice husk is approximately 120 million tons worldwide, with an annual energy generation potential of 109 GJ with a heating value of 15 MJ/kg. The gasification process is assumed to be the most effective biomass conversion method that can generate synthetic gas to operate IC engines, fuel cells, and boilers. Synthetic gas production from biomass using a gasification process is a significant source of future energy. Downdraft fixed-bed gasifiers are considered as a feasible option of biomass conversion in the gasification process. By optimizing the operating conditions of downdraft fixed-bed gasifier, such as reaction zone temperature, combustion zone temperature, intake air temperature, airflow rate, the humidity of intake air, a significant amount of synthetic gas can be produced from rice husks, waste plastic material, and sawdust.

**Keywords:** gasification, downdraft fixed-bed gasifier, rice husk, waste plastic, sawdust

## 1. Introduction

### 1.1 Global energy status

Human civilization and development have significantly increased world energy demand over the past years [1]. Consumption of world energy includes all energy sources consumed by humans in their economy and industrial purposes [2, 3]. Major factors that influence energy consumption are the high growth rate of population and per capita energy consumption. The globalization of international trade is another factor that affects the global energy profile [4]. **Figure 1** shows the global energy consumption from 2000 to 2020 and the forecast of future energy for 2035.

However, the world's population is the main global energy consumer [2–4]. According to the United Nations forecast data, the global population will reach

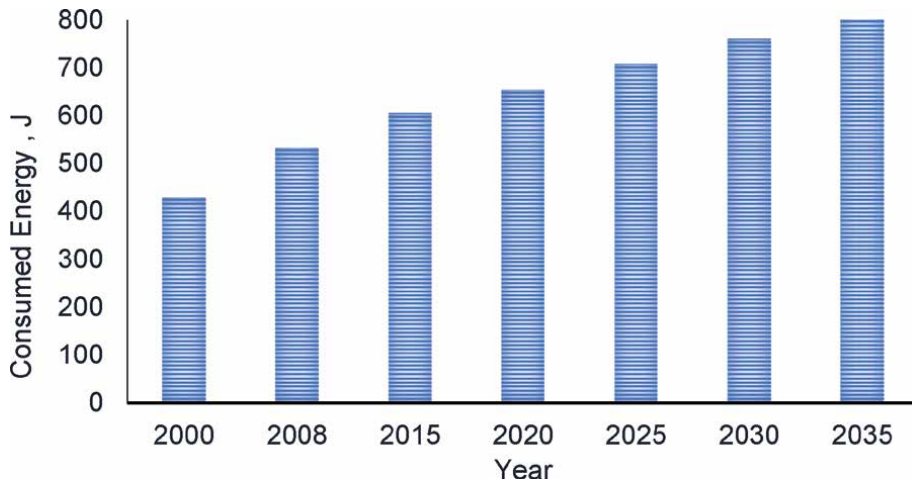


**Figure 1.**  
World's energy consumption scenario [1].

approximately 9.157 billion in 2040, which is around 2 billion higher than the population reached in 2015 [2]. **Figure 2** shows the global population in 2015 and the forecast for 2040. It is a challenge to provide sufficient energy to this huge population of around 2 billion using conventional energy sources.

All countries and regions worldwide are trying to reduce the use of conventional energy sources due to their low reserve and high rates of emission. However, due to the change in overall gross domestic product (GDP), failure of energy-saving technologies, and lack of investment for alternate energy, it is difficult to reduce the intense use of conventional energy. Consequently, the environment is largely polluted, and the world is moving towards an energy crisis era. The major sources of conventional energy are oil (33%), and the other sources of energy are coal provides 27%, and natural gas, 24% [6–8]. On the other hand, hydropower energy sources supply 6%, renewable sources 5%, and nuclear energy sources provide 4% world energy [7]. **Figure 3** presents the world's primary energy consumption sources. Overall around 84% of global energy is consumed from conventional fossil fuels. Therefore, finding new sources of energy is a major concern nowadays. In certain capacities, alternative renewable sources of energy are currently used with conventional fuels [9].

## 1.2 Renewable energy sources

Renewable energy sources can be utilized to generate energy again and again where wastes are minimized with less air pollution. Renewable sources of energy provide a significant contribution to global energy demand. It includes solar energy, energy from biomass, wind, ocean energy, and hydropower [10]. They supply clean energy and give less pollution than conventional sources of energy. Due to the depletion of conventional fuels and their negative impact on the environment, renewable energy sources would have a remarkable contribution to the world economy [11]. Again, fossil fuels reserve are diminishing, and they create an adverse effect on the environment that causes health hazard and change global climate condition [12]. Hence, the world's population moves slowly towards the generation of energy from sustainable renewable energy sources. **Table 1** shows the global consumption of renewable energy in a million tons of oil equivalent (Mtoe) and their forecast for 2040.



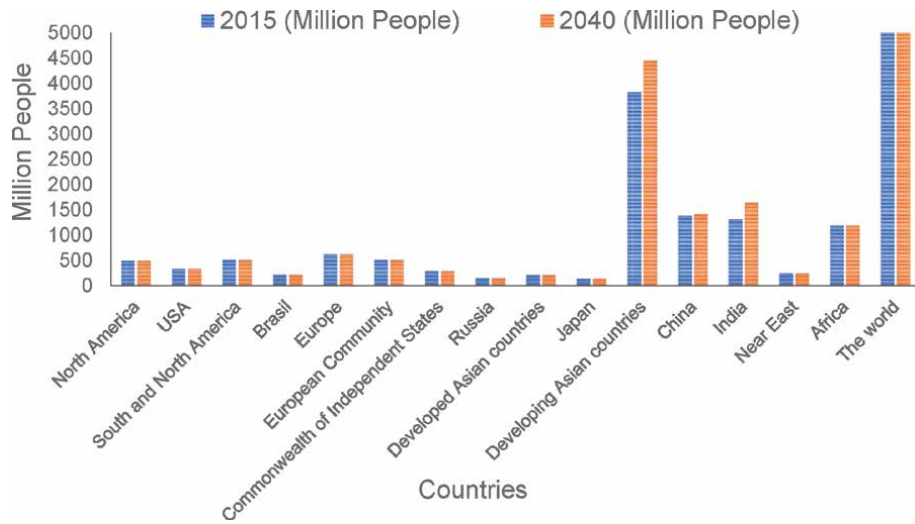


**Figure 2.** Global energy population by different countries in 2015 and 2040 [2, 5].

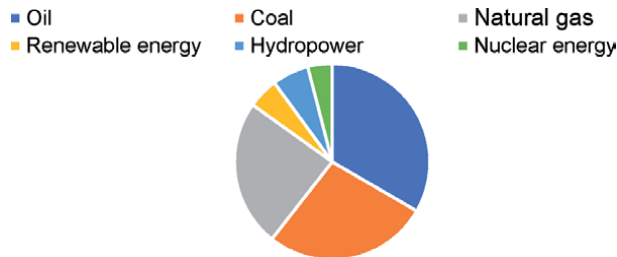


**Figure 3.** World's primary energy sources [6–8].

Renewable energy sources	Year				
	2001	2010	2020	2030	2040
Biomass energy	1080	1313	1791	2483	3271
Solar energy	4.10	15.0	66.0	244.0	480.0
Hydropower	22.70	266.0	309.0	341.0	358.0
Wind energy	4.70	44.0	266.0	542.0	688.0
Tidal/wave energy	0.050	0.10	0.40	3.0	20.0
Geothermal energy	43.20	86.0	186.0	333.0	493.0
Consumption of total energy (Mtoe)	10,038	10,549	11,425	12,352	13,310

**Table 1.** World's renewable energy consumption scenario in million tonne of oil equivalent (Mtoe) [13].

Overall, renewable sources of energy provide approximately 15% supply of global energy demand [14]. The use of renewable energy sources is now considered an alternate solution to meet the high energy demand [15, 16]. Major sources of renewable energy are solar, biomass, and hydropower. **Figure 4** shows the prospective usage options of renewable energy that can be applied to meet up the global energy demand [17–20].

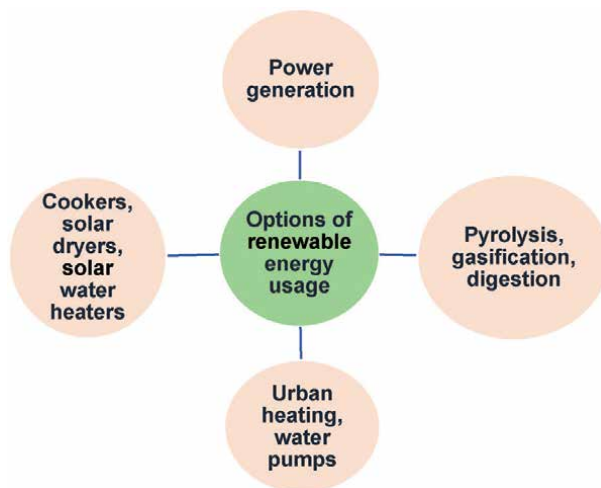


**Figure 4.**  
*Options of renewable energy usage [17–20].*

Energy generation from solar and hydropower sources are dependent on the weather condition of that country or regions of the world. Among different renewable sources, biomass plants require 0.820–1.130 relative units of energy to generate per unit of electricity, whereas solar photovoltaic requires 0.470 [17]. **Table 2** shows global renewable energy sources with their required relative units to generate per unit of energy.

### 1.3 Biomass renewable energy

Biomass renewable energy is a significant source of energy that can provide energy at a lower cost. It can maintain a sustainable energy supply and targeted greenhouse gas reduction all over the world. Moreover, energy generation methods related to biomass renewable sources are growing in interest due to the lower reserves of conventional fuels [21]. Also, regulations on low carbon dioxide emissions and reduced pressure on fossil fuels increase the interest in biomass renewable energy sources. Biomass renewable energy sources include waste produced from plants, rice husks, waste plastics, sawdust, algae, and trees [2]. Biomass renewable energy sources are mainly found in the wood form.

Usually, energy can be generated using thermal or chemical processes, as depicted in **Figure 5**. Gasification, pyrolysis, and combustion are the commonly used thermal processes to generate energy from biomass sources. In contrast, by applying chemical reagents and processes, biogas, hydrogen, and ethanol gas is generated from biomass renewable sources [22]. Gasification is now considered as one of the potential conversion processes, and therefore, this chapter presents the gasification methods of biomass sources.

Overall, biomass energy sources supply around 15% of the global energy and 35% for the developing countries. It is an effective bio-renewable energy source that is available globally. Production of biomass is approximately 146 billion metric tons per year globally [22]. It is approximated that 90% of the global population will depend on biomass renewable energy sources by the end of 2050 [22]. **Figure 6** shows the different usage options of biomass renewable energy that can be utilized to solve the high demand for future energy. It is seen from **Figure 6** that biomass renewable energy has the potentiality to use as energy and non-energy sources.

Renewable energy sources	Required quantity to generate per unit of electricity
Biomass energy plant	0.82–0.13.0
Solar PV plant	0.470
Tidal energy plant	0.070
Wind energy plant	0.06–1.920
Wave energy plant	0.30–0.580
Geothermal energy plant	0.080–0.370

**Table 2.**  
 Energy production from different renewable energy sources plant [17].

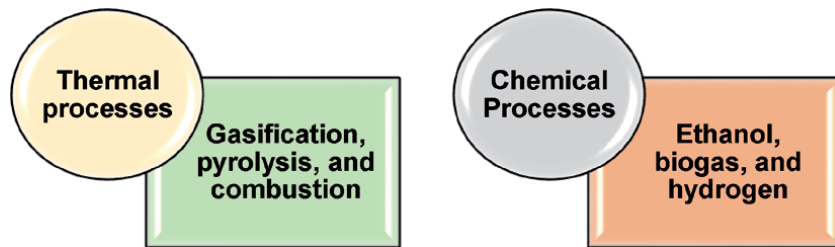


**Figure 5.**  
 Different power generation processes for biomass [22].

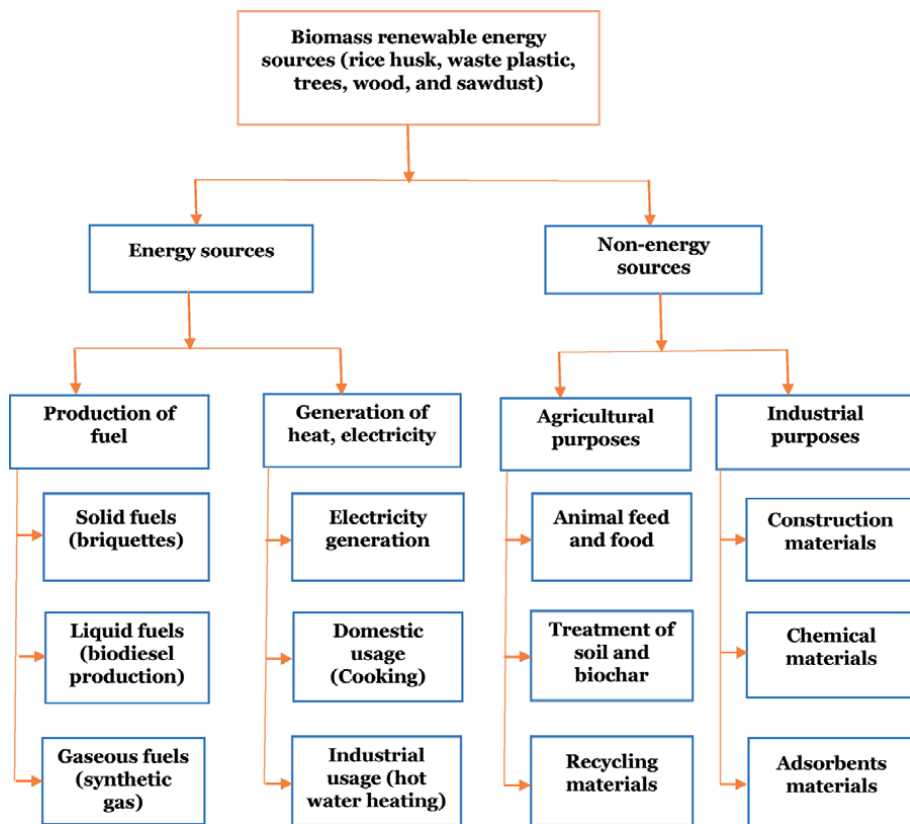


**Figure 6.**  
 Different applications of biomass renewable energy [22].

There are different types of biomass sources available in nature. The most common and available biomass sources are rice husk, sawdust, and waste plastics. Rice is the common food among the world's population. Hence, each year, millions of rice husks are wasted all over the world. On the other hand, plastics are used with a high growth rate due to their formability and higher durability. Therefore, turning waste plastic to generate energy is a potential way that can generate energy and reduce global environmental pollution. Sawdust can also be converted into energy using biomass anaerobic gasification method [23].

This chapter also presents the salient features and gasification method using a downdraft fixed-bed gasifier. It has been found in previous literature that the upper limit of moisture content of downdraft fixed-bed gasifier is 25% on a wet basis, while for updraft fixed-bed gasifier, it is 50% on the wet basis of measurement [24]. However, the high content of feed moisture negatively affects the gasification process and product gas [25, 26]. As a consequence, downdraft fixed-bed gasifier may provide better performance than updraft fixed-bed gasifier. Hence, this chapter considers the performance analysis of the downdraft fixed-bed gasifier.

## 2. Conventional biomass conversion technologies

### 2.1 Gasification

Gasification is the method that can convert carbonaceous biomass material to hydrogen, carbon dioxide, and carbon monoxide [27]. The method can be achieved by reaction of feed material at over 700 °C temperature, with a limited amount of oxygen and steam. In the gasification method, the feed material is processed without combustion. In this method, the generated mixture of gas is considered synthetic gas or producer gas utilized as fuel [28]. The produced power in the biomass gasification method and combustion of the generating gas can be considered as renewable energy source.

In chemical reactions of gasification method, char type carbonaceous feed material (C) is reacted with steam (H<sub>2</sub>O) and generates carbon monoxide (CO) and hydrogen (H<sub>2</sub>).



Therefore, in the gasification method, a small amount of air or oxygen is applied to the gasifier reactor to burn the organic feed material to generate energy and carbon dioxide. **Figure 7** shows the overall process of the gasification method to generate synthetic gas.

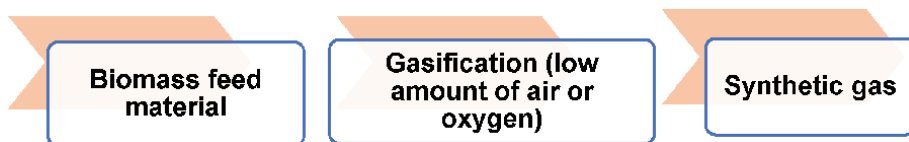


**Figure 7.** Flow diagram of biomass gasification process [29].

The gasification method of biomass renewable energy sources is the potential sources to generate energy, chemical energy, and biofuels. A gasifier is required to convert biomass renewable energy sources to synthetic gas in the gasification method. The generated synthetic gas is used to operate an internal combustion engine. They can also be used to produce electricity and heat energy by using a cogeneration system [30].

Again, the gasification process of biomass renewable energy sources is similar to the coal gasification method. Thermal decomposition of both biomass and coal gasification method generates the same output gases [31]. However, the operating conditions of gasification methods of biomass energy sources are less severe than coal gasification method [32]. In the biomass gasification method, cellulose and hemicellulose present in the feed material, whereas carbon is the main material of coal feed materials.

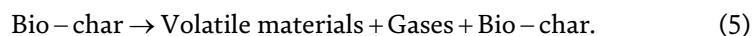
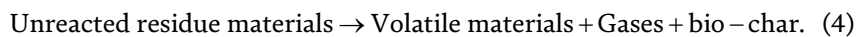
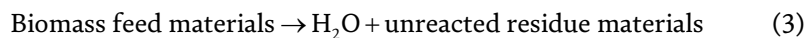
Practically, biomass energy sources are required to dry first. After that, the dried feed materials are required for the process of shrinkage and devolatilization [30]. Finally, the char gasification is applied from the surface of the material to the biomass center. **Figure 8** shows the overall process of biomass gasification to generate energy.

The overall power generation cost of the gasification process of biomass renewable energy includes labor cost 54%, cleaning cost of synthetic gas 28%, balancing of plant 9%, fuel cost 6%, and miscellaneous cost 3%. **Figure 9** represents the overall power generation cost of gasification methods.

## 2.2 Pyrolysis

Pyrolysis is the process where biomass materials are decomposed in absence of air or oxygen using heat energy. Therefore, the pyrolysis method generates bio-char as solid fuels, bio-oil as liquid fuels, and gases (non-condensable) [35]. **Figure 10** shows the overall process of pyrolysis method. The pyrolysis oil properties and yield of pyrolysis products depend on the operating conditions and parameters of the pyrolysis process. The pyrolysis process's operating parameters are the heating rate of feed material, the temperature of the reactor, residence time, catalysts, and reactor configurations.

The Pyrolysis process of biomass renewable energy sources can be simplified by the following Equations [36]:



Firstly, in the biomass pyrolysis method, feed materials are decomposed to remove the moisture contents and break the bond to form CO, CO<sub>2</sub>, and residues [37]. The remaining compounds are exposed to further conversion using cracking and polymerization that produces secondary char, tar, and gases [37]. In this method, at a lower temperature, such as less than 500 °C temperature, the organic vapor materials are not cracked. However, at higher temperatures, they convert readily with fewer residence times. The optimum temperature to generate the maximum quantity of bio-oil using the biomass pyrolysis method is over 500 °C.

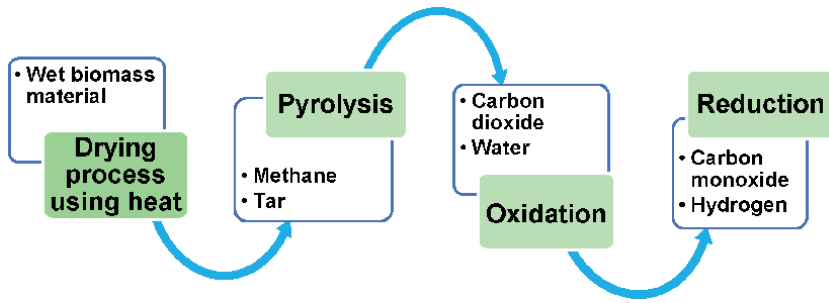


**Figure 8.**  
Energy generation process from biomass gasification method [33].

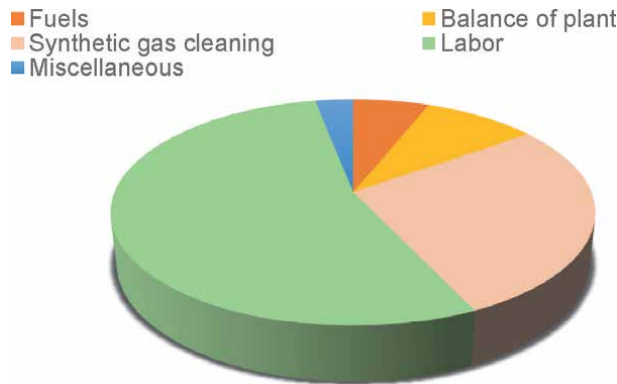


**Figure 9.**  
Power generation cost of biomass gasification method [34].

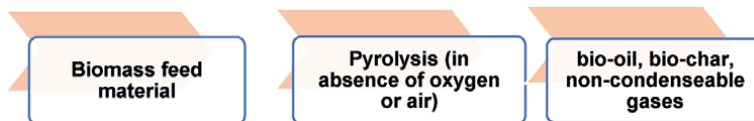


**Figure 10.**  
Flow diagram of pyrolysis methods [35].

The residence time of vapor materials and heating rate in the pyrolysis method can be classified into three major groups, as shown in **Figure 11**.

Fast and flash pyrolysis process generates lower amounts of char when compared with slow pyrolysis process. Flash and fast pyrolysis methods can produce bio-oil in high quantity. Hence, they are considered as a favorable method for the generation of bio-oil [35].

Slow pyrolysis is the process that occurs under a long residence time, lower temperature, and slow heating rate. In the slow pyrolysis method, cracking of the primary material generates a high yield of char.

Slow pyrolysis is the process that occurs under a long residence time, lower temperature, and slow heating rate. In the slow pyrolysis method, cracking of the primary material generates a high yield of char [40, 41]. The remaining non-condensed gases are used for drying purposes of raw biomass materials or as fuel gases. They can also be reflowed to the pyrolysis reactor to heat the pyrolysis method. Overall, biomass fast pyrolysis generates bio-oil (60–75%), bio-char (15–25%), and gaseous yield (10–20%) [42]. This process is preferable compared

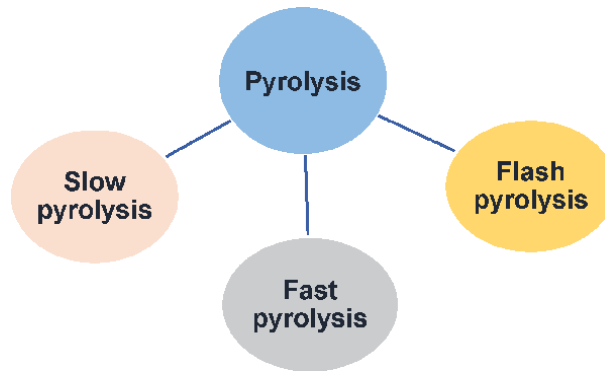


**Figure 11.**  
*Types of biomass pyrolysis methods [38, 39].*

to the slow and flash pyrolysis method based on the cost, transportability, and storability of liquid and gaseous fuels.

Flash pyrolysis is the third major group of pyrolysis methods that sometimes refer to a similar fast pyrolysis process. However, the flash pyrolysis method generates pyrolytic yield under a high heating rate, higher reaction temperature values, and short residence time [35]. This method has the capability to generate a high quantity of bio-oil from the conversion of biomass feed material. It has the capacity to convert a higher quantity of biomass to liquid bio-oil. However, the generated bio-oils in the flash pyrolysis method are unstable, acidic, and highly viscous in nature [43]. They even also contain solids and dissolve water. Hence, the yields of the flash pyrolysis method require up-gradation methods, such as hydrogenation and catalytic cracking to reduce the final product's oxygen content. **Table 3** shows the operating variables require to operate slow pyrolysis, fast pyrolysis, and flash pyrolysis method.

The pyrolytic reactor is considered the heart of the pyrolysis method and based on the types of reactors; the yields would change in the pyrolysis method. Several pyrolysis reactors are used in the pyrolysis process, such as a fixed-bed reactor, fluidized bed reactor, moving bed reactor, suspended bed reactor, inclined rotating bed reactor, etc. However, fixed and fluidized beds are commonly used in pyrolysis reactors. A fixed-bed reactor usually uses an external heating source by using a furnace. In contrast, the fluidized bed reactor uses a solid–fluid mixture of stable reactor bed where nitrogen is used to create an inert atmosphere. **Figure 12** shows the characteristic properties of a fixed-bed and fluidized bed reactor. Fluidized bed reactors are easy to operate, capable of transferring high heat rates, good at controlling temperature [44, 45]. Therefore, the pyrolysis method is an effective way of biomass to the energy conversion process.

### 2.3 Incineration

The process when the combustion of biomass materials occurs to generate heat, ash, and flue gases is known as incineration, as shown in **Figure 13** [46]. It is considered as the thermal treatment process of biomass materials. In this process, ash is produced due to the inorganic components contained in the biomass feed material. Ash and flues gases are required to clean, whereas the generated heat in the incineration process produces electricity. In recent practice, the generated heat is used to produce electricity effectively using combined heat energy and power systems. However, emission control is the main factor that needs to be considered during the biomass incineration process [30].

Types of pyrolysis method	Temperature (K)	Rate of heating (K/sec)	Residence time in sec	Size of particles (mm)
Slow	550–950	0.1–1	450–550	5–50
Fast	850–1250	500–10 <sup>5</sup>	0.5–10	Less than 1
Flash	1050–1300	Above 10 <sup>5</sup>	Less than 0.5	Less than 0.2

**Table 3.** Operating variables for fast, slow, and flash pyrolysis method [37, 42].

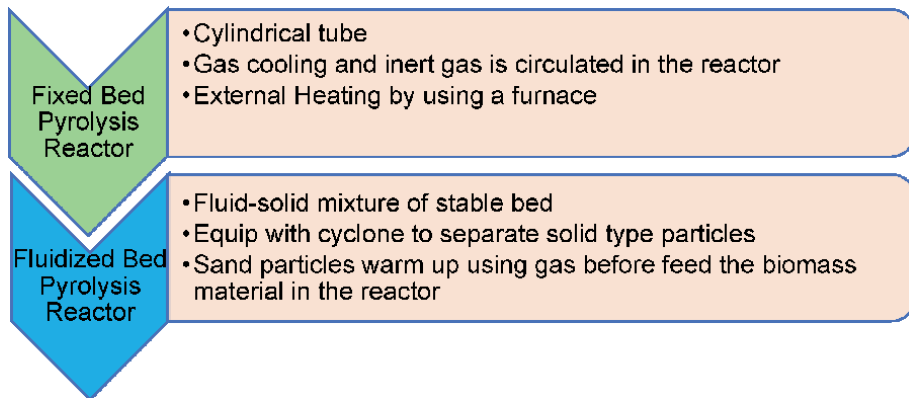


**Figure 12.** Major types of reactor use in pyrolysis method.

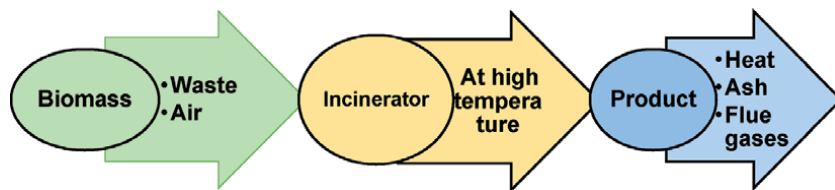


**Figure 13.** Biomass incineration process [47].

The incineration process is one of the several energy generation methods from wastes. Although gasification and incineration methods are considered similar, the generated energy is not the same for them. In the gasification method, combustible gas materials are the major energy product, whereas high-temperature heat is the main energy component in the incineration method [47, 48]. Both the gasification and incineration methods can be implemented without the recovery of energy.

### 3. Gasification method using different gasifiers

In the biomass gasification method, a gasifier is the core of the mechanism. There are different types of gasifiers commonly used in the gasification method. They can be classified depending on the ratio of dense phase biomass to the reactor's total volume. Therefore, dense phase gasifiers and lean phase gasifiers are two common types of gasifiers use in the gasification process. Dense phase biomass gasifiers have a density factor of between 0.08 to 0.3, whereas lean phase gasifiers' density factors vary between 0.05 to 2 [30, 49–51].



### 3.1 Counter-current or updraft gasifier

In counter-current or updraft gasifiers, the air or oxygen is passed through the gasifier's bottom level, and the generated product gases are left at the top of the gasifier [52]. Combustion reactions occur at the bottom side of the gasifier near the grate. After that, the reduction reactions occur at the somewhat upper level of the combustion zone, as shown in **Figure 14**. In the upper level of updraft gasifier, pyrolysis process and heating of the biomass materials occur using the forced convection and radiation heat transfer methods where the required heat is provided from the combustion and reduction zone in the lower part of the gasifier [53]. The generated volatile matters and tars in the updraft gasifier carry in the upper-level gas stream, as depicted in **Figure 14**. On the other hand, produced ash require to clean from the bottom layer of the updraft gasifier.

The main advantages of an updraft gasifier are simplicity in design, simplicity in operation, lower exit gas temperature, and high burning rate of feed materials. Therefore, the equipment efficiency of the updraft gasifier is high. This type of gasifier can be operated using different feed materials such as rice husk, waste plastics, and sawdust.

On the other hand, the disadvantages of updraft gasifiers are channeling that breaks the air or oxygen and creates harmful or explosive situations. Therefore, automatic grates are required in the updraft gasifier. Disposal of tar is another disadvantage in the case of an updraft gasifier.

### 3.2 Co-current or downdraft gasifier

In a downdraft gasifier, air or oxygen generally enters the middle zone of the downdraft gasifier above the grate, as presented in **Figure 15**. Air or oxygen enters at or above the oxygen region level in the downdraft gasifiers [54]. The feed materials are entered at the top of the gasifier, similar to the updraft gasifier. However, air and

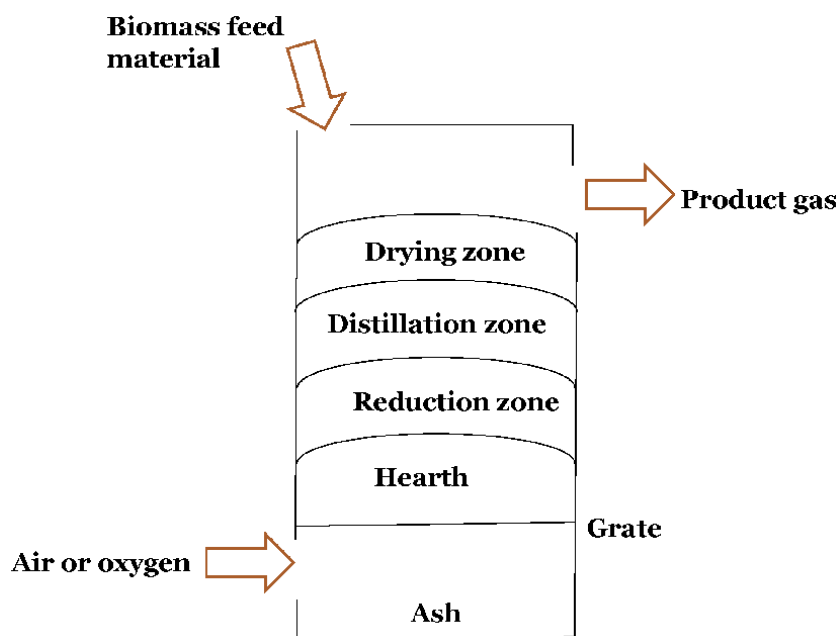


**Figure 14.**  
*Gasification process using updraft gasifier [54].*

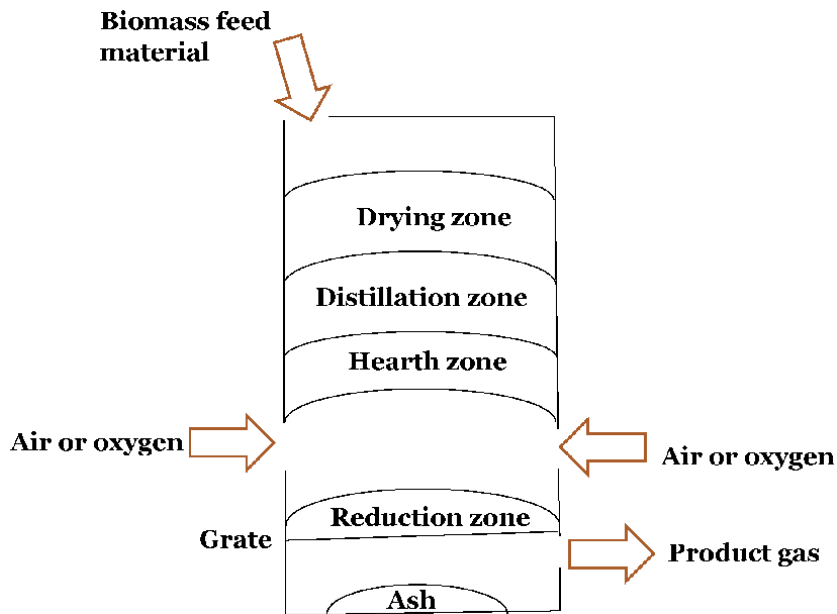


**Figure 15.**  
Gasification process using downdraft gasifier [54].

generated gas mixtures are passed through the oxidation region. In a downdraft gasifier, the producer gases are removed at the bottom level of the gasifier. Therefore, gases and fuels in co-current or downdraft gasifiers are moved in the same direction. When the gases and fuels move down, the fuel must pass through a charcoal bed and generate  $H_2$ ,  $CO$ ,  $CO_2$ , and  $CH_4$ . In a downdraft gasifier, based on the hot region temperature and residence time of tars, most of the tars are broken down. Therefore, the generated product gas in co-current or downdraft gasifier contains lower tar than updraft gasifier. Consequently, they are suitable to use in an internal combustion engine compared to the updraft gasifier gases.

The major advantages of downdraft gasifiers are tar-free gases, and they are suffered less from the environment compared with updraft gasifiers. **Figure 16** shows the salient features of the co-current or downdraft gasifier.

The main disadvantage of co-current or downdraft gasification is the inability to utilize or operate unprocessed fuel. Downdraft gasifier is suffered much from the high content of ash materials when compare with updraft gasifier.

### 3.3 Fluidized bed gasifier

In a fluidized bed gasifier, fuel fluidizes with air or oxygen and steam. Fuel is fed into a bubbling or circulating type fluidized bed. The bed of fluidized bed gasifier acts as fluid with high turbulence. In this system, ash materials are removed from the gasifier in a dry state that defluidize. The temperature in a fluidized bed gasifier is low, and the fuel is required to be highly reactive [55, 56]. However, the energy conversion efficiency is lower than the downdraft gasifier due to the elutriation of carbonaceous fuel [57]. There are three major types of fluidized bed gasifiers: circulating, bubbling, and dual fluidized bed.

The working principle of the operation of updraft and downdraft gasifier is affected by the fuel's chemical and physical properties. Fluidized bed gasifiers can solve a few of the drawbacks of updraft and downdraft gasifiers, such as pressure drop and low bunker flow over the updraft or downdraft gasifier [58].

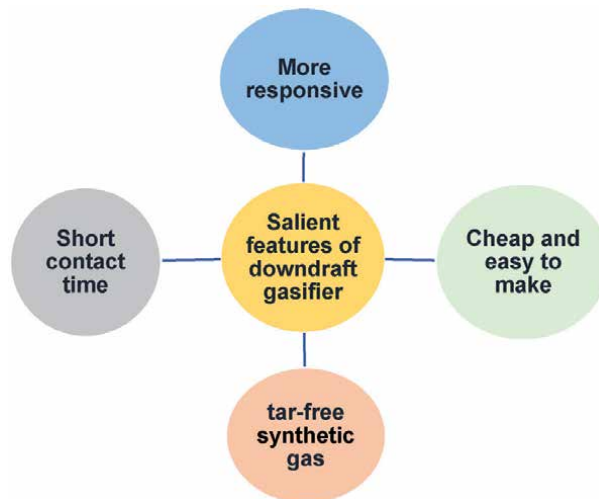


**Figure 16.**  
*Salient features of the gasification process using downdraft gasifier.*

Overall, a fixed-bed gasifier has the capacity for a wide range of temperature distribution. On the other hand, a fluidized bed gasifier can transfer heat between solid and gaseous phases with the best temperature distribution. Fluidized bed gasifiers can tolerate a high variation of fuel quality as well as a large particle distribution [58]. The major drawbacks of fluidized bed gasifiers are high dust contents that make the conflict between higher reaction temperatures with better energy conversion efficiency and lower melting temperature of ash.

### 3.4 Entrained flow gasifier

In an entrained flow gasifier, a dried solid pulverized, liquid fuel, or a slurry of fuel is reacted with oxygen or air in a gasification process using co-current flow [59]. In an entrained flow gasifier, gasification reactions are taken place in a dense cloud of fine particles. High throughput can be achieved, but the overall efficiency is relatively low than the downdraft or fluidized bed gasifier. The entrained flow gasifier system's residence time is approximately 5 seconds that is shorter than the residence time of the downdraft or fluidized bed gasifier. Most of the reactions of entrained flow gasifiers are endothermic. Therefore, high heat is required to be supplied using combustion of biomass feed material or from the outside sources of heat.

In this gasifier, finer coal with air is added co-currently in such a way that air and water steam surrounds the finer coal feed materials. This type of gasifier usually operates at very high pressure and temperature [60]. As a consequence, the flow is turbulent in an entrained flow gasifier. The rate of gasification reaction and efficiency of conversion of carbon is high, while the generation of hydrocarbons is low. Moreover, the coal devolatilization process generates oil, tar, other liquids, and phenols that can be decomposed into hydrogen ( $H_2$ ). This chapter describes gasification of rice husk, waste plastic, and sawdust biomass, therefore the entrained flow gasifier performance is not presented with their related analysis.

### 3.5 Plasma gasifier

In a plasma gasifier, high voltage and current are applied to a torch that can create an arc of high temperature. In the gasification method using plasma gasifier,

inorganic components of feed material are converted into a glass-like substance. It can also be used to gasify solid wastes mainly generated from municipal and households [61].

The plasma type gasifier mainly heats up by using a torch of plasma that is usually located at the bottom of the reactor [62]. At atmospheric pressure, feed materials are required to add to the reactor. The majority of the plasma gasifier is water-cooled on the outer side of the gasifier. In the gasification process of plasma gasifier, the generation of tar is usually eliminated by maintaining the temperature of the synthetic gas greater than 1000 °C.

#### 4. Different biomass feedstock materials

In the gasification method, carbonaceous materials such as rice husk, coal, waste plastics, and sawdust are turned into synthetic gas in the presence of limited air or oxygen, carbon dioxide, and steam. The generated synthetic gas includes hydrogen (H<sub>2</sub>), carbon dioxide (CO<sub>2</sub>), carbon monoxide (CO), Nitrogen (N<sub>2</sub>), char, tars, ash, and bio-oil [63].

This chapter presents the gasification of rice husk, waste plastic, and sawdust as biomass feed material due to their availability, high production rate, and reduction of environmental pollution. The majority of the world population use rice as their main food. Therefore, it was estimated that rice husk generation globally is about 80 million tons with an annual energy generation potential of 1.2 ~ 109 GJ. The estimated heating value of rice husk is approximately 15 MJ/kg [18]. In Asia and Africa, the annual generation of rice husk is  $1.5 \times 10^{11}$  kg [64].

On the other hand, the world's population uses plastic material in their daily activities due to its insolubility in liquid water, availability, resistance to corrosion, and lighter weight. The generation of plastic waste materials is increasing globally. For example, Asia regions possess maximum plastic waste, and they generate around 30% of plastic wastes in the world [65]. Therefore, if the plastic waste materials can be used as biomass feed material in the gasification method to generate energy, the waste materials are turned into energy. On the other hand, world environmental pollution due to waste plastics will also be reduced significantly. Waste plastic material can also be converted into oil by using fast pyrolysis.

Sawdust material is another potential biomass source use in the gasification process. Carbonaceous feed materials are effective for gasification methods. The ultimate and proximate analysis of sawdust material shows that sawdust contains approximately 50.90% carbon. **Table 4** shows the ultimate analysis results of rice husks, sawdust, and waste plastic material.

Biomass feed materials	Carbon C (%)	Oxygen O (%)	Nitrogen N (%)	Hydrogen H (%)	Sulfur S (%)
Rice husk [66]	45.2	47.6	1.02	5.8	0.2
Waste plastic [67]	77.10	11.20	0.20	11.50	—
Saw dust [23, 68]	50.9	45.03	0.27	3.7	0.05

**Table 4.**

*Ultimate analysis of rice husk, waste plastics, and sawdust biomass feed materials.*

## **5. Gasification method using downdraft gasifiers**

Downdraft fixed-bed gasifiers generate low tar content synthetic gas that can be used to operate an internal combustion engine. Hence, this chapter presents the gasification methods using the downdraft fixed-bed gasifier.

### **5.1 Gasification performance**

The performance of the gasification method mainly depends on the reactor temperature. With an increase in reactor temperature, the performance and yield of the gasification method are also increased. It was observed that with waste plastic gasification method using downdraft gasifier, at 600 °C synthetic gas yield was 112.4 (wt. %), whereas at 700 °C yield was 166.8% (wt. %), 800 °C generated 205.7% (wt. %) gaseous yield and maximum synthetic gaseous yield obtained at 900 °C (234.6 wt. %) [67].

In rice husk and sawdust gasification method, the performance of synthetic gas yield generation also depends on the reactor temperature. It was obtained that using a total 5 kg rice husk with 3.6 kg/h feed rate for 1.38-hour gasification in a downdraft fixed-bed gasifier; the generated synthetic gas yield was highest at 810 °C (0.27 wt.% CH<sub>4</sub> and other gases 61.09 wt.%) [18].

Catalytic temperature is another significant parameter of the biomass gasification method. With the increase of reactor temperature and catalytic temperature in the sawdust gasification method, the synthetic gas yield is also increased. It was found that at a constant gasification temperature of 800 °C in a downdraft fixed-bed gasifier, the synthetic gas yield was 63.43 (wt. %) at 600 °C catalytic temperature. In contrast, the gas yield was 71.35 (wt. %) at 700 °C catalytic temperature, 77.25 (wt. %) at 800 °C catalytic temperature, and 80.58 (wt. %) at 900 °C catalytic temperature [68].

### **5.2 Synthetic gas composition**

In this chapter, gasification method using downdraft fixed-bed gasifier generates synthetic gas from rice husk, waste plastic, and sawdust biomass energy sources. Among different gases, carbon monoxide, carbon dioxide, methane, hydrogen are significant. Carbon dioxide and carbon monoxide form a significant portion of synthetic gas, whereas methane generation is lower than carbon dioxide and carbon monoxide [18]. In the case of biomass feedstocks, the generation of H<sub>2</sub> and methane is higher for sawdust than rice husk biomass due to its higher heating value. In contrast, the heating value of plastic is higher than sawdust and rice husk. Therefore, it has a significant potential for H<sub>2</sub> (3–18 vol. %) rich and high methane synthetic gas generation using a downdraft fixed-bed gasifier. On the other hand, the gasification of plastic generates a high quantity of tar that reduces the efficiency of the gasification process. In addition, endothermicity is another drawback of the plastic gasification process. Overall, the gasification process using plastic material is still uncommon in practical cases although the efficiency can be improved by adding another feed material with plastic material as co-feedstocks.

### **5.3 Power generation using gasifier**

The generated synthetic gas from the gasification of rice husk, waste plastic, and sawdust is collected from the exhaust end by controlling the exhaust valve of

the downdraft fixed-bed gasifier. A gas analyzer is needed to analyze the contents of synthetic gas. The generated synthetic gas can be utilized to operate the engine, boiler, etc. It is possible to operate any prime movers, such as engines and boilers by connecting them at the exhaust end of a downdraft fixed-bed gasifier where the gasification of rice husk, sawdust, and waste plastic occurs.

The heating value of rice husk, sawdust, and waste plastic is 16.7 MJ/kg, 18.23 MJ/kg, and 40 MJ/kg, respectively.

However, in the biomass gasification method using downdraft fixed-bed gasifier, the heating value is within the range of 5.4 MJ/m<sup>3</sup> to 5.7 MJ/m<sup>3</sup> [69]. The generated synthetic gas from the biomass gasification method can also be used in diesel engines, dual-fuel engines, and petrol engines. Moreover, the produced heat in the rice husk, waste plastic, and sawdust gasification process can be used to generate electricity in an off-grid area. The typical size of an off-grid electricity system is 10–500 kW for the generated heat in these biomass gasification process [30]. The exact size of the off-grid energy system depends on the amount of feedstock materials use in the downdraft gasification process.

## **6. Conclusion**

Rice husk, waste plastic, and sawdust were used as feedstock materials in the gasification process using a downdraft fixed-bed gasifier. The generation of synthetic gas depends on the heating value of biomass feedstocks. It has been found that waste plastic has the highest heating value (40 MJ/kg) among the three biomasses. Therefore, it has the highest potential of H<sub>2</sub> rich (3–18 vol. %) synthetic gas generation than rice husk and sawdust biomasses. On the other hand, sawdust produces a high H<sub>2</sub> and methane content synthetic gas than rice husk. Moreover, the generation capacity and quantity of biomass gasification method depends on the type of gasifier. Downdraft fixed-bed gasifier is one of the effective gasifiers used in the gasification process. The generation of synthetic gas and heat from the biomass gasification method using a downdraft gasifier depends on the reactor temperature, residence time, catalytic temperature, and gasification duration.

## **Acknowledgements**

The authors would like to acknowledge the Department of Mechanical Engineering, Rajshahi University of Engineering & Technology, Bangladesh for the support of accessing the laboratory facilities to study the gasification process using the downdraft gasifier.

## Author details

Md. Emdadul Hoque\* and Fazlur Rashid  
Department of Mechanical Engineering, Rajshahi University of Engineering and  
Technology, Rajshahi, Bangladesh

\*Address all correspondence to: [mehoque@me.ruet.ac.bd](mailto:mehoque@me.ruet.ac.bd)

## IntechOpen

---

© 2021 The Author(s). Licensee IntechOpen. This chapter is distributed under the terms of the Creative Commons Attribution License (<http://creativecommons.org/licenses/by/3.0>), which permits unrestricted use, distribution, and reproduction in any medium, provided the original work is properly cited. 

## References

- [1] Ak, N. and A. Demirbas, Promising sources of energy in the near future. *Energy Sources, Part A: Recovery, Utilization, and Environmental Effects*, 2016. 38(12): p. 1730-1738.
- [2] Lizunkov, V., Population of the world and regions as the principal energy consumer. 2018.
- [3] Tvaronavičienė, M., J. Baublys, J. Raudeliūnienė, and D. Jatautaitė, Global energy consumption peculiarities and energy sources: Role of renewables, in *Energy Transformation Towards Sustainability*. 2020, Elsevier. p. 1-49.
- [4] Uddin, M.S., Islam, M.S., Rashid, F., Habibulla, I.M., and Haque, N. Energy and Carbon Footprint Analysis of University Vehicles in Bangladesh, in *Proceedings of the International Conference on Mechanical, Industrial and Materials Engineering*, 28-30 December 2017, RUET, Bangladesh.
- [5] Davis, N., V.G. Lizunkov, O. Ergunova, and E. Malushko, Phenomenon of migration and its manifestations in the modern world. *The European Proceedings of Social & Behavioural Sciences (EpSBS)*. Vol. 26: Responsible Research and Innovation (RRI 2016).—Nicosia, 2017., 2017. 262016: p. 550-556.
- [6] Asif, M. and T. Muneer, Energy supply, its demand and security issues for developed and emerging economies. *Renewable and sustainable energy reviews*, 2007. 11(7): p. 1388-1413.
- [7] Kok, B. and H. Benli, Energy diversity and nuclear energy for sustainable development in Turkey. *Renewable energy*, 2017. 111: p. 870-877.
- [8] Burnham, A., J. Han, C.E. Clark, M. Wang, J.B. Dunn, and I. Palou-Rivera, Life-cycle greenhouse gas emissions of shale gas, natural gas, coal, and petroleum. *Environmental science & technology*, 2012. 46(2): p. 619-627.
- [9] Rashid, F., Hoque, M.E., K. Peash, and F. Faisal, performance analysis and investigation for the development of energy efficient building, in *Proceedings of the International Conference on Mechanical Engineering and Renewable Energy*, 18-20 December 2017, CUET, Bangladesh.
- [10] Arent, D.J., A. Wise, and R. Gelman, The status and prospects of renewable energy for combating global warming. *Energy Economics*, 2011. 33(4): p. 584-593.
- [11] Dincer, I., Renewable energy and sustainable development: a crucial review. *Renewable and sustainable energy reviews*, 2000. 4(2): p. 157-175.
- [12] Farhad, S., M. Saffar-Avval, and M. Younessi-Sinaki, Efficient design of feedwater heaters network in steam power plants using pinch technology and exergy analysis. *International journal of energy research*, 2008. 32(1): p. 1-11.
- [13] Panwar, N., S. Kaushik, and S. Kothari, Role of renewable energy sources in environmental protection: A review. *Renewable and sustainable energy reviews*, 2011. 15(3): p. 1513-1524.
- [14] Fornasiero, P. and M. Graziani, Renewable resources and renewable energy: a global challenge. 2011: CRC press.
- [15] Iniyar, S. and K. Sumathy, An optimal renewable energy model for various end-uses. *Energy*, 2000. 25(6): p. 563-575.
- [16] Hoque, M. E., Biswas, A., Rashid, F., Saad, A.M., and Bir, P.K., production of electricity from renewable energy



sources for home appliances and nano-grid, in Proceedings of the International Conference on Mechanical Engineering and Renewable Energy, 26-29 November 2015, CUET, Bangladesh.

[17] Bezrukikh, P. and D. Strebkov, Alternative renewable energy in the world and Russia. The state, challenges, prospects. *Energy policy*, 2001. 3: p. 3-13.

[18] Hoque, M. E., Rashid, F., Aziz, S. S., Rahman, M. N., & Das, P. (2019, July). Process analysis and gasification of rice husk by using downdraft fixed bed gasifier. In *AIP Conference Proceedings* (Vol. 2121, No. 1, p. 130005). AIP Publishing LLC.

[19] Rashid, F., M. Sarker, S. Tuly, J. Ferdous, and R. Beg, Numerical Study of a Stand-alone Flat Plate Solar Water Heater using Rectangular Flow Channel with Fin, in Proceedings of the International Conference on Mechanical, Industrial and Energy Engineering, 23-24 December 2018, KUET, Bangladesh.

[20] Islam, T., M. Zaman, Rashid, F., and Hoque, M.E. Numerical Analysis of Solar Water Heater using Water-Glycerin Solution, in Proceedings of the International Conference on Mechanical, Industrial and Materials Engineering, 17-19 December 2019, RUET, Bangladesh.

[21] Yoon, S.J., Y.-I. Son, Y.-K. Kim, and J.-G. Lee, Gasification and power generation characteristics of rice husk and rice husk pellet using a downdraft fixed-bed gasifier. *Renewable Energy*, 2012. 42: p. 163-167.

[22] Balat, M. and G. Ayar, Biomass energy in the world, use of biomass and potential trends. *Energy sources*, 2005. 27(10): p. 931-940.

[23] Han, L., Q. Wang, Y. Yang, C. Yu, M. Fang, and Z. Luo, Hydrogen production

via CaO sorption enhanced anaerobic gasification of sawdust in a bubbling fluidized bed. *International journal of hydrogen energy*, 2011. 36(8): p. 4820-4829.

[24] Dogru, M., A. Midilli, and C.R. Howarth, Gasification of sewage sludge using a throated downdraft gasifier and uncertainty analysis. *Fuel Processing Technology*, 2002. 75(1): p. 55-82.

[25] Reed, T.B. and A. Das, Handbook of biomass downdraft gasifier engine systems. 1988: Biomass Energy Foundation.

[26] Dogru, M., C. Howarth, G. Akay, B. Keskinler, and A. Malik, Gasification of hazelnut shells in a downdraft gasifier. *Energy*, 2002. 27(5): p. 415-427.

[27] Baliban, R.C., J.A. Elia, and C.A. Floudas, Toward novel hybrid biomass, coal, and natural gas processes for satisfying current transportation fuel demands, 1: Process alternatives, gasification modeling, process simulation, and economic analysis. *Industrial & Engineering Chemistry Research*, 2010. 49(16): p. 7343-7370.

[28] Modell, M., R.C. Reid, and S.I. Amin, Gasification process. 1978, Google Patents.

[29] Wang, K., Q. Yu, Q. Qin, L. Hou, and W. Duan, Thermodynamic analysis of syngas generation from biomass using chemical looping gasification method. *international journal of hydrogen energy*, 2016. 41(24): p. 10346-10353.

[30] Das, B.K. and S. Hoque, Assessment of the potential of biomass gasification for electricity generation in Bangladesh. *Journal of Renewable Energy*, 2014. 2014.

[31] Milne, T.A., R.J. Evans, and N. Abatzoglou, Biomass gasifier "Tars": their nature, formation, and conversion.

1998, National Renewable Energy Laboratory, Golden, CO (US).

[32] Goldemberg, J. and S.T. Coelho, Renewable energy—traditional biomass vs. modern biomass. *Energy Policy*, 2004. 32(6): p. 711-714.

[33] Klass, D.L., Biomass for renewable energy, fuels, and chemicals. 1998: Elsevier.

[34] Indrawan, N., B. Simkins, A. Kumar, and R.L. Huhnke, Economics of distributed power generation via gasification of biomass and municipal solid waste. *Energies*, 2020. 13(14): p. 3703.

[35] Pourkarimi, S., A. Hallajisani, A. Alizadehdakheel, and A. Nouralishahi, Biofuel production through micro- and macroalgae pyrolysis—a review of pyrolysis methods and process parameters. *Journal of Analytical and Applied Pyrolysis*, 2019. 142: p. 104599.

[36] Demirbas, A., Effects of temperature and particle size on bio-char yield from pyrolysis of agricultural residues. *Journal of analytical and applied pyrolysis*, 2004. 72(2): p. 243-248.

[37] Balat, M., Mechanisms of thermochemical biomass conversion processes. Part 1: reactions of pyrolysis. *Energy Sources, Part A*, 2008. 30(7): p. 620-635.

[38] Chen, W.-H., B.-J. Lin, M.-Y. Huang, and J.-S. Chang, Thermochemical conversion of microalgal biomass into biofuels: a review. *Bioresource technology*, 2015. 184: p. 314-327.

[39] Balat, M., M. Balat, E. Kirtay, and H. Balat, Main routes for the thermo-conversion of biomass into fuels and chemicals. Part 1: Pyrolysis systems. *Energy conversion and Management*, 2009. 50(12): p. 3147-3157.

[40] Mourshed, M., M.H. Masud, F. Rashid, and M.U.H. Joardder, Towards the effective plastic waste management in Bangladesh: a review. *Environmental Science and Pollution Research*, 2017. 24(35): p. 27021-27046.

[41] Ellens, C.J., J.N. Brown, A.J.S. Pollard, and D.S. Banasiak, Methods for integrated fast pyrolysis processing of biomass. 2012, Google Patents.

[42] Jahirul, M.I., M.G. Rasul, A.A. Chowdhury, and N. Ashwath, Biofuels production through biomass pyrolysis—a technological review. *Energies*, 2012. 5(12): p. 4952-5001.

[43] Chiaramonti, D., A. Oasmaa, and Y. Solantausta, Power generation using fast pyrolysis liquids from biomass. *Renewable and sustainable energy reviews*, 2007. 11(6): p. 1056-1086.

[44] Borges, F.C., Q. Xie, M. Min, L.A.R. Muniz, M. Farenzena, J.O. Trierweiler, P. Chen, and R. Ruan, Fast microwave-assisted pyrolysis of microalgae using microwave absorbent and HZSM-5 catalyst. *Bioresource technology*, 2014. 166: p. 518-526.

[45] Caravella, A., G. Barbieri, and E. Drioli, Modelling and simulation of hydrogen permeation through supported Pd-alloy membranes with a multicomponent approach. *Chemical Engineering Science*, 2008. 63(8): p. 2149-2160.

[46] Lombana, L.A. and J.G. Campos, Incineration method and system. 1977, Google Patents.

[47] You, S., W. Wang, Y. Dai, Y.W. Tong, and C.-H. Wang, Comparison of the co-gasification of sewage sludge and food wastes and cost-benefit analysis of gasification-and incineration-based waste treatment schemes. *Bioresource technology*, 2016. 218: p. 595-605.

- [48] Dong, J., Y. Tang, A. Nzihou, Y. Chi, E. Weiss-Hortala, M. Ni, and Z. Zhou, Comparison of waste-to-energy technologies of gasification and incineration using life cycle assessment: Case studies in Finland, France and China. *Journal of Cleaner Production*, 2018. 203: p. 287-300.
- [49] Mosiori, G.O., C.O. Onindo, P. Mugabi, S.B. Tumwebaze, S. Bagabo, and R.B. Johnson, Characteristics of potential gasifier fuels in selected regions of the Lake Victoria Basin. *South African Journal of Science*, 2015. 111(5-6): p. 1-6.
- [50] Mosiori, G.O., Thermo-chemical characteristics of potential gasifier fuels in selected regions of the Lake Victoria basin, M. Sc., Kenyatta University, 2013.
- [51] Zhu, J.-g., Y. Yao, Q.-g. Lu, M. Gao, and Z.-q. Ouyang, Experimental investigation of gasification and incineration characteristics of dried sewage sludge in a circulating fluidized bed. *Fuel*, 2015. 150: p. 441-447.
- [52] Pedroso, D.T., E.B. Machín, J.L. Silveira, and Y. Nemoto, Experimental study of bottom feed updraft gasifier. *Renewable energy*, 2013. 57: p. 311-316.
- [53] Brandt, P. and U.B. Henriksen. Decomposition of tar in gas from updraft gasifier by thermal cracking. in 1st world conference and exhibition on biomass for energy and industry. 2000.
- [54] Phillips, J., Different types of gasifiers and their integration with gas turbines. *The gas turbine handbook*, 2006. 1.
- [55] Mansaray, K., A. Ghaly, A. Al-Taweel, F. Hamdullahpur, and V. Ugursal, Air gasification of rice husk in a dual distributor type fluidized bed gasifier. *Biomass and bioenergy*, 1999. 17(4): p. 315-332.
- [56] Black, J.W., G. Gravel, and R. Hoareau, Fluidized bed gasifier. 1990, Google Patents.
- [57] Basu, P., Combustion and gasification in fluidized beds. 2006: CRC press.
- [58] Warnecke, R., Gasification of biomass: comparison of fixed bed and fluidized bed gasifier. *Biomass and bioenergy*, 2000. 18(6): p. 489-497.
- [59] Wen, C.Y. and T. Chaung, Entrainment coal gasification modeling. *Industrial & Engineering Chemistry Process Design and Development*, 1979. 18(4): p. 684-695.
- [60] Kajitani, S., N. Suzuki, M. Ashizawa, and S. Hara, CO<sub>2</sub> gasification rate analysis of coal char in entrained flow coal gasifier. *Fuel*, 2006. 85(2): p. 163-169.
- [61] Hong, Y.C., D.H. Shin, B.J. Lee, H.S. Uhm, S.J. Lee, and H.W. Jeon, Power generation system using plasma gasifier. 2013, Google Patents.
- [62] Messerle, V., A. Mosse, and A. Ustimenko, Processing of biomedical waste in plasma gasifier. *Waste management*, 2018. 79: p. 791-799.
- [63] Ruiz, J.A., M. Juárez, M. Morales, P. Muñoz, and M. Mendívil, Biomass gasification for electricity generation: Review of current technology barriers. *Renewable and Sustainable Energy Reviews*, 2013. 18: p. 174-183.
- [64] Aulakh, D.S., J. Singh, and S. Kumar, The Effect of Utilizing Rice Husk Ash on Some Properties of Concrete-A Review. *Current World Environment*, 2017. 13(2).
- [65] Hossan, M.M., Evolution of environmental policies in Bangladesh (1972-2010). *Journal of the Asiatic Society of Bangladesh (Hum.)*, 2014. 59(1): p. 39-63.

[66] Efomah, A.N. and A. Gbabo, The physical, proximate and ultimate analysis of rice husk briquettes produced from a vibratory block mould briquetting machine. *International Journal of Innovative Science, Engineering & Technology*, 2015. 2(5): p. 814-822.

[67] Wu, C. and P.T. Williams, Pyrolysis–gasification of post-consumer municipal solid plastic waste for hydrogen production. *International Journal of Hydrogen Energy*, 2010. 35(3): p. 949-957.

[68] Hu, M., L. Gao, Z. Chen, C. Ma, Y. Zhou, J. Chen, S. Ma, M. Laghari, B. Xiao, and B. Zhang, Syngas production by catalytic in-situ steam co-gasification of wet sewage sludge and pine sawdust. *Energy Conversion and Management*, 2016. 111: p. 409-416.

[69] Asadullah, M., Barriers of commercial power generation using biomass gasification gas: A review. *Renewable and Sustainable Energy Reviews*, 2014. 29: p. 201-215.

# Performance Assessment of the Thermodynamic Cycle in a Multi-Mode Gas Turbine Engine

*Viktors Gutakovskis and Vladimirs Gudakovskis*

## Abstract

This chapter discusses the direction of development of promising multimode aviation gas turbine engines (GTE). It is shown that the development of GTE is on the way to increase the parameters engine workflow: gas temperatures in front of the turbine ( $T^*_G$ ) and the degree of pressure increase in the compressor ( $P^*_C$ ). It is predicted that the next generation engines will operate with high parameters of the working process,  $T^*_G = 2000\text{--}2200\text{ K}$ ,  $\pi^*_C = 60\text{--}80$ . At this temperature of gases in front of the turbine, the working mixture in the combustion chamber (CC) is stoichiometric, which sharply narrows the range of stable operation of the CC and its efficiency drops sharply in off-design gas turbine engine operation modes. To expand the range of effective and stable work, it is proposed to use an advanced aviation GTE: Adaptive Type Combustion Chamber (ATCC). A scheme of the ATCC and the principles of its regulation in the system of a multi-mode gas turbine engine are presented. The concept of an adaptive approach is given in this article. There are two main directions for improving the characteristics of a promising aviation gas turbine engine. One is a complication of the concepts of aircraft engines and the other one is an increase in the parameters of the working process, the temperature of the gases in front of the turbine ( $T^*_G$ ) and the degree of increasing pressure behind the compressor ( $\pi^*_C$ ). It is shown how the principles of adaptation are used in these areas. The application of the adaptation principle in resolving the contradiction of the possibility of obtaining optimal characteristics of a high-temperature combustion chamber (CC) of a gas turbine engine under design (optimal) operating conditions and the impossibility of their implementation when these conditions change in the range of acceptable (non-design) gas turbine operation modes is considered in detail. The use of an adaptive approach in the development of promising gas turbine engines will significantly improve their characteristics and take into account unknown challenges.

**Keywords:** thermodynamic cycle, gas turbine engine, combustion chamber, adaptation principle, aviation

## 1. Introduction

This chapter analyses the main trends in the development of an aviation multi-mode gas turbine engine (GTE) of direct reaction, examines its thermodynamic cycle and determines the influence of the multi-mode GTE on its efficiency,

analyses the multi-mode operation of a multi-purpose aircraft and analyses ways to improve operation of the thermodynamic cycle in non-design modes of GTE operation. The energy capabilities of traditional aviation fuels for the implementation of high thermodynamic characteristics in non-design gas turbine engine operation are studied. The adaptive approach is determined as the main one in the creation of promising aviation GTEs. The concept of an adaptive approach is given. There are two main directions for improving the characteristics of the promising aviation GTE.

One is the sophistication of the schematic diagrams of aircraft engines and the second one is an increase in the parameters of the working process, the temperature of the gases in front of the turbine ( $T_G^*$ ) and the degree of pressure rise behind the compressor ( $\pi_C^*$ ).

It is shown how the principles of adaptation are used in these areas. The application of the adaptation principle in resolving the contradiction of the possibility of obtaining the optimal characteristics of the high-temperature combustion chamber (CC) of the GTE under the design (optimal) conditions of operation and the impossibility of their implementation when these conditions change in the range of permissible (non-design) operating modes of the GTE are considered in detail. The use of an adaptive approach in the development of promising gas turbine engines will significantly improve their characteristics and take into account unknown challenges.

## **2. The main trends in the development of aviation gas turbine engines**

The world leaders in aircraft engine manufacturing prefer the traditional (“soft”) direction of the development of aircraft gas turbine engines. In accordance with the theory of aircraft engines, the development of the traditional direction of aircraft gas turbine engines occurs in accordance with the following priorities:

- ensuring high efficiency;
- stable operation in a wide range of speeds and flight altitudes of the aircraft;
- ensuring high dynamic characteristics;
- reliable high-altitude and ground launch;
- ensuring high environmental performance (reducing harmful emissions and reducing noise levels);
- ensuring acceptable performance under icing conditions and other difficult climatic conditions;
- widening of the range of work due to ensuring the operation of the engine with a minimum degree of stability;
- the ability to operate on various fuels (alternative).

At present, aviation GTEs has reached a high level of development and has:

- a high level of thermodynamic perfection;
- high aerodynamic loading of blades (compressors, turbines);

- marginal combustion intensity and ecological perfection of combustion chambers;
- effective thermal protection of the elements of the hot path of the engine;
- low specific gravity;
- multi-mode operation;
- new materials in engine design (steel and composite materials);
- highly efficient constructive and technological solutions.

The main regularity in the development of aviation GTEs is the consistent improvement of the indicators of technical perfection and the efficiency of their use on aircraft. This pattern is continuous and progressive, reflecting the need to accumulate the required amount of knowledge, understanding the experience of previous developments and operation, mastering new technologies for creating highly efficient units and elements of aviation GTE.

The traditional way to improve the efficiency and traction characteristics of a GTE is to increase the efficiency of the thermodynamic cycle of the engine:

- increase in the total degree of pressure increase in the cycle (1):

$$\pi_{C\Sigma}^* = P_C^*/P_A^*, \quad (1)$$

where:

( $P_C^*$  – pressure behind the compressor,  $P_A^*$  – engine entrance pressure);

- increase in turbine intake temperature ( $T_G^*$ );
- reduction of total pressure losses in the air intake and outlet devices.

Within the framework of the traditional approach of improving the efficiency of aircraft gas turbine engines, there is also some reserve associated with improving the main components of the aircraft engine.

However, it should be stated that further improvement of the characteristics of aviation GTEs within the framework of traditional layouts is associated with ever-increasing difficulties.

The main qualitative changes, in accordance with thermodynamics and heat exchange, are associated with the creation of turbines and combustion chambers capable of operating at turbine intake temperature which is at the level of 2100–2400 K, bringing the turbine inlet temperature closer to the maximum energy potential of aviation fuel, and requiring new solutions for realization of such temperatures in aircraft gas turbine engines.

As noted earlier, the development of aircraft gas turbine engines follows the path of a constant increase in the parameters of the working process, an increase in the turbine inlet temperature ( $T_G^*$ ) and an increase in the total of pressure increase degree in the engine ( $\pi_{C\Sigma}^*$ ).

An increase in  $T_G^*$  with a simultaneous increase in  $\pi_{C\Sigma}^*$  leads to an increase in the specific engine thrust  $R_S = R/G_A$  ( $R$  - engine thrust,  $G_A$  - air flow through the engine) and frontal thrust  $R_F = R_{TO} / F_m$  ( $R_{TO}$  - engine thrust at take-off,  $F_m$  - the area of the mid-section of the engine) .

GTE generation	I	II	III	IV	V	VI
$T_G^*$ , K	1000–1150	1150–1250	1300–1450-	1500–1650	1700–1900	2100–2200
$\pi_{C\Sigma}^*$	3–5	7–13	14–20	20–35	20–50	60–80

**Table 1.**

The growth trend of  $T_G^*$  and  $\pi_{C\Sigma}^*$  for different generations of aviation gas turbine engines.

The higher  $R_F$ , the smaller the frontal dimensions of the engine and the specific gravity of the engine  $Y_{ENG} = G_{ENG}/R_F$  ( $G_{ENG}$  - engine mass). Parameters  $R_F$  and  $Y_{ENG}$  - characterize the level of perfection of the engine.

An increase in the values of  $T_G^*$  and  $\pi_{C\Sigma}^*$  lead to an increase in the work of the thermodynamic cycle and efficiency. **Table 1** shows the growth trend of  $T_G^*$  and  $\pi_{C\Sigma}^*$  for different generations of aviation gas turbine engines [1].

One important feature of a promising multi-mode aircraft is flight at supersonic cruising modes, which should be carried out at non-boosted engine operating modes.

A promising direction for meeting this requirement is the creation of the so-called stoichiometric motors. In these engines, all of the oxygen in the air entering the gasifier is used to burn fuel in the main combustion chamber to obtain a high  $T_G^*$ .

Obtaining  $T_G^* = 2000\text{--}2200$  K in the combustion chamber of a promising gas turbine engine requires that the excess air ratio of the combustion chamber  $\alpha_{CC} = G_A/G_{FL0}$  ( $G_A$  - the air flow rate entering the combustion chamber,  $G_F$  - the fuel flow rate entering the combustion chamber,  $L_o$  - the theoretically required amount of air for complete combustion of 1 kg of fuel, for aviation kerosene  $L_o = 14.8$ ) was  $\alpha_{CC} = 1.1\text{--}1.2$  (to describe the fuel composition a description of the following dependence is used: air / fuel ratio).

The urgency of creating high-temperature (stoichiometric) gas turbine engines, in the direction of increasing the efficiency of the thermodynamic cycle and ensuring their multimodality, poses a number of new problems. These tasks are associated with the peculiarities of the organization of the fuel combustion workflow to obtain high turbine inlet temperature and the efficient use of the energy potential of the fuel in the entire range of the GTE operation.

### 3. Thermodynamic cycle of the direct reaction aircraft GTE

As mentioned above, the parameters of the working process of aviation GTE  $\pi_{C\Sigma}^*$  and  $T_G^*$  with the development of engines are constantly increasing. Such a tendency in the development of aviation GTE as a heat engine, in accordance with the theory of aircraft engines, is natural. Put simplistically, the main components of a modern aviation GTE are:

- a heat engine operating according to a thermodynamic cycle with heat supply to the working fluid (implementing the Brighton cycle);
- propulsion device - a device for converting the available work, obtained as a result of the thermodynamic cycle, into thrust, depending on the type of gas turbine engine;
- automatic control system (ACS), which ensures the maintenance of the necessary engine operating modes.



Based on the basic provisions of the theory of aircraft engines, the energy balance of aviation GTE of a direct reaction can be represented in a simplified way by a diagram that displays all stages of the process of converting the chemical energy of fuel into useful work.

In a direct reaction GTE, atmospheric oxygen is used to convert the chemical energy of the fuel into thermal energy. Air serves as the main component of the working fluid for the thermodynamic cycle, in which thermal energy is converted into mechanical energy. Receiving acceleration in the propulsion system, it creates a thrust force, i.e. serves as a propulsion device. Direct reaction engines are turbojet engines and turbofan engines. **Figure 1** shows a simplified diagram of the energy balance of a direct reaction GTE.

In the diagram on the **Figure 1**:

$Q_0 = \frac{G_F H_u}{G_A}$  - the amount of thermal energy introduced into the engine with fuel per 1 kg of working body (chemical energy of the fuel);

$G_F$  - fuel consumption;

$G_A$  - air consumption;

$H_u$  - lower calorific value of fuel;

$Q$  - the actual amount of heat energy received during fuel combustion.

The real process of heat release is accompanied by losses and is characterized by the fuel combustion efficiency ( $\eta_g = Q/Q_0$ ).

$L_C$  - the work of the thermodynamic cycle of the engine, which results in an increase in the kinetic energy of the exhaust gases, can be represented for multimode aircraft real cycle in the following formula (2) [1]:

$$L_C = C_p T_H \frac{e - 1}{\eta_c} \left( \frac{\bar{m} \Delta \eta_c \eta_e}{e} - 1 \right), \quad (2)$$

where:  $\eta_c, \eta_e$  - the efficiency of the compression and expansion processes, i.e., they characterize the technical perfection of the compression and expansion process;

$\Delta = \frac{T_G^*}{T_H}$  - working body heating degree;

$T_H$  - ambient air temperature;

$\bar{m}$  - coefficient taking into account the difference in the physical properties of air and gas;

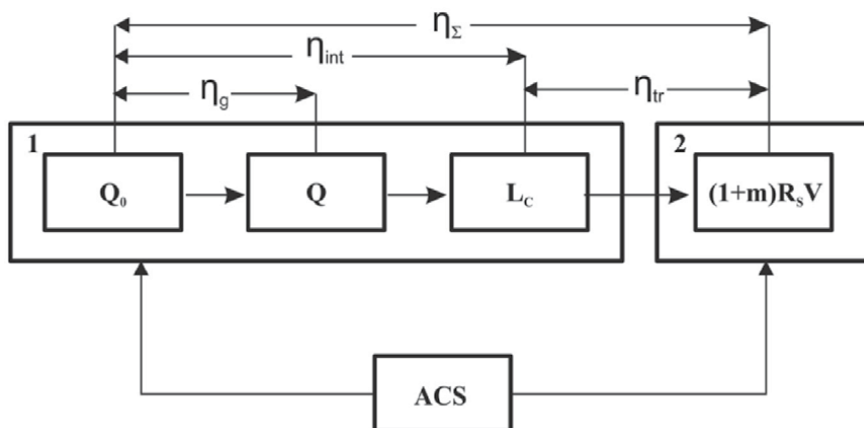


**Figure 1.**  
 Simplified diagram of the energy balance of a direct reaction GTE: 1 - heat engine; 2 - propulsion device;  
 ACS - automatic control system.

$$e = \pi_{k\Sigma}^* \frac{k-1}{k};$$

$C_p$  – specific heat of heat supply at constant pressure.

The operation of the actual thermodynamic cycle of a GTE depends both on the parameters of the working process  $\pi_{C\Sigma}^*$ ,  $\Delta$ , and on the technical perfection of the compression and expansion processes ( $\eta_c, \eta_e$ ).

$\eta_{int} = \frac{L_C}{Q_0}$  - internal coefficient efficiency of the GTE thermodynamic cycle (motor thermodynamic efficiency), i.e. the efficiency of the engine as a heat engine serves to assess the efficiency of heat conversion into cycle work, is given in the following relation: ( $\eta_{int} = \frac{L_C \eta_k}{Q}$ ).

The internal efficiency of the GTE thermodynamic cycle takes into account the inevitable heat losses associated with the costs of overcoming hydraulic losses, as well as heat losses due to incomplete fuel combustion and recoil to the engine walls.

$\eta_{tr} = \frac{2}{1 + \frac{C_j}{V}}$  - propulsive efficiency, which characterizes the operation of a direct reaction gas-turbine engine as a propulsion device [1]:

where:

$C_j$  – nozzle flow rate;

$V$  – flight speed.

$(1 + m)R_S V$  – effective work (jet thrust),

where:  $m = \frac{G_{A2}}{G_{A1}}$  - bypass ratio ( $G_{A2}$  – air flow through the second engine circuit,  $G_{A1}$  – air flow through the gas generator).

$\eta_{\Sigma} = \eta_{int} \eta_{tr}$  – the overall efficiency of the direct reaction GTE, which characterizes the share of chemical energy of the fuel converted into effective work, takes into account all the losses in the process of converting heat into effective work, and thus most fully characterizes the efficiency of the GTE .

ACS - automatic engine control system that regulates the operation of the GTE of both the heat engine and the propulsion unit in various flight modes of the aircraft, in order to obtain maximum performance.

**Figure 2** shows the values of the level of efficiency of GTE for some engines of civil aviation, considering the degree of bypass ( $m$ ) [2, 3].

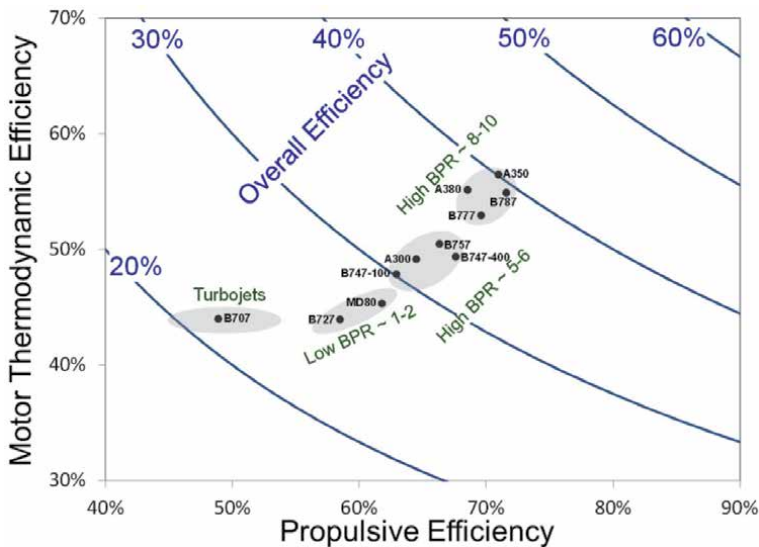


**Figure 2.** Commercial aircraft gas turbine engine efficiency trend BPR, bypass ratio. Reproduced with the permission of United Technologies Corporation, Pratt & Whitney [2, 3].

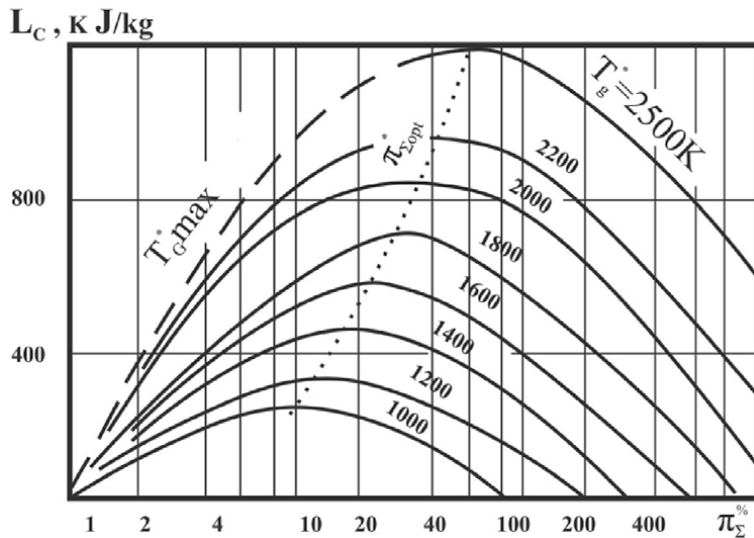


**Figure 3.**  
 Dependence of the cycle  $L_C$  from  $\pi_{C\Sigma}^*$  if  $T_G^* = \text{var.}$  and  $T_H^* = \text{const.}$

**Figure 3** shows the dependence of the cycle  $L_C$  on the parameters of the working process of the direct reaction gas turbine engine. The graph shows that for a promising multi-mode bypass turbofan engine at  $\pi_{C\Sigma}^* = 28$  the turbine inlet temperature will be  $T_G^* \approx 1700$  K, while the degree of bypass is  $m \approx 0.57$ .

#### 4. Multi-mode aviation GTE of direct reaction

As a rule, aviation GTEs are designed for the maximum power mode, which provides the maximum parameters of the thermodynamic cycle and which are optimal. The geometry of the gas-turbine engine flow path also optimally corresponds to this mode and the parameters of the thermodynamic cycle. Other modes of GTE operation, which have their own optimal parameters of the thermodynamic cycle and which must correspond to their own geometry of the GTE flow path, are taken as compromises with the engine flow path unchanged. Engines of multipurpose supersonic aircraft differ from engines of subsonic aircraft in the requirement of multimode.

In a certain sense, any aircraft is multimode, but the most multimode is typical for military aircraft, the aircraft which must perform a wide range of varied tasks, which are characterized by a wide range of speeds and flight altitudes. Thus, the fighter's engine must provide high thrust when accelerating and intercepting supersonic targets at high altitudes and when conducting air combat at medium altitudes in a wide range of aircraft flight speeds, as well as having high efficiency when flying at subsonic speeds at high altitudes and near the ground. Since each flight mode of an aircraft is characterized by its own optimal parameters of the thermodynamic cycle, compromise decisions are made in the design of the engine and its control systems.

The provision of supersonic flight in non-afterburner mode is especially acute for engines of military multipurpose aircraft. Provision of supersonic cruise flight in non-afterburner mode requires the creation of a large thrust from the engine. One of the ways to solve this problem is to increase the turbine inlet temperature ( $T_G^*$ ), in the future to stoichiometric. The result of analyzing the main flight modes of a

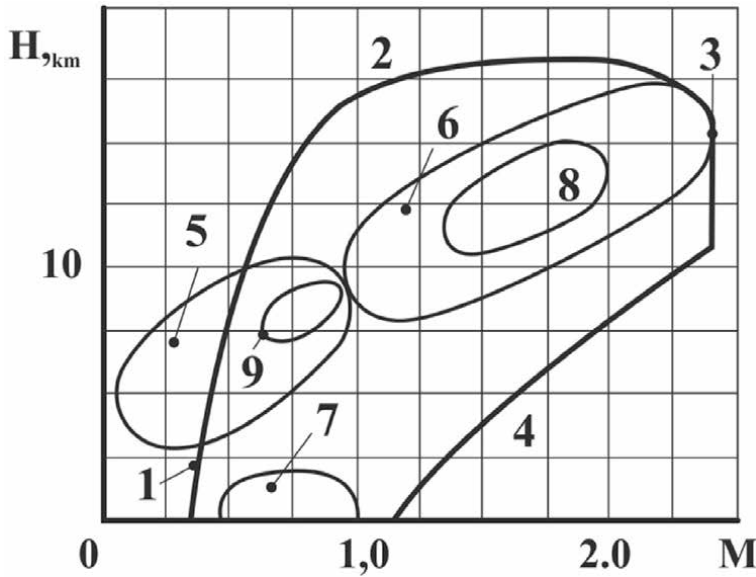


**Figure 4.** Areas of the main flight modes of a multi-mode aircraft: 1- on the bearing properties of the wing, 2- on the thrust capabilities of the engine (static ceiling), 3- on kinetic heating, 4- on the strength of the aircraft (high-speed head); flight modes: 5- subsonic maneuverable combat, 6- interception, 7- attacks of ground targets, 8- supersonic cruising flight, 9- subsonic cruising flight.

multi-mode aircraft [4, 5] is represented in **Figure 4**, it shows the areas of the main flight modes of a multipurpose aircraft.

The engines of multi-mode aircraft have high values of the parameters of the working process. This is due to gaining an advantage over a potential enemy. Engines of civil aircraft with high parameters of the working process have an advantage in the combat, because their efficiency will be better. It becomes important to create aviation gas turbine engines that work effectively in all flight modes of aircraft, i.e. adapt the engine to the appropriate operating mode. The higher the thrust-to-weight ratio of the aircraft, the more it is necessary to throttle the engine in cruise mode, especially for stoichiometric engines.

When the engine is throttled, its internal efficiency decreases sharply due to a strong decline  $\pi_{C\Sigma}^*$  when decreasing  $T_G^*$ . This leads to a decrease of  $L_C$  at this engine operating mode.

To increase  $L_C$  at throttle modes (non-design modes of GTE operation), as can be seen from formula (1), it is necessary to increase the efficiency of compression ( $\eta_C$ ) and efficiency enlargement ( $\eta_e$ ) of the thermodynamic cycle.

## 5. The main directions of increasing the efficiency of GTE of direct reaction in non-design (throttle) modes

Increasing the efficiency of the GTE of direct reaction in off-design modes is achieved by regulating the elements of its flow path. To increase the efficiency of compression ( $\eta_C$ ) in non-design modes, regulation elements are used:

- air intake device for supersonic aircraft;
- rotation of the engine fan blades with a high bypass ratio;

- rotation of the guide vanes of the compressors of individual stages or a group of stages;
- the use of a bypass GTE scheme, which makes it possible to redistribute the air flow between the gas generator by the second or third circuits (regulation of the degree of bypass ( $m$ ));
- the use of two or three compressor stages in the design of a gas turbine engine, while there is a spontaneous change in the rotational speed of individual stages;
- the use of a slotted air bypass above the rotor blades of the first compressor stages;
- regulation of the radial clearance in the last stages of the compressor;
- bypassing air from individual sections of the compressor flow path to the atmosphere, the second circuit, or into any section of the gas-air duct with reduced pressure (as a rule, it is not used in advanced engines).

A characteristic feature of promising aircraft gas turbine engines is the use of complex schemes with high parameters of the working process, in which several methods of compressor control are used. To increase the efficiency enlargement ( $\eta_e$ ) the following regulation elements are applied:

- regulation of gas turbines GTE by turning the nozzle apparatus;
- regulation of radial clearances of working blades of gas turbines;
- regulation of mixing chambers (for gas turbine engines with mixing flows);
- regulation of output devices.

It should be noted that in modern and promising gas-turbine engines, the regulation of the flow path occurs in a complex manner according to regulation programs, depending on the properties of the joint operation of the elements of the flow path of the aviation GTE. At the same time, the greatest effect of obtaining high values of efficiency of compression and expansion processes at non-design modes of GTE operation is observed.

## **6. Influence of the GTE operating mode on the energy characteristics of the fuel**

The source of thermal energy for the implementation of the thermodynamic cycle of aviation GTE is aviation fuel. In connection with the aforesaid, there is an acute issue of the efficiency of fuel use, reduction of its consumption while obtaining the maximum possible thermal energy. The main aviation fuel, today, for jet aviation is aviation kerosene, obtained from oil. Despite the development of alternative fuels, aviation kerosene will remain the main fuel for jet aircraft in the near future. The most common brands of aviation kerosene used in civil and military aviation, and their main characteristics, are presented in the source [6, 7].

An important parameter characterizing the energy capabilities of fuel for a multi-mode GTE is the fuel heat output. Heating capacity characterizes the energy capabilities of the fuel-air mixture, taking into account the efficiency of the

organization of the working process in the engine combustion chamber. Fuel heating capacity ( $Q_t$ ) is determined from the relation (3):

$$Q_t = \frac{H_u \eta_g}{1 + \alpha_{cc} L_0}, \quad (3)$$

where:

$Q_t$  – heating capacity (lowest), kJ/kg;

$H_u$  – lower calorific value, kJ/kg;

$L_0$  – stoichiometric coefficient, kg air/kg fuel;

$\eta_g$  – fuel combustion efficiency;

$\alpha_{cc}$  – excess air ratio in the combustion chamber.

From formula (3) it follows that the fuel heat output depends on the operating mode of the gas turbine engine.

Thus in non-design modes  $\alpha_{cc}$  will take on larger values than in the design mode of operation of the GTE, then the heat output of the fuel in these modes will decrease. This will lead to an increase in fuel consumption in these engine operating modes.

The results of previous research in the field of changes in  $\alpha_{cc}$  can be represented in the following way in **Figure 5**. It shows the range of variation of the excess air ratio in the combustion chamber of a turbojet engine of a maneuverable aircraft. For a turbofan engine the excess air ratio will vary in a smaller range. This is due to the fact that part of the air will be bypassed into the second circuit, bypassing the gas generator (first circuit).

A typical change in the excess air ratio can be shown schematically in the following form in **Figure 6**. It shows a typical change in the excess air ratio in the combustion chamber when changing the operating mode of the gas turbine engine. Point 2 corresponds to the maximum operating mode of the engine (design mode), point 1 corresponds to the operating mode of the minimum power, which is

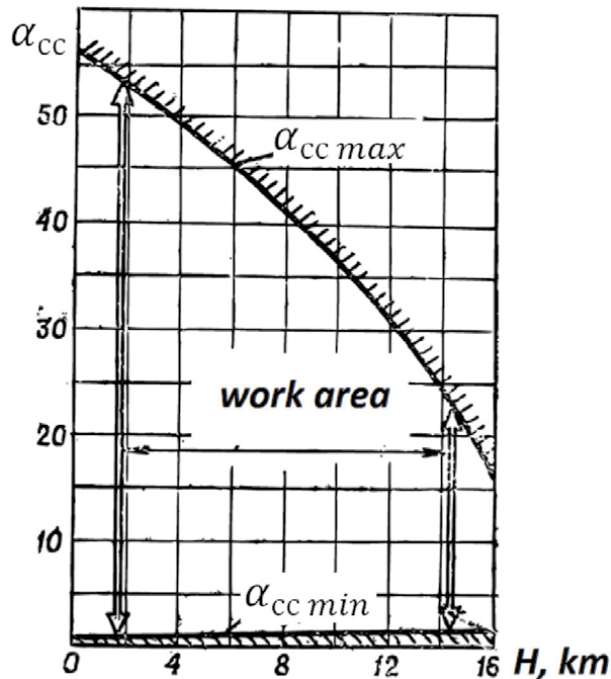


**Figure 5.**  
Range of  $\alpha_{cc}$  variation in GTE multi-mode (maneuverable) aircraft.

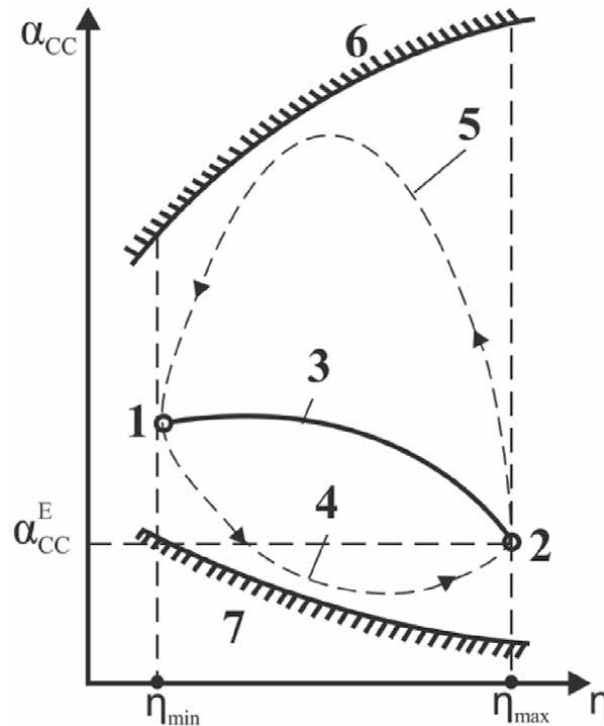


**Figure 6.**  
 Typical change in excess air ratio  $\alpha_{cc}$  in the combustion chamber of a gas turbine engine when changing its operating mode.

characterized by increased values of the excess air factor in the engine compressor, 3- steady-state modes of GTE operation, 4- throttle response, 5- gas discharge, 6- lean flameout in the combustion chamber, 7- rich flameout in the combustion chamber,  $\alpha_{cc}^E$  – the calculated value of the excess air ratio in the combustion chamber.

As it can be seen from **Figure 6**, a change in the operation of a gas turbine engine leads to a strong change in the excess air ratio in the combustion chamber, which greatly affects the efficiency of fuel combustion efficiency ( $\eta_g$ ) this also reduces the heat output of the fuel ( $Q_t$ ), which, accordingly, reduces the coefficient of the GTE thermodynamic cycle  $\eta_{int}$ , and in the end full efficiency of the engine ( $\eta_{\Sigma}$ ) decreases. This situation is typical for any direct reaction aircraft GTE, and the parameter values depend on the specific engine and its purpose.

At the design operating mode of the GTE (maximum power mode),  $\alpha_{cc} = 2.0-2.5$ ,  $\eta_g = 0.98-0.99$ , which corresponds to the modern level of development of aviation gas turbine engines, the heat output of aviation kerosene is 1103–1385 kJ/kg - design modes, fuel heating capacity ( $Q_t$ ) less than 500 kJ/kg.

For promising high-temperature (stoichiometric) aviation GTEs in the design mode (maximum power mode),  $\alpha_{cc} = 1.0$ ,  $\eta_g = 0.99$ , the heating capacity will be approximately 2682 kJ/kg. Thus, the multimodality of aviation GTE significantly determines the efficiency of fuel use in an engine. As noted earlier, each mode of operation of aviation GTE also corresponds to its own optimal parameters of the thermodynamic cycle, which are characterized by the effective operation of the engine in this mode. Therefore, it is important to ensure optimal and efficient use of fuel in all modes of GTE operation to obtain these parameters, taking into account that the geometry of the engine is optimally designed for efficient operation only at

the maximum power mode. Fuel properties play one of the key functions in the formation of the technical appearance of an aviation GTE and its design.

Flight technical and operational characteristics of an aircraft to the greatest extent depend on such fuel properties as density ( $\rho$ ), and heat of combustion ( $H_u$ ). Influence of the type of fuel on the working process and the main parameters of the GTE, thrust ( $R$ ) and specific fuel consumption ( $C_R$ ), is (mainly) due to the calorific value of the fuel and the thermophysical properties of combustion products with air. Maximum possible theoretical turbine inlet temperature ( $T_G^*$ ) (in the first approximation) for aviation kerosene can be determined by the relation (from the basic course in the aviation engine technology):

$$T_{Gmax}^* = T_C^* + \frac{H_u \eta_g}{\alpha_{cc} L_0 C_p}. \quad (4)$$

From the Eq. (4) it follows that  $T_{Gmax}^*$  generally depends on  $T_C^*$ , excess air ratio in the combustion chamber ( $\alpha_{cc}$ ) and the relation  $H_u/L_0$ . By increasing  $\alpha_{cc}$  the temperature  $T_{Gmax}^*$  decreases.

As follows from **Figure 7**, the maximum gas temperature ( $T_{Gmax}^*$ ) is achieved at  $\alpha_{cc} = 1.0$ , thus, at the stoichiometric value. The range of maximum value of  $T_G^*$  is very narrow and by increasing  $\alpha_{cc}$ ,  $T_{Gmax}^*$  will decrease rapidly. This leads to a decrease in the possibilities of full use of the energy potential of the fuel, and in some cases it can lead to the impossibility of the combustion process.

**Figure 8** shows a typical characteristic of the combustion chamber from which it follows that in the entire range of variation of the excess air coefficient in the combustion chamber ( $\alpha_{cc}$ ) there is a single value  $\alpha_{cc}^E$  at which the combustion

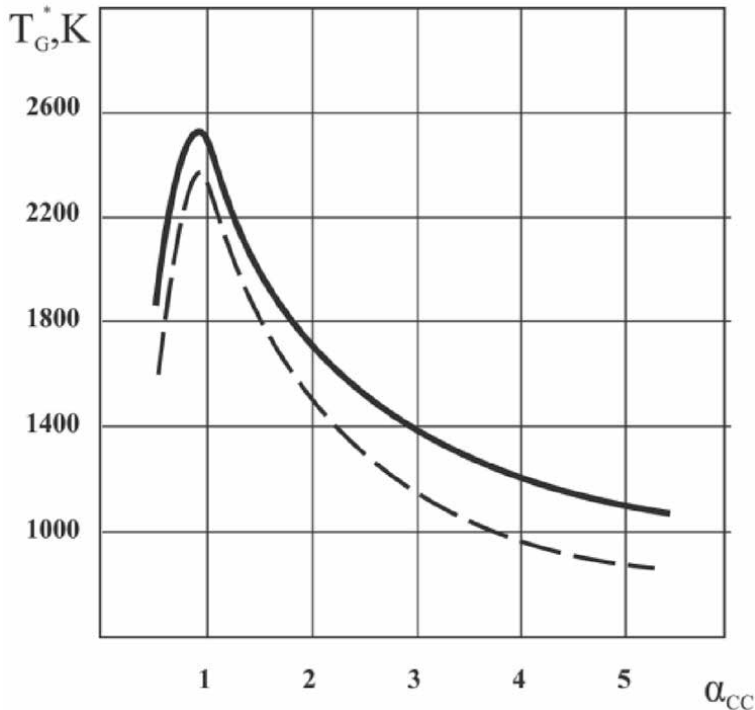


**Figure 7.** Calculated dependence of the temperature of fuel oil combustion products on the excess air ratio: — at  $T_C^* = 600$  K; - - -  $T_C^* = 300$  K.



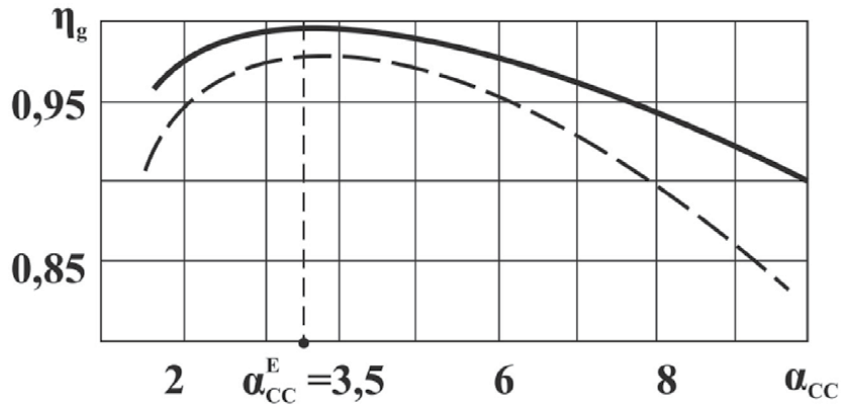


**Figure 8.** Typical characteristic of the combustion chamber is represented in the following way: The dependence of the fuel combustion efficiency ( $\eta_g$ ) from the excess air ratio in the combustion chamber ( $\alpha_{CC}$ ). The calculated excess air ratio for a given combustion chamber is  $\alpha_{CC}^E = 3,5$ , —————  $T_{Cmax}^*$ , - - - -  $T_{Cmin}^*$ .

efficiency ( $\eta_g$ ) has a maximum value. This is true for all combustion chambers of a conventional GTE.

Thus, it follows from the above analysis that the maximum energy characteristics of jet fuel can be obtained in a very narrow range of operation of traditional (non-regulated) combustion chambers. And the optimal operating mode of the compressor station at which the maximum heat release occurs corresponds only to a single value of the excess air coefficient ( $\alpha_{CC}^E$ ) in the combustion chamber and it corresponds to the calculated (maximum) value of the engine operating mode.

To evaluate the operation of the compressor station with control elements in the multi-mode GTE system, we introduce the coefficient of fuel heat output ( $q_t$ ) (5):

$$q_t = \frac{Q_{ti}}{Q_{tr}}, \quad (5)$$

where:

$Q_{ti}$  - fuel heating capacity at the  $i$ -th mode of GTE operation;

$Q_{tr}$  - heating capacity of fuel at the design (maximum) mode of operation of the GTE.

The coefficient of fuel heat output shows the use of the thermal capabilities of the fuel depending on the operating mode of the GTE. Each mode of GTE operation corresponds to its own excess air ratio in the combustion chamber ( $\alpha_{CCi}$ ). For high-temperature (stoichiometric) combustors with elements for regulating the geometric dimensions and composition of the mixture in the combustion zone, the coefficient of heat output shows their technical perfection, i.e. obtaining the maximum possible heating capacity of the fuel in throttle (non-design) modes of the GTE.

The above analysis shows that, aviation kerosene still has a sufficient reserve for the implementation of high thermodynamic characteristics for promising GTEs for the near future. However, in order to realize the great thermodynamic capabilities of fuel in a multi-mode GTE, a new approach to the development of promising GTEs is required.

## 7. The principles of adaptation of a promising multi-mode GTE

The essence of the approach for realizing the large thermodynamic capabilities of the GTE should be based on the fact that each operating mode of the engine

should be optimal (calculated). This means that the gas path of the GTE and the engine automatics must correspond to obtaining the maximum engine characteristics in these modes. In other words, the gas path of the GTE and the automatic engine control system must adjust (adapt) to each operating mode of the engine in order to increase the work of the thermodynamic cycle in these modes, i.e. increase in total efficiency of GTE.

Adaptation refers to the ability of technical devices or systems to adapt to changing environmental conditions or to their internal changes, which leads to an increase in the efficiency of their functioning. For promising aircraft gas turbine engines, this is expressed in the application of regulation of the elements of its flow path, depending on the mode of its operation, as well as the use of an adaptive control system for its operation. The means of adaptation are the adjustable elements of the GTE flow path (part 5) and the engine control system. Continuous increasing requirements for the flight performance of maneuverable aircraft necessitate continuous improvement of the characteristics of the aviation GTE. As already noted, the improvement of the characteristics of the aviation GTE goes along two” soft “directions.

The first is the complication of the schematic diagrams of aviation GTEs, with the simultaneous implementation of regulation of the elements of its flow path, in accordance with the operating mode of the engine, that is, the use of its adaptation.

The second is to increase the parameters of the GTE working process, the turbine inlet temperature ( $T_G^*$ ) and the degree of compressor delivery pressure ( $\pi_C^*$ ).

Moreover, in these areas of development of aviation GTE, the adaptation process is widely used in order to obtain high performance in all modes of GTE operation.

If the adaptation of promising aircraft GTEs is carried out mainly by adjusting the elements of the flow path of the engine, as is customary, according to rigidly specified programs, depending on the operating mode, then it is clear that automatic control according to a given rigid program does not implement extensive adaptation and automation capabilities. In other words, there is a shortage of potential capabilities of the characteristics of the GTE, from this it follows that the evolution of the means of adaptation of the GTE comes into conflict with the control methods.

The operational ranges of changes in the characteristics of promising multi-mode aircraft are so wide that the control of the GTE without adaptation means becomes more and more difficult.

The rigidity of the program for regulating the elements of the GTE reduces the achievable effect of automation of maintaining the constraints. With tough regulation programs, the engine does not pick up its potential capabilities, i.e. its potential for gas-dynamic stability in the area of possible operation is not fully used.

The contradictions between the completeness of using the capabilities of the GTE and its limitations can be resolved only on the basis of the use of adaptive multi-parameter control systems with the simultaneous development of regulation of the elements of the GTE flow path in accordance with the mode of its operation, i.e. engine adaptation.

## 8. The application of adaptive approach in complicating the concept of aviation GTEs

**Figure 9** shows a hypothetical adaptive GTE with control elements for its flow part, where: 1-rotary guide vanes of the fan; 2- air bypass into the second circuit; 3-rotary guide vanes of the compressor; 4-adjustable radial clearances in the last

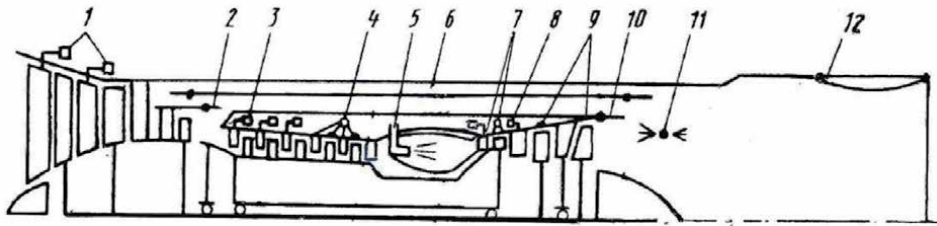


**Figure 9.** Hypothetical adaptive GTE: Source [8, 9] provides information about the Adaptive Versatile Engine Technology (ADVENT) program, which later switched to the Adaptive Engine Technology Development (AETD) program, which provides for the creation of a new type of aviation GTE for aircraft of the 5th and 6th generation.

stages of the compressor; 5-fuel supply to the adaptive combustion chamber; 6-adjustable third circuit; 7- adjustment of the compressor turbine (rotary blades of the nozzle apparatus and adjustable radial clearance of the impeller); 8-rotary blades of the nozzle apparatus of the fan turbine; 9-adjustable radial clearances of the fan turbine; 10- adjustable mixing chamber; 11-fuel supply to the afterburner; 12-adjustable nozzle.

The overall goal of the programs is to create a promising GTE, which consumes 25% less fuel, creates 10–20% more traction than existing GTEs.

Such a significant improvement in the parameters is achieved due to the complexity of the concept of a GTE and the use of various adaptation mechanisms.

The bypass turbofan engine provides for the availability of an adjustable third circuit (**Figure 9**, item 6), which is included in the operation only in the cruise (economic) flight mode, while significantly increasing the overall bypass ratio ( $m$ ).

At high and maximum power modes, the circuit switches to low bypass levels, which allow increasing the traction characteristics of the engine in these modes.

Analyzing changes in specific thrust ( $R_S$ ) and specific fuel consumption ( $C_R$ ) depending on the bypass ratio, we calculate (from the basic aviation engine technology theory) (6):

$$C_R = \frac{3600 * Q_1}{(1 + m) * \eta_g * H_u * R_S}, \quad (6)$$

where:

$m$  – bypass ratio;

$Q_1$  – the amount of heat supplied to the primary circuit (core engine circuit);

$\eta_g$  – fuel combustion efficiency;

$H_u$  – thermal conductivity of fuel;

$R_S$  – engine specific thrust.

$$R_S = \sqrt{\frac{2 * L_{C1}}{1 + m} + V^2} - V, \quad (7)$$

where:

$L_{C1}$  – inner loop operation;

$V$  – flight speed;

$M$  – bypass ratio.

Eqs. (6) and (7) show that an increase in the bypass ratio ( $m$ ) in the cruise aircraft flight modes leads to a decrease in specific fuel consumption ( $C_R$ ), while a decrease in the bypass ratio at the maximum power modes leads to an increase in specific thrust ( $R_S$ ).

This example also shows that the use of an adaptive approach to increasing the complexity of the schematics of an aircraft GTE provides a significant boost to improving the performance of promising engines.

## 9. Increasing the parameters of the GTE workflow using the adaptation approach of high-temperature main combustion chamber

The above mentioned graph also shows that, to ensure the possibility of a stable and efficient operation of high-temperature stoichiometric combustion chamber (CC) and  $T^*_G = 2000\text{--}2200\text{ K}$  in a multi-mode GTE, it is necessary to use elements of the control of the combustion chamber (from the previous information analysis).

In [6] various methods of regulating the main CC of a multimode GTE are described. Although these methods of regulating the main CC were mainly aimed at obtaining better characteristics for the emission of pollutants, they can also be used to improve the characteristics of the high-temperature main CC.

Adjustment in the main CC is aimed at maintaining the specified composition of the fuel-air mixture in the combustion zone. Maintaining the required composition of the mixture in the CC can be facilitated by the supply of fuel, distributing it to the combustion zones. Several combustion zones are created that operate on the corresponding GTE operation modes. **Figure 10** shows the sample CC by the [6, 7] with two zones of combustion chamber areas. The main drawback of such burning is the inefficient use of the volume of the CC. In some modes of operation, the GTE of the zone type uses only half of its working volume.

Another way to maintain a given composition of the mixture in the CC is the redistribution of air entering the CC, depending on the mode of operation of the GTE. Air is distributed by using, for example, an adjustable front device. **Figure 11** shows CC with an adjustable head.

By means of changing the flow area of the holes in the flame tube, it is possible to vary the air supply to the combustion zone in various combinations to maintain a given  $\alpha_{CC}$  [7].

Currently, the adjustability of the elements of the CC is sufficiently broadly developed.

Various adjustable nozzles, swirlers with adjustable blade installation angle and a change in the cross-sectional area, heads with preliminary organization of the air mixture fuel and control of its supply, adjustment of the CC volume with redistribution of air throughout the flame tube, etc., may be applied [10].

Based on the above, it is possible to schematically present a hypothetical high-temperature CC for a multi-mode perspective GTE. **Figure 12** shows a hypothetical

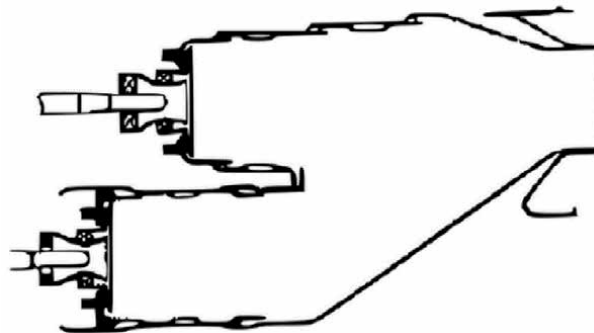


**Figure 10.**  
Double zone CC [6, 7].

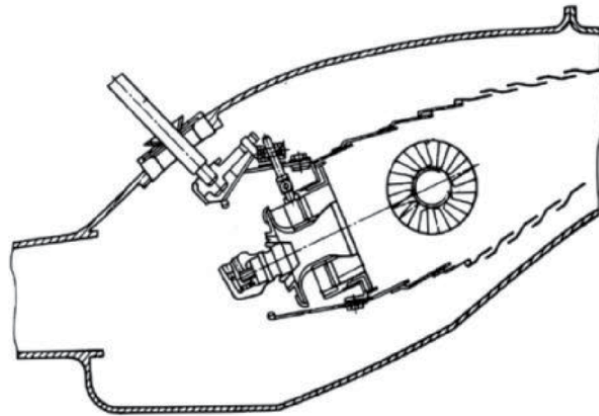


**Figure 11.**  
 The possible CC scheme with an adjustable head.

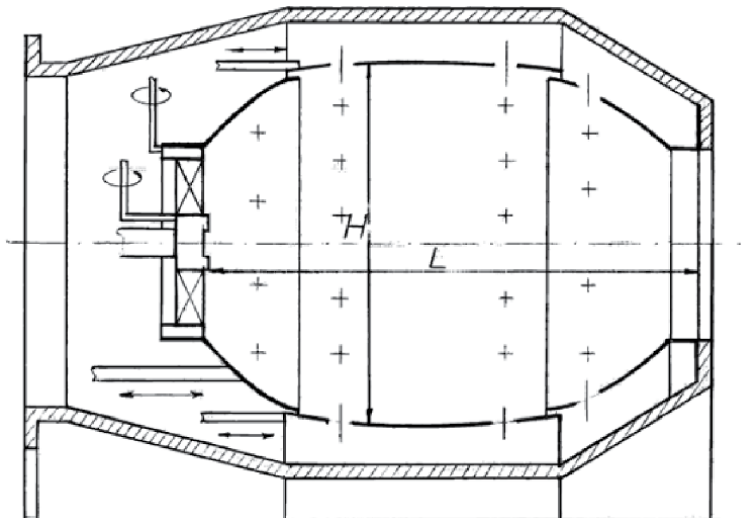


**Figure 12.**  
 Diagram of a hypothetical adaptive type combustion chamber (ATCC).

high-temperature CC with workflow control element or adaptive type CC (ATCC). A combustion chamber in which elements of adjustable geometric dimensions are used in accordance with the operation mode of the GTE, as a rule, the volume of CC and, accordingly, redistribution of air supply to the combustion and mixing zone, is called an adaptive type CC (ATCC).

An obstacle for use of effective control of multi-mode CC of the GTE is the design complexity of the controlled CC, high-temperature GTE operation modes and limitations in the level of development of modern materials science and technology.

The application of adjustability in a high-temperature ATCC is aimed at maintaining a given  $\alpha_{CC}$ , at which the combustion chamber operates quite efficiently, with a high fuel combustion efficiency ( $\eta_g$ ) and a high coefficient of fuel heat output ( $q_t$ ) (4) which also leads to the expansion of its range of stable operation.

**Table 2** shows the adjustable parameters, control actions and the achievable control goals for a hypothetical ATCC multi-mode GTE. The implementation of the ATCC control is an adaptive control system.

No	Adjustable parameter	Designation	Control action	The purpose of regulating GTE modes
1.	Air supply to the fuel injector	$F_{IA}$	The area of the orifices of the air flow through the nozzle	Coordination of the spray angle of the geometry of the CC
2.	Spinning the air in the head	$\varphi_S$	Swirl blade installation angle	Coordination of the sizes of the zone of processing currents of the geometry of the CC
3.	Air flow through the head	$F_S$	The area of the orifices of the flow sections of the air supply through the swirler	Maintaining a given $\alpha_{CC}$ in the primary combustion zone
4.	Changing the geometric dimensions of the CC	$V_C$	The volume of the flame tube CC (change in length- L and height - H)	Coordination of the volume of the flame tube CC and its dimensions to the mode of operation of the GTE
5.	Supply of secondary air flow along the length of the CC	$F_{SA}$	The area of the orifices of the flow areas of the secondary air supply to the flame tube	The distribution of the secondary air supply throughout the volume of the CC to maintain a given $\alpha_{CC}$
6.	Fuel supply to the CC	$G_{FJ}$	Adjustable fuel supply through the nozzle	Specified fuel supply, depending on the mode of operation of the GTE

**Table 2.**  
The adjustable parameters, the control actions and the achieved adjustment objectives for the hypothetical ATCC of multimode GTE.

An adaptive control system for a high-temperature CC of a multi-mode GTE can be implemented in two directions:

First - an adaptive choice of options, as the simplest [11].

Second - a self-adjusting adaptive system, as a more complex [12].

Adjustment by the method of adaptive choice of options is a choice of control actions (variant of the CC) under conditions of a priori uncertainty.

In this direction, the ATCC has several fixed positions of all control actions distributed over the GTE operation modes. Where for each range of GTE operation mode there is “its own” version of the CC, which in these conditions realizes the best performance. Each variant of the CC corresponds to a fixed position of the control action. In this way (8):

$$\alpha_{CCi} = f(G_{FJi}; F_{IAi}; \varphi_{Si}; F_{Si}; V_{Ci}; F_{SAi}). \quad (8)$$

Graphically the characterization of the relative fuel combustion efficiency  $\bar{\eta}_g = \eta_g / \eta_{g \max}$  (where  $\eta_g$  – current fuel combustion efficiency,  $\eta_{g \max}$  – maximum fuel combustion efficiency) depending on the  $\alpha_{CC}$  for ATCC with an adaptive choice of options can be represented in the following form in **Figure 13**  $\bar{\eta}_g = f(\alpha_{CC})$ .

The generalized characteristic of the ATCC is the curve of the peaks of the options. Thus, given the formula (7) we get (9):

$$\bar{\eta}_g = f\left(\sum_{i=1}^n \alpha_{CCi}^E\right). \quad (9)$$

When using the self-regulated adaptive system ATCC, the rule for determining the control actions changes in the course of GTE operation. In this case, the adaptive

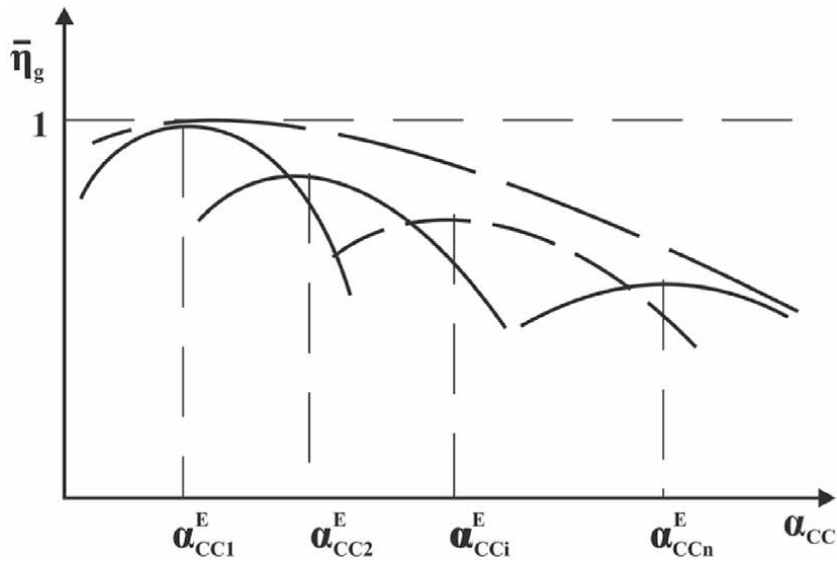


**Figure 13.**  
 Graphical characteristic of the ATCC with an adaptive choice of options.

control algorithm will be a combination of adjustment and adaptation algorithms. The adaptive control system will be a dynamic system consisting of an ATCC and a device implementing an adaptive control algorithm, with the control algorithm to be determined over the entire range of operation of a multimode GTE. In this case, the ATCC characteristic will appear as follows, see **Figure 14**.

In this way:

$$\bar{\eta}_g = f(\alpha_{CC}(\bar{u})), \quad (10)$$

where:

$\bar{u}$ – vector of control actions.

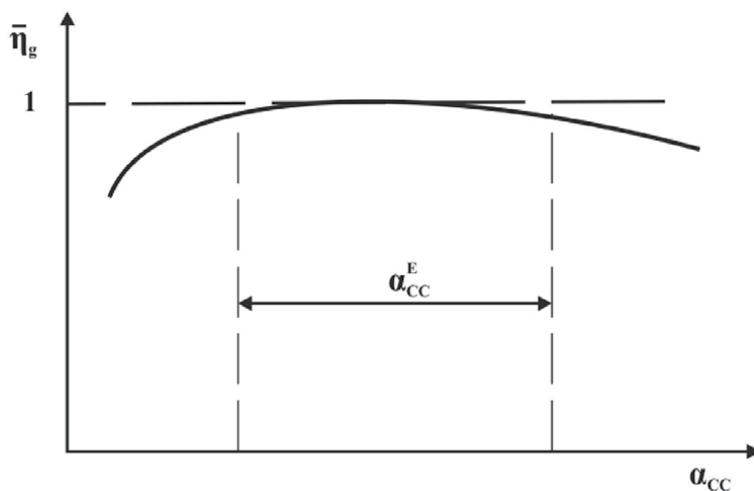


**Figure 14.**  
 The characteristic of the ATCC with a self-adjusted adaptive system of regulation, where  $\alpha_{CC}^E$  – The range of calculated modes of the excess air ratio in the combustion chamber for this method of controlling the organization of the combustion process.

It is necessary to clarify the definition of CC of the adaptive type (ATCC). Based on the above, the ATCC of a multi-mode GTE is a CC with a large number of control actions on the organization of the working process (developed control) and an adaptive control system.

**Figures 13 and 14** show that, the use of ATCC in a high-temperature multi-mode GTE will significantly reduce its specific fuel consumption  $C_R$  in all operating modes. Since an increase in the fuel combustion efficiency ( $\eta_g$ ) and the coefficient of thermal performance of fuel ( $q_t$ ) lead to a decrease of  $C_R$  (6). At the same time, the task of expanding the range of stable work is being solved.

## 10. Conclusions

To meet the requirements for promising aviation GTEs, it is necessary to increase the parameters of the thermodynamic cycle of the engine, while simultaneously applying complications of the GTE concept and its elements. This will make it possible to apply the principles of adaptation of the engine in non-design modes of operation, and to obtain the best characteristics of the GTE in these modes.

The use of adaptation principles in the development of future-generation aviation GTEs makes it possible to quite effectively resolve the contradictions of the possible obtaining of the best (optimal) characteristics under certain (calculated) conditions of GTE functioning and the impossibility of their implementation when these conditions change (non-design modes) in the range of permissible (or necessary) engine operating modes.

The use of an adaptive approach in the development of promising aviation GTEs will allow to take into account many uncertainties of the challenges of the future, which at the time of the start of work are not known or only assumed. This is due to the fact that the creation of an engine is characterized by a significant time interval within which various influencing factors can appear or change, and the adaptive approach takes into account the uncertainty and limited information of many influencing factors.

### List of the acronyms

$C_j$	nozzle flow rate
$C_p$	specific heat of heat supply at constant pressure
$C_R$	specific fuel consumption
$F_{IA}$	the area of the orifices of the air flow through the nozzle
$F_m$	the area of the mid-section of the engine
$F_S$	the area of the orifices of the flow sections of the air supply through the swirler
$F_{SA}$	the area of the orifices of the flow areas of the secondary air supply to the flame tube
$G_A$	air flow through the engine
$G_{A1}$	air flow through the gas generator
$G_{A2}$	air flow through the second engine circuit
$G_{AC}$	air flow rate entering the combustion chamber
$G_{ENG}$	engine mass
$G_F$	fuel flow rate entering the combustion chamber
$G_{Fj}$	adjustable fuel supply through the nozzle
$H_u$	lower calorific value of fuel
$L_o$	theoretically required amount of air for complete combustion of 1 kg of fuel



$L_C$	work of the thermodynamic cycle of the engine, which results in an increase in the kinetic energy of the exhaust gases, for a real cycle has the following form
$L_{C1}$	inner loop operation
$m$	bypass ratio
$\bar{m}$	coefficient taking into account the difference in the physical properties of air and gas
$P_A^*$	engine entrance pressure
$P_C^*$	pressure behind the compressor
$Q$	the actual amount of heat energy received during fuel combustion
$Q_0$	the amount of thermal energy introduced into the engine with fuel per 1 kg of working body
$Q_t$	fuel heating capacity
$Q_{ti}$	fuel heating capacity at the i-th mode of GTE operation
$Q_{tr}$	heating capacity of fuel at the design (maximum) mode of operation of the GTE
$Q_1$	the amount of heat supplied to the primary circuit (core engine circuit)
$q_t$	the coefficient of fuel heat output
$R$	engine thrust
$R_F$	frontal thrust
$R_C$	specific engine thrust
$R_{TO}$	engine thrust at takeoff
$T_C^*$	air temperature behind the compressor (at the inlet to the combustion chamber)
$T_G^*$	gas temperature in front of the turbine
$T_{Gmax}^*$	the maximum possible theoretical turbine inlet temperature
$T_H$	ambient air temperature
$\bar{u}$	vector of control actions
$V$	flight speed
$V_C$	the volume of the flame tube CC
$Y_{ENG}$	the specific gravity of the engine
$\alpha_{CC}$	air ratio of the combustion chamber
$\alpha_{cc}^E$	the calculated excess air ratio for a given combustion chamber
$\alpha_{CCi}^E$	the calculated excess air ratio for the current position of the control elements of the adaptive type combustion chamber
$\Delta$	working body heating degree
$\eta_e$	the efficiency of the expansion processes
$\eta_c$	the efficiency of the compression
$\eta_g$	the fuel combustion efficiency
$\eta_{int}$	internal coefficient efficiency of the GTE thermodynamic cycle
$\eta_{g \max}$	the maximum fuel combustion efficiency
$\eta_{tr}$	propulsive efficiency
$\eta_{\Sigma}$	the overall efficiency of the direct reaction GTE
$\bar{\eta}_g$	the relative fuel combustion efficiency
$\pi_C^*$	compressor pressure rise
$\pi_{C\Sigma}^*$	cumulative pressure rise in the engine
$\rho$	density
$\varphi_S$	swirl blade installation angle

## **Author details**

Viktors Gutakovskis<sup>1\*</sup> and Vladimirs Gudakovskis<sup>2</sup>


1 Riga Technical University (RTU), Riga, Latvia

2 Kaunas University of Applied Engineering and Sciences (KTK), Kaunas, Lithuania

\*Address all correspondence to: viktors.gutakovskis@rtu.lv

## **IntechOpen**

---

© 2021 The Author(s). Licensee IntechOpen. This chapter is distributed under the terms of the Creative Commons Attribution License (<http://creativecommons.org/licenses/by/3.0>), which permits unrestricted use, distribution, and reproduction in any medium, provided the original work is properly cited. 

## References

- [1] S. Farokhi, Aircraft Propulsion, John Wiley & Sons Ltd, 2014, 999 p.
- [2] Committee on Propulsion and Energy Systems to Reduce Commercial Aviation Carbon Emission Aeronautics and Space Engineering Board Division on Engineering and Physical Sciences THE NATIONAL ACADEMIES PRESS 500 Fifth Street, NW Washington, DC. 2001, 108 p.
- [3] A.H. Epstein, 2014, Aeropropulsion for commercial aviation in the twenty-first century and research directions needed, AIAA Journal 52(5):901–911
- [4] Leland M. Nicilai, Grant E. Caricher, Fundamentals of Aircraft and Airship Design Volume I — Aircraft Design, American Institute of Aeronautics and Astronautics Inc., 2017, 755 p.
- [5] Mario Asselin, An Introduction to Aircraft Performance, Royal Military College of Canada , 1997. 337 p.
- [6] Lefebvre A.H., Dilip R. Ballal. Gasturbine combustion: Alternative Fuels and Emissions. – 3rd Edition. – London: Taylor & Francis, 2010. 537 p.
- [7] A. K. Gupta, D. G. Lilley, and N. Syred, Swirl flows., Abacus Press, Tunbridge Wells, England, 1984, 475 p.
- [8] GE Adaptive Cycle Engine. Available from: <https://www.geaviation.com/military/engines/ge-adaptive-cycle-engine>.
- [9] D. Culley., S.Garg., and others, More Intelligent Gas Turbine Engines, ISBN 978–92–837-0080-7, 2009. 177 p.
- [10] Gudakovskis V., Kovalev V. A method for burning fuel in a gas turbine engine and a device for its implementation. Inv.S. No. 1378525, registered 11/01/1987 g.
- [11] Nazin A., Poznyak A., Responsive choice of options. Recurrent algorithms - M. Science 1986, 288 p.
- [12] Lozano R., Adaptive Control, Springer, 2012. 562.p.



# Graphical Analysis of Gasification Processes

*Shehzaad Kauchali*

## Abstract

Gasification processes incorporate many reactions that are fairly complex to analyse making their design difficult. In this chapter it is shown that general gasification systems are limited by consideration of mass and energy balances only. Here, a ternary Carbon-Hydrogen-Oxygen diagram is developed to represent gasification processes. The diagram incorporates basic chemistry and thermodynamics to define a region in which gasification occurs. The techniques are further validated from data obtained from pilot or laboratory experiments available in literature. In this chapter we develop graphical representation for sawdust gasification and underground coal gasification (UCG), a clean coal technology. The methods described allow for further analysis without considerations to thermodynamic equilibrium, reactor kinetics, reactor design and operation. This analysis is thus an indispensable tool for flowsheet development using gasification and an excellent tool for practitioners to rapidly understand gasification processes.

**Keywords:** gasification, biomass, sawdust, CHO-diagram, coal, UCG

## 1. Introduction

Biomass gasification processes produce a versatile fuel-gas using a thermochemical conversion of the biomass in a reducing environment in the presence of air, oxygen or steam. The resulting gas is cleaned and is generally suitable for heating, power generation or liquid fuel production. The important drivers towards biomass utilisation include renewable and sustainable energy sources, the Kyoto protocol addressing the need to lower carbon dioxide emissions and the CO<sub>2</sub>-neutrality of biomass emissions. However, it is argued that biomass conversion systems be as efficient as existing fossil fuel technologies [1]. It is stated that gasification is one of the least efficient processes in the biomass-to-energy value chain and a study on the gasifier alone can lead to substantial improvements [2].

Large amounts of literary work, including theoretical and experimental developments, on biomass gasification have been published [3–11].

The use of bond-equivalent percentages to study conversion of coal to other materials on a ternary Carbon-Hydrogen-Oxygen (CHO) diagram has been advocated by [12]. [13] have used a CHO diagram to determine the feasible operating region of a moving bed gasification reactor. In an important follow on work, by [14], it was shown that any coal gasification process can be constrained to a region, by stoichiometry, and further to a line or plane by energy considerations. Thus complex coal gasification reaction schemes can be interpreted readily before the consideration of thermodynamic equilibrium, kinetics, reactor design and

operation. This work forms the basis of the sawdust gasification analysis in this paper. Recently [15] use a graphical targeting approach, on the CHO diagram, to design a biomass gasification process for methanol production. This chapter seeks to provide design options for biomass gasification, on the CHO diagram, in order to evaluate theoretical limitations of the complex reacting systems. Moreover, these options are envisaged to assist in the design of new pilot-scale experiments or commercial operation of biomass and underground coal gasification systems.

There is a lack of coherent approaches to designing gasification processes. This is partly due to the fact that most approaches rely heavily on reactor types, where the information is proprietary and partly due to non-existence of fundamental explanations based on simple chemistry and thermodynamics. It is thus useful to develop a method that enables the understanding of gasification from basic principles. Lastly, and more importantly, it would be useful to empower a designer to suggest experimental validity, for given solid-feedstock, based on preliminary designs derived from the methods discussed in this chapter. This will invariably lead to honing into final designs quicker, with less experimental effort and cost.

The chapter is ordered according to the following: first the bond-equivalent CHO diagram is introduced, followed by the determination of the important gasification reactions and stoichiometric region for sawdust and underground coal gasification, followed by the determination of autothermal operation and the representation of experimental data on the CHO diagram.

## 2. Bond-equivalent CHO diagram

The bond-equivalent percentages, as introduced by [12], implement the bonding capability of each element in the CHO system. Bond-equivalent percentages spread data points uniformly in the CHO diagram, making analysis visually appealing, and this technique is used for the remainder of the discussions in this work.

### 2.1 Introduction to CHO diagram

The bond-equivalent CHO diagram is shown in **Figure 1**, below, where the apexes represent pure C, H and O as well as pure C, H<sub>2</sub> and O<sub>2</sub>. The other important permanent species that need to be represented are CO<sub>2</sub>, CO, H<sub>2</sub>, CH<sub>4</sub> and H<sub>2</sub>O [5]. For example, to obtain the bond equivalent fraction for a species C<sub>x</sub>H<sub>y</sub>O<sub>z</sub>, the contribution by carbon is 4(x), hydrogen is 1(y) and oxygen is 2(z), which is normalised for each species. Thus CH<sub>4</sub> is represented by C = 4/(4 + 4) and H = 4/(4 + 4) and places the point midway between C and H. Similarly CO<sub>2</sub> and H<sub>2</sub>O are midway between C-O and H-O respectively. CO is a third between C-O.

### 2.2 Representing chemical species and reactions

Chemical species, as individual or in a mixture (such as feed to a process), can thus be represented as single points on the CHO diagram. For example, a synthesis gas of composition 33.3% CO and 67.7% H<sub>2</sub> (CO:2H<sub>2</sub>) may be represented as a single COH<sub>4</sub> species and is plotted in **Figure 1**. Dry sawdust represented by CH<sub>1.35</sub>O<sub>0.617</sub> [16] is also shown.

A further property of the diagram is that reactions may be represented as intersections of two lines: one representing the reactants and, the other, products. For example, the line joining CH<sub>4</sub> to O<sub>2</sub> intersecting with the line joining CO and H<sub>2</sub> represents partial oxidation of methane to form H<sub>2</sub> and CO, in the ratio 2:1.

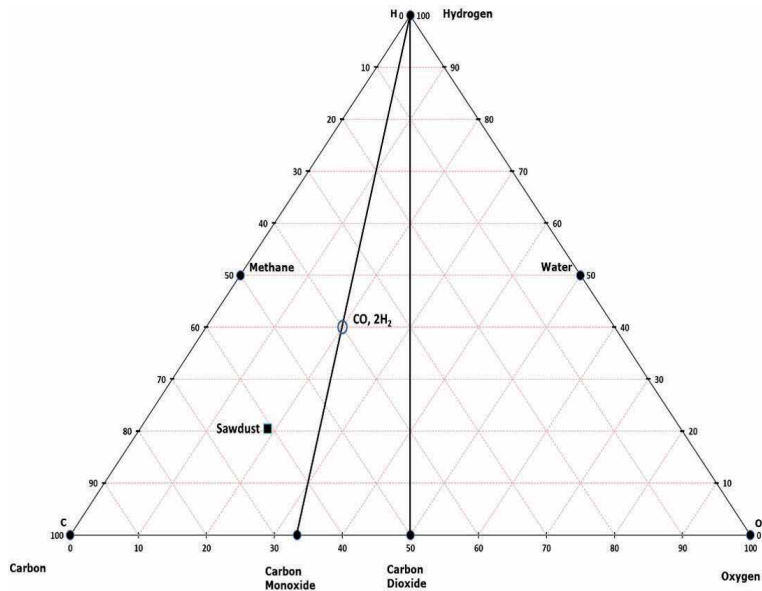


**Figure 1.**  
 Representation of chemical species on the bond equivalent CHO diagram.

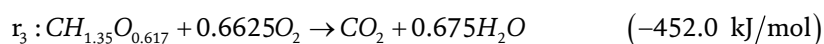
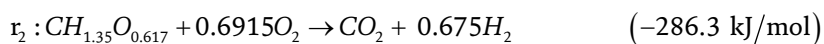
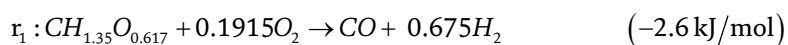
### 3. Stoichiometric region of operation for sawdust

The analysis performed here utilises dry sawdust with chemical formula  $CH_{1.35}O_{0.617}$  with HHV of 476 kJ/mol [16] and a calculated  $\Delta H$  of formation of  $-107.77$  kJ/mol. The nitrogen, sulphur and other elements (including ash) are considered inerts within the CHO diagram and are excluded from analysis. The theoretical development here seeks to determine the region in the CHO triangle where the gasification of sawdust is feasible and attractive energy-wise. Furthermore, the theoretical result will be compared with those from pilot scale experiments in a later section.

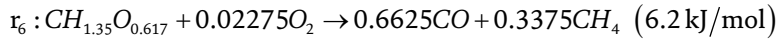
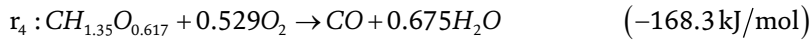
#### 3.1 Stoichiometric region of operation for sawdust

It is acknowledged that gasification reactions are complex comprising of numerous reactions occurring on solid surface or in gas phase. The gasification system considered here comprises of sawdust, steam and oxygen (or air with nitrogen as inert). In contrast, [14] considers a similar system with fixed carbon, steam and oxygen to represent a coal gasification system. Furthermore, a simplified set of reactions are provided that limit the product species from the list of permanent gases ( $CO$ ,  $CO_2$ ,  $H_2O$ ,  $CH_4$  &  $H_2$ ) that occur in appreciable amounts between 650 K–1500 K [5].

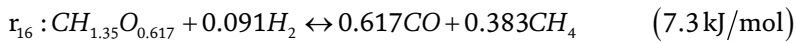
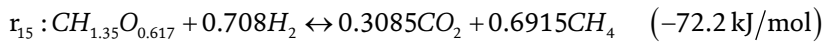
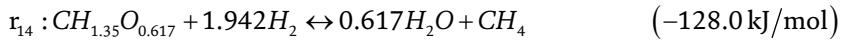
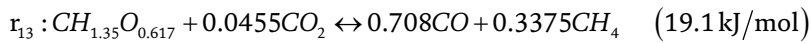
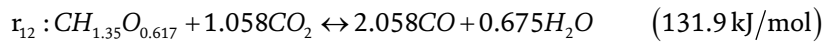
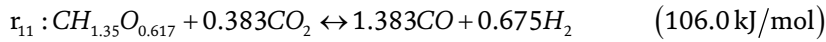
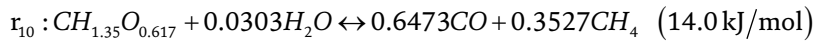
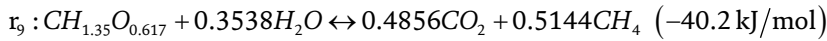
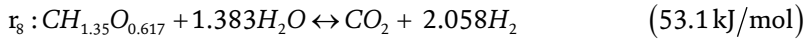
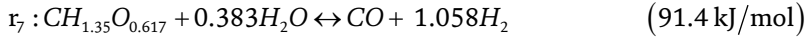
For the sawdust system, the following reactions at 650 K will thus be considered:  
 Combustion



## Gasification



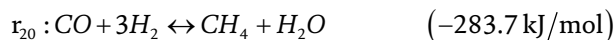
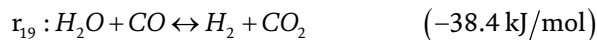
## Gasification



## Gas combustion



## Gas reactions



The reactions ( $r_1$ - $r_{16}$ ) are not chosen arbitrarily. The reactions are chosen on the basis that sawdust will react with a number of gases, some from feed (oxygen, steam) while others from primary products such as hydrogen or carbon dioxide.



### 3.2 Graphical representation of sawdust reactions

The reactions ( $r_1$ - $r_{16}$ ) are plotted on the CHO diagram in **Figure 2**. The dotted line represents combustion reactions and the dashed lines are gasification reactions. It is noted that there are no reactions with  $\text{CH}_4$  and biomass or CO and biomass as these lines ( $\text{CH}_4$ -sawdust & CO-sawdust) do not intersect with any other lines since they are on the extreme edges. There are other reaction schemes plausible that have not been included as they shall not form part of the important subset shown later.

#### 3.2.1 The non-negative basis reactions

From the reactions given above, some reactions are dependent on each other. Furthermore, the gasification system, and hence the analysis, requires only those reactions to form the basis reactions which are able to: 1) obtain other reactions by positive linear combinations, and 2) do not produce the original feed reactants, in particular  $\text{O}_2$ ,  $\text{H}_2\text{O}$  and C. The reader is directed to [14] for further clarity. The eight important basis reactions that satisfy the two conditions are given in **Table 1**.

A method for determining which reactions are part of the basis set can be described as follows: Firstly, connect all product species, excluding the ones that appear in the feed (steam and oxygen). Note, water-methane, water-carbon dioxide and water-carbon monoxide are thus also omitted. Secondly, connect the feed (sawdust) to the feed oxidants (steam and oxygen). The intersections that are formed (within the diagram – excluding edges) are the basis reactions where the connected points form the reactants and products respectively. Also note hydrogen is not forming part of the reactants in the basis reactions as it is not specified as a feed and thus is excluded.

Any sawdust gasification overall reaction can be obtained by positive linear combinations of the eight basis reactions in **Table 1**. This is translated graphically by implying that an interior point in the space (formed by the basis reactions) can be obtained by connecting any boundary points.

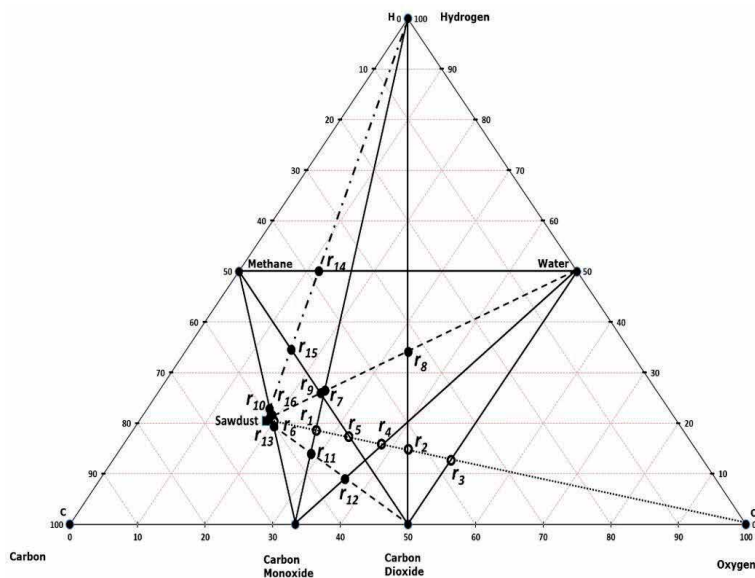


**Figure 2.**  
 Graphical representation of sawdust reactions.

**Table 1** summarises the important reactions between sawdust, oxygen and steam. Notice, the reactions also represent the line, which in turn, determine the reactants or products. This is shown in **Figure 3**. For example, a line representing the reactants (sawdust and oxygen) is obtained by connecting the sawdust point with the pure oxygen point. However, the products obtained from this reactant line (sawdust-oxygen) are dependent on which product line is intersected. The product line is one which contains two of the permanent gases listed previously. For illustration purposes, consider the two product lines obtained from H<sub>2</sub>-CO and H<sub>2</sub>-CO<sub>2</sub> – these are strictly products as none of them feature in the feed given. Finally, to obtain the reactions, say  $r_1$ , the intersection of the lines joining sawdust-oxygen and CO-H<sub>2</sub> are considered. In **Figure 3**, this intersection point is presented by point A. It also represents the bond equivalent point plotted for either the feed or product. The relevant stoichiometric values are then used to balance the reaction and are listed in **Table 1**. The process was thus repeated for all possible intersection points and a set of balanced reactions were obtained ( $r_1$ - $r_{16}$ ). Moreover, the heat of reactions were determined based on the balanced reactions. The values have been provided in brackets after every reaction. Whilst, the reactions are not meant to represent reaction sequence or mechanism they do provide for a macro representation of the possible outputs from a sawdust gasification system. This is useful when predictions of syngas composition is critical for design.

$r_1 : CH_{1.35}O_{0.617} + 0.1915O_2 \rightarrow CO + 0.675H_2$	(-2.6 kJ / mol)
$r_2 : CH_{1.35}O_{0.617} + 0.6915O_2 \rightarrow CO_2 + 0.675H_2$	(-286.3 kJ / mol)
$r_3 : CH_{1.35}O_{0.617} + 1.383H_2O \leftrightarrow CO_2 + 2.058H_2$	(53.1 kJ / mol)
$r_7 : CH_{1.35}O_{0.617} + 0.383H_2O \leftrightarrow CO + 1.058H_2$	(91.4 kJ / mol)
$r_5 : CH_{1.35}O_{0.617} + 0.354O_2 \rightarrow 0.6625CO_2 + 0.3375CH_4$	(-181.8 kJ / mol)
$r_6 : CH_{1.35}O_{0.617} + 0.02275O_2 \rightarrow 0.6625CO + 0.3375CH_4$	(6.2 kJ / mol)
$r_3 : CH_{1.35}O_{0.617} + 0.3538H_2O \leftrightarrow 0.4856CO_2 + 0.5144CH_4$	(-40.2 kJ / mol)
$r_{10} : CH_{1.35}O_{0.617} + 0.0303H_2O \leftrightarrow 0.6473CO + 0.3527CH_4$	(14.0 kJ / mol)

**Table 1.**  
Non-negative basis reactions for sawdust.

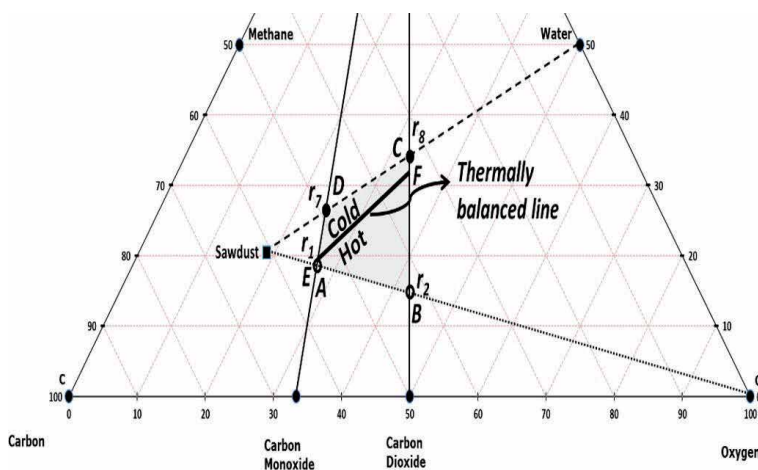


**Figure 3.**  
Stoichiometric region for sawdust without methane formation.

The heat of reactions listed with the various reactions are important as they provide the necessary energy for gasification processes to occur. It is noted that some heat of reactions are endothermic (positive) and some exothermic (negative). Of particular interest are the heat of reactions for  $r_6$ ,  $r_9$  and  $r_{10}$ .  $r_9$  depicts the exothermic nature of steam reaction producing syngas rich in  $\text{CO}_2$  and  $\text{CH}_4$  – this has not been reported elsewhere and is of commercial interest requiring low temperature (<400C) and perhaps even the use of catalysts.  $r_6$  and  $r_9$  both demonstrate the lowest amount of oxygen and steam required to gasify sawdust, to produce syngas rich in CO and  $\text{CH}_4$ , at high temperatures and non-catalytically.

The sawdust-oxygen intersection with the product lines were depicted in **Figure 2**. These are represented, in order from the sawdust point, by  $r_6$ ,  $r_1$ ,  $r_5$ ,  $r_4$ ,  $r_2$  and  $r_3$ . Of these points, it is noted that  $r_3$  and  $r_4$  do NOT form part of the basis reactions as one of the products (water) is already accounted for in the feed. This leaves only reactions that form either one of the products: CO,  $\text{CO}_2$ ,  $\text{H}_2$  and  $\text{CH}_4$ . The same analysis applied to sawdust-water intersections with the product lines requires that those reactions that produce only the products CO,  $\text{CO}_2$ ,  $\text{H}_2$  and  $\text{CH}_4$  are included.

For most gasification systems, the compositions of the syngas desired is dependent on the end use for the gas. For example for liquid chemicals production syngas rich in  $\text{H}_2$  and CO, with minimal  $\text{CH}_4$ , is required. The system can be designed for low methane production. When methane is not formed, then only the first four reactions (**Table 1** and region ABCD in **Figure 3**) will provide the possible products obtainable from the gasification system using sawdust, oxygen and steam. This fundamentally implies that any sensible gasification (conversion of sawdust to gas with significant calorific value/energy content) will occur inside the stoichiometric region ABCD. Operating outside of this region will result in material not converted in the gasification process and leave the gasifier unreacted – which is not a preferred mode of operation.

### 3.2.2 Stoichiometric regions without methane reactions

When methane reactions are excluded from the reactor product, such as required for liquid fuel or chemicals production, the basis reactions as from **Table 1**, form a region (ABCD) as shown in **Figure 3**, above. It is noted that these reactions, which form part of the extreme boundary, span all sensible gasification products within the region. Any interior point inside region ABCD can be obtained by linear combinations of reactions  $r_1$ ,  $r_2$ ,  $r_7$  and  $r_8$  where the final products will be a combination of  $\text{H}_2$ , CO and  $\text{CO}_2$  only. Moreover, the edges of the region comprise of oxygen (air) gasification processes, on the lower side (AB), and steam gasification (CD) on the top side of ABCD. Furthermore, these reactions are chosen on the initial premise that no product should contain any reactant, hence any reaction that forms steam (or oxygen) is automatically rejected. Also, operation of a gasification system to the left of AD implies that the feed contains more sawdust than steam and oxygen, which inherently implies that unreacted sawdust should be expected at the exit of the reactor. Similarly, operating to the right of BC implies that the feed contains more steam/oxygen which will leave the gasifier unreacted, implying non-optimal usage of steam/oxygen. It is in this context that it is implied that sensible gasification occurs within the region ABCD. The case where methane is formed is omitted from further interpretation and will form part of a future publication.

## 4. Autothermal operation

When gasifiers run under adiabatic conditions, without heat loss or added heat, the system balances the exothermic reactions with the endothermic reactions. In

$E: CH_{1.35}O_{0.617} + 0.186O_2 + 0.0107H_2O \rightarrow CO + 0.686H_2$	(0kJ / mol)
$F: CH_{1.35}O_{0.617} + 0.108O_2 + 1.17H_2O \rightarrow CO_2 + 1.84H_2$	(0kJ / mol)

**Table 2.**  
Thermally balanced basis reactions without methane formation.

**Figure 3**, the two exothermic reactions  $r_1$  and  $r_2$  can be used to balance the endothermic reactions  $r_7$  &  $r_8$ . Line EF forms the thermally balanced line and the product temperature equals the inlet temperature. The thermally balanced equations for reactions E and F are given in **Table 2** for the case where no methane forms.

When methane is not produced, any thermally balanced process can be obtained by the linear combination of the two thermally balanced basis reactions. In **Figure 3**, below line EF products emerge hotter, while above the line they are colder. Furthermore, point E is preferred under low  $H_2O/O_2$  ratios while F would be preferred for high  $H_2O/O_2$  ratios. According to [14] practical gasification processes occur below the thermally balanced line and on the hot side. The reason is a combination of compensation for heat losses as well as methanation in real gasification systems. Operating in the colder section is an indication of external heat sources used to drive the endothermic reactions. Section 6 looks at some experimental points for sawdust gasification in relation to the thermally balanced line EF.

### 5. Carbon boundary and contours of higher heating value

The work of [17] studied the effect of temperature and pressure on carbon formation in gasification systems. It was identified that it is common for carbon to partially gasify and, due to kinetic limitations, solid carbon does not achieve equilibrium. Furthermore, the carbon boundary, under thermodynamic limits, may be represented on the CHO diagram as isotherms at constant pressure. Two such isotherms have been depicted in **Figure 4** at 1000 K [7] and 733 K [5]. Operating a

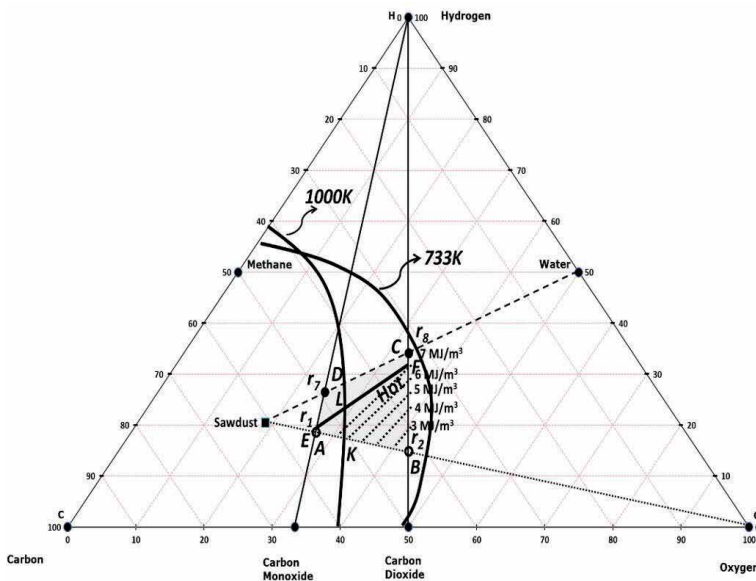


**Figure 4.**  
Carbon boundaries at 733 K and 1000 K with HHV contours.

gasification process within the carbon boundary indicates that there is a propensity for unreacted carbon to occur in the product stream.

This results in low carbon conversions with some carbon remaining in the ash. Moreover, it is desirable to operate in a carbon-free region. In **Figure 4**, it is evident that operating a process with feed within the stoichiometric region ABCD, at low temperatures (733 K), will invariably lead to carbon deposition. It is therefore important to determine the average maximum temperature achievable in the gasification system in order to assess the location of the carbon boundary. **Figure 4** also shows a carbon boundary for a system that operates at 1000 K. The presence of the high temperature carbon boundary further reduces the stoichiometric region in which it is desirable to operate a gasification system. For exothermic gasification, with 100% carbon conversion, it is favourable to operate in the region defined by KBFL (**Figure 4**). **Figure 4** also shows the calorific value (HHV) contours (3–7 MJ/m<sup>3</sup>) for the idealised stoichiometric region when only air (Nitrogen 79%) is used. These contours are useful when deciding on the targeted calorific value of the product syngas as well as air and steam requirements.

## 6. Representation of experimental points for sawdust gasification

**Tables 3–5** summarise some experimental data available for analysis on the CHO-diagram. It is notable to see that the fuels used have similar C,H and O content. In this analysis the chemical representation of [16] was used to determine

Reference	Comments	Gasifier type	Sawdust chemical formula (dry, ash-free)		
			C	H	O
Basu [16]	Basis for Heat of Reaction calculations		1	1.35	0.617
Li et al. [7]	Syngas data from Figure 15. 4 extreme points taken from set of 15 experimental runs. Average sawdust composition reported from 7 wood species	Circulating Fluidised Bed	1	1.55	0.597
Zainal et al. [10]	Calculated from modelled data in <b>Table 5</b> (Dry gas) including steam in product stream	Fixed Bed Downdraft	1	1.44	0.66
Li et al. [18]	Calculated from Figure 2a (S/B = 0.8) including steam in product stream	Circulating Fluidised Bed	1	1.46	0.75
Qin et al. [19]	Calculated from Figure 15 (1400C) including steam in product stream	Entrained Flow	1	1.53	0.66
Fletcher et al. [20]	CFD modelling of gasifier	Entrained Flow	1	1.68	0.6
Meng et al. [21]	Calculated from Figure 2 (S/B = 0.8 & 2.9) including steam in product stream. Representation of 8 experimental points	Bubbling Fluidised Bed	1	1.39	0.79

**Table 3.**  
*Sawdust characterisation and gasifier type used from literature.*

Reference	Mol composition (syngas)			Syngas composition (mol %)					
	C	H	O	H <sub>2</sub>	CO	CO <sub>2</sub>	CH <sub>4</sub>	H <sub>2</sub> O	C <sub>2</sub> H <sub>4</sub>
Basu [16]				—	—	—	—	—	—
Li et al. [7]	18.5	39.0	42.6	—	—	—	—	—	—
	24.6	29.8	45.6						
	21.0	39.6	39.5						
	24.8	36.4	38.8						
Zainal et al. [10]				31.9	30.5	18.2	0.2	19.2	—
Li et al. [18]				13.1	23.3	14.8	8.0	40.8	—
Qin et al. [19]				24.3	26.6	11.1	—	38.0	—
Fletcher et al. [20]				24.0	13.0	14.0	5.0	11.0	—
Meng et al. [21]				13.9	23.8	7.8	4.4	47.5	2.6
				9.9	9.3	5.4	1.9	72.7	0.8

**Table 4.**  
Syngas data from various experimental runs.

Reference	Bond equivalent composition (syngas)		
	C	H	O
Basu [16]	—	—	—
Li et al. [7]	0.38	0.22	0.40
	0.48	0.22	0.29
	0.41	0.19	0.39
	0.47	0.18	0.35
Zainal et al. [10]	0.42	0.22	0.36
Li et al. [18]	0.36	0.27	0.37
Qin et al. [19]	0.39	0.24	0.37
Fletcher et al. [20]	0.39	0.28	0.33
Meng et al. [21]	0.34	0.31	0.35
	0.16	0.41	0.43

**Table 5.**  
Bond equivalent composition for syngas from various experiments.

the heat of reaction for sawdust and used subsequently for all the other reactions in the respective calculations. It is also noted, that the experimental results have been performed in various types of gasifiers ranging from fixed bed, circulating, entrained flow reactors and even catalytic systems.

Sawdust gasification tests in a pilot-scale air blown circulating fluidized bed gasifier have been performed by [7]. 15 runs were performed with over 6 species of sawdust (with varying moisture content) at atmospheric pressure and temperature ranging from 700–815°C. With air as gasification medium, syngas contaminated with nitrogen was produced with dry gas heating values ranging from 2.43–4.82 MJ/m<sup>3</sup> (STP) and 3.59–6.13 MJ/m<sup>3</sup> (STP) if tar and light hydrocarbons are produced. A CHO diagram was used to analyse the experiments relative to the carbon boundaries with the conclusion that there are kinetic limitations restricting the full conversion of carbon. **Figure 5** depicts the collection of extreme

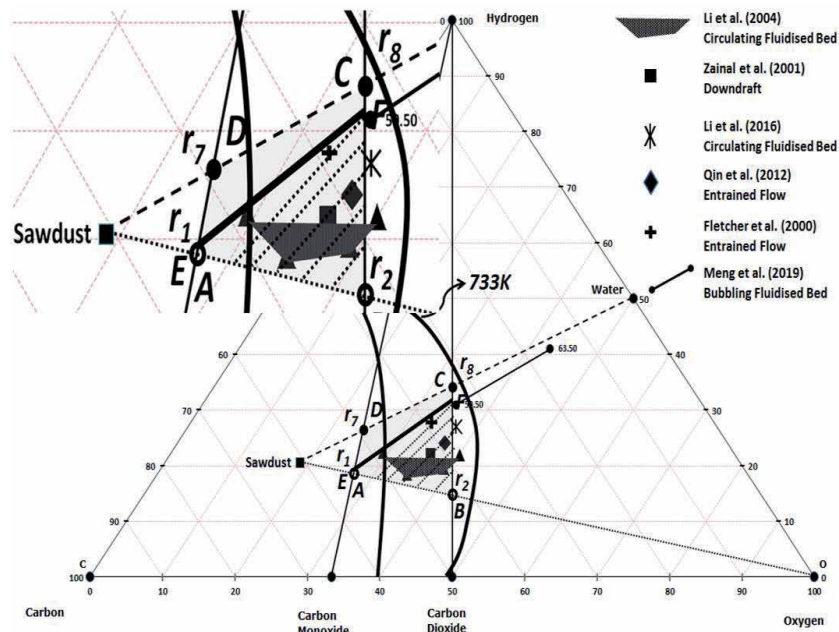


**Figure 5.**  
 Representation of experimental points for sawdust gasification.

experimental points from [4] as indicated by the shaded region. It is of interest to observe that the points lie within the stoichiometric boundary, and on the hot side. Moreover, there are experimental points that lie on the carbon boundary. It is noted that the sawdust used in the experiment have a slightly higher hydrogen content than the one used for the analysis so some deviations are expected.

Zainal et al. [10] develop an equilibrium model to predict the gasification process in an adiabatic downdraft gasifier. The result is plotted in **Figure 5** for an adiabatic downdraft gasification of sawdust. The downdraft gasifier lies once again in the stoichiometric region and on the hot side of the thermally balance line. Also, it is found that a downdraft gasifier can be modelled using an equilibrium model provided the gasification temperature is known.

The effects of metal salt catalyst on gasification of sawdust in a fluidized bed gasifier was studied by [18]. For sawdust it was noted that using NaCl and K<sub>2</sub>CO<sub>3</sub> as salt catalyst increased yields of CO and CH<sub>4</sub>. Excess steam was used in the gasification system and the reported data in **Table 4** was determined by analysing the dry syngas data, the feed mass balance and the WGS reaction.

Qin et al. [19] performed a laboratory scale entrained flow gasifier at temperatures of 1400C using feedstock comprising wood, straw and dried lignin. The experiments were conducted using excess steam but report the syngas on a dried basis. The values for the syngas immediately after the entrained flow gasifier reported in **Table 4** have thus been recalculated based on the known feed mass balance, the gasification temperature and the syngas output composition (dried). It is noted some WGS reaction had to be included to obtain the final compositions.

A Computational Fluid Dynamics (CFD) model developed by [20] predicted the output performance of an entrained flow gasifier using biomass (sawdust and cotton trash). The output of the syngas is suitable for gas-to-liquid process such as methanol or Fischer-Tropsch liquids.

A novel pilot scale bubbling fluidized gasifier was built by [21] to study the effects of gasification oxidants. 8 such points have been included and represented

by a single straight line in **Figure 5**. It is noted that excess steam has been used and hence the points lie out of the stoichiometric region (grey shaded region). The product syngas is then further dehydrated in an additional step to obtain the dry gas reported by [21].

The CHO diagram development and the analysis performed in this work have thus been validated by experimental data. In summary, sensible biomass gasification systems will operate in a well-defined mass balance region (grey shaded region ABCD in **Figure 5**). This region is further divided by the presence of the energy balance and the carbon boundary (derived from maximum temperature achievable for gasification). With the additional information of the HHV contours, a desirable operating point (for high HHV syngas) can be determined at the intersection of the thermally balanced line and the carbon boundary (maximum gasification temperature). The experimental points from literature also confirm the operational regions for sawdust gasification. Hence, preliminary designs or experimental programs can greatly benefit as a targeted approach is used prior to expensive trials.

## 7. Equilibrium and thermodynamics

While the basis reactions in **Table 1** provide the necessary process schemes required for gasification, they do not explicitly say how the specific stoichiometry is to be obtained. The restricting factor here is thermodynamic equilibrium limitations and, in the case of [7], kinetic limitations. In general, some aspects of gasification processes may be modelled as equilibrium systems. However, thermodynamics restricts the theoretically achievable CO:H<sub>2</sub> ratios as required by the ideal stoichiometric region. For example, if reaction F is desired at say 1000 K, the equilibrium compositions are H<sub>2</sub>O: 0.19, CO:0.19, CO<sub>2</sub>:0.16, H<sub>2</sub>:0.44 and negligible CH<sub>4</sub>. In this case we are seeking a ratio (CO:H<sub>2</sub>) of infinity instead of the one limited by thermodynamics at 2.3. In order to achieve the composition from the idealised stoichiometric region steam injection (for H<sub>2</sub> deficient gas) or CO<sub>2</sub> (for CO deficient gas) addition is required to adjust the ratios of the species in the Water-Gas-Shift (WGS) reaction.

### 7.1 Circumventing thermodynamic limitations using WGS reaction

It is possible to use steam injection to obtain the thermally balanced reaction (F) (**Table 2**). This is in accordance with the Water-Gas-Shift reaction:  $\text{CO} + \text{H}_2\text{O} \leftrightarrow \text{CO}_2 + \text{H}_2$ . Steam is added to increase H<sub>2</sub> content from a CO rich equilibrium steam. Conversely, CO<sub>2</sub> may be added to increase CO content from a H<sub>2</sub> rich stream although it is not commonly practiced. In this particular case, at 1000 K, the steam per mol of sawdust is >55. This means that a large quantity of steam needs to be raised and condensed after the gasifier. Although this ratio (55) is an extreme case, it is commonly found that ratios of up to 3–7 are used in practice. It is also noted here that the steam assists in obtaining the stoichiometry of the basis reactions and is recycled after the gasifier in a recycle loop comprising of steam generation, condensation, treatment and make-up water stream.

## 8. Application to underground coal gasification (UCG)

UCG, a clean coal technology, is widely understood as a disruptive mining method that is efficient and environmentally benign. This method extracts deep and stranded coal by performing complex gasification reactions in-situ within the



coal seam. The products of UCG are exactly the same as a surface gasifier without the ash component which is designed to be left underground. Whilst the literature on UCG technology is vast, in this chapter the analysis is limited to the syngas products and region of gasification as demonstrated by CHO-diagram. As an example, consider two UCG projects in Australia performed on Macalister Coal Seam at Bloodwood Creek and Chinchilla.

### 8.1 Analysis of UCG at Bloodwood Creek and Chinchilla

Macalister Coal Seam,  $\text{CH}_{0.898}\text{O}_{0.108}$ , has a heat of formation of  $-112.27 \text{ kJ/mol}$ . With this information it can be shown (developed elsewhere), that 8 non-negative basis reactions are possible if the coal is gasified with oxygen and steam where methane production is allowed in the product stream. Furthermore, only 4 independent reactions lead to the thermally balanced operation where the heat of reactions are zero. These reactions are represent in **Table 6** and the thermally balanced region (shaded in grey) in **Figure 6**.

### 8.2 Representation of UCG processes at Bloodwood Creek and Chinchilla

**Figure 6** represents the gasification tendencies for the Macalister Coal Seam, oxygen and steam. The shaded region indicates where the thermally balanced region is for the coal, representing a net zero input/output of energy into the gasifier – a preferred scenario for any ideal gasification process. The Chinchilla syngas output are represented by the triangles and the cross represents Bloodwood Creek

No.	Reaction
G	$\text{CH}_{0.898}\text{O}_{0.108} + 0.4476\text{O}_2 \rightarrow 0.9964\text{CO} + 0.0036 \text{CO}_2 + 0.4489 \text{H}_2$
H	$\text{CH}_{0.898}\text{O}_{0.108} + 1.167 \text{H}_2\text{O} + 0.3623 \text{O}_2 \rightarrow \text{CO}_2 + 1.6159 \text{H}_2$
I	$\text{CH}_{0.898}\text{O}_{0.108} + 0.5251 \text{H}_2\text{O} + 0.1962 \text{O}_2 \rightarrow 0.487 \text{CH}_4 + 0.513 \text{CO}_2$
J	$\text{CH}_{0.898}\text{O}_{0.108} + 0.3494 \text{O}_2 \rightarrow 0.2244 \text{CH}_4 + 0.0317 \text{CO}_2 + 0.7438 \text{CO}$

**Table 6.**  
 Thermally balanced reactions for Macalister coal.

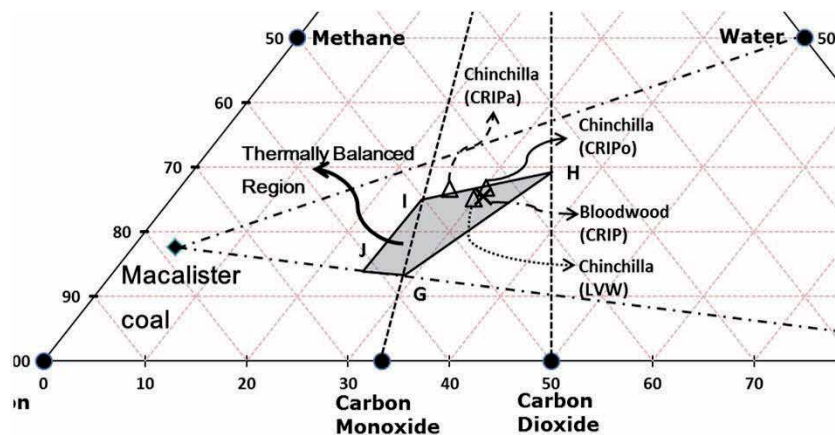


**Figure 6.**  
 Representation of gasification region for Macalister underground coal gasification.

respectively. Two different UCG techniques have been used: Linked Vertical Wells (LVW) and Controlled Retractable Injection Point (CRIP) [22].

The syngas compositions may be found in the works of [22]. It is noted that the output from the UCG field trials lie within the theoretically predicted shaded thermally balanced region. The choice of where to operate the UCG process depends on the final use of the syngas. In these trials, a syngas feed for liquid-fuel production was desired – hence a higher hydrogen to carbon monoxide ratio was required which is achievable around the line HI. For power generation, a syngas with a higher calorific value gas would be required and would thus operate closer to line JI which is richer in methane, carbon monoxide and hydrogen.

## **9. Conclusions**

While gasification systems are complex, the important reactions are represented by basis reactions that span the stoichiometric region of operation on a CHO diagram. The operation of autothermal sawdust gasification systems, without methane formation, is further represented by a line within the stoichiometric region. It is verified, from pilot plant data for gasification of sawdust that the operation occurs within the stoichiometric region and on the hot-side of the thermally balanced line. The analysis in this chapter thus enables the determination of outputs from sawdust gasification which can further be used to design downstream processes. It is shown that a desirable point to operate an air–steam gasification system for power generation (syngas with highest HHV) lies at the point of intersection between the thermally balanced line and the carbon boundary. This intersection represents the point where the maximum HHV is obtained for the gasification system.

The application of the CHO-diagram has been extended to underground coal gasification processes where thermally balanced regions for a given coal was developed. Field trial data were then plotted and found to be in the theoretically predicted thermally balanced region.

The method developed in this chapter provides a high-level analysis to practitioners who are doing basic design in gasification processes – it enables some predictions of syngas possible based on the carbon source and possible oxidants. The output is independent of major parameters such as gasifier type, kinetics or reaction parameters. Lastly, the method provides predictions of syngas compositions possible from a gasification system, enabling design tasks to be completed with reasonable accuracy.

## **Acknowledgements**

Acknowledgments are due to the NRF Grant No. 81248 for funding this work.

## Author details

Shehzaad Kauchali  
School of Chemical and Metallurgical Engineering, University of the  
Witwatersrand, Johannesburg, South Africa

\*Address all correspondence to: [shehzaad.kauchali@wits.ac.za](mailto:shehzaad.kauchali@wits.ac.za)

## IntechOpen

---

© 2021 The Author(s). Licensee IntechOpen. This chapter is distributed under the terms of the Creative Commons Attribution License (<http://creativecommons.org/licenses/by/3.0>), which permits unrestricted use, distribution, and reproduction in any medium, provided the original work is properly cited. 

## References

- [1] Prins MJ, Ptasiński KJ, Janssen FJJG. From coal to biomass gasification: Comparison of thermodynamic efficiency. *Energy*. 2007;**32**:1248-1259
- [2] Ptasiński KJ, Prins MJ, Pierik A. Exergetic evaluation of biomass gasification. *Energy*. 2007;**32**:568-574
- [3] Melgar A, Pérez JF, Laget H, Horillo A. Thermochemical equilibrium modelling of a gasifying process. *Energy Conversion and Management*. 2007;**48**:59-67
- [4] Ahmed TY, Ahmad MM, Yusup S, Inayat A, Khan Z. Mathematical and computational approaches for design of biomass gasification for hydrogen production: A review. *Renewable and Sustainable Energy Reviews*. 2012;**16**:2304-2315
- [5] Prins MJ, Ptasiński KJ, Janssen FJJG. Thermodynamics of gas-char reactions: first and second law analysis. *Chemical Engineering Science*. 2003;**58**:1003-1011
- [6] Prins MJ, Ptasiński KJ, Janssen FJJG. Exergetic optimisation of a production process of Fischer-Tropsch fuels from biomass. *Fuel Processing Technology*. 2004;**86**:375-389
- [7] Li XT, Grace JR, Lim CJ, Watkinson AP, Chen HP, Kim JR. Biomass gasification in a circulating fluidized bed. *Biomass and Bioenergy*. 2004;**26**:171-193
- [8] Radwan AM. An overview on gasification of biomass for production of hydrogen rich gas. *Der Chemica Sinica*. 2012;**3**(2):323-335
- [9] Sadaka SS, Ghaly AE, Sabbah MA. Two phase biomass air-steam gasification model for fluidized bed reactors: Part I-model development. *Biomass and Bioenergy*. 2002;**22**:439-462
- [10] Zainal ZA, Ali R, Lean CH, Seetharamu KN. Prediction of a downdraft gasifier using equilibrium modelling for different biomass materials. *Energy Conversion and Management*. 2001;**42**:1499-1515
- [11] Wander PR, Altafini CR, Barreto RM. Assessment of a small sawdust gasification unit. *Biomass and Bioenergy*. 2004;**27**:467-476
- [12] Battaerd HAJ, Evans DG. An alternative representation of coal composition data. *Fuel*. 1979;**58**(2):105-108
- [13] Yoon H, Wei J, Denn MM. Feasible operating regions for roving bed coal gasification reactors. *Ind. Eng. Chem. Process Des. Dev.* 1979;**18**(2):306-312
- [14] Wei J. A stoichiometric Analysis of Coal Gasification. *Ind. Eng. Chem. Process Des. Dev.* 1979;**18**(3):554-558
- [15] Han Shin Tay D, Kok Sum Ng D, Kheireddine H, El-Halwagi M. Synthesis of an integrated biorefinery via the C-H-O ternary diagram. *Clean Techn Environ Policy*. 2011;**13**:567-579
- [16] Basu P. Biomass Gasification & Pyrolysis: Practical Design & Theory. Oxford: Elsevier Inc.; 2010
- [17] Li X, Grace JR, Watkinson AP, Lim CJ, Ergudenler A. Equilibrium modelling of gasification: a free energy minimization approach and its application to a circulating fluidized bed coal gasifier. *Fuel*. 2001;**80**:195-207
- [18] Li Y, Yu M, Fan Y, Li R, Yang T, Chi Y. Effects of metal salt catalysts on fluidized bed gasification characteristics of source-collected combustible solid waste. *BioResources*. 2016;**11**(4):10314-10328
- [19] Qin K, Jensen PA, Lin W, Jensen AD. Biomass Gasification Behavior in an

Entrained Flow Reactor: Gas Product  
Distribution and Soot Formation.  
Energy & Fuels. 2012;**26**(9):5992-6002

[20] Fletcher DF, Haynes BS, Christo FC,  
Joseph SD. A CFD based combustion  
model of an entrained flow biomass  
gasifier. Applied Maths Modelling.  
2000;**24**:165-182

[21] Meng F, Ma Q, Wang H, Liu Y,  
Wang D. Effect of Gasifying Agents on  
Sawdust Gasification in a Novel Pilot  
Scale Bubbling Fluidized Bed System.  
Fuel. 2019;**249**:112-118

[22] Perkins G. Underground  
coal gasification – Part I: Field  
demonstrations and process  
performance. Progress in Energy and  
Combustion Science. 2018;**67**:158-187



*Edited by Valter Silva  
and Celso Eduardo Tuna*

Gasification is the thermochemical process of converting carbonaceous material in the presence of an oxidant less than stoichiometric to form a gaseous product, known as synthesis gas or syngas, at high temperatures. The gas produced can have different uses depending on its quality. Among these uses are to drive internal combustion engines and gas turbines, direct burning, and synthesis of chemical components. This book provides a comprehensive overview of the various techniques and applications of syngas developed thus far to contribute to a better understanding of this important process of obtaining a renewable fuel, which is essential for the development of a sustainable economy.

Published in London, UK

© 2021 IntechOpen  
© Bet\_Noire / iStock

**IntechOpen**

